OIL RESERVOIR DISTRIBUTION MAPPING

OF MAE-SOON OIL FIELD, FANG BASIN

Makara Laikanok

A Thesis Submitted in Partial Fulfillment of the Requirements for the

Degree of Master of Engineering in Geotechnology

Suranaree University of Technology

Academic Year 2014

การทำแผนที่การกระจายตัวของชั้นกักเก็บน้ำมัน ของแหล่งน้ำมันแม่สูน แอ่งฝาง

นายมกรา ลายกนก

มหาวิทยาลัยเทคโนโลยีสุรนารี

วิทยานิพนธ์นี้เป็นส่วนหนึ่งของการศึกษาตามหลักสูตรปริญญาวิศวกรรมศาสตรมหาบัณฑิต
สาขาวิชาเทคโนโลยีธรณี
มหาวิทยาลัยเทคโนโลยีสุรนารี
ปีการศึกษา 2557

OIL RESERVOIR DISTRIBUTION MAPPING

OF MAE-SOON OIL FIELD, FANG BASIN

Suranaree University of Technology has approved this thesis submitted in partial fulfillment of the requirements for a Master's Degree.

Thesis Examining Committee

_____

(Prof. Dr. Kittitep Fuenkajorn)

Chairperson

_____

(Asst. Prof. Dr. Akkhapun Wannakomol)

Member (Thesis Advisor)

_____

(Assoc. Prof. Kriangkrai Trisarn)

Member

_____

(Prof. Dr. Sukit Limpijumnong)

Vice Rector for Academic Affairs and Innovation

_____

(Assoc. Prof. Flt. Lt. Dr. Kontorn Chamniprasart)

Dean of Institute of Engineering

มกรา ลายกนก : การทำแผนที่การกระจายตัวของชั้นกักเก็บน้ำมันของแหล่งน้ำมันแม่สูน แอ่งฝาง (OIL RESERVOIR DISTRIBUTION MAPPING OF MAE-SOON OIL FIELD, FANG BASIN) อาจารย์ที่ปรึกษา : ผู้ช่วยศาสตราจารย์ ดร.อัฆพรรค์ วรรณโกมล, 209 หน้า

การศึกษาครั้งนี้มีเป้าหมาย เพื่อการวิเคราะห์คุณภาพและการกระจายตัวเชิงพื้นที่ของชั้นกักเก็บน้ำมันที่มีศักยภาพของแหล่งน้ำมันแม่สูน แอ่งฝาง จังหวัดเชียงใหม่ โดยการใช้ข้อมูลการหยั่งธรณีหลุมเจาะและระบบภูมิศาสตร์สารสนเทศเป็นเครื่องมือในการทำแผนที่และแสดงการกระจายตัวของชั้นกักเก็บน้ำมันที่มีศักยภาพของแหล่งน้ำมันแม่สูน ผลการศึกษาทำให้เห็นว่ามีชั้นกักเก็บน้ำมันที่เป็นหินทรายอยู่ในชั้นหินแม่สอดของแหล่งน้ำมันแม่สูน ชั้นกักเก็บน้ำมันที่เป็นหินทรายนี้สามารถจัดแบ่งได้เป็น 19 ชั้นหินทรายหลัก ซึ่งสามารถจัดเป็นกลุ่มได้ 3 กลุ่ม เป็นชั้นหินทรายกลุ่มเอ (A) ชั้นหินทรายกลุ่มบี (B) และชั้นหินทรายกลุ่มซี (C) ตามลำดับ โดยอ้างอิงจากคุณสมบัติทางด้านรังสีแกมมา ค่าศักย์ทางไฟฟ้า และค่าความต้านทานไฟฟ้าของชั้นหิน ชั้นหินทรายกลุ่มเอ มีบริเวณที่มีศักยภาพในการเป็นชั้นกักเก็บ ไฮโดรคาร์บอนอยู่ 2 บริเวณ ซึ่งได้แก่ บริเวณพื้นที่ทางตะวันตกเฉียงเหนือ และพื้นที่ทางตะวันตกเฉียงใต้ของแหล่ง ชั้นหินทรายกลุ่มบี มีบริเวณที่มีศักยภาพในการเป็นชั้นกักเก็บไฮโดรคาร์บอนอยู่ 3 บริเวณ ซึ่งได้แก่ บริเวณพื้นที่ทางตะวันตกเฉียงเหนือ พื้นที่ทางตะวันออก และพื้นที่ทางตะวันตกของแหล่ง ตามลำดับ ส่วนชั้นหินทรายกลุ่มซี มีบริเวณที่มีศักยภาพในการเป็นชั้นกักเก็บไฮโดรคาร์บอนอยู่ 4 บริเวณ ซึ่งได้แก่ บริเวณพื้นที่ทางตะวันตกเฉียงเหนือ พื้นที่ทางตะวันออกเฉียงเหนือ พื้นที่ทางตะวันออก และพื้นที่ทางตะวันตกเฉียงใต้ ตามลำดับ

มหาวิทยาลัยเทคโนโลยีสุรนารี

สาขาวิชา เทคโนโลยีธรณี ลายมือชื่อนักศึกษา_____

ปีการศึกษา 2557 ลายมือชื่ออาจารย์ที่ปรึกษา_____

MAKARA LAIKANOK : OIL RESERVOIR DISTRIBUTION MAPPING OF MAE-SOON OIL FIELD, FANG BASIN. THESIS ADVISOR : ASST. PROF. AKKHAPUN WANNAKOMOL, Ph.D., 209 PP.

OIL RESERVOIR DISTRIBUTION MAP/ WIRELINE LOGGING/ MAE-SOON OIL FIELD

This study is aimed to analyze the quality and spatial distribution of the potential oil reservoirs of Mae-Soon oil file, Fang Basin, Chiang Mai province by using wireline logging data and Geographic Information Systems (GIS) as the tool for mapping and demonstrating the distribution of the potential oil reservoirs of Mae-Soon oil field. The results of the study revealed that there were oil sandstone reservoirs in Mae Sod Formation of Mae-Soon oil field. These sandstone reservoirs could be divided into 19 major sandstones layers which could be grouped into three groups as group A, group B and group C based on their gamma ray, spontaneous potential, and resistivity characteristics, respectively. Sandstone Group A has 2 potential hydrocarbon-bearing zones which are located in the north-western and south-western part of the field. Sandstone Group B has 3 potential hydrocarbon-bearing zones which are located in the north-western, eastern, and western part of the field, respectively. Sandstone Group C has 4 potential hydrocarbon-bearing zones which are located in the north-western, north-eastern, eastern, and south-western part of the field, respectively.

School of Geotechnology Student's Signature_____

Academic Year 2014 Advisor's Signature_____

ACKNOWLEDGEMENTS

Completion of this report would have been impossible without the interest and direct participation of a member of individuals to whom I owe everlasting gratitude sincere appreciation in extended to everyone who I worked in connection with this scholastic achievement.

In particular, I would like to acknowledge the efforts of Assistant Professor Akkhapun Wannakomol, Ph.D, my advisor, for his intellectual insights guidance; Professor Dr. Kittitep Fuenkajorn, Associate Professor Kriangkrai Trisarn, Dr. Chongpan Chonglakmani, Mr. Chatetha Chumkratoke for their intellectual insights guidance and encouragement to conduct this thesis.

The Exploration and Production Division Northern Petroleum Development Centre for giving an opportunity to use the data needed for this report.

All my friends and classmates, for their constant encouragement and moral support; and finally, my beloved parents for their constant and affectionate understanding, inspiration and unfading love.

Makara Laikanok

TABLE OF CONTENTS

Page

ABSTRACT (THAI) I

ABSTRACT (ENGLISH) II

ACKNOWLEDGEMENTS III

TABLE OF CONTENTS IV

LIST OF TABLES VII

LIST OF FIGURES VIII

SYMBOLS AND ABBREVIATIONS XIII

CHAPTER

I INTRODUCTION 1

1.1 Background and rationale 1

1.2 Study area 2

1.3 Objectives of the study 2

1.4 Scope and limitation of the study 2

1.5 Research methodology 4

1.6 Thesis contents 4

II LITERATURE REVIEW 5

2.1 Geology of the Fang Basin 5

2.2 Petroleum geology of the Fang Basin 8

2.3 Other research use ARCGIS for study 11

TABLE OF CONTENTS (Continued)

Page

III METHODOLOGY 15

3.1 Wireline log data interpretation 15

3.1.1 Gamma ray (GR) log 15

3.1.2 Spontaneous potential (SP) log 18

3.1.3 Resistivity log 18

3.2 Porosity and permeability 21

3.2.1 Porosity 21

3.2.2 Permeability 21

3.3 Wireline log data calculation 22

IV RESULTS 27

4.1 Wireline log data interpretation results 27

4.1.1 Gamma ray, Spontaneous potential and Resistivity log interpretation 27

4.1.2 Sandstone layer thickness maps 27

4.2 Stratigraphic section 52

4.3 Potential reservoir rock properties 52

4.3.1 Porosity and permeability 52

4.3.2 The relationship between rock properties and depth 89

4.3.3 Grouped sandstone layers thickness, porosity, permeability and hydrocarbon saturation map 91

TABLE OF CONTENTS (Continued)

Page

4.4 Potential hydrocarbon-bearing zones of Mae-Soon oil field 106

4.5 Three-dimensional map of the potential reservoirs..... 113

V CONCLUSIONS, DISCUSSIONS AND RECOMMENDATIONS 121

5.1 Conclusions 121

5.2 Discussions..... 123

5.3 Recommendations 123

REFERENCES..... 124

APPENDICES

APPENDIX A GAMMA RAY AND SPONTANEOUS POTENTIAL LOG INTERPRETATION 134

APPENDIX B RESISTIVITY LOG INTERPRETATION..... 168

APPENDIX C PERMEABILITY AND POROSITY OF SANDSTONE LAYER OF MAE-SOON OIL FIELD 202

BIOGRAPHY..... 209

LIST OF TABLES

Table **Page**

3.1 Borehole name and well location of 33 boreholes which were used in the study. 16

3.2 Sandstone type classification guideline based on resistivity data and mud logging data (modified after DED) 19

3.3 Total thickness of 19 sand layers of 33 boreholes drilled in Mae-Soon oil field 20

3.4 The quality of sandstone based on permeability (after Dickker, 1985) 21

3.5 The quality of sandstone based on porosity (after Dickker, 1985) 22

4.1 Three main grouped sandstone layer of Mae-Soon oil field 113

มหาวิทยาลัยเทคโนโลยีสุรนารี

LIST OF FIGURES

Figure **Page**

1.1 Structure of oil field in Fang Basin (modified after Polachan and Sattayarak, 1989)..... 3

2.1 The geological map of Fang area and the study area is bounded by (modified after DMR, 2007). 6

2.2 The geological symbols of Fang area (modified after DMR, 2007). 7

2.3 Diagram of petroleum system of Mae-Soon and San-Sai plays (Defence Energy Department, 2006). 10

3.1 Location map of the 33 boreholes which were used in this study 16

4.1 Isopach map of sandstone layer 01 of Mae-Soon oil field..... 28

4.2 Isopach map of sandstone layer 02 of Mae-Soon oil field..... 29

4.3 Isopach map of sandstone layer 03 of Mae-Soon oil field..... 30

4.4 Isopach map of sandstone layer 04 of Mae-Soon oil field..... 32

4.5 Isopach map of sandstone layer 05 of Mae-Soon oil field..... 33

4.6 Isopach map of sandstone layer 06 of Mae-Soon oil field..... 34

4.7 Isopach map of sandstone layer 07 of Mae-Soon oil field..... 35

4.8 Isopach map of sandstone layer 08 of Mae-Soon oil field..... 37

4.9 Isopach map of sandstone layer 09 of Mae-Soon oil field..... 38

4.10 Isopach map of sandstone layer 10 of Mae-Soon oil field..... 39

4.11 Isopach map of sandstone layer 11 of Mae-Soon oil field..... 40

LIST OF FIGURES (Continued)

Figure **Page**

4.12 Isopach map of sandstone layer 12 of Mae-Soon oil field..... 42
4.13 Isopach map of sandstone layer 13 of Mae-Soon oil field..... 43
4.14 Isopach map of sandstone layer 14 of Mae-Soon oil field..... 44
4.15 Isopach map of sandstone layer 15 of Mae-Soon oil field..... 45
4.16 Isopach map of sandstone layer 16 of Mae-Soon oil field..... 47
4.17 Isopach map of sandstone layer 17 of Mae-Soon oil field..... 48
4.18 Isopach map of sandstone layer 18 of Mae-Soon oil field..... 49
4.19 Isopach map of sandstone layer 19 of Mae-Soon oil field..... 50
4.20 Stratigraphic section of well no. FA-MS-08-12 52
4.21 Stratigraphic section of well no. FA-MS-08-18 53
4.22 Stratigraphic section of well no. FA-MS-27-46 54
4.23 Stratigraphic section of well no. FA-MS-28-47 55
4.24 Stratigraphic section of well no. FA-MS-28-48 56
4.25 Stratigraphic section of well no. FA-MS-28-49 57
4.26 Stratigraphic section of well no. FA-MS-28-50 58
4.27 Stratigraphic section of well no. FA-MS-30-54 59
4.28 Stratigraphic section of well no. FA-MS-31-55 60
4.29 Stratigraphic section of well no. FA-MS-32-56 61
4.30 Stratigraphic section of well no. FA-MS-33-58 61
4.31 Stratigraphic section of well no. FA-MS-34-59 63
4.32 Stratigraphic section of well no. FA-MS-34-60 64

มหาวิทยาลัยเทคโนโลยีสุรนารี

LIST OF FIGURES (Continued)

Figure **Page**

4.33 Stratigraphic section of well no. FA-MS-34-61 65
4.34 Stratigraphic section of well no. FA-MS-35-62 66
4.35 Stratigraphic section of well no. FA-MS-36-65 67
4.36 Stratigraphic section of well no. FA-MS-36-66 68
4.37 Stratigraphic section of well no. FA-MS-36-67 69
4.38 Stratigraphic section of well no. FA-MS-40-69 70
4.39 Stratigraphic section of well no. FA-MS-46-70 71
4.40 Stratigraphic section of well no. FA-MS-47-71 72
4.41 Stratigraphic section of well no. FA-MS-48-73 73
4.42 Stratigraphic section of well no. FA-MS-48-75 74
4.43 Stratigraphic section of well no. FA-MS-49-76 75
4.44 Stratigraphic section of well no. FA-MS-49-77 76
4.45 Stratigraphic section of well no. FA-MS-50-78 77
4.46 Stratigraphic section of well no. FA-MS-51-79 78
4.47 Stratigraphic section of well no. FA-MS-51-80 79
4.48 Stratigraphic section of well no. FA-MS-53-83 80
4.49 Stratigraphic section of well no. FA-MS-54-84 81
4.50 Stratigraphic section of well no. FA-MS-54-85 82
4.51 Stratigraphic section of well no. FA-MS-54-86 83
4.52 Stratigraphic section of well no. FA-MS-55-87 84
4.53 Porosity quality distribution of sandstone of Mae-Soon oil field 85

มหาวิทยาลัยเทคโนโลยีสุรนารี

LIST OF FIGURES (Continued)

Figure **Page**

4.54 Frequency distribution of Permeability, Depth, Grain Size, Cementing Material and Matrix for fair porosity of Mae-Soon oil field 86

4.55 Distribution of Permeability, Depth, Grain size, Cementing material and Matrix of 19 sandstone layers of Mae-Soon oil field..... 87

4.56 Cross-plot between porosity and depth of sandstone of Mae-Soon oil field..... 88

4.57 Cross-plot between porosity and permeability of sandstone of Mae-Soon oil field..... 89

4.58 Isopach map of sandstone Group A of Mae-Soon oil field 91

4.59 Porosity distribution map of sandstone Group A..... 92

4.60 Permeability distribution map of sandstone Group A..... 93

4.61 Hydrocarbon saturation distribution map of Sand Group A..... 94

4.62 Isopach map of sandstone Group B of Mae-Soon oil field..... 96

4.63 Porosity distribution map of sandstone Group B..... 97

4.64 Permeability distribution map of sandstone Group B..... 98

4.65 Hydrocarbon saturation distribution map of sandstone Group B 99

4.66 Isopach map of sandstone Group C of Mae-Soon oil field..... 101

4.67 Porosity distribution map of sandstone Group C..... 102

4.68 Permeability distribution map of sandstone Group C..... 103

4.69 Hydrocarbon saturation distribution map of sandstone Group C 104

LIST OF FIGURES (Continued)

Figure **Page**

4.70 Isopach, porosity, permeability and hydrocarbon saturation map of sandstone Group A 106
4.71 Hydrocarbon-bearing potential zone of sandstone Group A 107
4.72 Isopach, porosity, permeability and hydrocarbon saturation map of sandstone Group B..... 108
4.73 Hydrocarbon-bearing potential zone of sandstone Group B..... 109
4.74 Isopach, porosity, permeability and hydrocarbon saturation map of sandstone Group C..... 110
4.75 Hydrocarbon-bearing potential zone of sandstone Group C..... 111
4.76 Three-dimensional model of three main sandstone groups of Mae-Soon oil field..... 113
4.77 Three-dimensional model of sandstone Group A of Mae-Soon oil field..... 114
4.78 Three-dimensional model of sandstone Group B of Mae-Soon oil field..... 114
4.79 Three-dimensional model of sandstone Group C of Mae-Soon oil field..... 115
4.80 Location of geologic cross-section line A-A' 116
4.81 Lithologic cross-section line A-A'..... 117
4.82 Location of geologic cross-section line B-B' 118
4.83 Lithologic cross-section line B-B' 119

SYMBOLS AND ABBREVIATIONS

ANN	=	Artificial Neural Network
Bbls	=	Barrels
Bopd	=	Barrels per day
DMR	=	Department of Mineral Resources
E.	=	East
EON	=	One billion years
F	=	Formation factor
FA	=	Fang
ft.	=	Feet
FTB	=	fold-thrust belt
GIS	=	Geographic Information Systems
GR	=	Gramma ray
IF	=	in fang
kft^2	=	Square kilo feet
km	=	Kilometer
km^2	=	Square kilometer
L	=	Luang
m.	=	Meter
Ma	=	Millions of years ago
md.	=	Millidarcy
MFS	=	Maximum flooding surface

มหาวิทยาลัยเทคโนโลยีสุรนารี

SYMBOLS AND ABBREVIATIONS (Continued)

mm.	=	Millimeter
MMbbls	=	One million barrels
MS	=	Mae-soon
N.	=	North
NS	=	North to South
No.	=	Number
Ohm-m	=	Ohmmeter
PCR	=	Petro Canada Resources
PN	=	Pong-nok
Ro	=	rock saturated with water 100%
Rw	=	all spaces of the rock layers
RTDS	=	Real Time Digital Simulator
S.	=	South
SIDS	=	Seismic interactive data Interpretation System
SP	=	Spontaneous potential
Sw	=	water saturation
TM	=	Thematic Mapper
UTM	=	Universal Transverse Mercator
W.	=	West
WE	=	West to East
2-D	=	Two-Dimension
3-D	=	Three-Dimension

มหาวิทยาลัยเทคโนโลยีสุรนารี

SYMBOLS AND ABBREVIATIONS (Continued)

°API	=	American Petroleum Institute gravity
°C	=	Degree Celsius
°F	=	Degree Fahrenheit
%	=	Percent
%wt	=	Percent by weight
ϕ	=	porosity

มหาวิทยาลัยเทคโนโลยีสุรนารี

CHAPTER I

INTRODUCTION

1.1 Background and rationale

Production and exploration of petroleum at Fang Oil Field has been proceeding for over 50 years, but there is some spare amount of it (Settakul, 1985). According to the present day economic and political situation more studies of Fang oil field to increase its level of production are needed. Fang oil field is an intermontane basin where its average present production rate is about 1,000 barrel per day. These oils have been produced under the supervision of the Defence Energy Department (DED) by the Petroleum Development Act 1956. The majority of oil are produced from Mae-Soon oil field while the rest are from Nong-Yao, San-Sai, and Sam-Jang oil field which are located in Huai Ngu Sub basin (Petro Canada Resources, 1988. To study the distribution of oil-bearing formations, which is important in determining the amount of oil reserves and in oil and gas production wells planning, the applications of spatial information techniques can be applied.

Therefore, this study emphasis on the spatial distribution and the quality of petroleum reservoirs in the Mae-Soon oil field by applying Geographic Information Systems (GIS) and wireline logging techniques. The spatial information systems was used to collect, analyze and evaluate data of which could be displayed in a mapping format whereas the wireline logging techniques was used to study the quality of the potential reservoir in terms of its physical properties, e.g. porosity, permeability,

hydrocarbon saturation concentration. As a result, this spatial approach and analysis capable to increases the better concrete results in visual format of the distribution of the potential oil-bearing formations of Mae-Soon oil field.

1.2 Study area

Mae-Soon oil field is located between latitude 19°49'16" and 19°53'24" North and between longitude 99°07'35" and 99°11'28" East (Figure 1.1). It covers an area of about 5 square kilometers including the area of Ban San Par Dang, Ban Huang Ao, Ban San Ton Muang and Ban Nong Yao, Mae Soon Sub district, Fang district, Chiang Mai province.

1.3 Objectives of the study

The thesis aimed to analyze spatial distribution and quality of the potential petroleum reservoirs in the Mea-Soon oil field, Fang basin, by using Geographic Information Systems (GIS) and wireline logging data as the tool for mapping and demonstrating distribution and determine quality.

1.4 Scope and limitation of the study

The study is focused mainly on the spatial distribution and determine the quality of petroleum reservoirs in the Mae-Soon oil field. This research uses the subsurface data including lithological logs, wireline logs, and 2D seismic profiles stratigraphic, reports of 33 boreholes drilled in Mae-Soon oil field which were provided by the Thai Defense Energy Department.

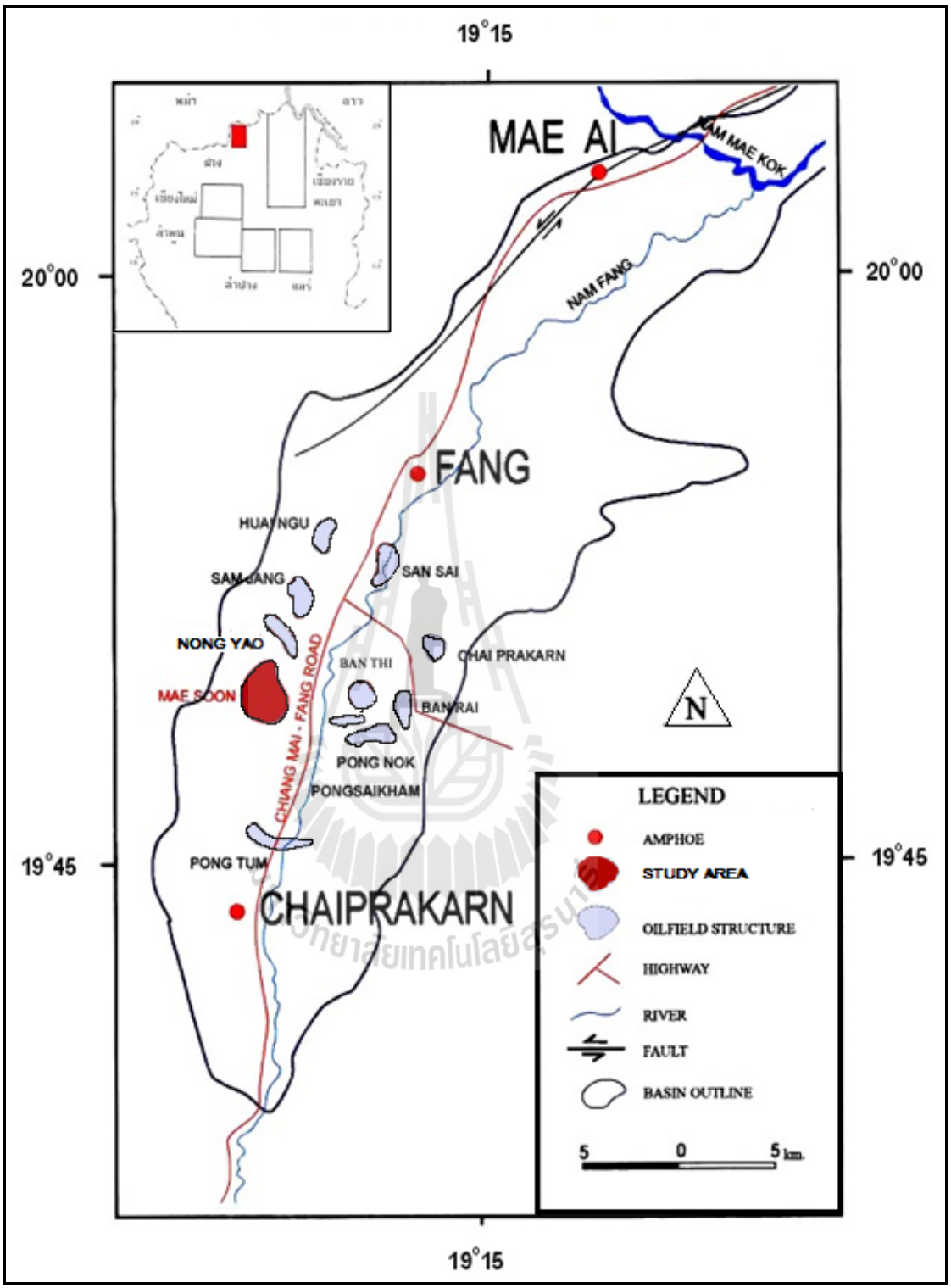

Figure 1.1 Structure of oil field in Fang Basin (modified after Polachan and Sattayarak, 1989)

1.5 Research methodology

Research strategies and activities had been performed as followings:

1. Relevant literatures were searched, reviewed, summarized and documented.

2. Subsurface data including lithological logging, wireline logging data of 33 boreholes in the study area were collected, calculated, and interpreted in order to generate porosity, permeability, hydrocarbon saturation and isopach map.

3. ArcGIS, Surfer8, and Rockwork14 software were used in this study as tools for mapping and demonstrating distribution and determine quality of the potential petroleum reservoirs.

1.6 Thesis contents

Chapter I introduces the thesis by briefly describing the background and rationale of the study, the study objectives, methodology, scope and limitations of the study. **Chapter II** summarizes the results of the literature review. **Chapter III** describes the methodology of the study. **Chapter IV** shows the results and some discussions on the study. **Chapter V** concludes the study results and provides some recommendations for future study, respectively.

CHAPTER II

LITERATURE REVIEW

2.1 Geology of the Fang Basin

The geology of the Fang Basin and the adjacent areas were previously studied by numerous workers, namely, Dutescu et al. (1980), Bunopas and Vella (1983), Braun and Hahn (1976), Settakul (1985).

The Fang Basin is located on the western side of the Sukhothai Fold Belt, which comprises Paleozoic and Triassic strata and volcanic rocks that were accumulated on the eastern margin of the Shan-Thai Craton prior to the Indosinian orogeny. This fold belt is complex and trends north and northeast southwest. These rocks were uplifted and deformed by granitic intrusions during the collision of the Indochina and the Shan-Thai Craton (Bunopas and Vella, 1983). The base of sedimentary sequence in Fang Basin is marked by unconformity as a result of a great period of erosion that preceded the sedimentation of Miocene-Pliocene deposits. At the end of Pliocene the series of deposits was followed by sedimentation of fluviatile environment.

The Fang Basin was filled with rocks of Tertiary and Quaternary age. These Cenozoic rocks and sediments consist of shale, sandstone, conglomerate, sand and gravel (Braun and Hahn, 1976) which is then modified and published by the Department of Mineral Resources (DMR) in 2007 (Figure 2.1 and Figure 2.2).

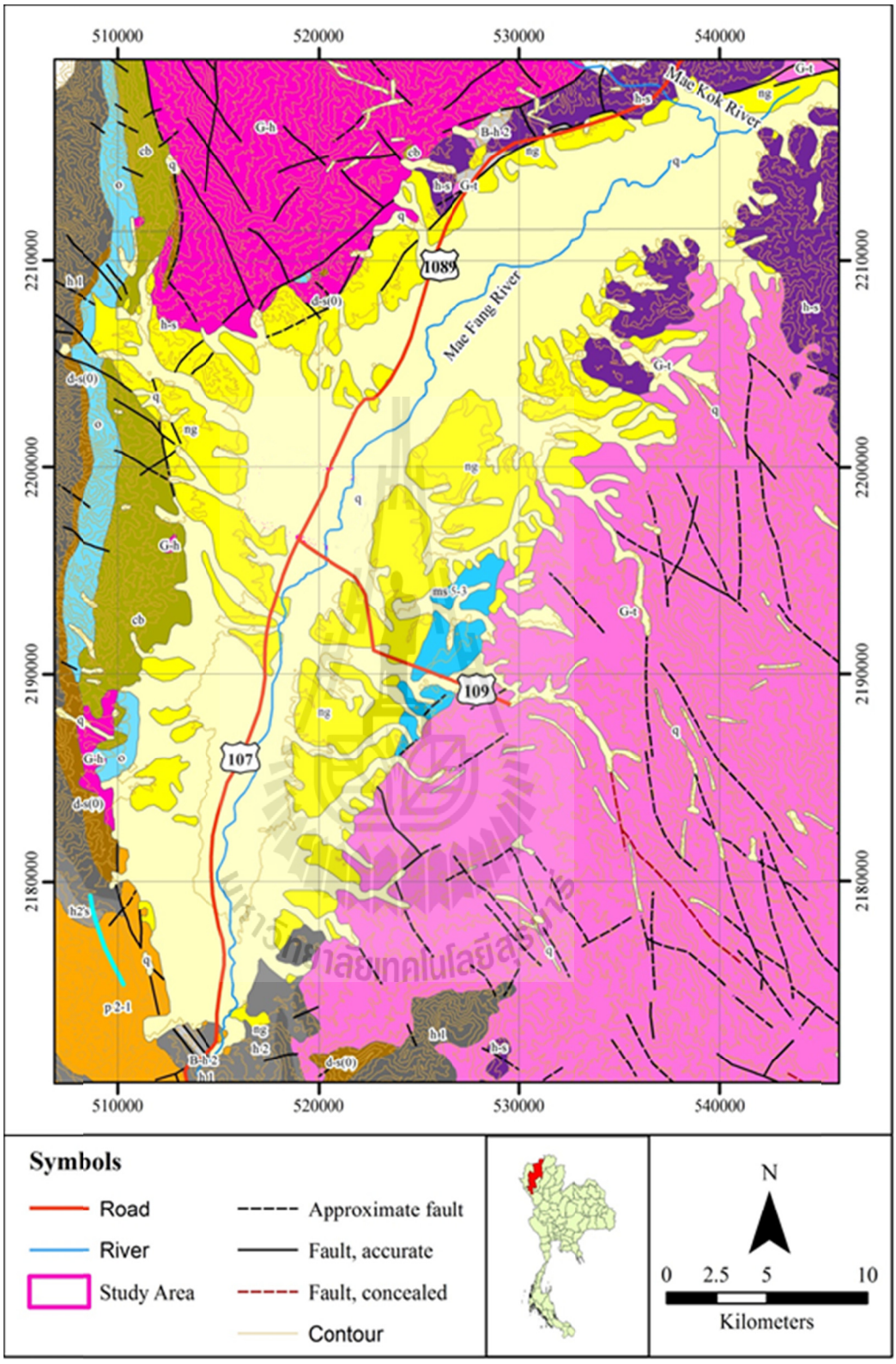

Figure 2.1 The geological map of Fang area and the study area is bounded by (modified after DMR, 2007).

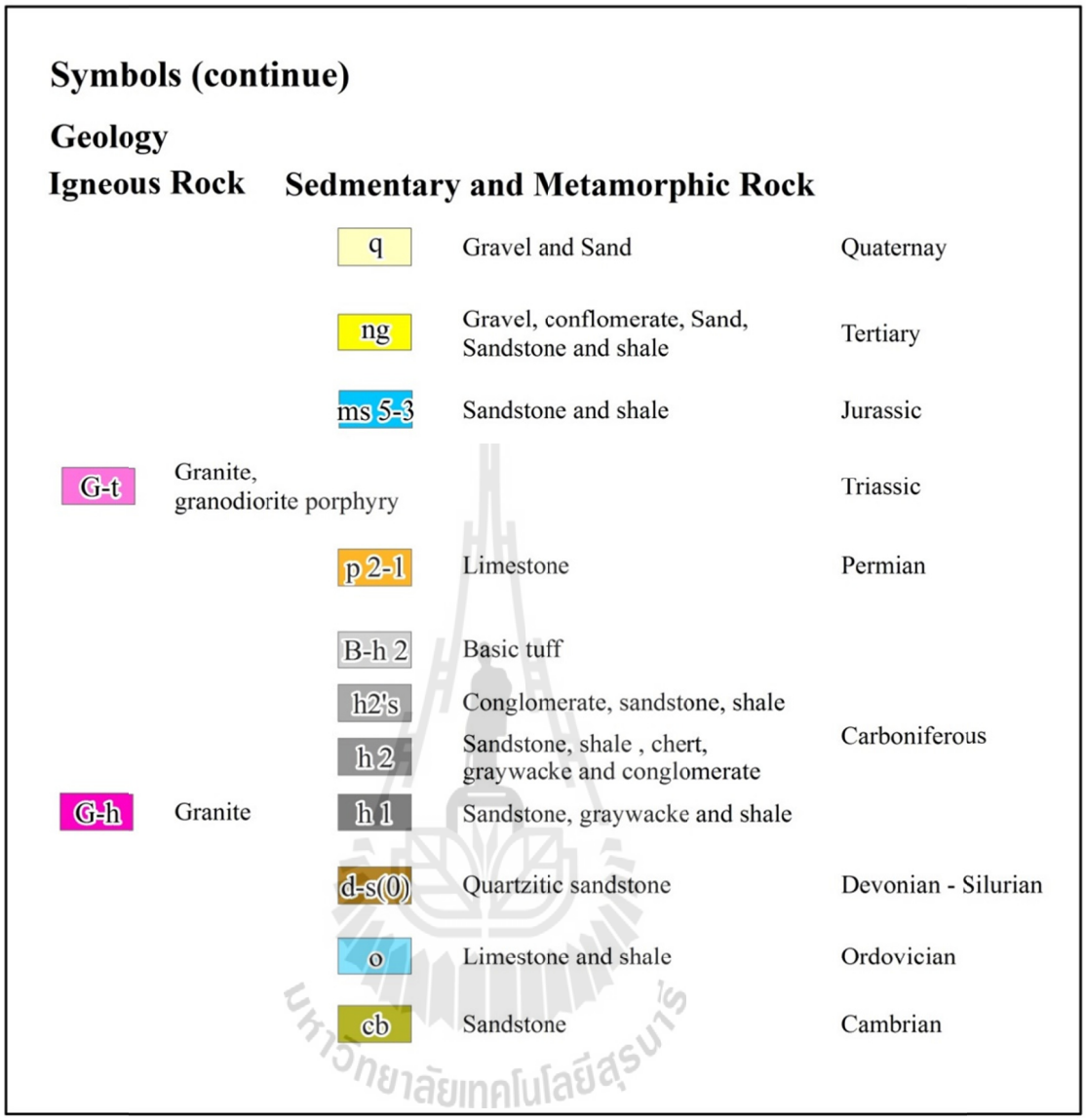

Figure 2.2 The geological symbols of Fang area (modified after DMR, 2007).

The character of lacustrine deposit of Miocene-Pliocene age is indicated by numerous coal seams and carbonaceous sediments. The dominant lithologic type of Miocene-Pliocene deposits is dark clays and sandy clays with lignite. The Fang Basin was subsided in the central part with about 3,000 meters thick of sediment accumulated. The wedging out of the beds and the prograding sedimentation are characteristics of fluvialtile deltaic zone (Dutescu et al, 1980).

Settakul (1985) classified sediments and rocks in the Fang Basin into 2 units. These units are the Mae Fang Formation and the Mae Sod Formation. The depositional environment in the Tertiary time was fluvial-lacustrine and changed to fluvial and alluvial in Quaternary time. The Tertiary rocks of the Fang Basin are conglomerate, sandstone, claystone and shale. The Quaternary deposits are silt, clay, sand and gravel and they occur as stream channels, terrace deposits and alluvial fans. These sediments are covered by recent soil and lateritic sand. The pre-Tertiary basement rocks consist of sedimentary, metamorphic and igneous rocks. On the western side of the basin, the rocks are Cambrian-Permian age and include Carboniferous granite. On the eastern side of the basin, the rocks are Silurian-Devonian and Jurassic, along with Triassic granite.

2.2 Petroleum geology of the Fang Basin

Historically, the Fang Basin area is well known for oil seeps and the first petroleum production in the country was established here over five decades ago. The basin is divided by strike-slip faults into 3 sub-basins separated by horst of older rocks. The Miocene-Pliocene lacustrine sediments of the Mae Sod Formation are the main exploration target, with sediment in the main depocentre including organic-rich shales,

lignites and reservoir quality sandstone. The oils are waxy and were sourced from fresh water lacustrine shales which contained a high proportion of algal material (Petersen et al., 2006). Maximum Tertiary sediment thickness is 3,000 meters. The geothermal gradient is high at 7.5°C/100 meters and possible as high as 9.3°C/100 meters. (Petersen et al., 2006). The onset of oil generation is at 1,400 meters depth, which indicates that the main source-rock interval has been generating oil for about 6 Ma. The onset of wet gas generation is 1,900 meters. The deepest part of the basin is at 3,500 meters. Five small oil fields have been discovered to date and yield a total production rate of 800 bopd (with a historical maximum of 1,500 bopd). These fields produced from Miocene fluvial sandstones in a variety of traps including rollovers and possibly stratigraphic traps. The estimated original reserve of these fields was 50 MMbbl. According to the Department of Mineral Fuels, 2.7 MMbbl proven recoverable reserve remains. The first discovery was the Chai Pra Karn Field in 1953 which encountered a combined structural and/or stratigraphic trap at 230 meters. depth with production from coarse fluvial-lacustrine sandstones of the inferred Mae Sot Formation, sourced and sealed by lacustrine shales of similar age. The reservoir interval comprises thin poorly sorted sands in an interval of 30-100 meters. thick. Twenty wells were drilled on the field with production rates of 10-35 bopd per well. The field was abandoned in 1974, having produced 200,000 barrels of 16°API oil.

Mae-Soon oil field was discovered in 1961 and comprises a simple roll-over on the Mae-Soon Fault in the center of the basin (Figure 2.3). It has reserves of 3.5 MMbbl of 28.3°API oil with high wax content (15.6%). Thirty wells have been drilled, with one reaching basement at 1,005 meters. The reservoirs are stacked, fluvial-lacustrine sandstones of the Mae Sot Formation at 580-690 meters and 730-770

meters depth. The net pay of individual sandstone reservoirs is 2-5 meters and they are separated by inter-bedded shale and mudstones. Porosities are 22-26% and permeability are 552-2,026 md. Oil has been produced from 12-18 wells since 1970 and the field-production rate has averaged 91,000 bbls per year from the upper interval and 120,000 bbls per year from the lower interval.

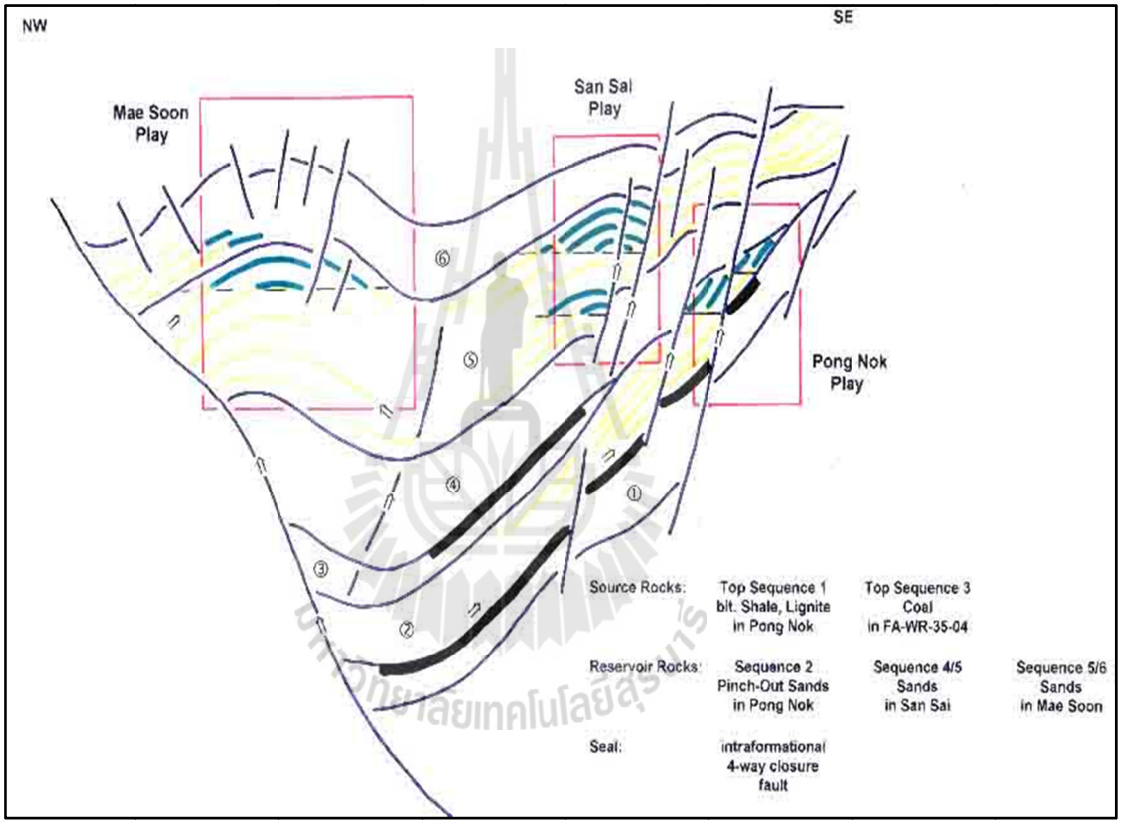

Figure 2.3 Diagram of petroleum system of Mae-Soon and San-Sai plays (Defence Energy Department, 2006).

The Pong Nok Field was discovered in 1979 and produced 30,000 barrels per year of 37°-38°API oil from four wells but is now abandoned. The San Sai discovery was made on the eastern margin of basin and flowed 300 bopd of 33°API oil from

possibly Pliocene sands at 1,280 meters from a combined structural and stratigraphic trap. The Nong Yau discovery produced 600 bopd from one well.

2.3 Other research use ARCGIS for study

Harding (2008) presented ArcGIS used to analyze water access in Mae La, Thailand, home to 45,000 residents living as refugees in a temporary camp. Drinking water for the shelter is supplied at public tap stands while water for hygienic purposes such as bathing and laundry is available via covered rope-pump wells which reach shallow ground water; stream and river surface water; and hand-dug wells. In all 7,117 homes were identified using Google Earth and the corresponding proximity to the nearest tap stand and rope-pump well was calculated. ArcGIS was used together with an EPANET water-distribution model created by Rahimi (2008) to evaluate the predicted daily volume of drinking water available per home. Overall this research shows that the vast majority of residents in Mae La have sufficient access to water. Homes located further than 115 meters from a tap stand, located further than 180 meters from a rope-pump well, or having access to less than 50 liters of water per day were considered a cause for concern. Approximately one in four homes met these criteria. Only 5% of homes are located more than 115 meters from a tap stand. Approximately 14% of homes did not meet the rope-pump proximity criterion, and 15% of homes did not meet the available volume criterion. The tap-stand proximity results provide a much higher degree of confidence compared to the other results. Alternative sources for hygienic water besides rope-pump wells exist, suggesting the number of homes with sufficient access to hygienic water is likely underestimated. Flow rates, predicted by the EPANET model, are highly dependent on the elevation of

distribution system infrastructure points (e.g. storage tanks and tap stands), which are difficult to determine accurately. Thus, while the final results show one in four homes are a cause for concern, the reliability of the rope-pump well proximity assessment and volume per home assessment is insufficient, and the findings could be overly pessimistic.

Lagason (2008) reported Flood-map modeling that an integral part in determining flood-prone areas. This information will help planners and local authorities of future development in the areas affected, propose mitigation measures and also contingency plan in case of flooding. In this research, Geographic Information System (GIS) is coupled with HEC-RAS to produce a flood map of Kota Marudu. GIS provides a broad range of tools for determining area affected by floods and for forecasting areas that are likely to be flooded due to high water level in a river. HEC-RAS is capable of performing one-dimensional open channel steady-state hydraulics. In ArcView, Triangular Irregular Network (TIN) is developed for floodplain processing. Stream centerline, Bank, flow paths and cross sections are digitized to prepare the floodplain geometry for further analysis in HEC-RAS. The rainfall data is taken as 150 mm/hr from the IDF curve. Thus, the obtained flow rate using Rational method is 498.8 m^2/s. A flood map is later produced for the Kota Marudu floodpain the depicts the flood depth and extent for 100 years ARI.

Ing, Cajthaml, and Hutchinson (2008) explained annual 90m x 90m resolution raster datasets of mean temperatures covering the Czech Republic were created for the 1998-2007 period in ArcGIS using linear regression. Linear regression was based on correlation between dependent climate variable – mean temperature and independent variable – altitude. Altitude information was taken from a digital elevation model

(DEM) acquired by the Space Shuttle Radar Topographic Mapping Mission (SRTM). Climate data were obtained from a small subset of meteorological stations (22 stations total) supervised by the Czech Hydrometeorological Institute. Annual variation in mean temperature was visualized in an animated map and published on the Internet. Mean temperature maps were published as a web map service. This web-based environment was created using ArcGIS Server software using a web server managed by the Department of Geography at Kansas State University.

Hasani (2013) presented several methods have been presented to flood administration and reduction and the results of flood risks until now. One of the employed methods is the Flood Plain Zoning (FPZ) method using hydraulic analysis that is based on a hydraulic model. Hydraulic models can draw the water surface profile in each arbitrary section. At first, the flood period is given; then the water surface level in different cross sections is calculated using the model, subsequently these points over the topographic plan of the zone are compared, to find the flood plain zone; and finally we can make required predictions to flood administration on the risk of flood. The current case study is an interval of Zaringol river in Golestan province in Northern Iran which is 24,210 meters long. Golestan province is the first region in Iran with the most detrimental floods and is always at risk because of its position, so presentation of accurate methods to determination of the accurate plain zone of flood is necessary to prevent the probable risks. To this end, the hydraulic model of HEC-RAS to hydraulics calculations and the ArcView software are employed to extract the cross section using topographic plans of river and FPZ in Geographical Information System (GIS) with flood periods: 2, 5, 10, 50 & 100 years and the scale of plans is 1:10000. The zones that were at risk were determined and finally several methods were

recommended to prevent the zone reduction and the detriments of flood. This inquiry completely showed that incorporation of the hydraulic model of HEC-RAS and GIS is a useful implement to analyze FPZs.

CHAPTER III

METHODOLOGY

3.1 Wireline log data interpretation

In this study gamma ray (GR), spontaneous potential (SP) and resistivity logs data of Mae-Soon oil field were gathered from 33 boreholes and were interpreted. These wireline logs data were provided by the Exploration and Production Division of the Northern Petroleum Development Center. These log data were used to identify rock type and rock properties within boreholes, e.g. porosity and permeability. Borehole names and location used in this study are listed in Table 3.1 and Figure 3.1.

3.1.1 Gamma ray (GR) log

The GR log records the radioactivity of the formation along the borehole. The GR reading tends to increase in proportion to the amount of clay present in sediment, which tends to increase with decreasing particle size. Therefore, the GR log can be used as a grain size profile. Sand line (lowest GR) and shale base line (highest GR) values can be calibrated to particle size. Pure coals have low GR response while shaly coals have a GR value which depends on the shale content. High GR values often correspond to source rock interval rich in organic matters, but such intervals do not always have a high GR value. The contrast between pure coals and organic shales is remarkable, and often seen in cyclic deltaic sequences, where a low GR coal is overlain by a high GR, organic rich shale. GR peaks in shale sequences representing condensed sections or maximum flooding surface (MFS). Quartzite shows

no radioactivity and sandstone usually shows low GR values (Jankaew, 2002). In this study GR log data had been used to separate shale bed from sandstone bed since it has a great amount of gamma ray compared with sandstone.

Table 3.1 Borehole name and well location of 33 boreholes which were used in the study.

Borehole	UTM X	UTM Y
FA-MS-08-12	516070.00	2193810.00
FA-MS-08-18	516688.00	2192832.00
FA-MS-27-46	517950.00	2193500.00
FA-MS-28-47	517070.00	2193950.00
FA-MS-28-48	517508.00	2193800.00
FA-MS-28-49	516630.00	2193400.00
FA-MS-28-50	517350.00	2192550.00
FA-MS-30-54	517581.00	2194001.00
FA-MS-32-56	516684.00	2193528.00
FA-MS-33-58	517082.00	2193707.00
FA-MS-34-59	516916.00	2193868.00
FA-MS-34-60	516680.00	2193290.00
FA-MS-34-61	517218.00	2194035.00
FA-MS-35-62	516894.00	2194060.00
FA-MS-35-64	517401.00	2193902.00
FA-MS-36-65	517340.00	2193616.00
FA-MS-36-66	517056.00	2193104.00

Borehole	UTM X	UTM Y
FA-MS-36-67	516554.00	2193248.00
FA-MS-40-69	517288.00	2192918.00
FA-MS-46-70	516665.44	2193697.04
FA-MS-47-71	516961.88	2193369.45
FA-MS-48-73	516675.00	2193061.00
FA-MS-48-75	517425.75	2193211.93
FA-MS-49-76	517125.00	2193595.00
FA-MS-49-77	516998.18	2193643.75
FA-MS-50-78	517214.00	2192821.00
FA-MS-51-79	516938.00	2192821.00
FA-MS-51-80	517044.00	2192942.00
FA-MS-53-83	517236.00	2193419.00
FA-MS-54-84	516835.00	2193268.00
FA-MS-54-85	517255.00	2193321.00
FA-MS-54-86	516957.00	2192967.00
FA-MS-55-87	517062.00	2193353.00

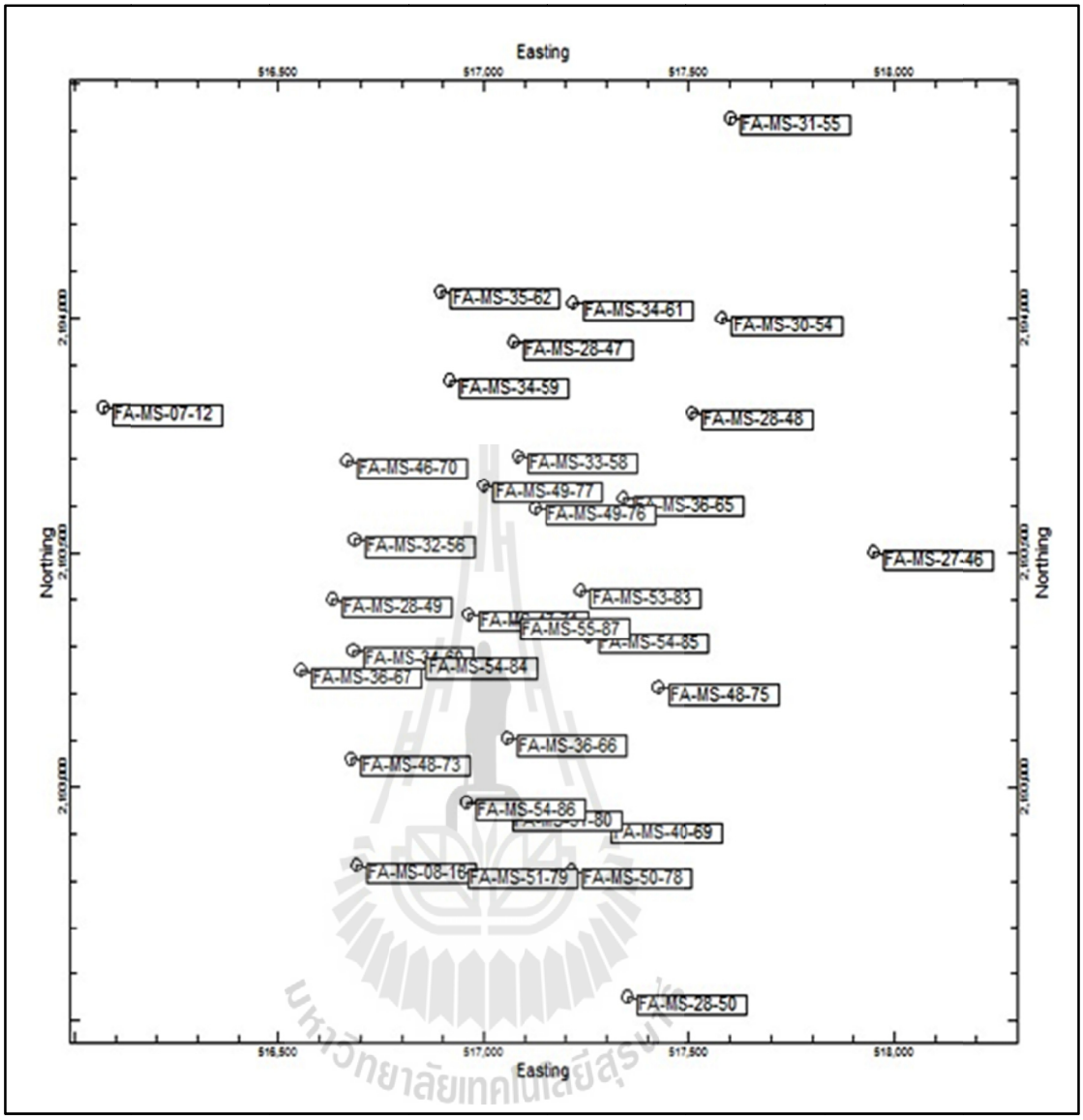

Figure 3.1 Location map of the 33 boreholes which were used in this study.

3.1.2 Spontaneous potential (SP) log

SP log measures the natural electric potential of formation. It is measured in millivolts on relative scale only because the absolute value of the potential depends not only on the properties of the rock and interstitial fluid, but also on the properties of the drilling mud. The SP log is used to detect bed boundaries, identify permeable zones, calculate formation water resistivity, and determine the volume of shale (shaliness) in permeable beds. The SP response is relatively constant in shaly sections and it is used to define a "shale line". Zones of permeable bed containing interstitial fluid with a salinity contrast to drilling mud are indicated by deflections from shale line. The SP log will be a good lithological indicator if it is calibrated against cores and cuttings (Chinabutr, 1987). Lithological interpretation of SP logs shape is similar to those of GR logs, i.e. changes in SP log response are in the same direction as GR logs. Thus, SP and GR logs are substituted for one another in the absence of the other in interpreting lithology.

3.1.3 Resistivity log

Resistivity logs respond to two features involving change in texture and change in composition. Compositional changes include changes in organic matter content and amount of silt. Facies and facies change can be followed on the resistivity logs. A resistivity log can register changes in quartzose (sand) - shale mixtures where an increase in resistivity corresponds to an increase in the silt (quartz) content.

Textural variation such as fine lamination of organic rich shale causes distinctive, low resistivity. Resistivity of rock is closely related to texture, e.g. when porosity decreases resistivity increases. High resistivity values may indicate a porous, hydrocarbon-bearing formation. Hydrocarbons have very high resistivity contrast with

aqueous fluids, which have high conductivities. There are no characteristic resistivity limits for shale or limestone or sandstone. The values depend on many variations, e.g. compaction, composition and fluid content. High resistivity will also be associated with tight limestone and dolomite (Jankaew, 2002).

To identify rock type in this study gamma ray, spontaneous potential, and resistivity logs data were interpreted according to sandstone type classification guideline of DED (Table 3.2) together with the mud logging data of 33 boreholes which were drilled in Mae-Soon oil field and then sandstones of each well could be classified into 19 layers (Table 3.3), respectively.

Table 3.2 Sandstone type classification guideline based on resistivity data and mud logging data (modified after DED).

Sandstone type	Depth (feet)	Long resistivity (ohm-meter)	Short resistivity (ohm-meter)	Ratio (%)
very fine Lithic Greywacke	1,400-2,600	40	12	0.30
fine Lithic Greywacke		94	31	0.33
Intermediate Lithic Greywacke		110	40	0.36
Coarse Lithic Greywacke		140	54	0.39
very fine Quartz Wacke	2,600-3,500	20	8.3	0.42
fine Quartz Wacke		71	32	0.45
Intermediate Quartz Wacke		124	60	0.48

Table 3.3 Total thickness of 19 sand layers of 33 boreholes drilled in Mae-Soon oil field.

Sandstone layer	Range (feet)	Total Thickness (feet)	Mean (feet)	Max (feet)	Min (feet)
Layer 1	1295-1730	435	20	60	5
Layer 2	1450-1844	395	18	64	5
Layer 3	1540-1992	452	14	28	5
Layer 4	1574-2028	454	16	70	5
Layer 5	1642-2085	443	21	56	5
Layer 6	1777-2140	363	16	48	4
Layer 7	1868-2260	392	20	68	6
Layer 8	1972-2340	368	17	41	4
Layer 9	2014-2430	458	19	72	4
Layer 10	2124-2530	406	20	58	5
Layer 11	2150-2636	486	16	52	5
Layer 12	2248-2688	440	17	58	5
Layer 13	2322-2720	398	15	38	5
Layer 14	2410-2800	390	17	44	7
Layer 15	2456-2879	423	14	36	4
Layer 16	2534-2970	436	16	40	4
Layer 17	2628-3110	482	15	34	5
Layer 18	2704-3312	608	15	32	5
Layer 19	2815-3434	619	17	32	5

3.2 Porosity and permeability

3.2.1 Porosity

Porosity is the ratio between the volume of all spaces to the total volume of the rock mass and porosity indicates the volume in the storage of liquids or gases in the rock (Selley, 1976). Porosity depends on sorting and grain shape (Mayer-Gurr, 1976). Porosity has two types which are 1) absolute (total porosity) as a percentage of the gap in the rocks and 2) effective porosity as a percent of spaces are connected (Pettijohn, Potter, and Siever, 1973 and Pettijohn, 1975). Dickker (1985) determined by the quality of the porosity of sandstone in term of its capacity retention based on porosity percent as depicted in Table 3.4.

Table 3.4 The quality of sandstone based on permeability (after Dickker, 1985).

Porosity (percent)	Capacity retention
<10	poor
10-15	fair
15-25	good (mostly the oil bearing formations)
>25	very good (but a little)

3.2.2 Permeability

Permeability is the ability to allow the flow of liquid or gas through a gap in the rocks (Selley, 1976). Properties of the rock affects the permeability are viscosity, pressure gradient, capillary force, throats, tortuosity of space, geometry of pores, the effective porosity of the stone, grain size, cementation, orientation, packing of framework grains, sorting and bedding. Permeability changes in the vertically

upward direction and down is measured in Darcy. Pettijohn, Potter, and Siever (1973) indicates that permeability of the sandstone and siltstone (with small effective porosity) would be lower when grain size decreases. Surface area increases should result in obstruction of the flow of the fluid. Development of the interface surface area and porosity reduction sometimes cause the permeability to deteriorate. Muskat (1949) found that the permeability of the sandstone in the range of 5-5,000 milliDarcy. Dickker (1985) classified sandstone quality in term of its storage capacity based on permeability as depicted in Table 3.5.

Table 3.5 The quality of sandstone based on porosity (after Dickker, 1985).

Permeability (milliDarcy)	Storage capacity
10	poor
100	fair to good
1000 (1 Darcy)	very good

3.3 Wireline log data calculation

Gamma ray (GR), resistivity, and spontaneous potential (SP) logs data were used to discriminate the subsurface lithology of 33 boreholes of Mae-Soon oil filed based on the following steps.

Step 1 Sand and shale layers identification

The SP log data were used to separate hydrocarbon zone which are sandstone layers (SP-) and shale break (SP+) from each other. Then the result from SP log interpretation were rechecked by using gamma ray log data to clearly identify shale layers.

Step 2 Potential hydrocarbon zones identification

Porosity determination

Resistivity log data were used to determine porosity of sand layers of each boreholes. In this step, Formation factor (F) which is the ratio between the clean formation resistivity of rock saturated with water 100% (Ro) and the electrical resistance of the water in all spaces of the rock layers (Rw) were calculated by the following equation (Erickson and Stephanie, 1998).

$$F = \frac{R_o}{R_w} \tag{3.1}$$

From equation, it indicates that the formation factor (F) is directly proportional to the formation resistivity (Ro). However, the formation factor (F) is inversely proportional to the porosity (ϕ) according to the Archie's equation as presented in equation 3.2.

$$F = \frac{0.62}{\phi^{2.15}} \quad \text{or} \quad F = \frac{0.81}{\phi^{2.0}} \tag{3.2}$$

Therefore, the porosity of each interesting layer can be calculated from this relationship.

Hydrocarbon saturation (Shc) determination

Hydrocarbon saturation (Shc) could be determined by known clean formation water saturation (Sw) (Jordan and Rachel, 2011). Therefore, in this study the water saturation of each interesting zone was calculated by Archie's equation (equation 3.3)

$$S_w = \sqrt[n]{\frac{FR_w}{R_t}} = \sqrt[n]{\frac{R_o}{R_t}} \quad (3.3)$$

Where n = saturation exponent (generally 2.0)

Rt = observed total resistivity

Thus, the hydrocarbon saturation (Shc) can be obtained from equation 3.4.

$$S_{hc} = 1 - S_w \quad (3.4)$$

Permeability determination

Permeability values used in this study were obtained and supported by the Exploration and Production Division of the Northern Petroleum Development Center which were measured from core samples directly in laboratory.

Then porosity, permeability and hydrocarbon saturation data were used to classify the quality of the studied sandstone layers based on Muskat (1949) and Dickker (1985) theory.

Step 3 Lithostratigraphic correlation from wireline log data

Lithostratigphy obtained from wireline logs interpretation in the first and second step of each well was then correlated to each other and made up the lithostratigraphic correlation in the north-south and west-east direction.

Step 4 Database make up

All acquired and obtained data from literature reviews, wireline log data interpretation and calculation, e.g. porosity, permeability, hydrocarbon saturation, sand layer thickness, were saved as in Microsoft Excel format and prepared for exporting to ArcGIS, Surfer8, and Rockwork14 program to generated maps.

The algorithm used by ArcGIS to calculate area is called the shoelace formula or Gauss's area formula. Thesis uses a normalized form of this formula to preserve numeric precision.

The algorithm calculates the area for each ring (part) in a polygon. If the ring is clockwise (outer ring) the area is positive, and if the ring is counterclockwise (inner ring) the value is negative.

A partial sum of a trapezoid's area is used where:

partialSums[0]	- Array of double
cPoints	- Number of points in the ring
points	- Array of point structure, the structure as X and Y as attributes
yOrigin	- Double equal to the Y value of the last point (cpoints-1)

The first trapezoid's area is:

partialSums[0] = (points[1].x - points[cPoints-1].x) * (points[0].y - yOrigin)

For each point starting at index 1:

for j = 1 to j < cPoints-1

partialSums[j] = (points[j+1].x - points[j-1].x) * (points[j].y - yOrigin)

If the ring contains nonlinear segments, such as Circular Arc, Elliptic Arc, and Bezier Curve, a correction of the area is applied for each trapezoid.

The final area of the ring is : SUM(PartialSums)/2

The final area of the polygon is : SUM(Area of each ring)

Here is an example with the following points (one square ring) zz:

X0 = 0; Y0 = 0

X1 = 0; Y1 = 10

X2 = 10; Y2 = 10

X3 = 10; Y3 = 0

X4 = 0; Y4 = 0

partialSums(0) = (X0 - X4) * (Y0 - Y4) = (0 - 0) * (0 - 0) = 0

partialSums(1) = (X2 - X0) * (Y1 - Y4) = (10 - 0) * (10 - 0) = 100

partialSums(2) = (X3 - X1) * (Y2 - Y4) = (10 - 0) * (10 - 0) = 100

partialSums(3) = (X4 - X2) * (Y3 - Y4) = (0 - 10) * (0 - 0) = 0

There is no correction to apply in this case because only lines are used:

sum (partialSums)/2 = 200/2 = 100

มหาวิทยาลัยเทคโนโลยีสุรนารี

CHAPTER IV

RESULTS

4.1 Wireline log data interpretation results

The interpretation of the data in order to see the relationship of the sandstone layer. Interpretation will use the wireline logging and mud logging in view of the relationship of sandstone that has similar properties. It is used to divide the properties of the sandstone layers of the DED (Table 3.2) is determined. The potential of the sandstone layers is used to divide the property. Dekker (Table 3.4 and 3.5) is determined.

4.1.1 Gamma ray, Spontaneous potential and Resistivity log interpretation

Based on sandstone type classification guideline of DED (Table 3.2) and the mud logging data of 33 boreholes which were drilled in Mae-Soon oil field (Table 3.3) gamma ray, spontaneous potential data (Appendix A) and resistivity logs data (Appendix B) were interpreted and results from each wireline log interpretation was presented in Appendix A and Appendix B respectively.

4.1.2 Sandstone layer thickness maps

Method of create map:

1. From define the scope study area that needs to be studied.
2. The data in the study that there is sufficient data and collect the necessary data to create maps for most.
3. The data acquisition, processing and analysis in the form of files.

4. Data files into the program to create the map.

Results from gamma, spontaneous potential, and resistivity log interpretation in the previous step together with mud log data of selected 33 boreholes were then used to generate isopach map of 19 sandstone layers which are potential oil reservoirs of Mae-Soon oil filed. Isopach map of identified 19 potential oil sandstone reservoirs are showed in Figures 4.1 to Figure 4.19, respectively.

Figure 4.1 revealed the distribution of thickness of sandstone layer 01 in the study area. This layer is found at depth between 1,295 and 1,730 feet and the thickest (60 feet) is found at well no. FA-MS-51-79 whereas the thinnest layer (5 feet) is found at well no. FA-MS-49-76. This sandstone layer is very fine sand Lithic Greywacke with an average grain size of 0.07 millimeters. It contains 3% cementing materialand 18% Matrix.

Figure 4.2 revealed the distribution of thickness of sandstone layer 02 in the study area. This layer is found at depth between 1,450 and 1,844 feet and the thickest (38 feet) is found at well no. FA-MS-36-68 whereas the thinnest layer (5 feet) is found at well no. FA-MS-35-63. This sandstone layer is very fine sand Lithic Greywacke with an average grain size of 0.09 millimeter. It contains 5% cementing material and 20% Matrix.

Figure 4.3 revealed the distribution of thickness of sandstone layer 03 in the study area. This layer is found at depth between 1,540 and 1,992 feet and the thickest (64 feet) is found at well no. FA-MS-54-85 whereas the thinnest layer (7 feet) is found at well no. FA-MS-28-48. This sandstone layer is fine sand Lithic Greywacke with an average grain size of 0.15 millimeter. It contains 3% cementing material and 18% Matrix.

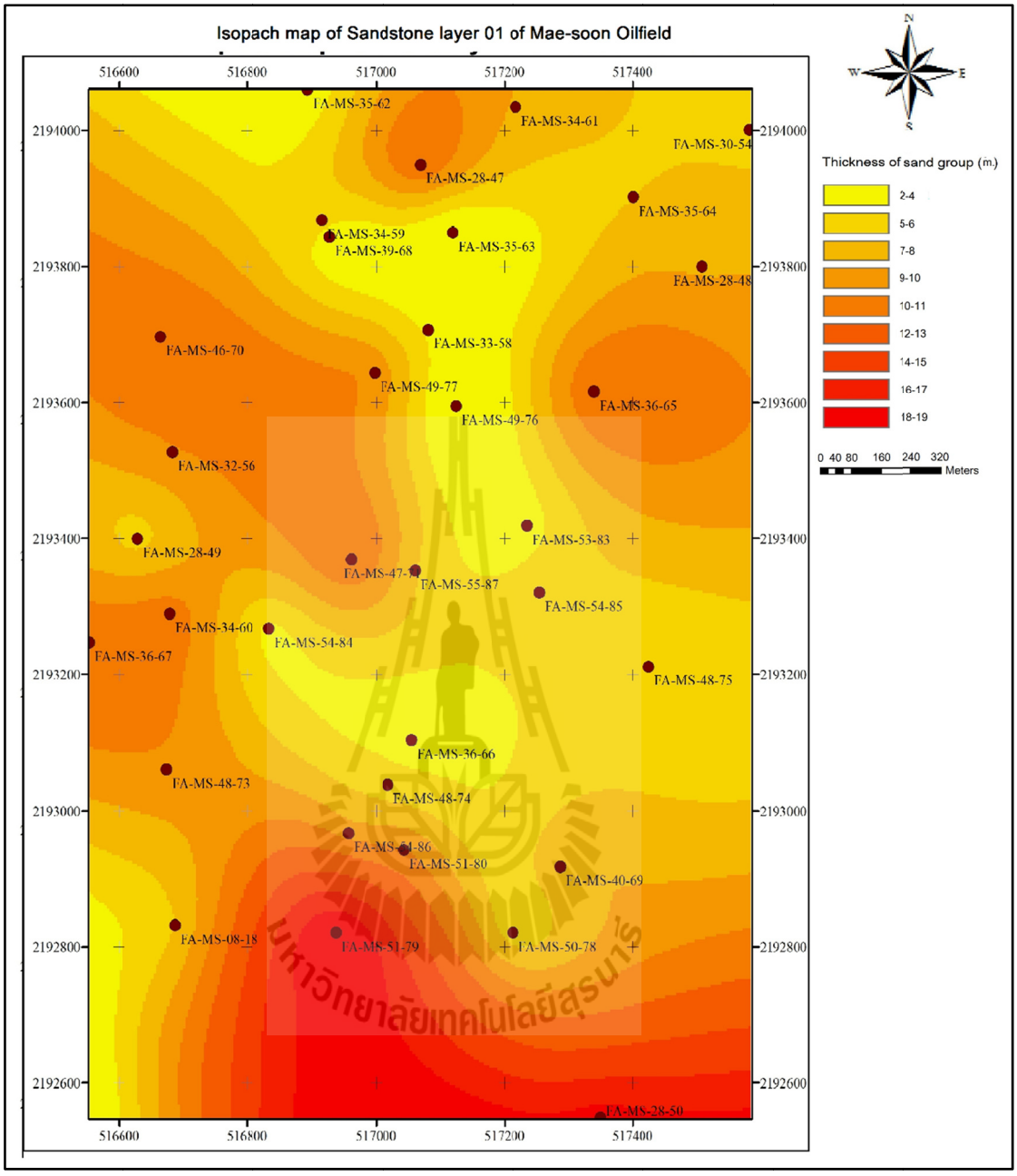

Figure 4.1 Isopach map of sandstone layer 01 of Mae-Soon oil field.

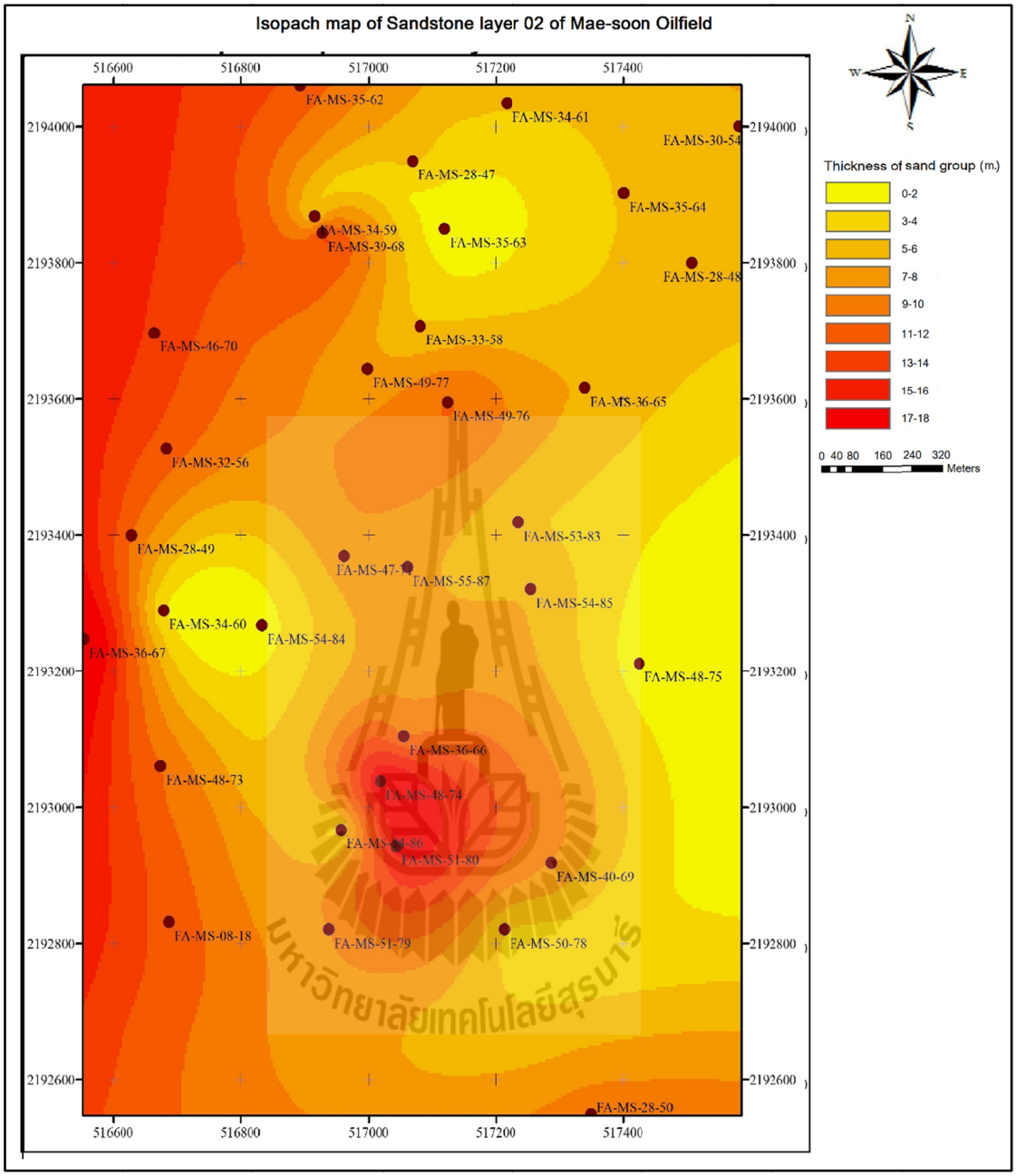

Figure 4.2 Isopach map of sandstone layer 02 of Mae-Soon oil field.

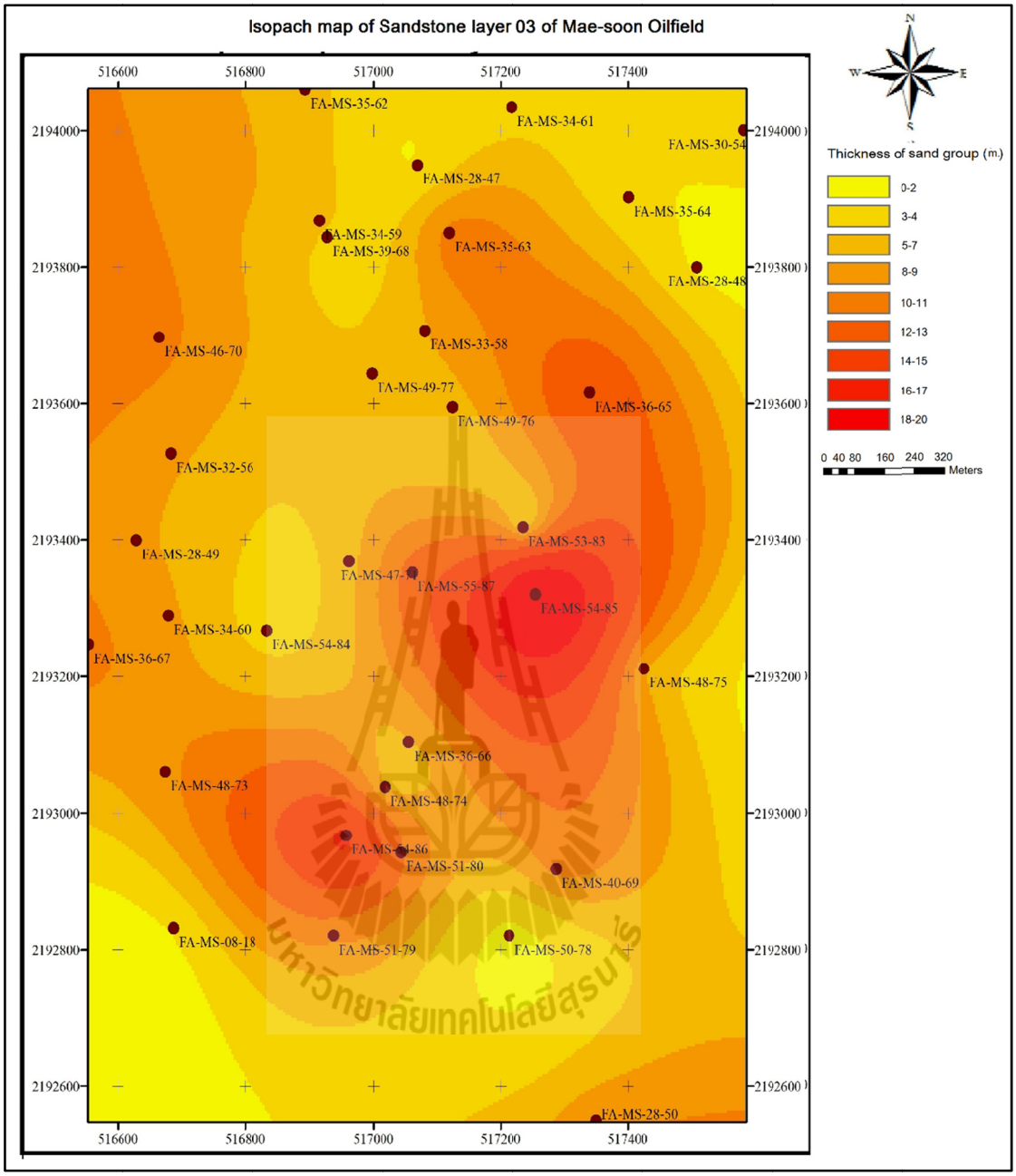

Figure 4.3 Isopach map of sandstone layer 03 of Mae-Soon oil field.

Figure 4.4 revealed the distribution of thickness of sandstone layer 04 in the study area. This layer is found at depth between 1,574 and 2,028 feet and the thickest (70 feet) is found at well no. FA-MS-51-79 whereas the thinnest layer (5 feet) is found at well no. FA-MS-28-48. This sandstone layer is medium sand Lithic Greywacke with an average grain size of 0.2 millimeter. It contains 2% cementing material and 23% Matrix.

Figure 4.5 revealed the distribution of thickness of sandstone layer 05 in the study area. This layer is found at depth between 1,642 and 2,085 feet and the thickest (56 feet) is found at well no. FA-MS-49-76 and FA-MS-48-74 whereas the thinnest layer (5 feet) is found at well no. FA-MS-32-56. This sandstone layer is medium sand Lithic Greywacke with an average grain size of 0.2 millimeter. It contains 2% cementing material and 21% Matrix.

Figure 4.6 revealed the distribution of thickness of sandstone layer 06 in the study area. This layer is found at depth between 1,777 and 2,140 feet and the thickest (48 feet) is found at well no. FA-MS-48-73 whereas the thinnest layer (4 feet) is found at well no. FA-MS-48-75. This sandstone layer is medium sand Lithic Greywacke with an average grain size of 0.3 millimeter. It contains 3% cementing material and 25% Matrix.

Figure 4.7 revealed the distribution of thickness of sandstone layer 07 in the study area. This layer is found at depth between 1,868 and 2,260 feet and the thickest (58 feet) is found at well no. FA-MS-46-70 whereas the thinnest layer (6 feet) is found at well no. FA-MS-33-58. This sandstone layer is fine sand Lithic Greywacke with an average grain size of 0.17 millimeter. It contains 2% cementing material and 20% Matrix.

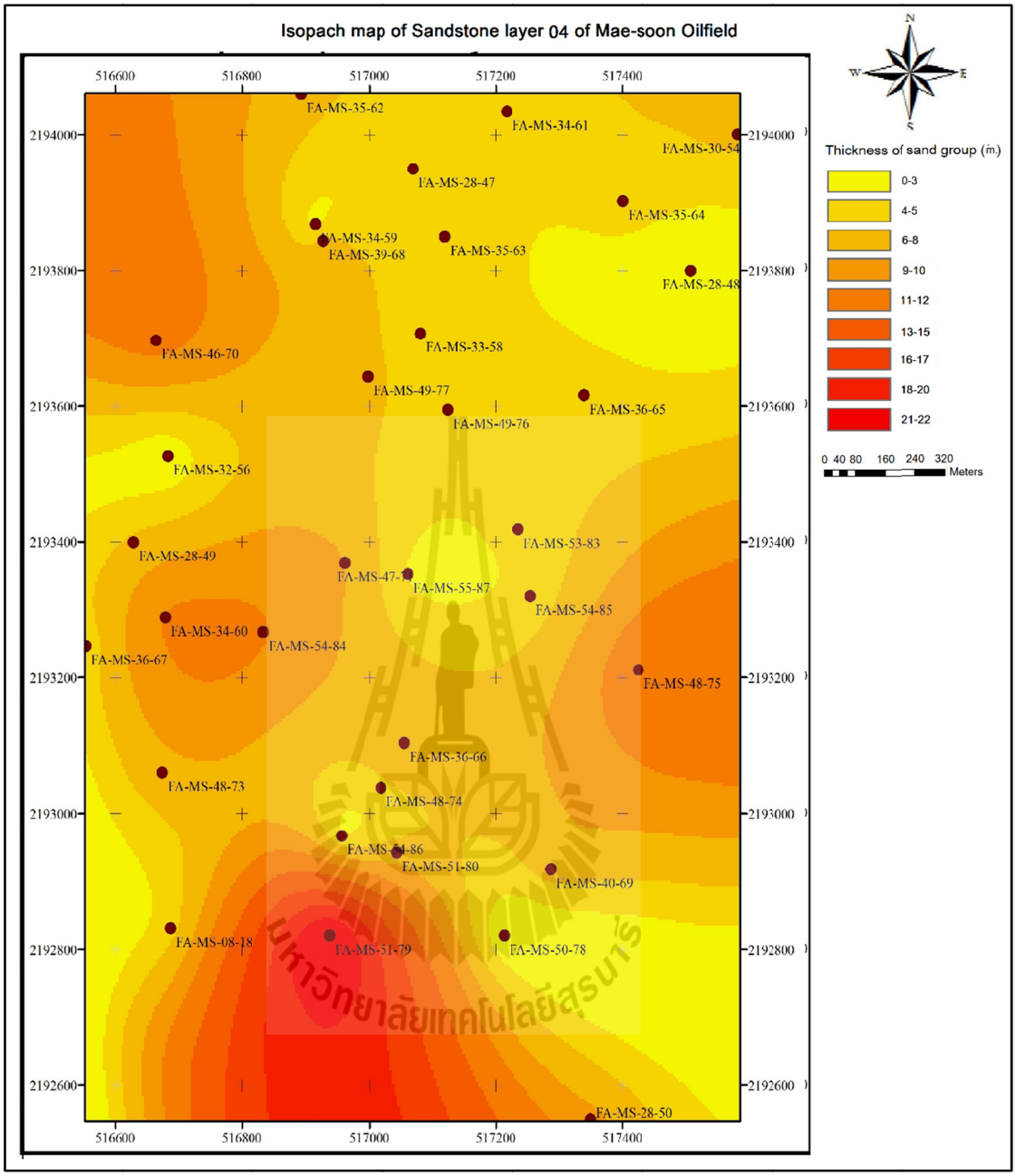

Figure 4.4 Isopach map of sandstone layer 04 of Mae-Soon oil field.

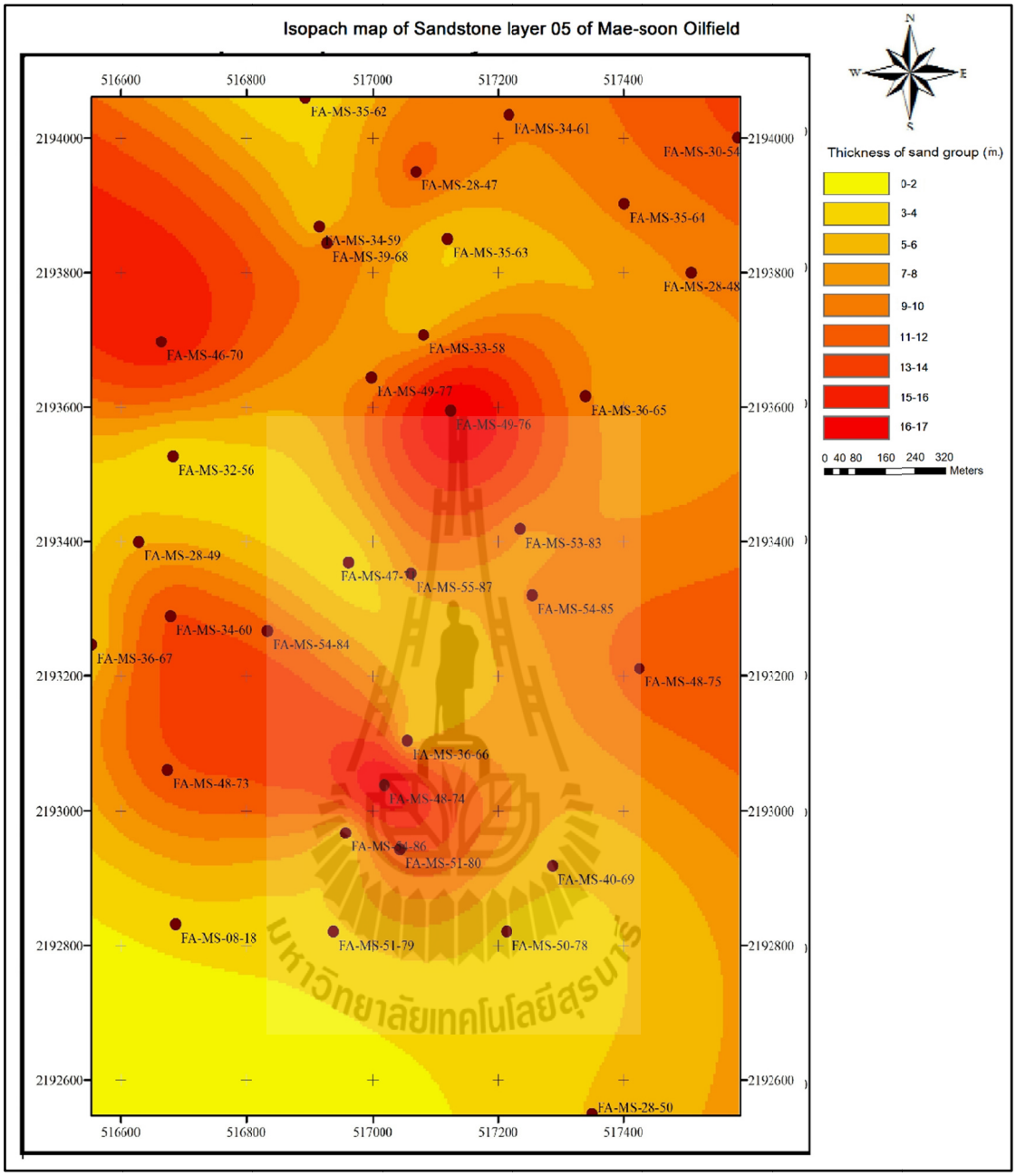

Figure 4.5 Isopach map of sandstone layer 05 of Mae-Soon oil field.

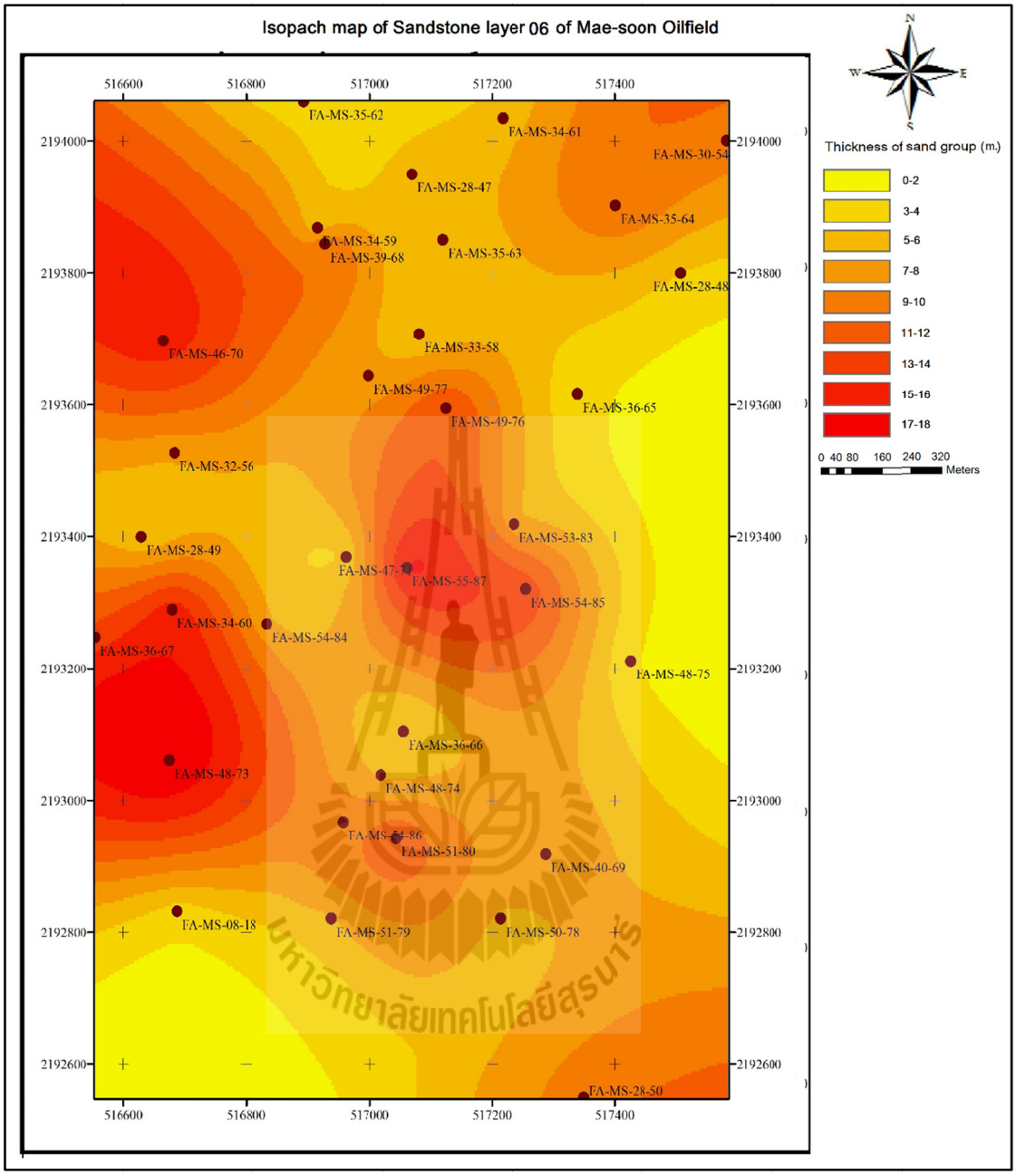

Figure 4.6 Isopach map of sandstone layer 06 of Mae-Soon oil field.

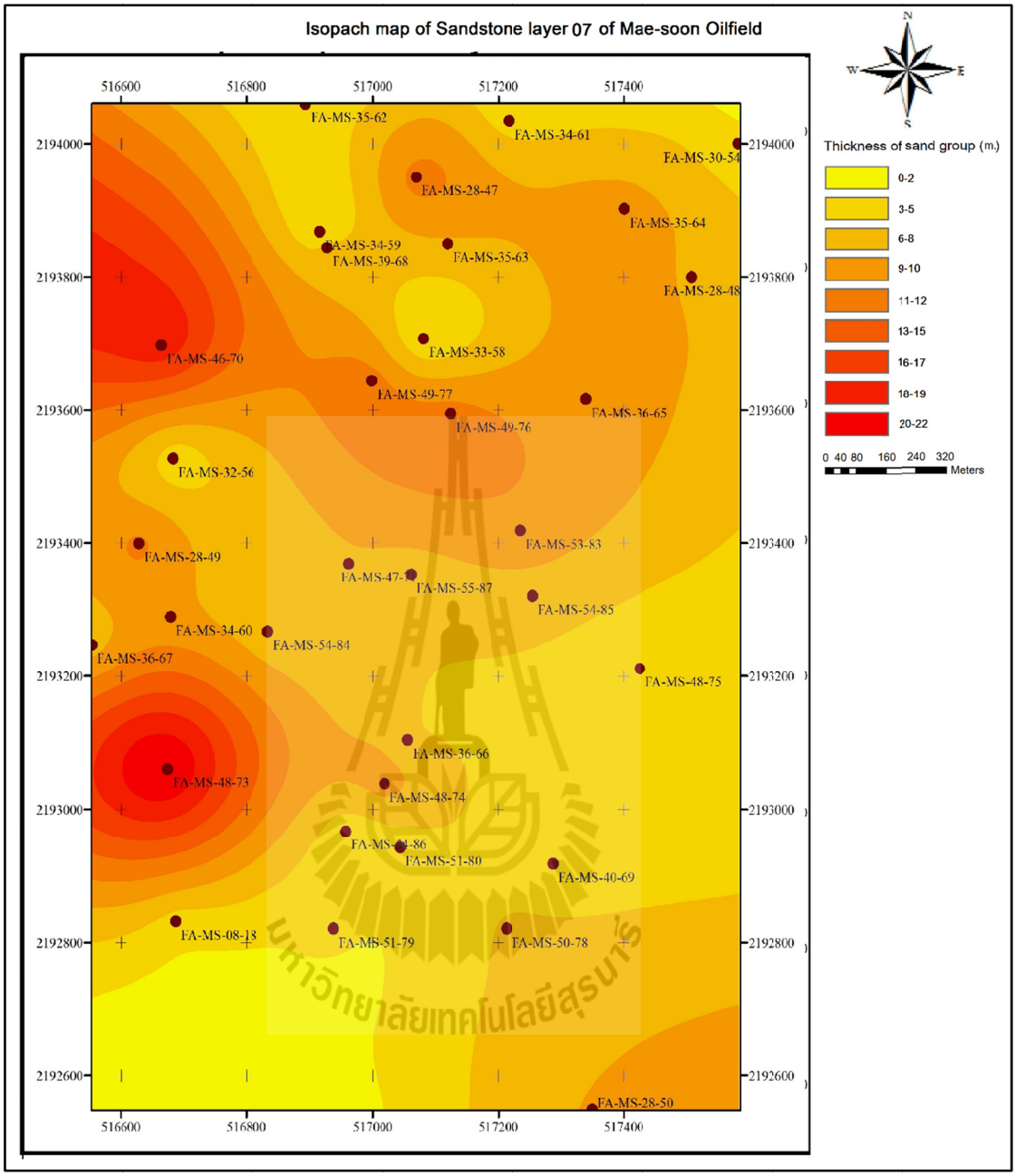

Figure 4.7 Isopach map of sandstone layer 07 of Mae-Soon oil field.

Figure 4.8 revealed the distribution of thickness of sandstone layer 08 in the study area. This layer is found at depth between 1,972 and 2,340 feet and the thickest (41 feet) is found at well no. FA-MS-28-47 whereas the thinnest layer (4 feet) is found at well no. FA-MS-35-64 and FA-MS-08-18. This sandstone layer is medium sand Lithic Greywacke with an average grain size of 0.2 millimeter. It contains 2% cementing material and 23% Matrix.

Figure 4.9 revealed the distribution of thickness of sandstone layer 09 in the study area. This layer is found at depth between 2,014 and 2,430 feet and the thickest (72 feet) is found at well no. FA-MS-46-70 whereas the thinnest layer (4 feet) is found at well no. FA-MS-28-48. This sandstone layer is medium sand Lithic Greywacke with an average grain size of 0.27 millimeter. It contains 3% cementing material and 25% Matrix.

Figure 4.10 revealed the distribution of thickness of sandstone layer 10 in the study area. This layer is found at depth between 2,124 and 2,530 feet and the thickest (58 feet) is found at well no. FA-MS-48-75 whereas the thinnest layer (5 feet) is found at well no. FA-MS-35-64. This sandstone layer is medium sand Lithic Greywacke with an average grain size of 0.35 millimeter. It contains 2% cementing material and 16% Matrix.

Figure 4.11 revealed the distribution of thickness of sandstone layer 11 in the study area. This layer is found at depth between 2,150 and 2,636 feet and the thickest (52 feet) is found at well no. FA-MS-46-70 whereas the thinnest layer (5 feet) is found at well no. FA-MS-28-48. This sandstone layer is coarse sand Lithic Greywacke with an average grain size of 0.6 millimeter. It contains 2% cementing material and 20% Matrix.

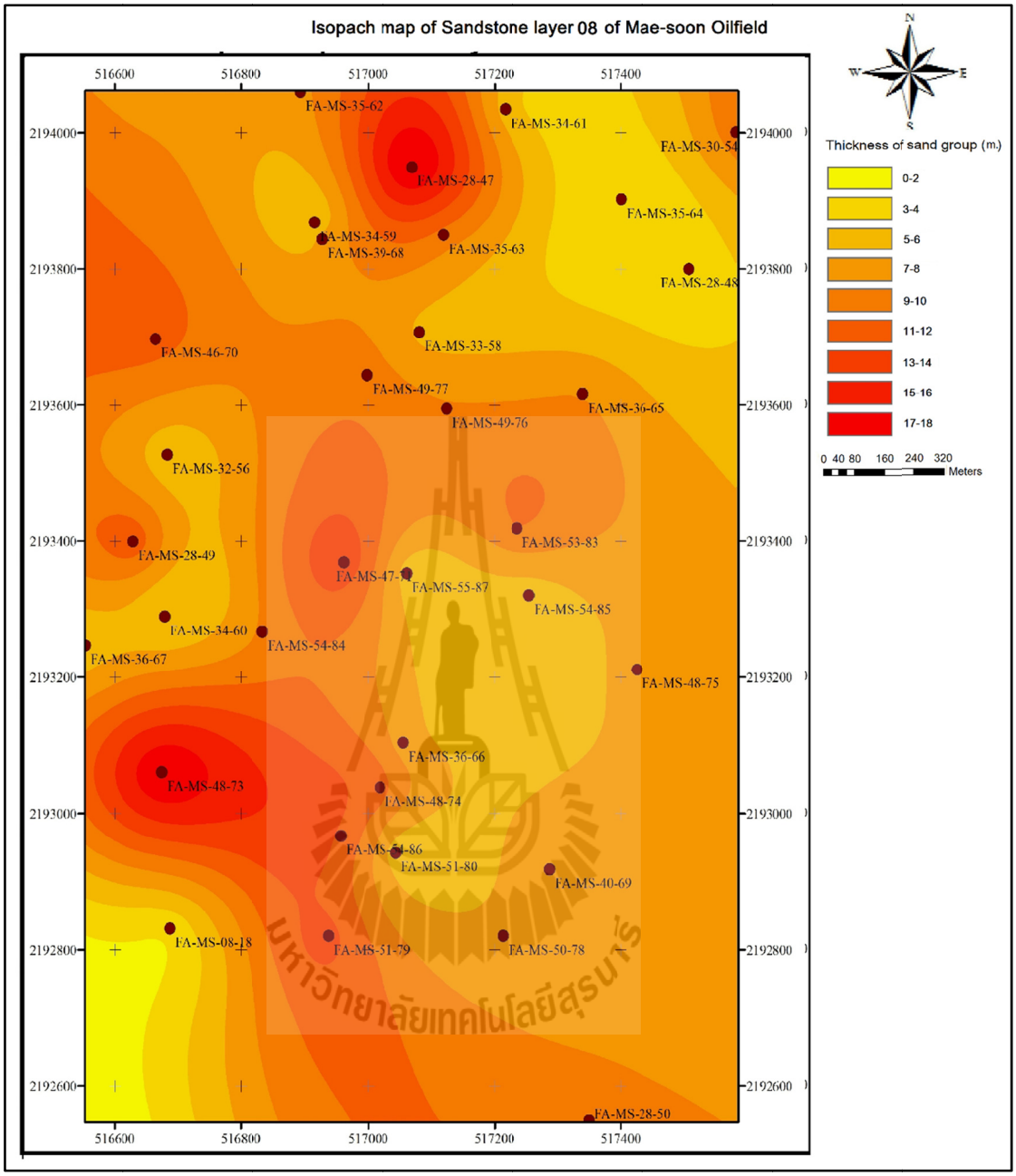

Figure 4.8 Isopach map of sandstone layer 08 of Mae-Soon oil field.

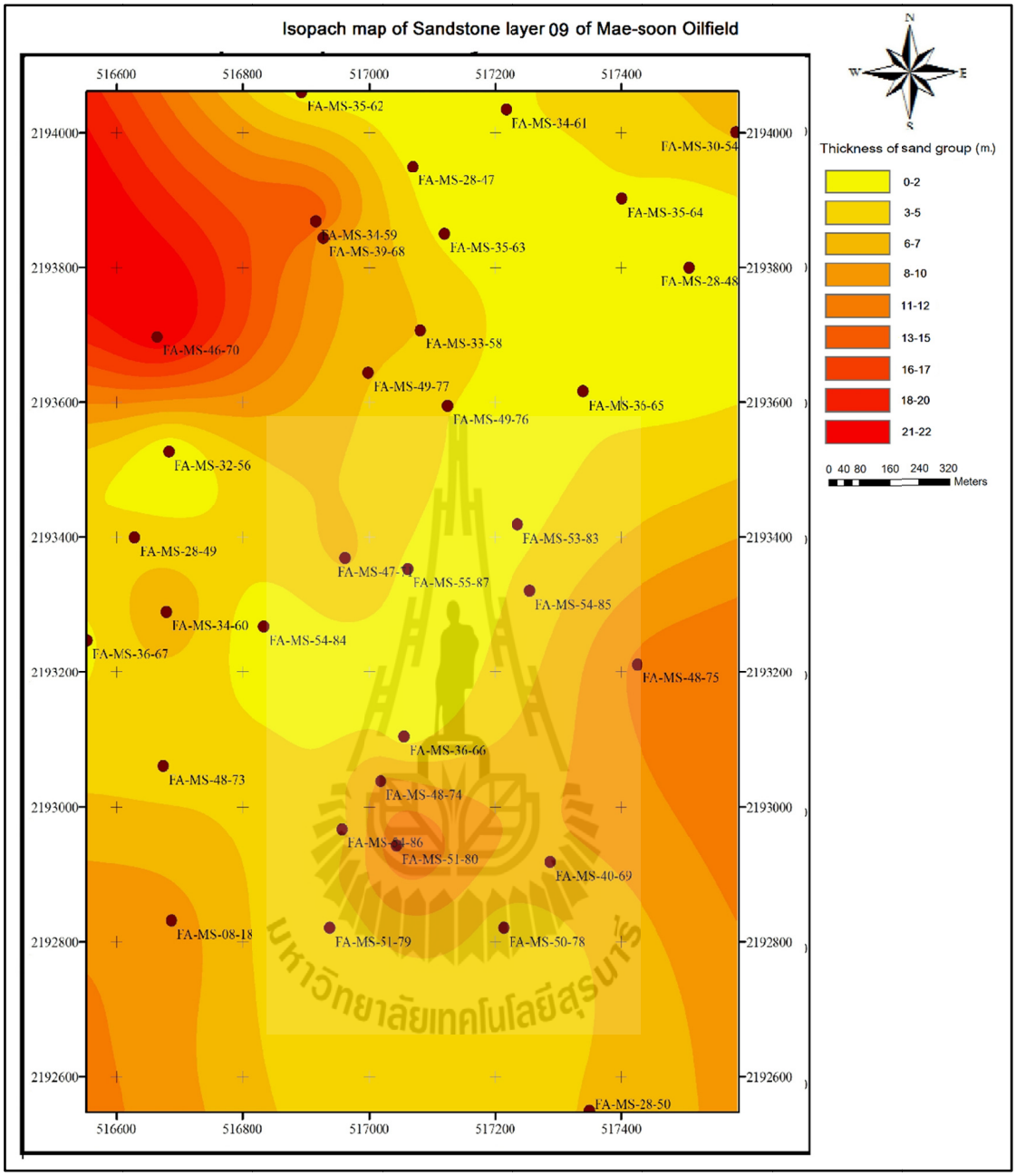

Figure 4.9 Isopach map of sandstone layer 09 of Mae-Soon oil field.

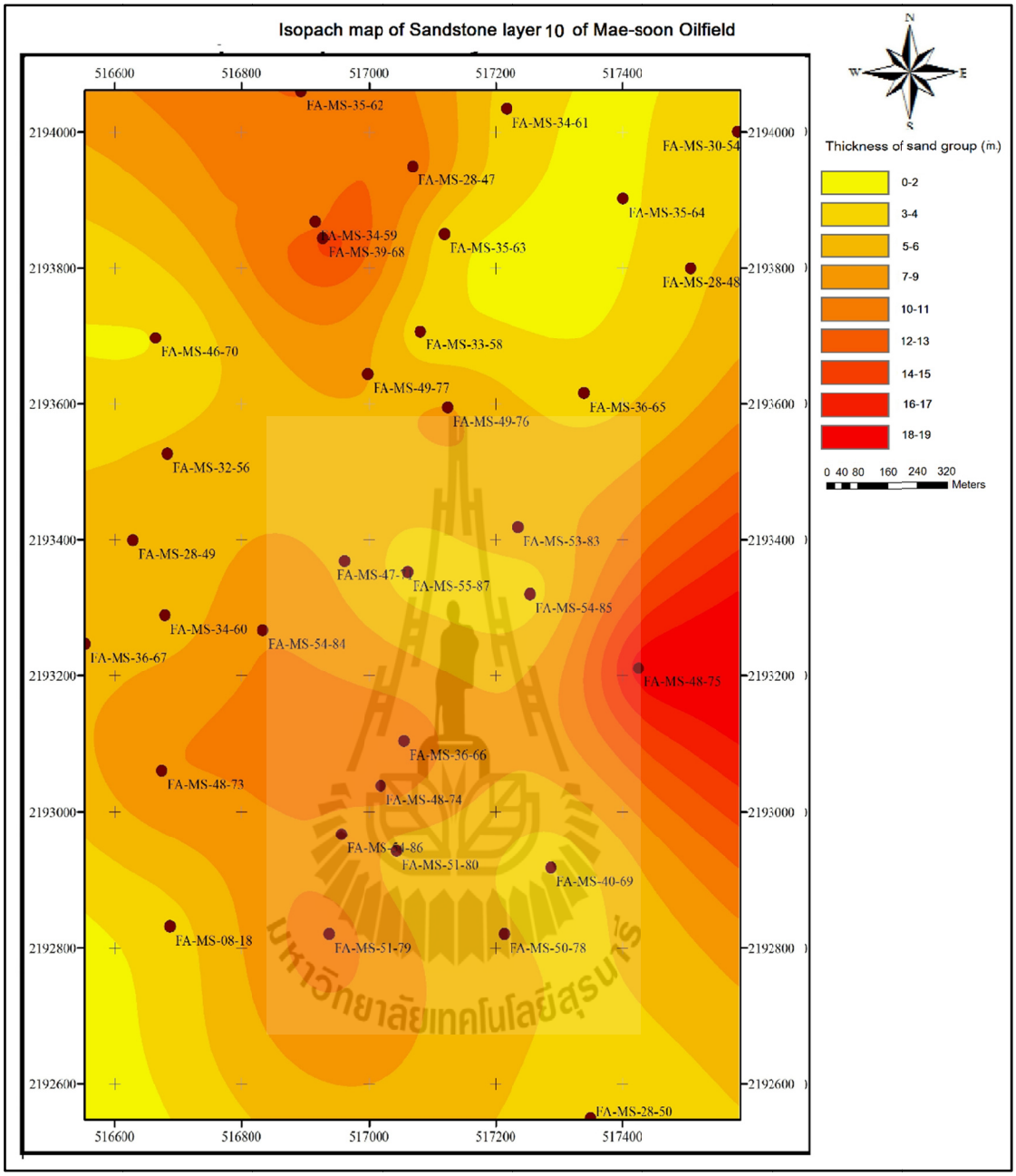

Figure 4.10 Isopach map of sandstone layer 10 of Mae-Soon oil field.

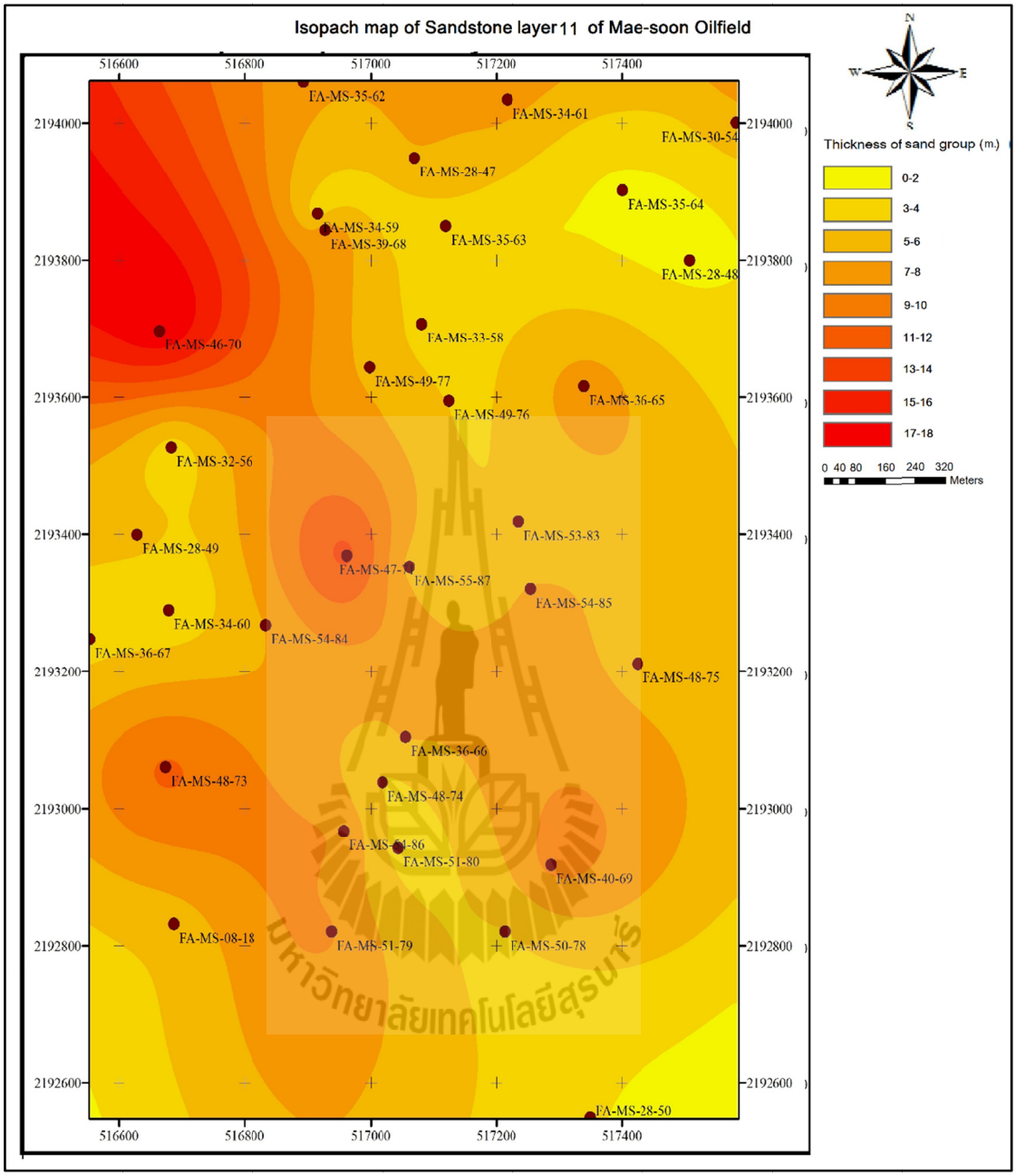

Figure 4.11 Isopach map of sandstone layer 11 of Mae-Soon oil field.

Figure 4.12 revealed the distribution of thickness of sandstone layer 12 in the study area. This layer is found at depth between 2,248 and 2,688 feet and the thickest (58 feet) is found at well no. FA-MS-46-70 whereas the thinnest layer (5 feet) is found at well no. FA-MS-34-61. This sandstone layer is coarse sand Lithic Greywacke with an average grain size of 0.8 millimeter. It contains 3% cementing material and 19% Matrix.

Figure 4.13 revealed the distribution of thickness of sandstone layer 13 in the study area. This layer is found at depth between 2,322 and 2,735 feet and the thickest (38 feet) is found at well no. FA-MS-39-68 whereas the thinnest layer (5 feet) is found at well no. FA-MS-34-61. This sandstone layer is very fine sand Quartz Greywacke with an average grain size of 0.07 millimeter. It contains 3% cementing material and 22% Matrix.

Figure 4.14 revealed the distribution of thickness of sandstone layer 14 in the study area. This layer is found at depth between 2,410 and 2,800 feet and the thickest (38 feet) is found at well no. FA-MS-39-68 whereas the thinnest layer (5 feet) is found at well no. FA-MS-34-61. This sandstone layer is very fine sand Quartz Greywacke with an average grain size of 0.09 millimeter. It contains 2% cementing material and 23% Matrix.

Figure 4.15 revealed the distribution of thickness of sandstone layer 15 in the study area. This layer is found at depth between 2,456 and 2,879 feet and the thickest (36 feet) is found at well no. FA-MS-39-68 whereas the thinnest layer (4 feet) is found at well no. FA-MS-28-50. This sandstone layer is very fine sand Quartz Greywacke with an average grain size of 0.125 millimeter. It contains 2% cementing material and 20% Matrix.

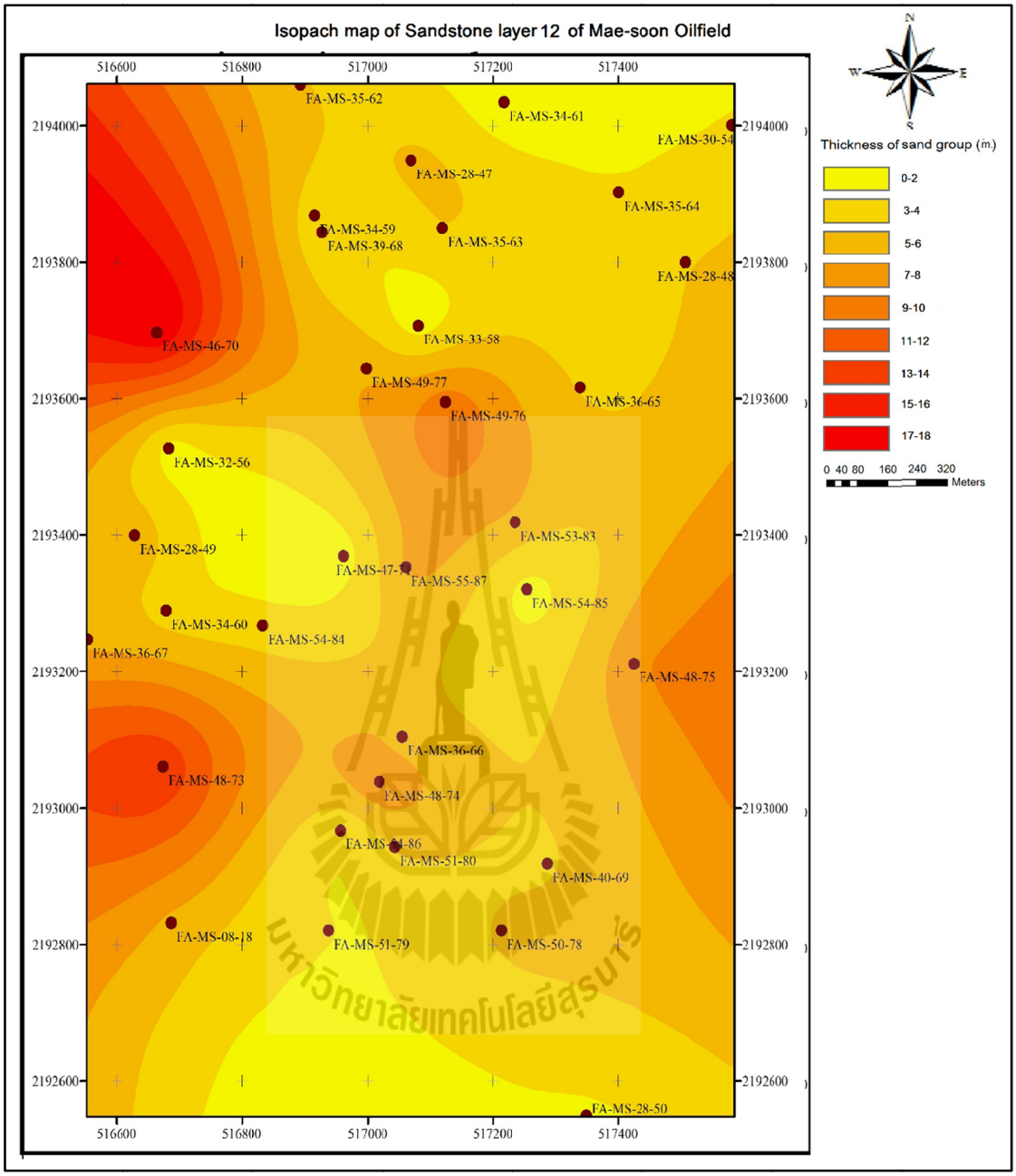

Figure 4.12 Isopach map of sandstone layer 12 of Mae-Soon oil field.

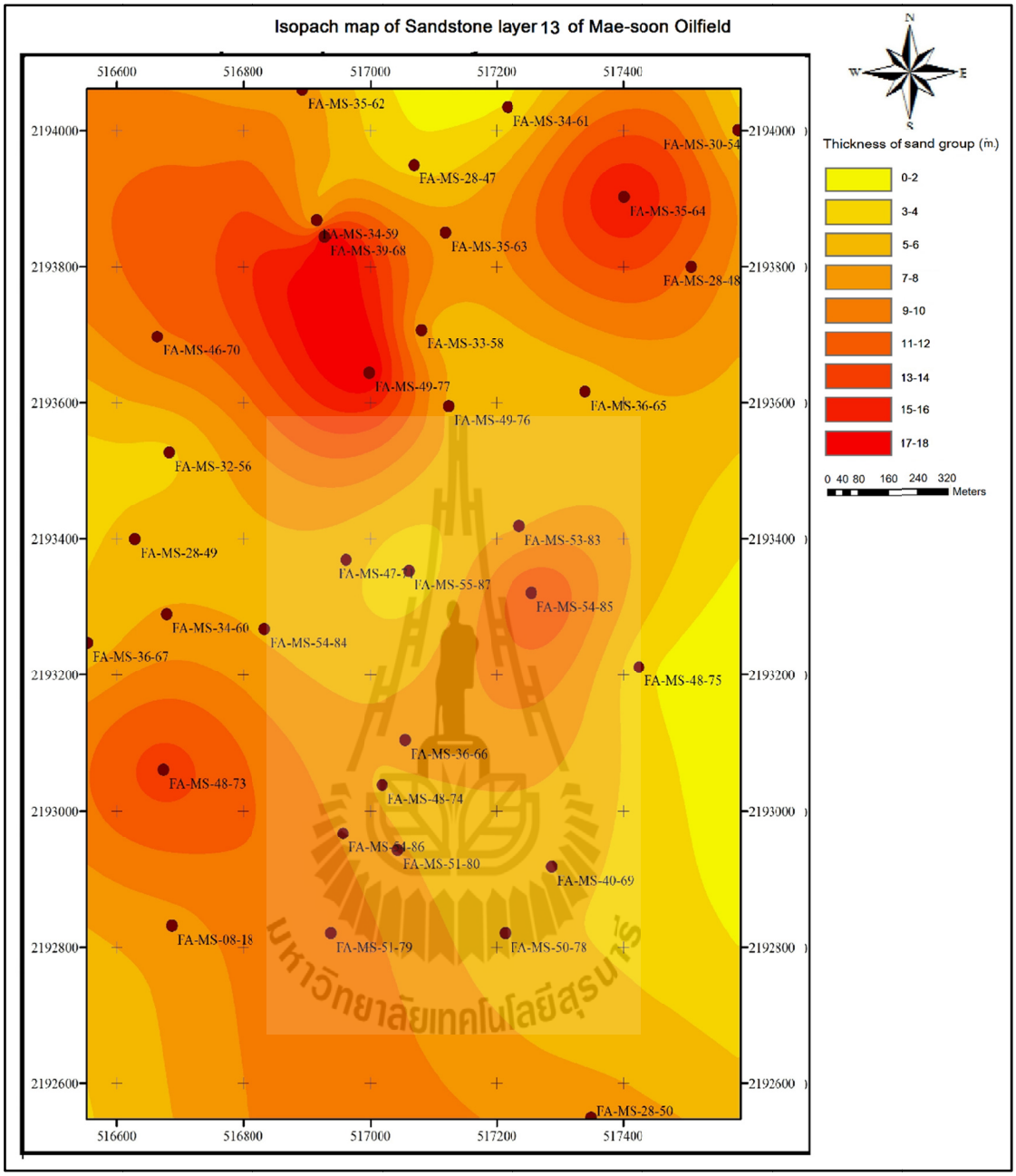

Figure 4.13 Isopach map of sandstone layer 13 of Mae-Soon oil field.

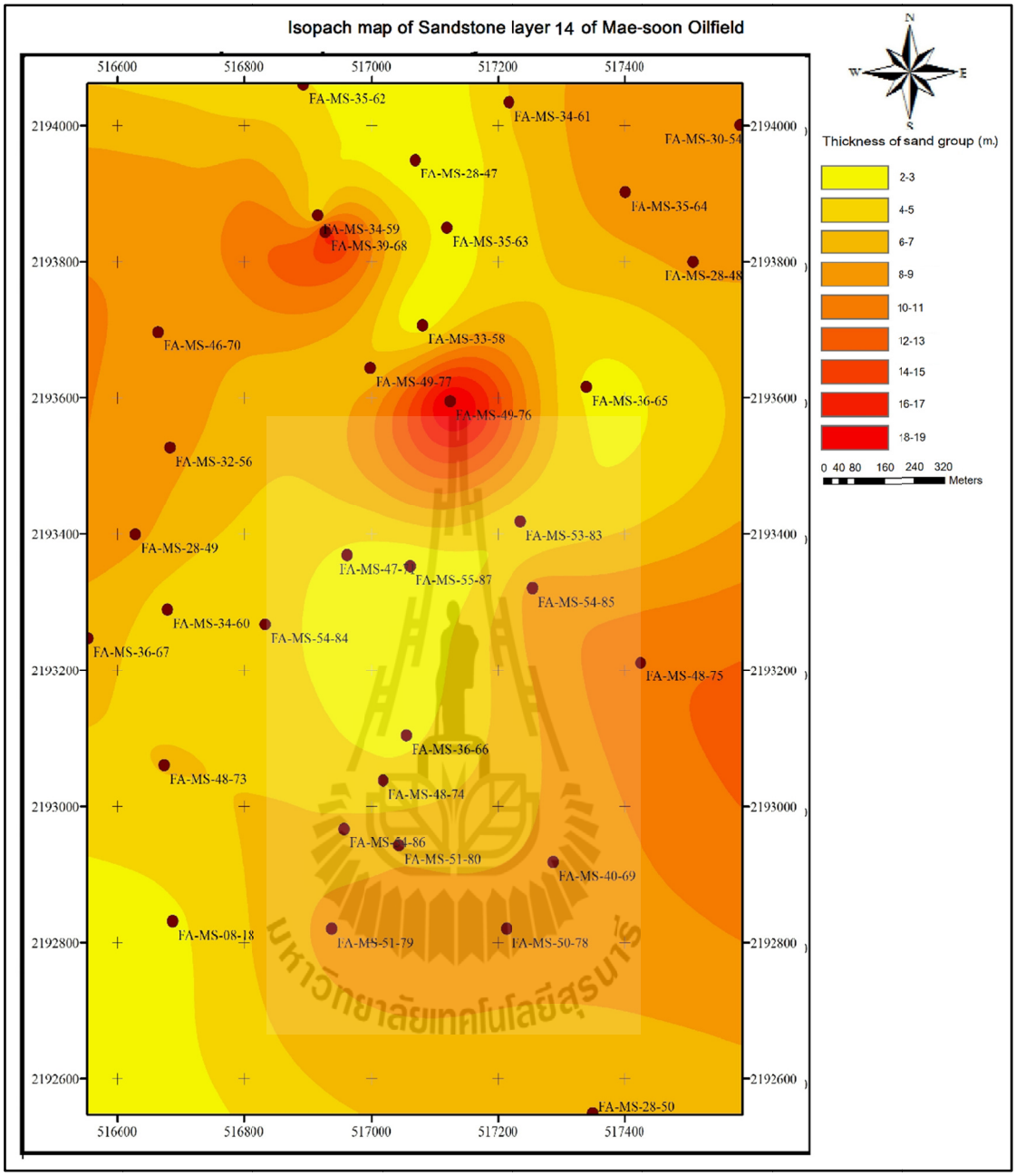

Figure 4.14 Isopach map of sandstone layer 14 of Mae-Soon oil field.

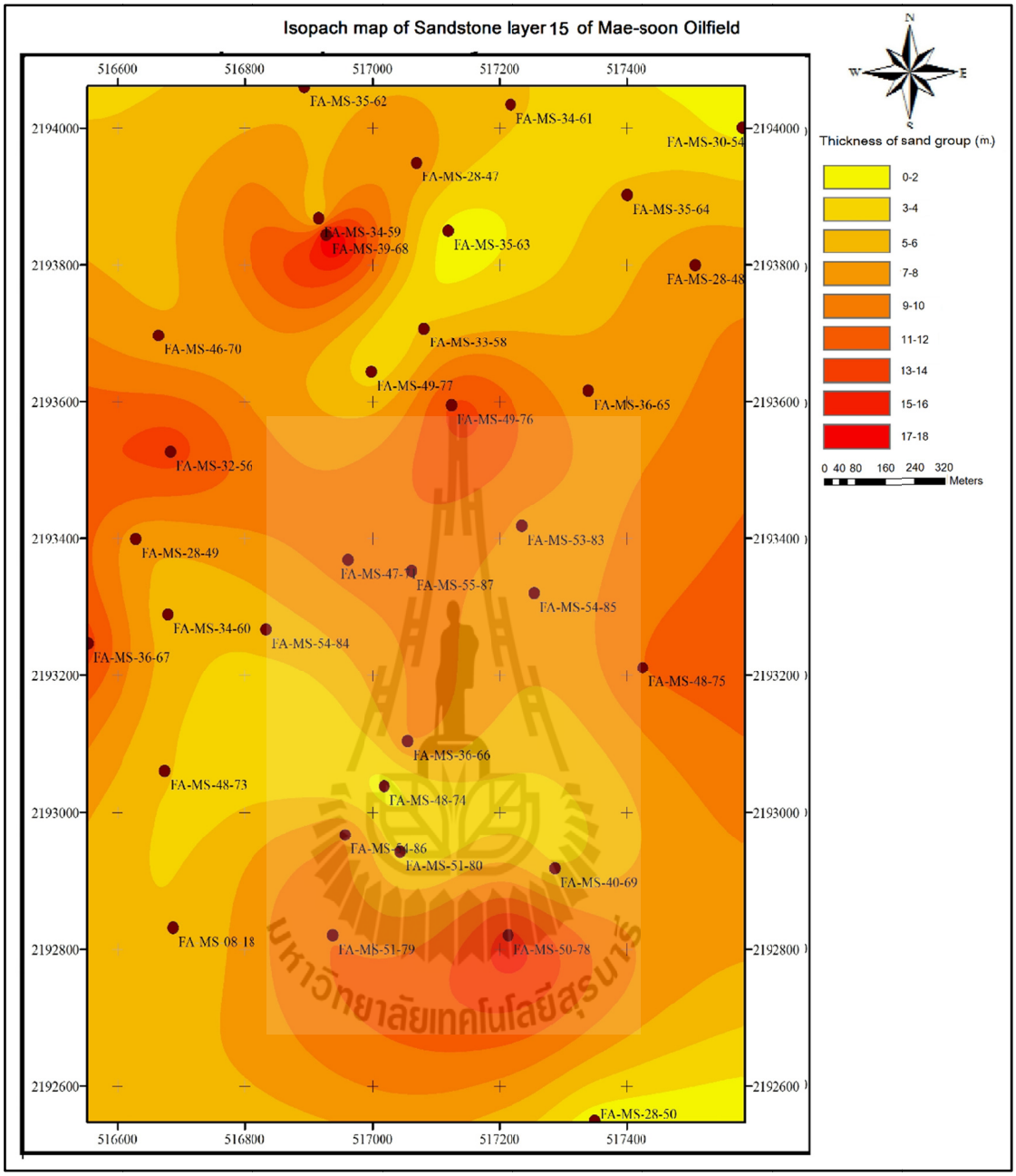

Figure 4.15 Isopach map of sandstone layer 15 of Mae-Soon oil field.

Figure 4.16 revealed the distribution of thickness of sandstone layer 16 in the study area. This layer is found at depth between 2,534 and 2,970 feet and the thickest (40 feet) is found at well no. FA-MS-40-69 whereas the thinnest layer (4 feet) is found at well no. FA-MS-51-80. This sandstone layer is fine sand Quartz Greywacke with an average grain size of 0.15 millimeter. It contains 3% cementing material and 22% Matrix.

Figure 4.17 revealed the distribution of thickness of sandstone layer 17 in the study area. This layer is found at depth between 2,628 and 3,110 feet and the thickest (34 feet) is found at well no. FA-MS-35-64 whereas the thinnest layer (5 feet) is found at well no. FA-MS-33-58. This sandstone layer is fine sand Quartz Greywacke with an average grain size of 0.17 millimeter. It contains 2% cementing material and 25% Matrix.

Figure 4.18 revealed the distribution of thickness of sandstone layer 18 in the study area. This layer is found at depth between 2,704 and 3,312 feet and the thickest (32 feet) is found at well no. FA-MS-48-73 whereas the thinnest layer (5 feet) is found at well no. FA-MS-28-47. This sandstone layer is medium sand Quartz Greywacke with an average grain size of 0.25 millimeter. It contains 4% cementing material and 21% Matrix.

Figure 4.19 revealed the distribution of thickness of sandstone layer 19 in the study area. This layer is found at depth between 2,815 and 3,434 feet and the thickest (32 feet) is found at well no. FA-MS-40-70 whereas the thinnest layer (5 feet) is found at well no. FA-MS-51-80. This sandstone layer is medium sand Quartz Greywacke with an average grain size of 0.4 millimeter. It contains 3% cementing material and 22% Matrix.

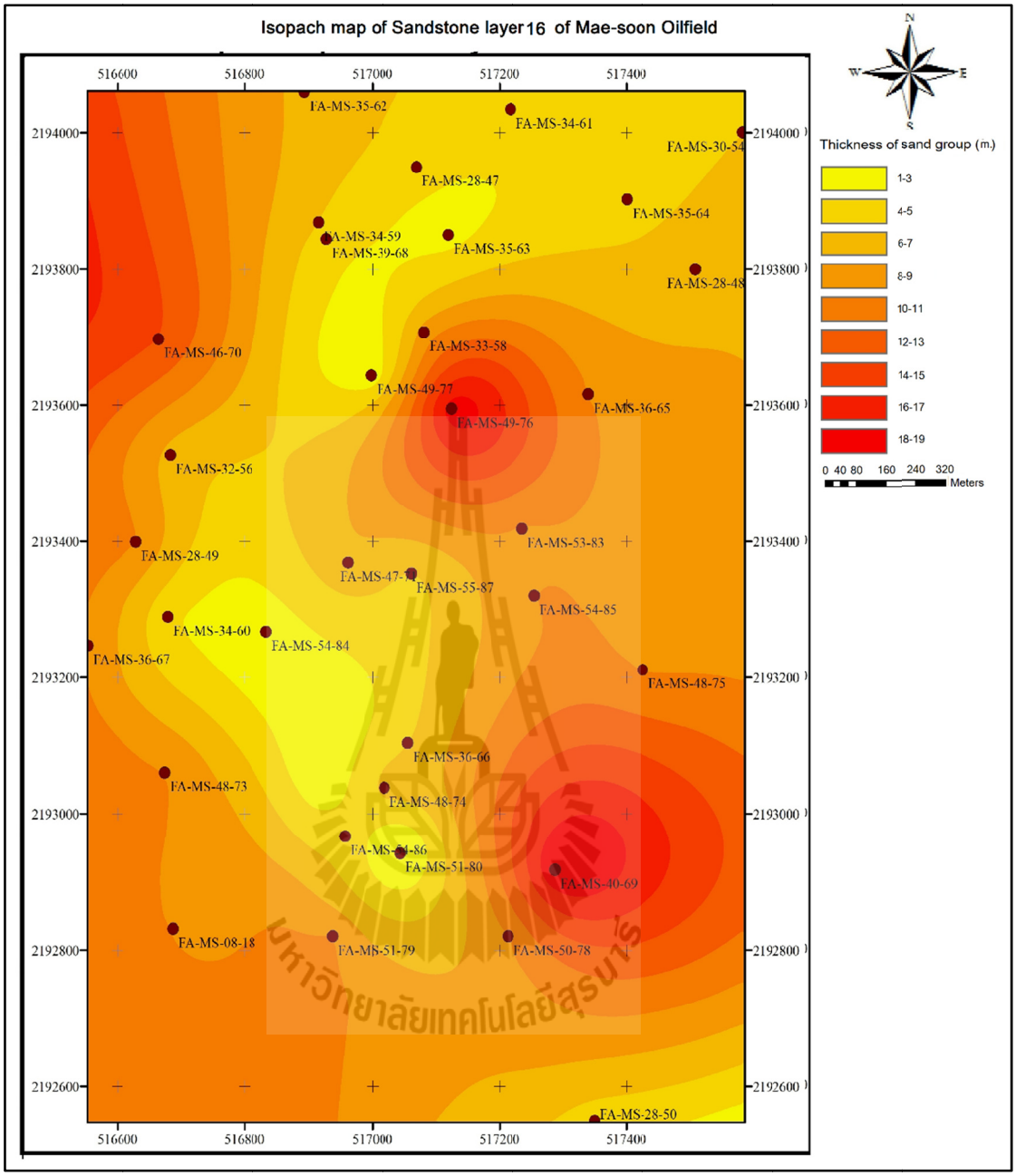

Figure 4.16 Isopach map of sandstone layer 16 of Mae-Soon oil field.

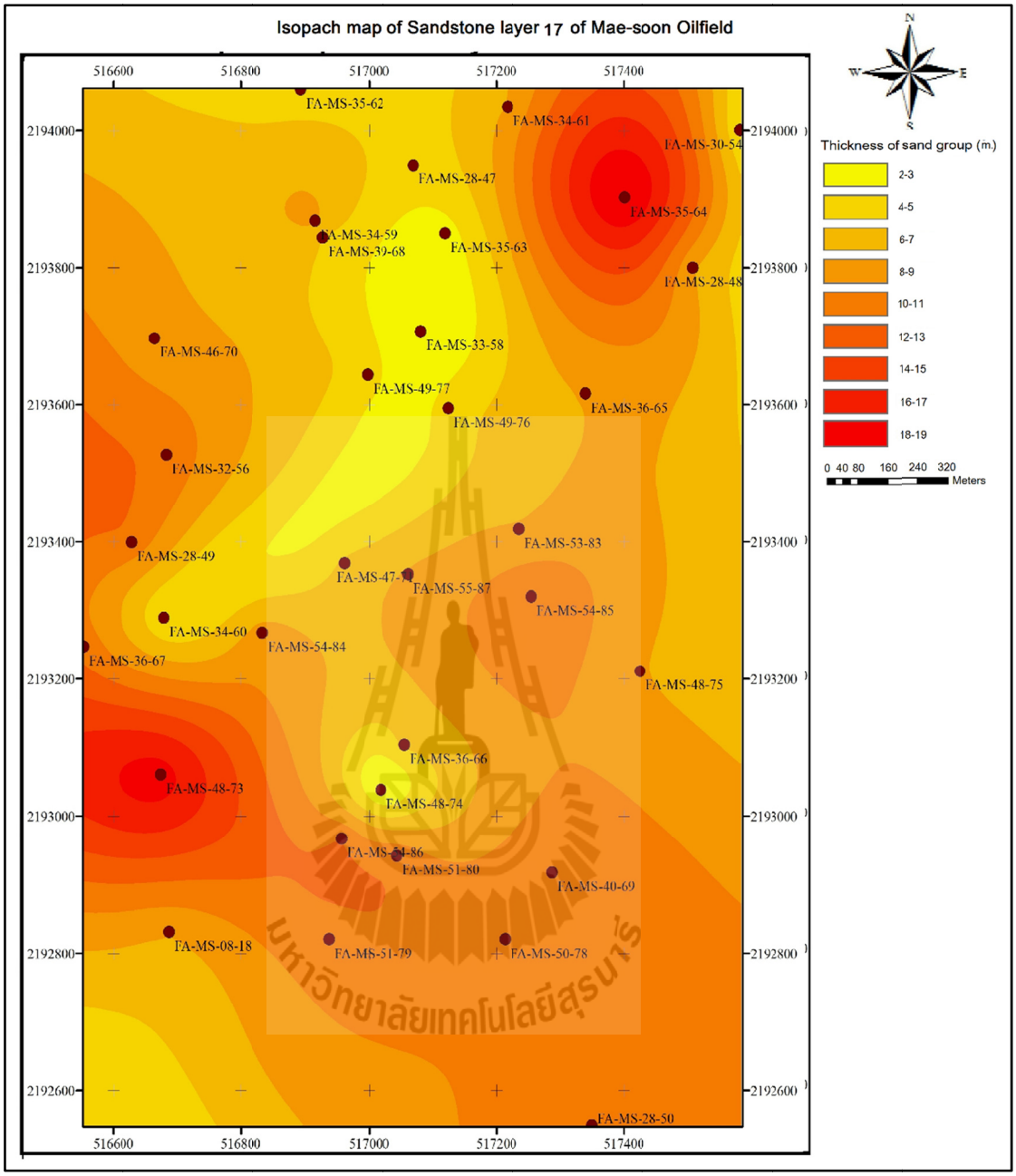

Figure 4.17 Isopach map of sandstone layer 17 of Mae-Soon oil field.

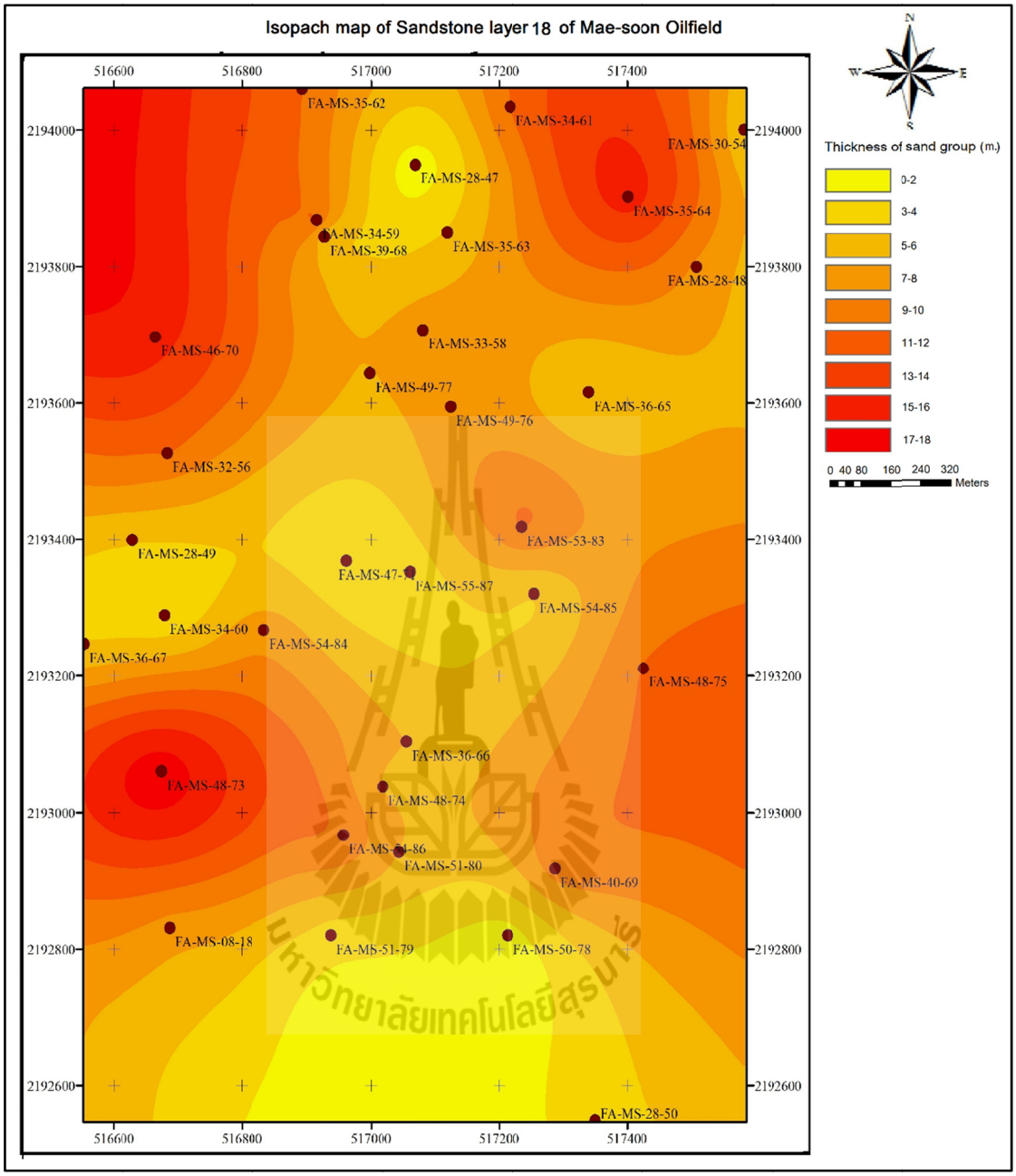

Figure 4.18 Isopach map of sandstone layer 18 of Mae-Soon oil field.

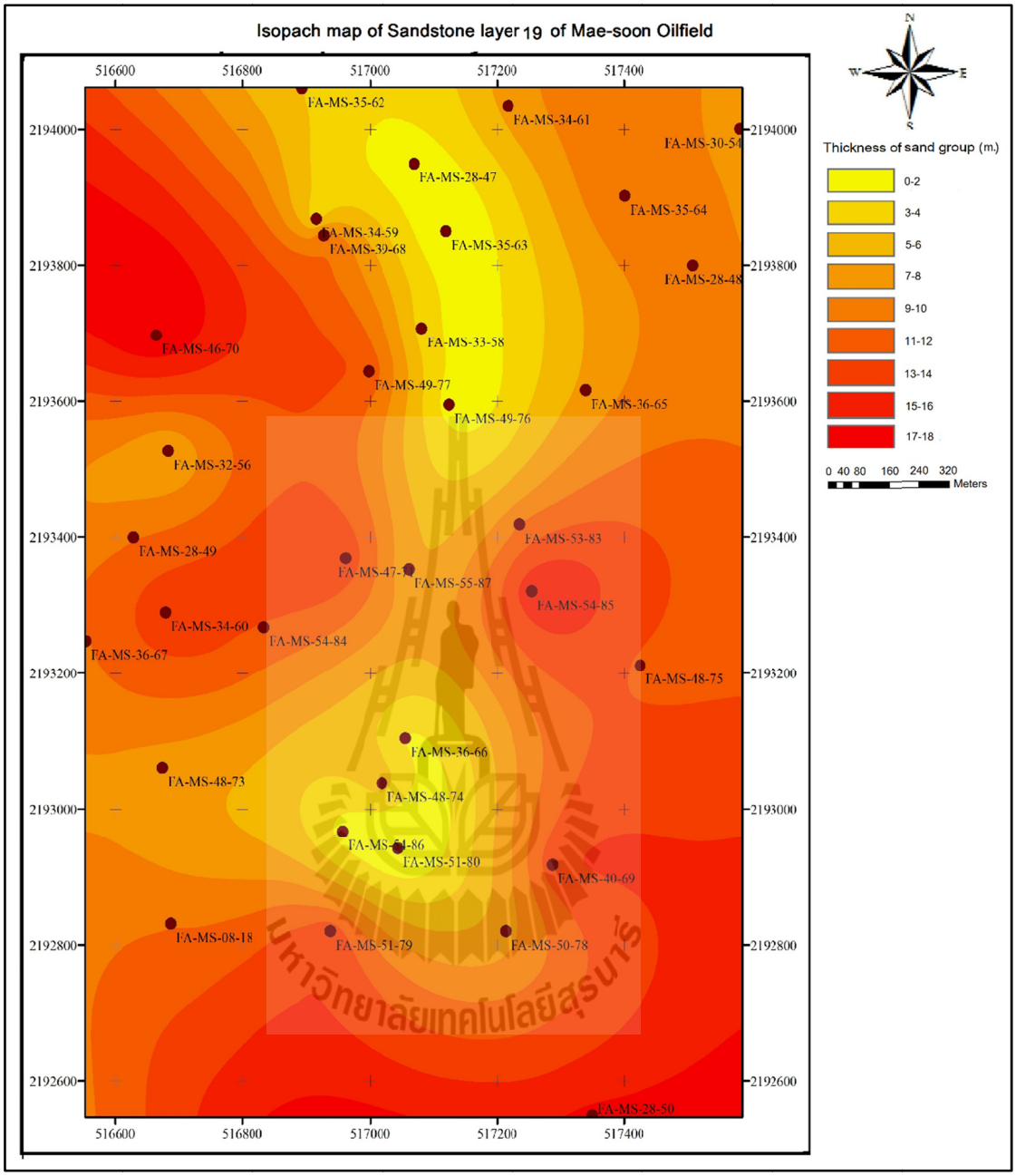

Figure 4.19 Isopach map of sandstone layer 19 of Mae-Soon oil field.

4.2 Stratigraphic section

Results from wireline log interpretation together with some other informative geological data, e.g. mud log data and seismic data, which were reviewed at the first step of the study, could be used to generate stratigraphic section of the 33 boreholes of Mae-Soon oil field. Consequently, the stratigraphic section of 33 boreholes can be generated as depicted in Figure 4.20 to Figure 4.52, respectively.

4.3 Potential reservoir rock properties

4.3.1 Porosity and permeability

Results from porosity and permeability calculation together with well name, depth of collected core samples, sandstone type, average grain size (mm), cementing material (percent) and matrix (percent) of all 19 potential sandstone reservoirs of Mae-Soon oil filed are concluded and depicted in Appendix C

To illustrate the porosity quality distribution of all 19 potential sandstone reservoirs, all available porosity data both from direct measuring in laboratory and from wireline log calculation were plotted and showed in Figure 4.53. It was found that most of sandstone shows fair to medium porosity quality according to Muskat (1949) and Dickker (1985) classification and showed in Figure 4.54.

Figure 4.55 illustrates the distribution of permeability (milliDarcy), depth (meter), average grain size (millimeter), cementing material (percent) and matrix (percent) data of all 19 potential sandstone reservoirs of Mae-Soon oil field, respectively.

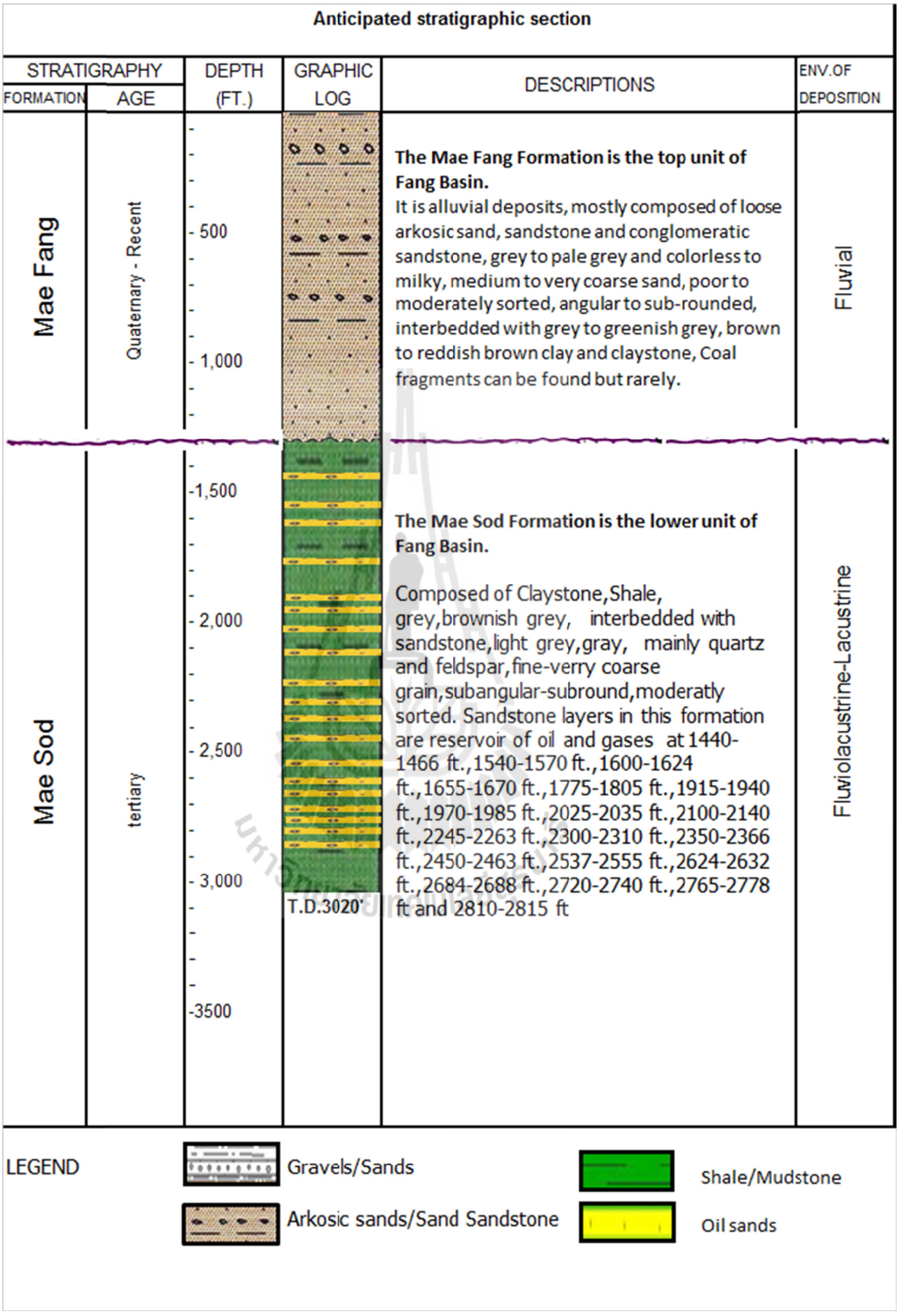

Figure 4.20 Stratigraphic section of well no. FA-MS-08-12.

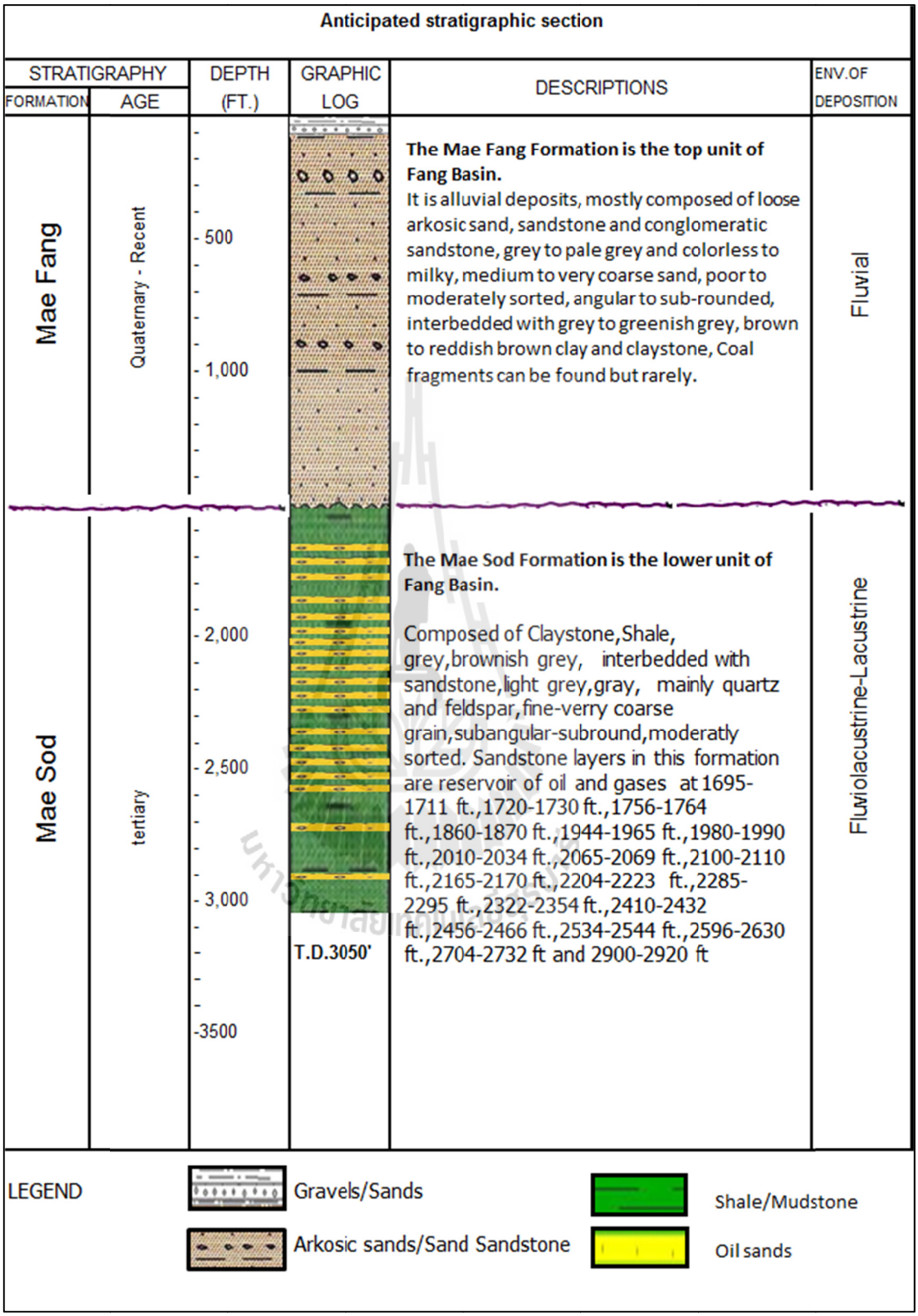

Figure 4.21 Stratigraphic section of well no. FA-MS-08-18.

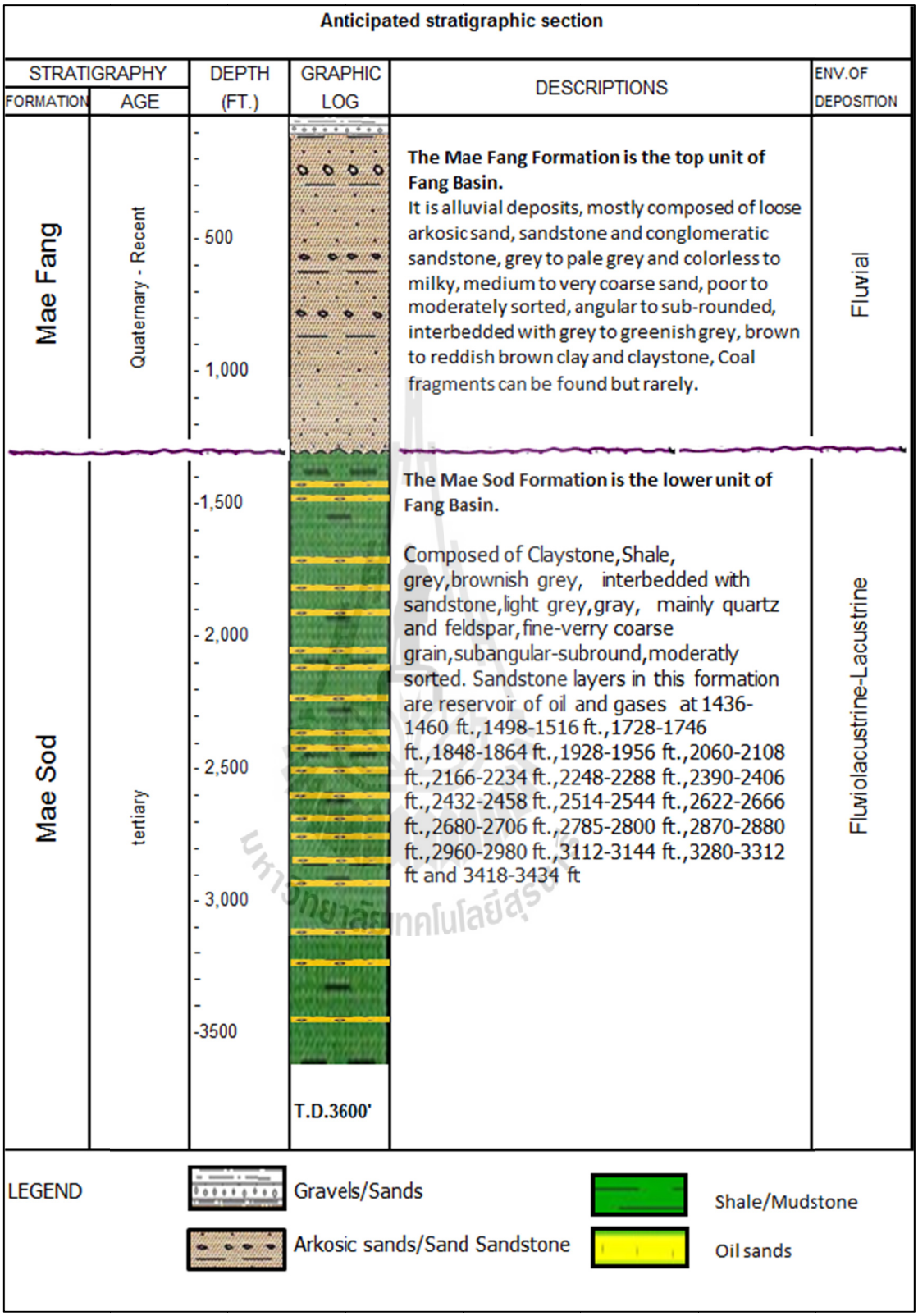

Figure 4.22 Stratigraphic section of well no. FA-MS-27-46.

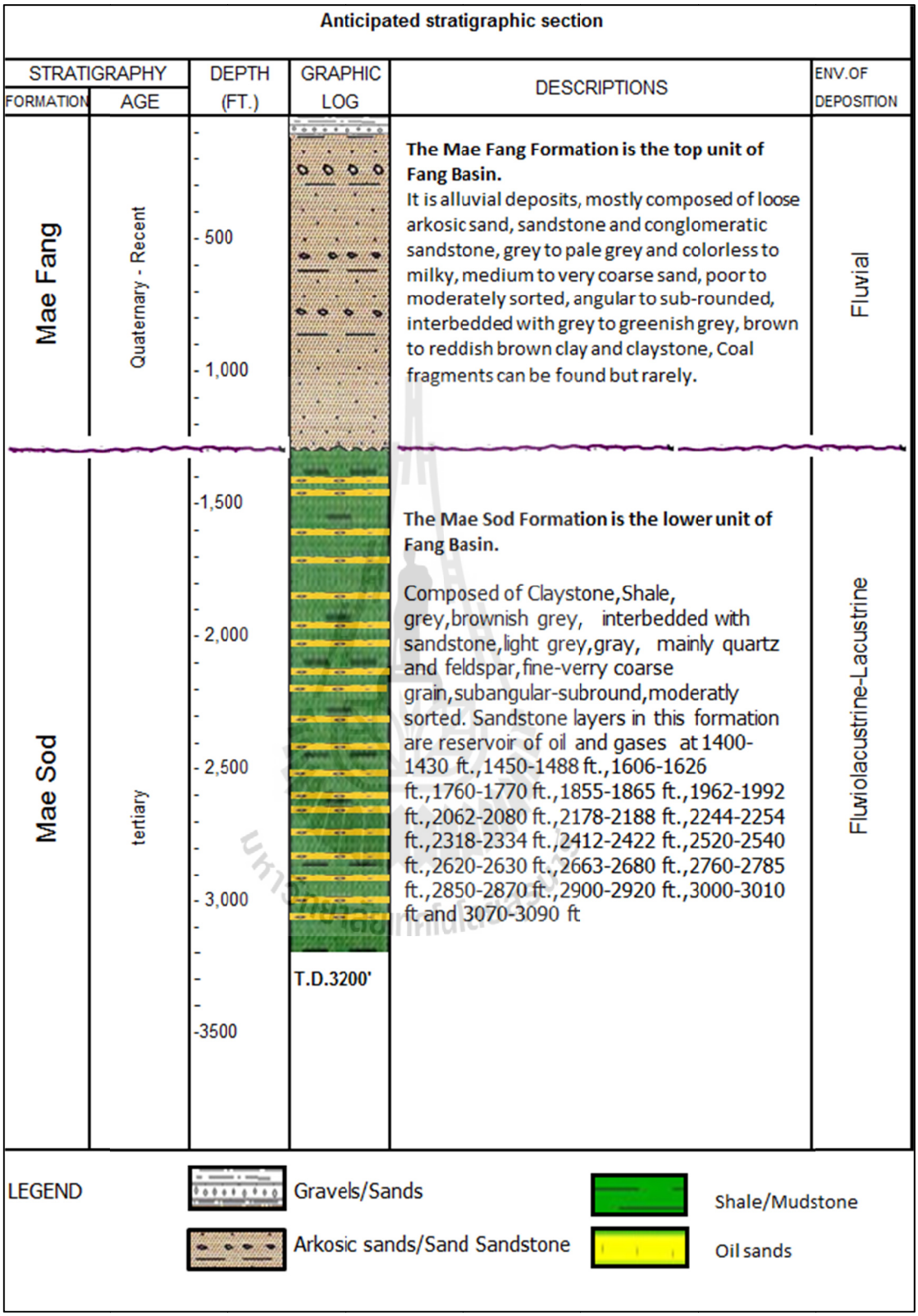

Figure 4.23 Stratigraphic section of well no. FA-MS-28-47.

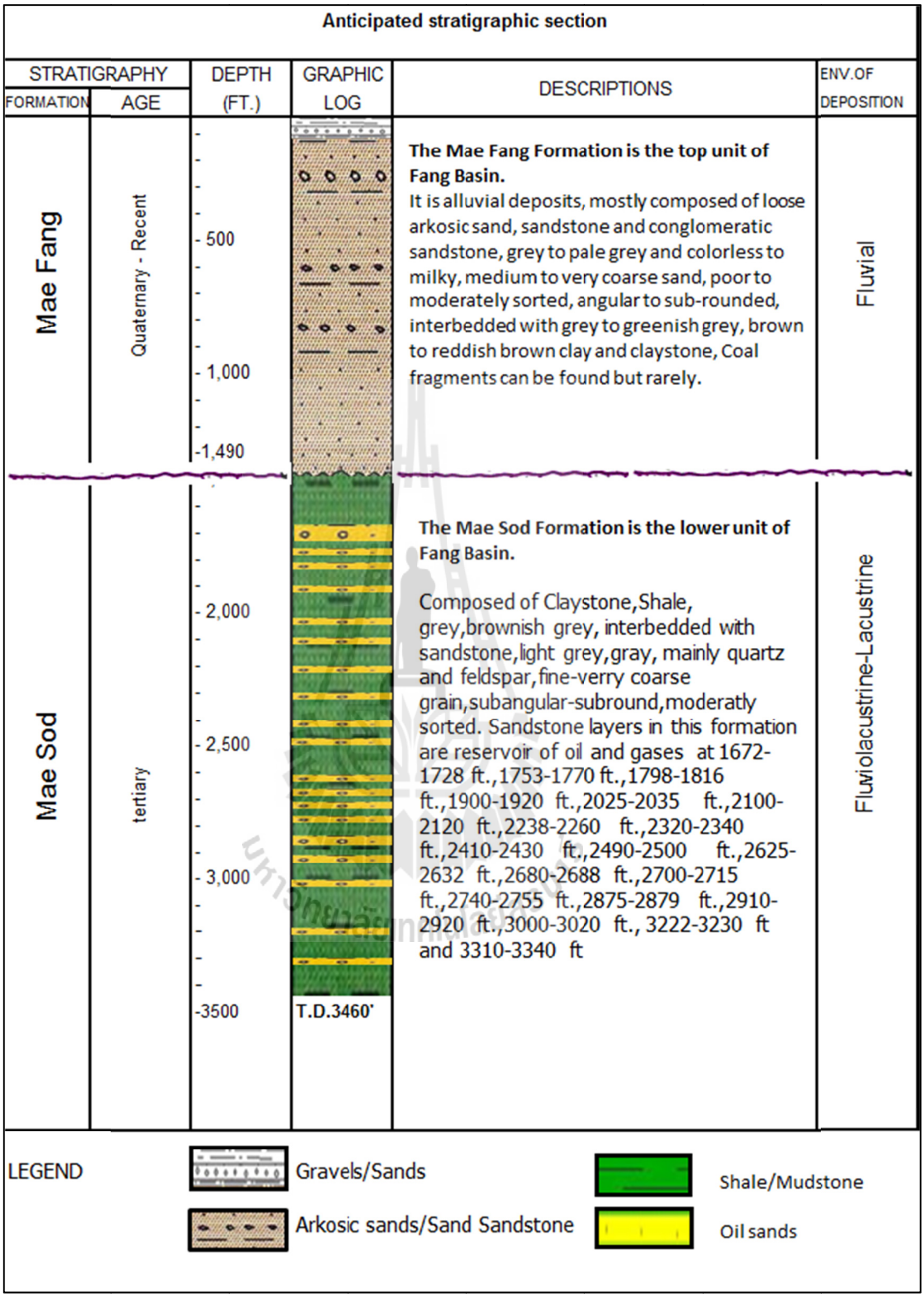

Figure 4.24 Stratigraphic section of well no. FA-MS-28-48.

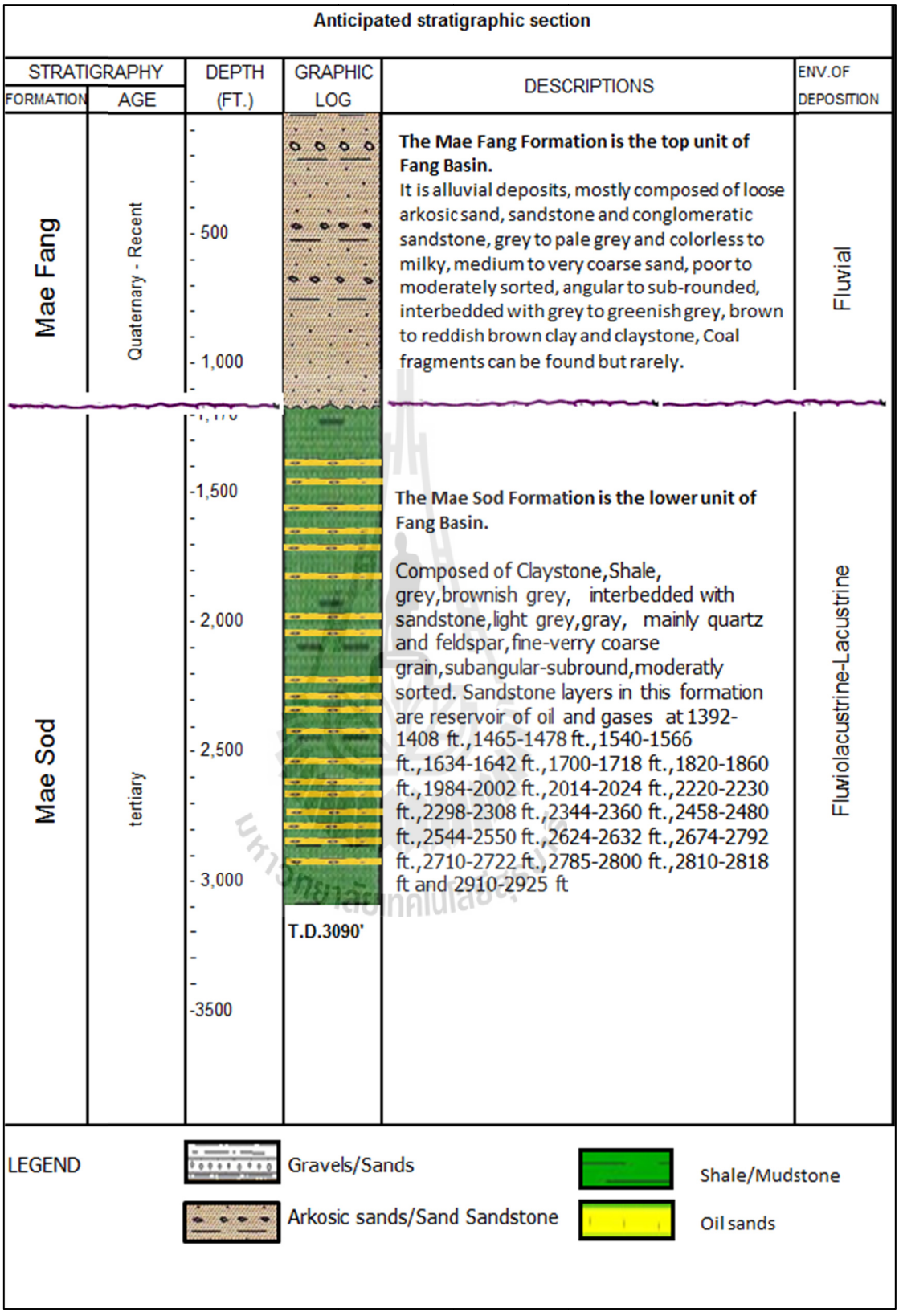

Figure 4.25 Stratigraphic section of well no. FA-MS-28-49.

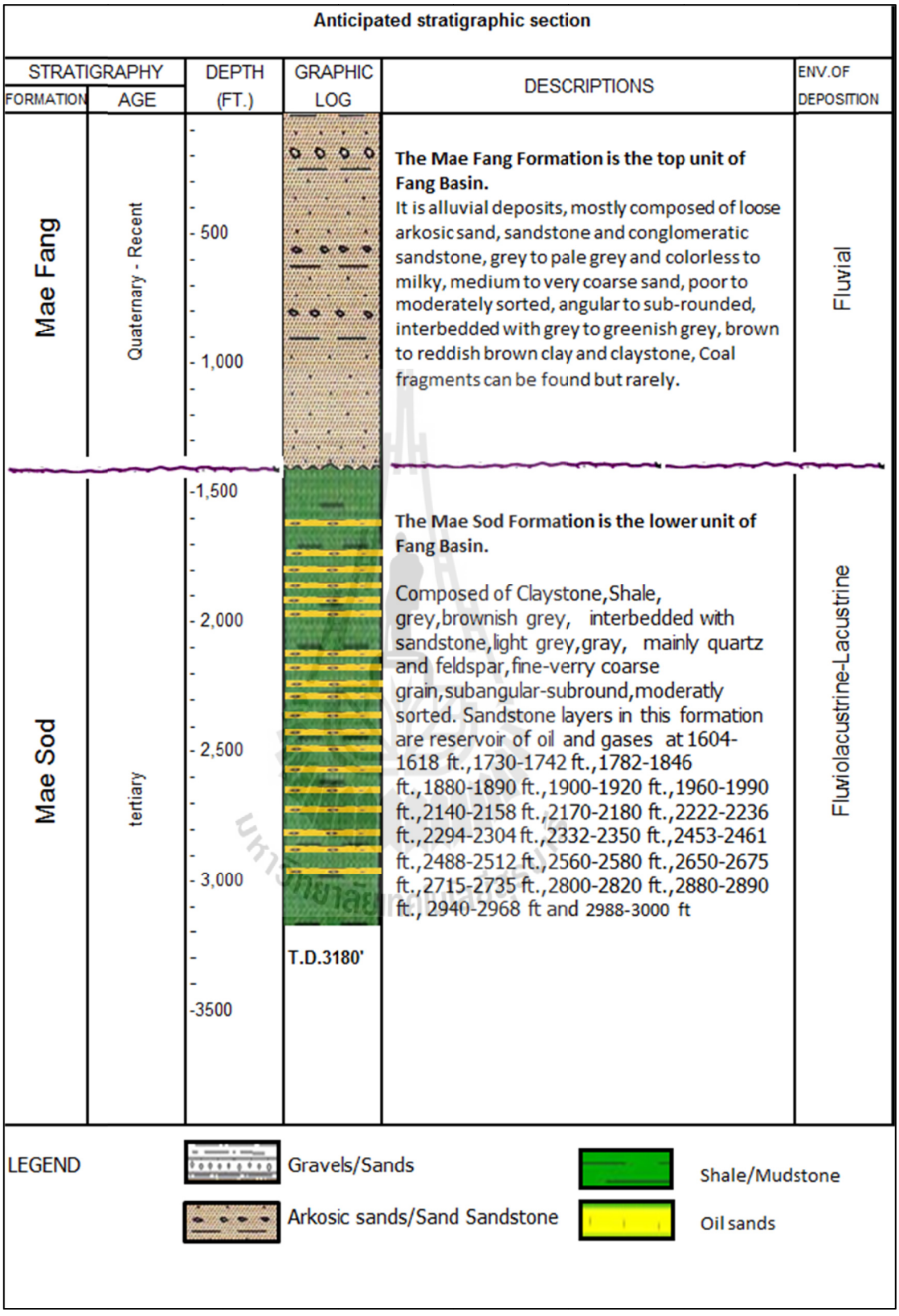

Figure 4.26 Stratigraphic section of well no. FA-MS-28-50.

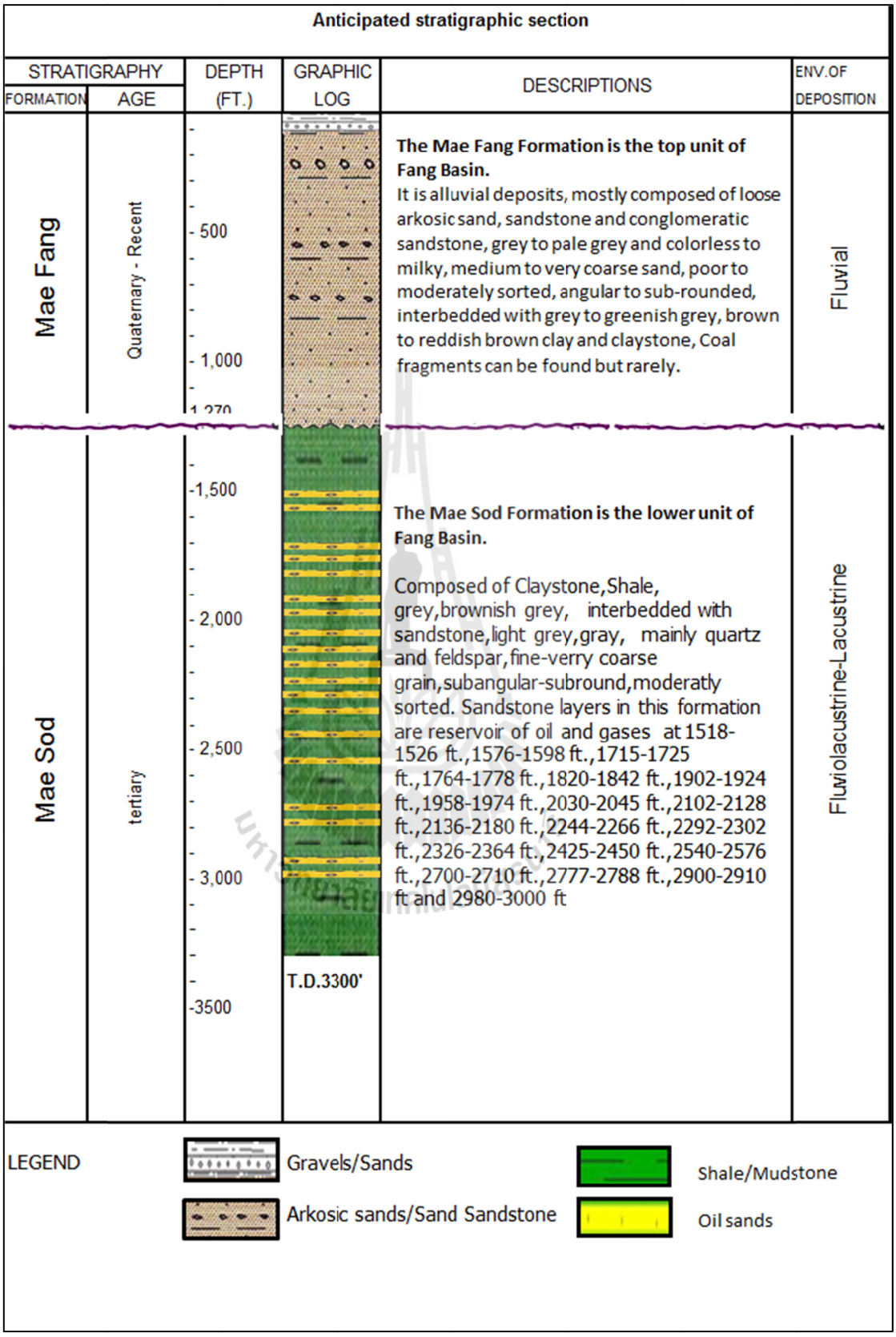

Figure 4.27 Stratigraphic section of well no. FA-MS-30-54.

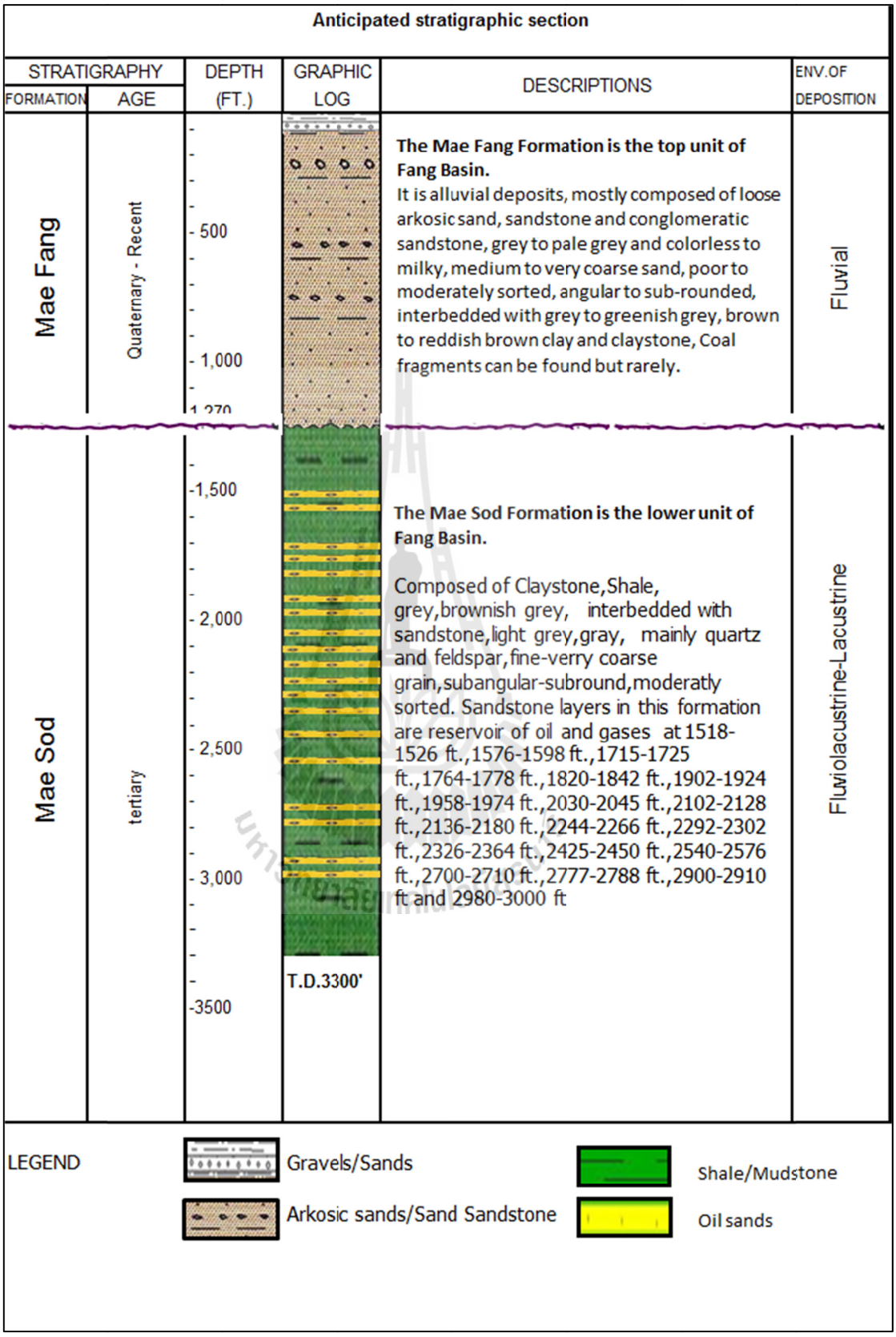

Figure 4.28 Stratigraphic section of well no. FA-MS-31-55.

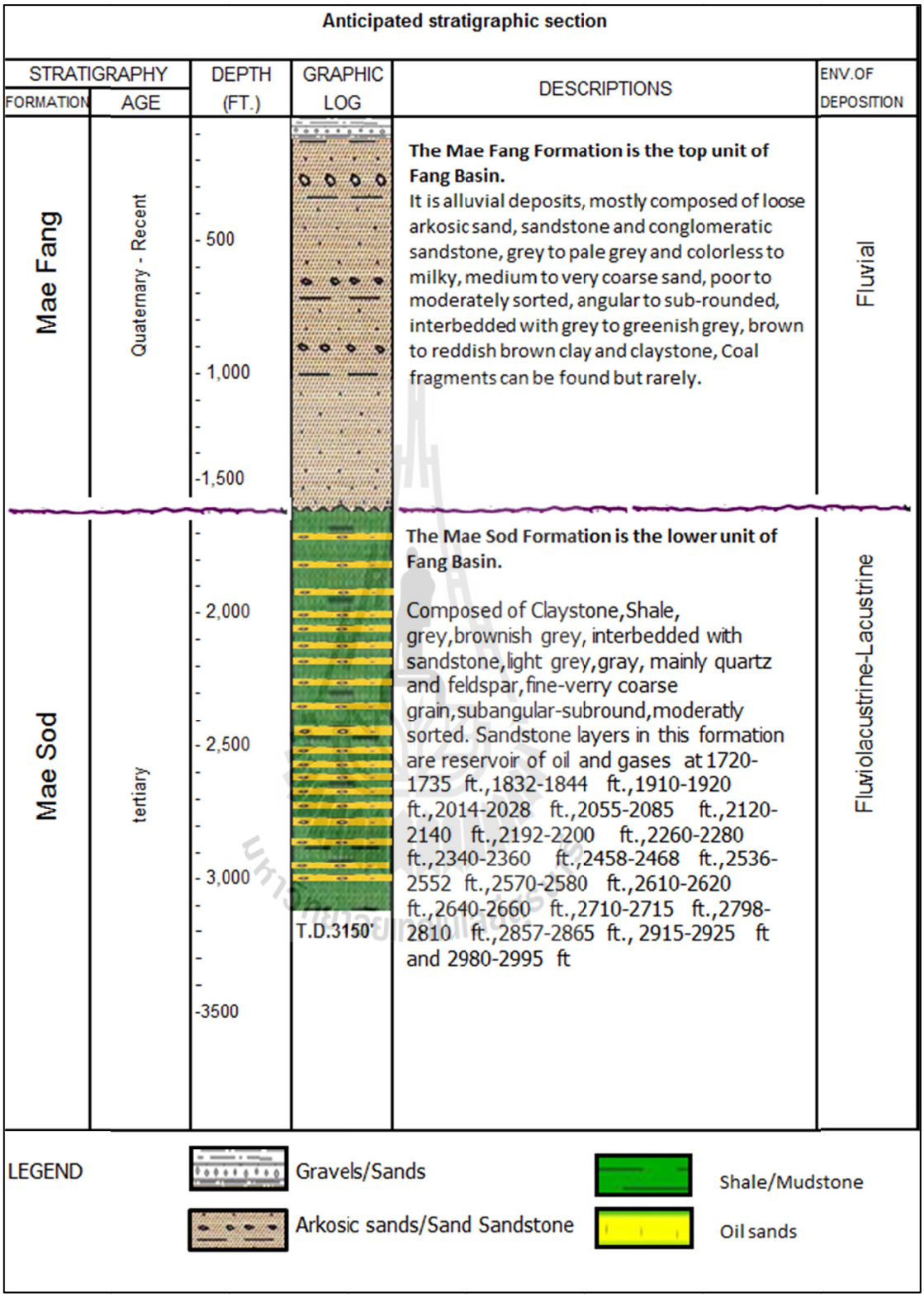

Figure 4.29 Stratigraphic section of well no. FA-MS-32-56.

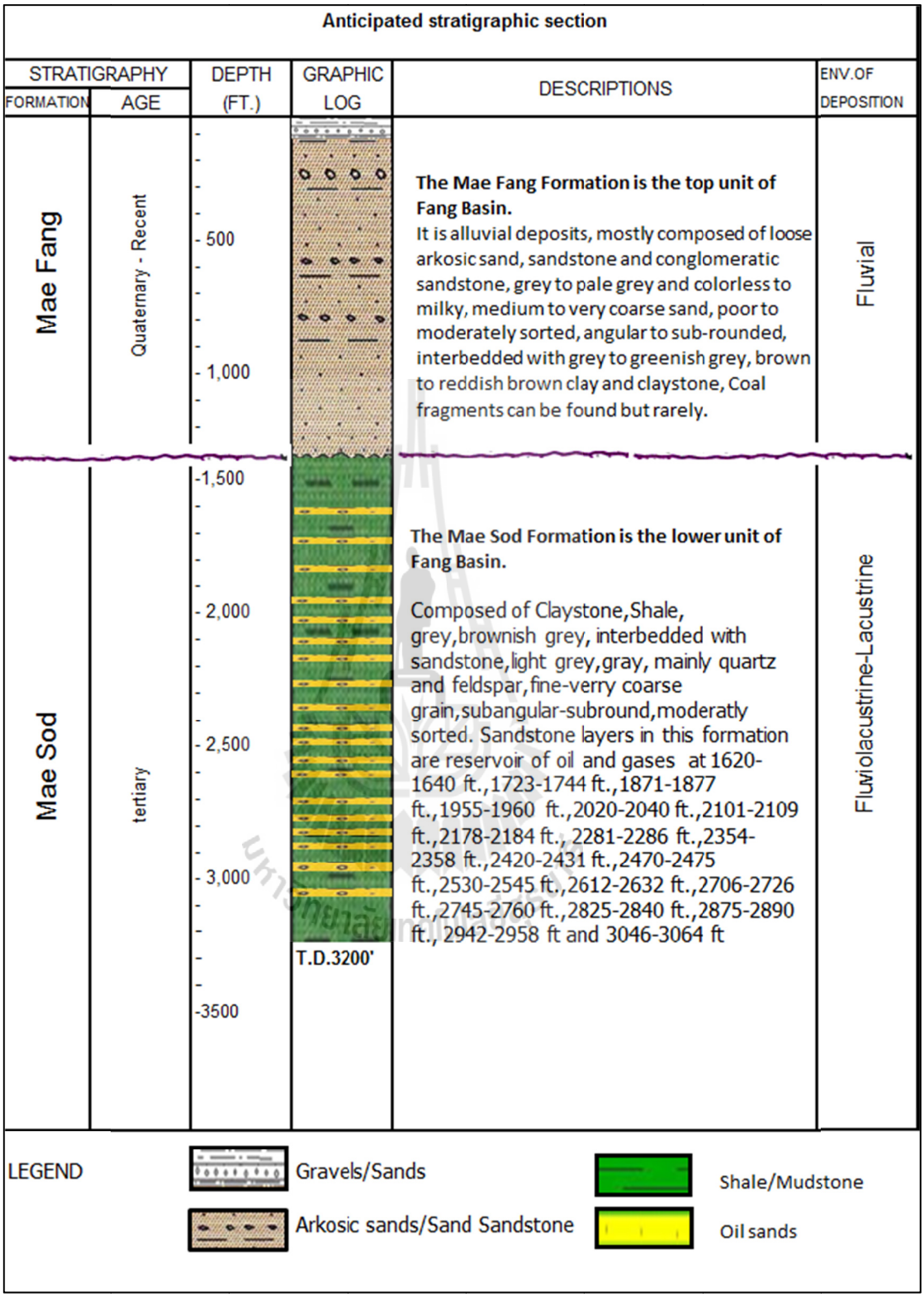

Figure 4.30 Stratigraphic section of well no. FA-MS-33-58.

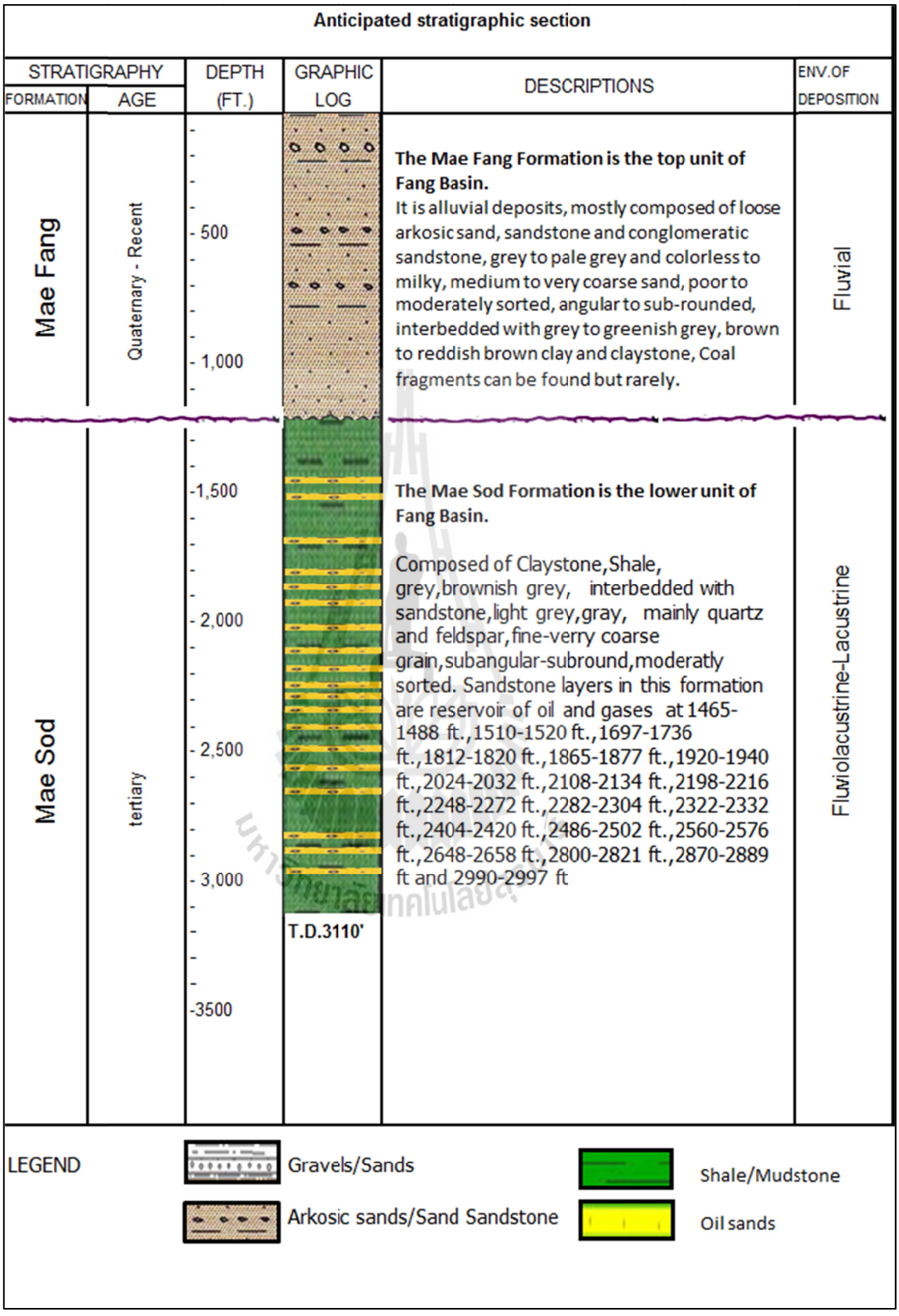

Figure 4.31 Stratigraphic section of well no. FA-MS-34-59.

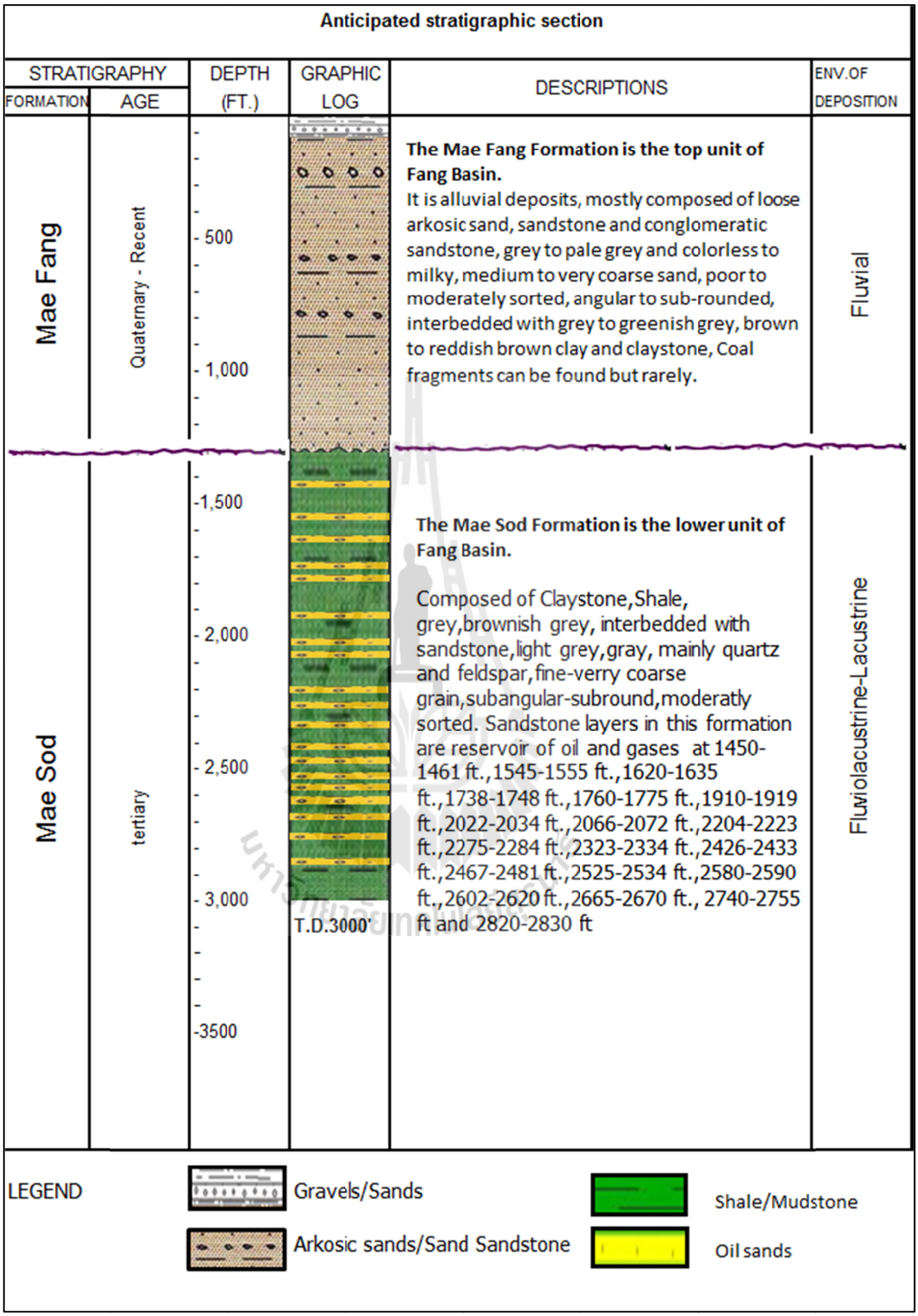

Figure 4.32 Stratigraphic section of well no. FA-MS-34-60.

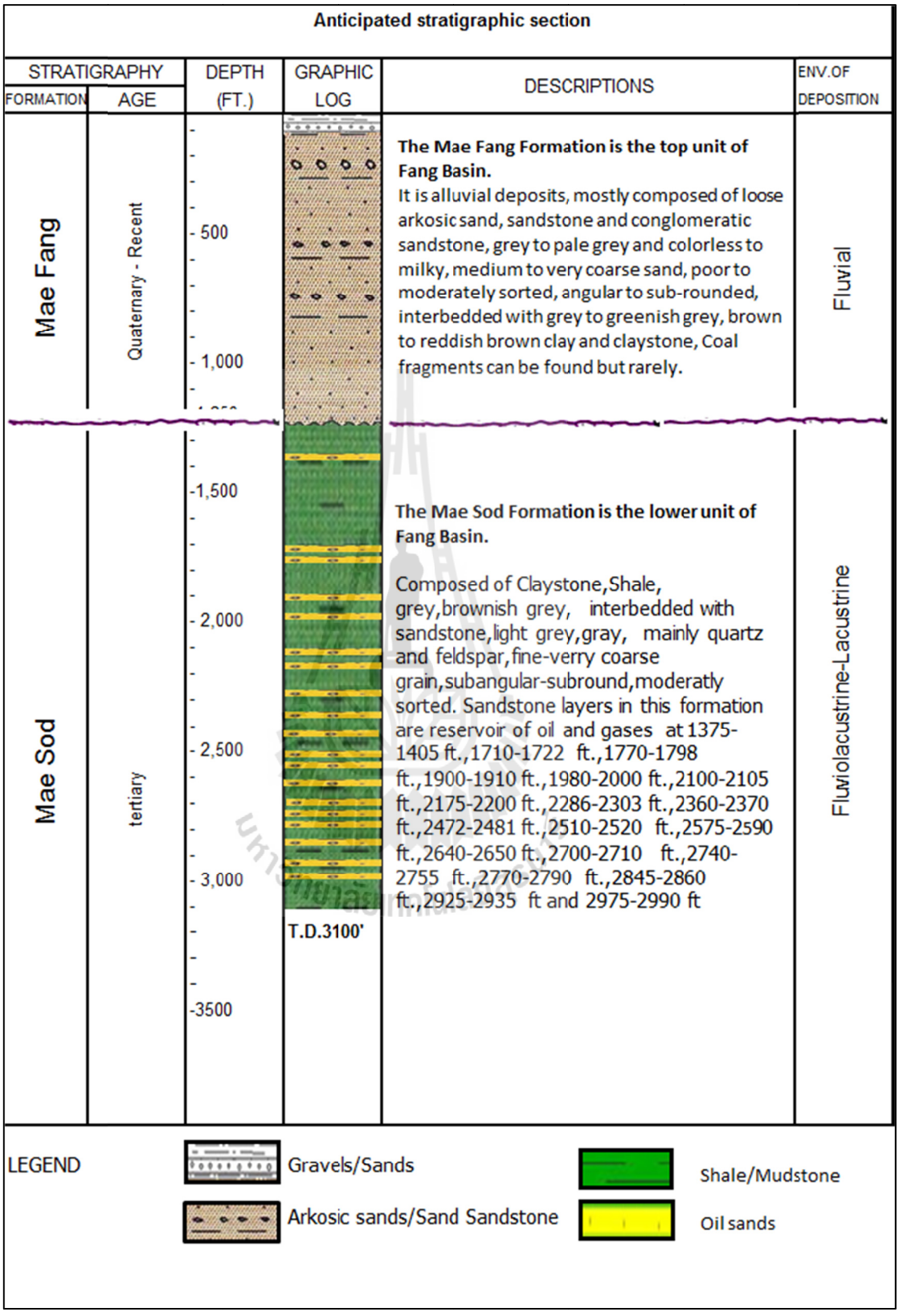

Figure 4.33 Stratigraphic section of well no. FA-MS-34-61.

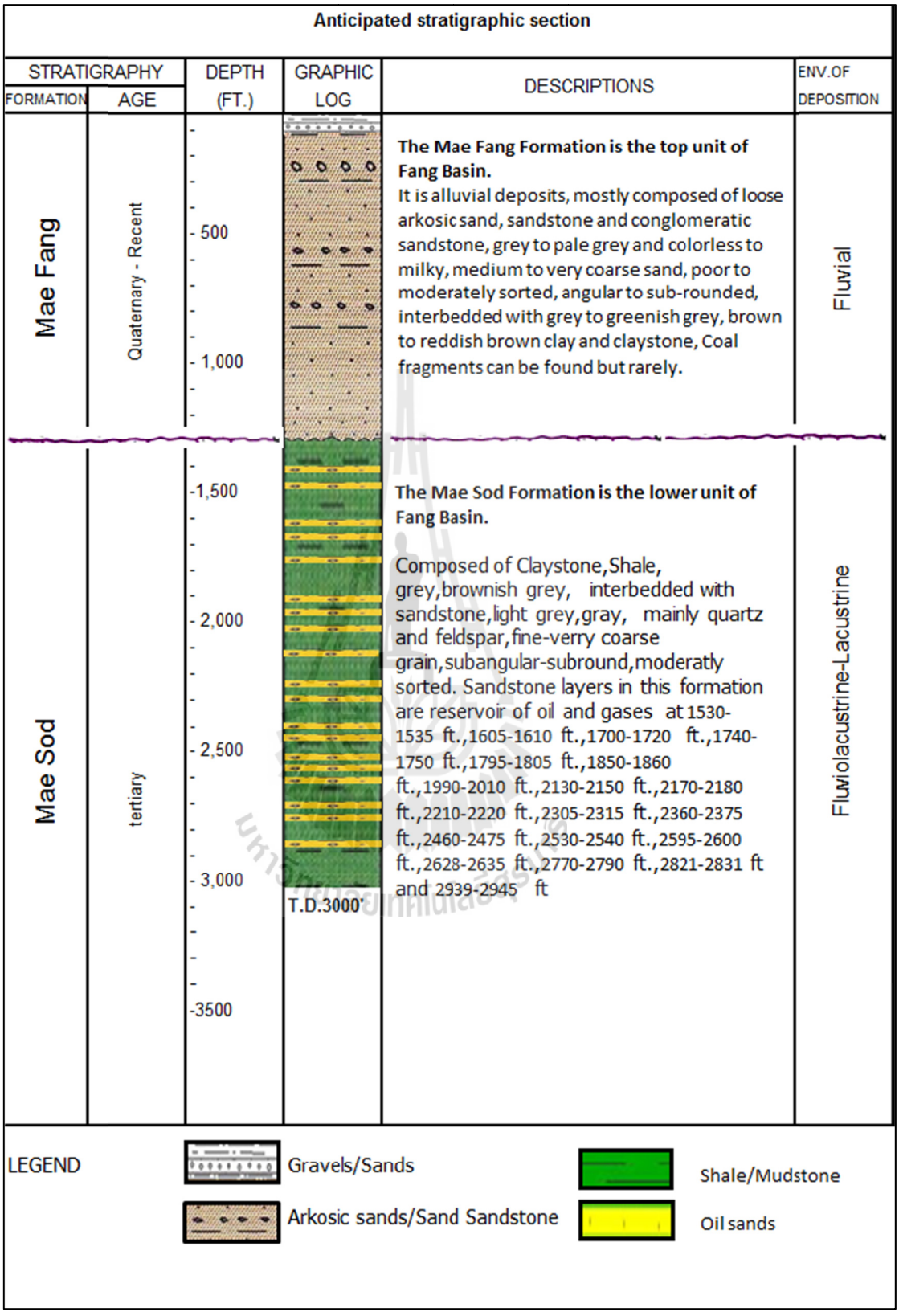

Figure 4.34 Stratigraphic section of well no. FA-MS-35-62.

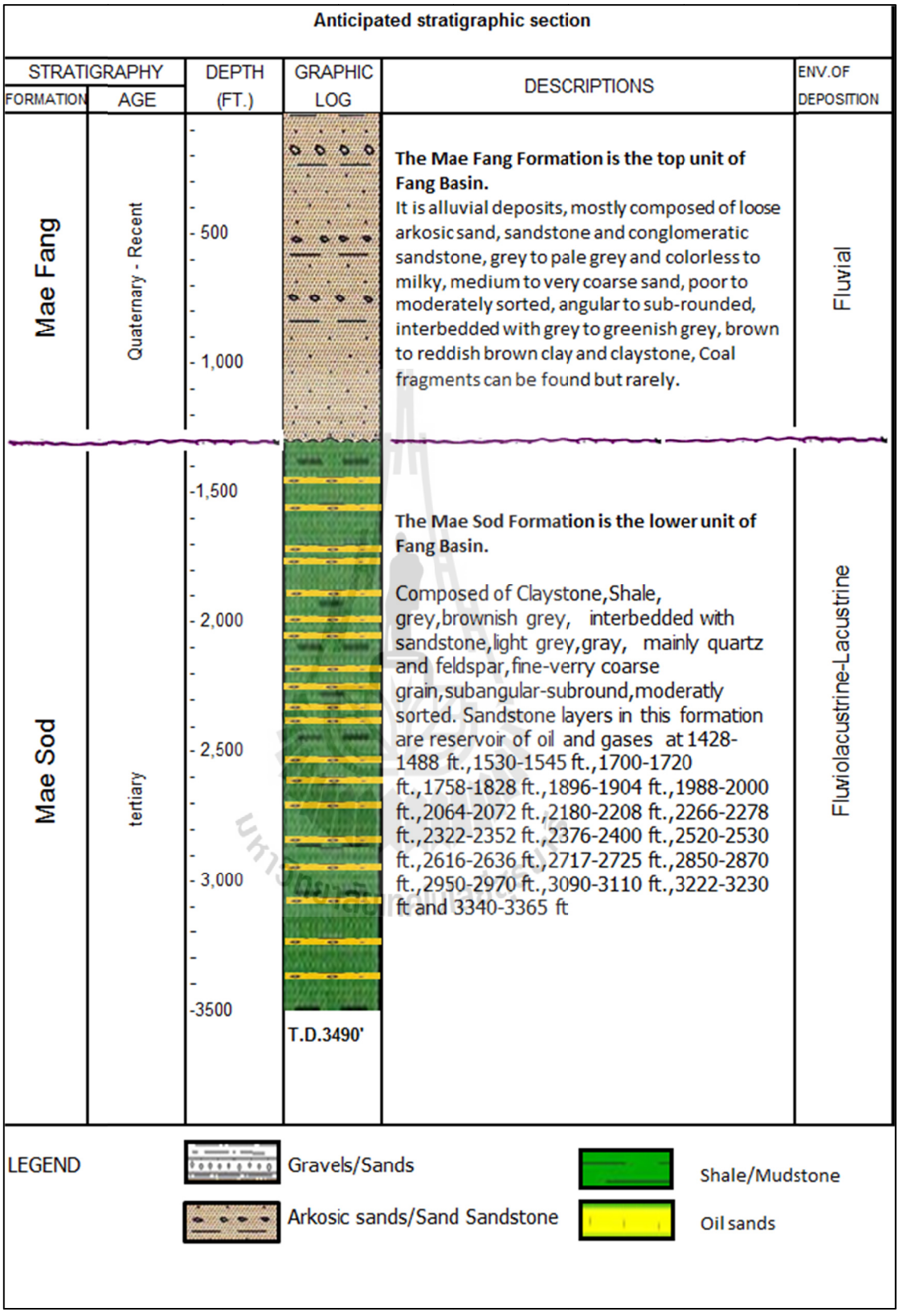

Figure 4.35 Stratigraphic section of well no. FA-MS-36-65.

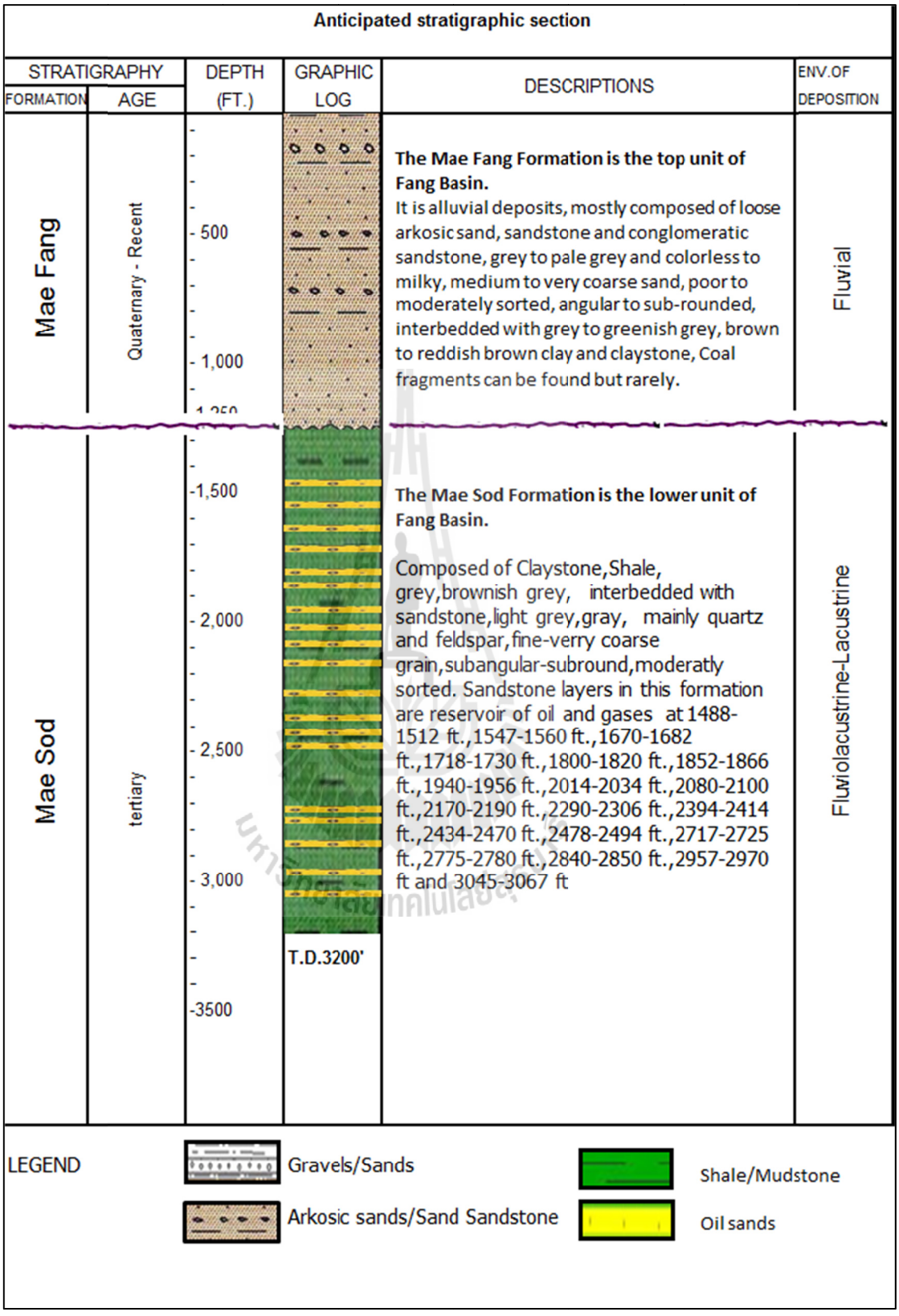

Figure 4.36 Stratigraphic section of well no. FA-MS-36-66.

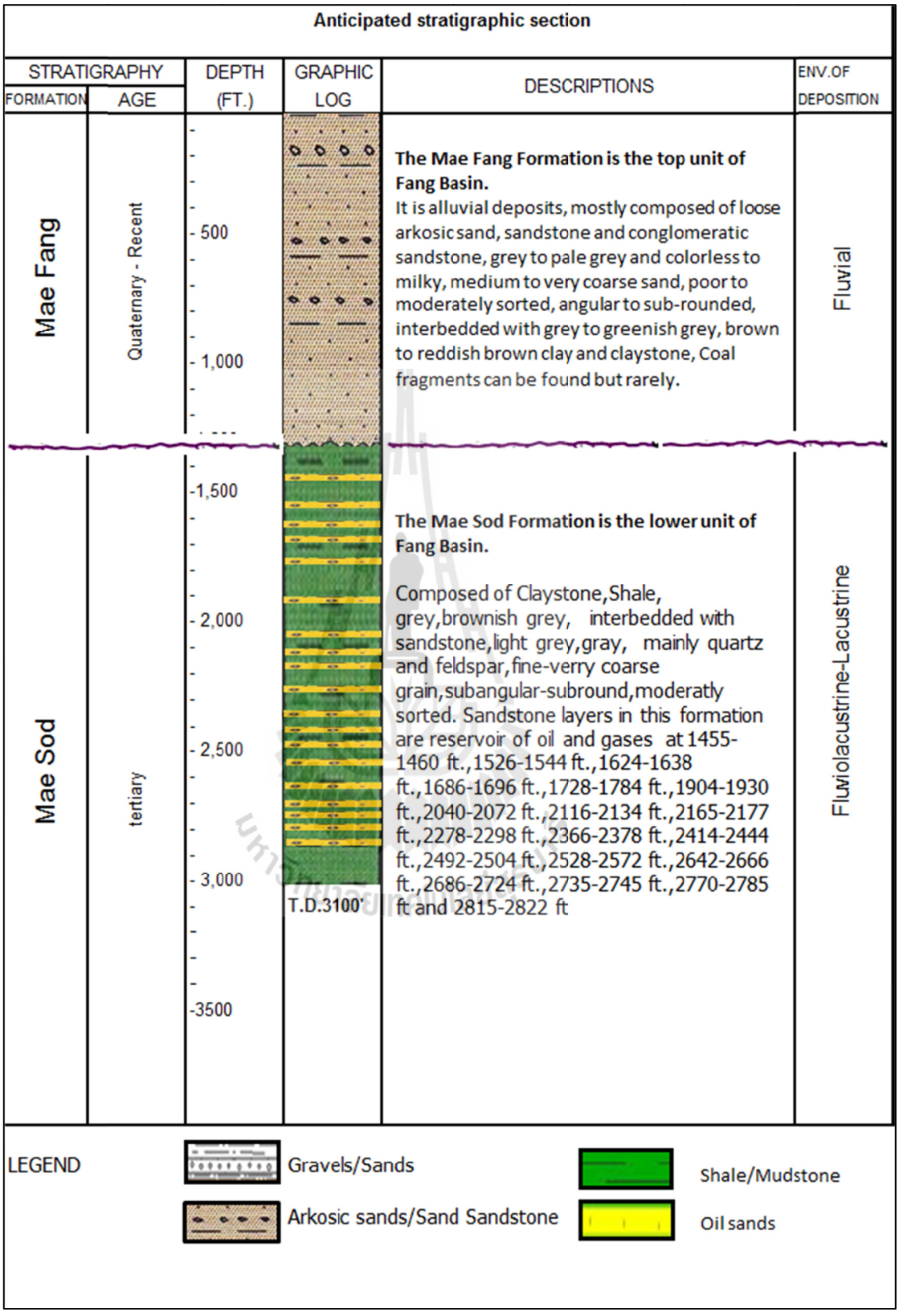

Figure 4.37 Stratigraphic section of well no. FA-MS-36-67.

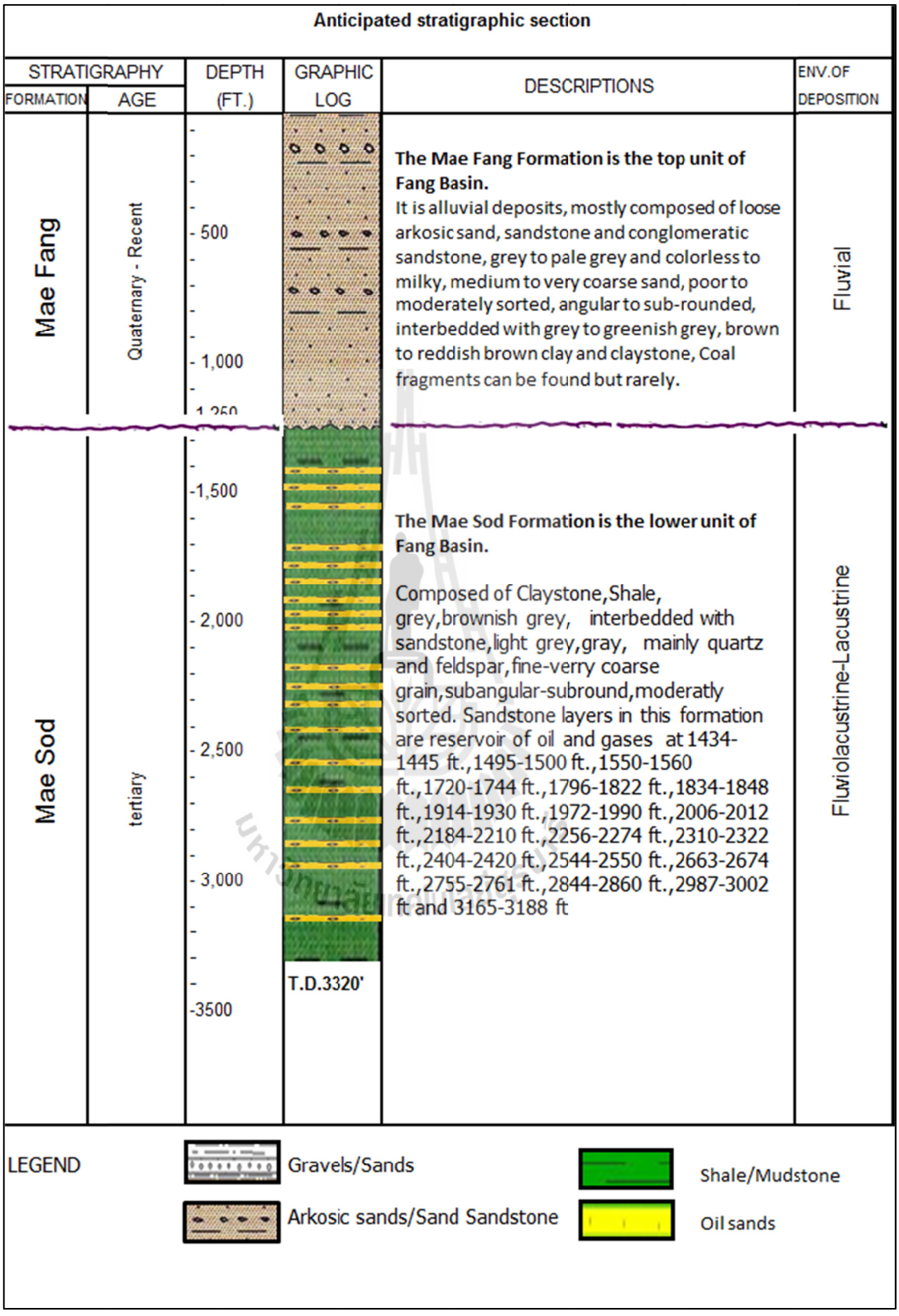

Figure 4.38 Stratigraphic section of well no. FA-MS-40-69.

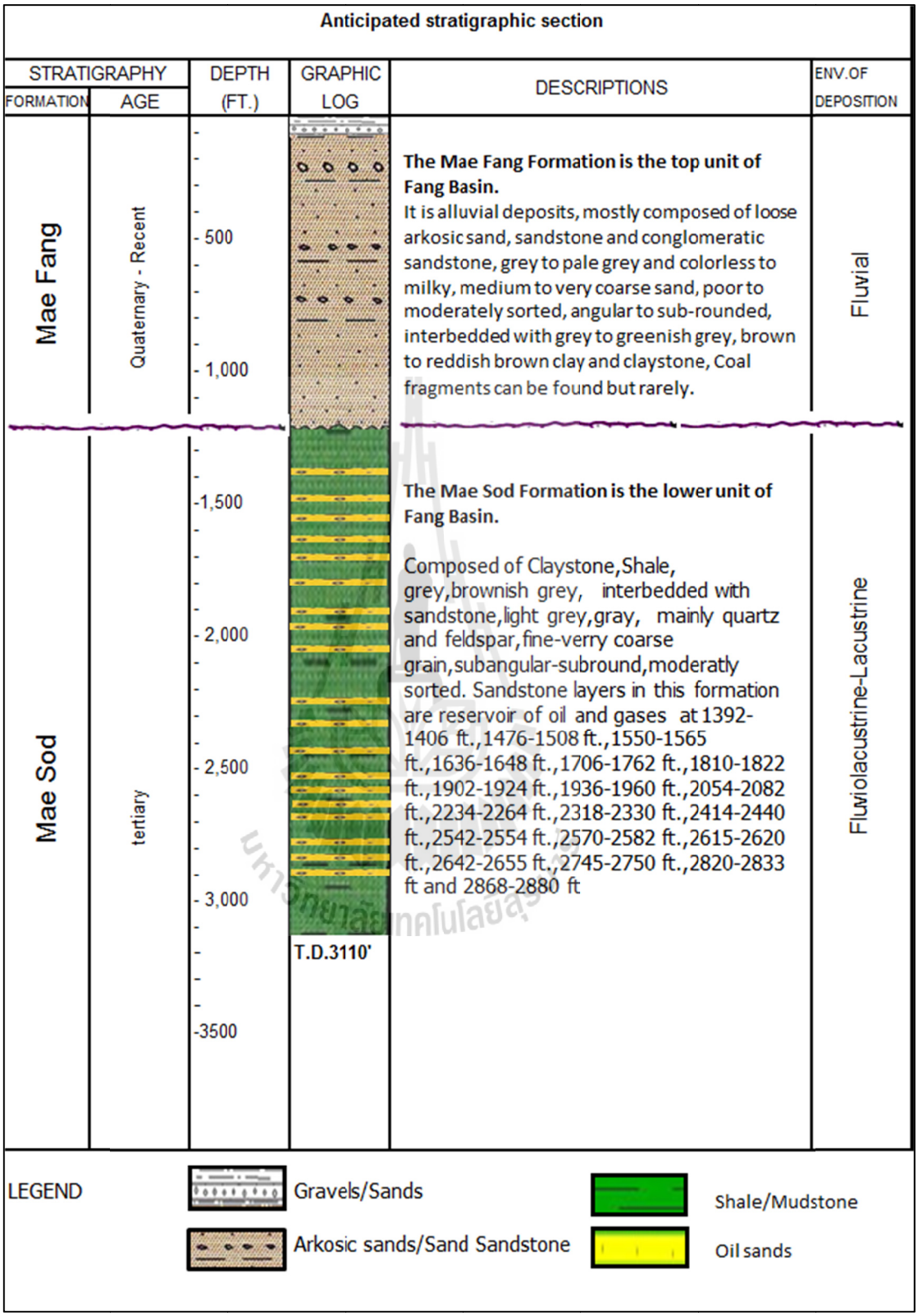

Figure 4.39 Stratigraphic section of well no. FA-MS-46-70.

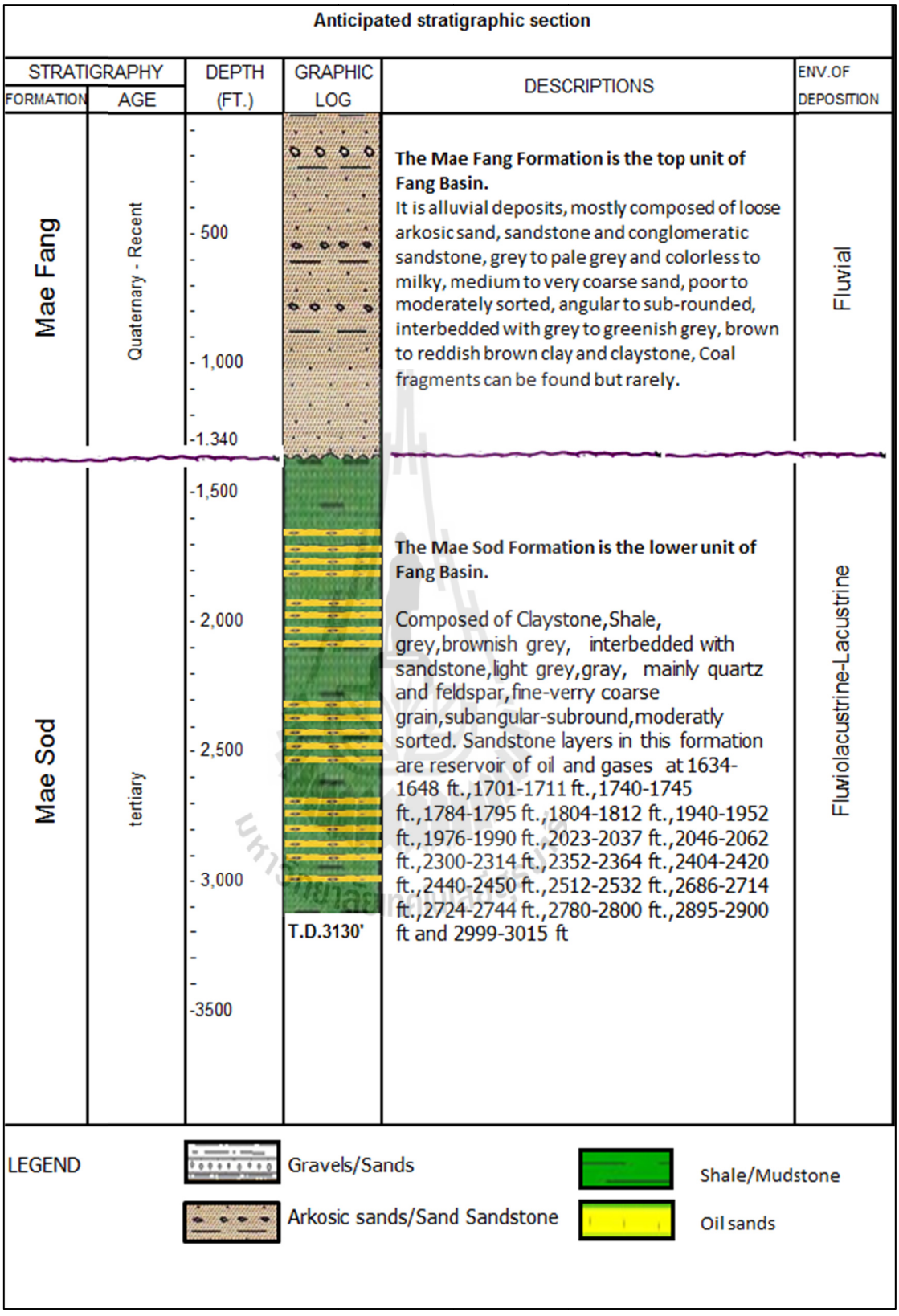

Figure 4.40 Stratigraphic section of well no. FA-MS-47-71.

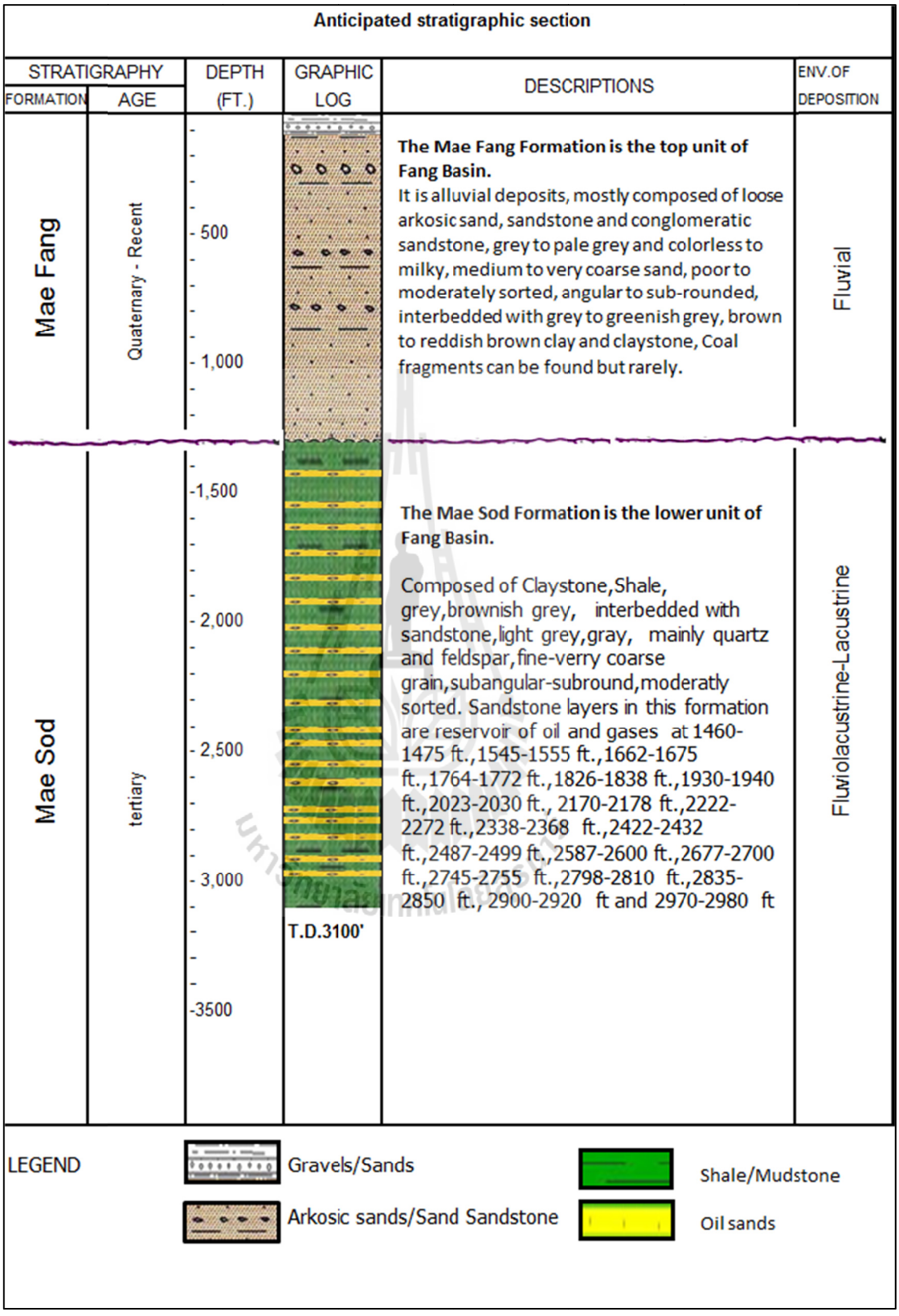

Figure 4.41 Stratigraphic section of well no. FA-MS-48-73.

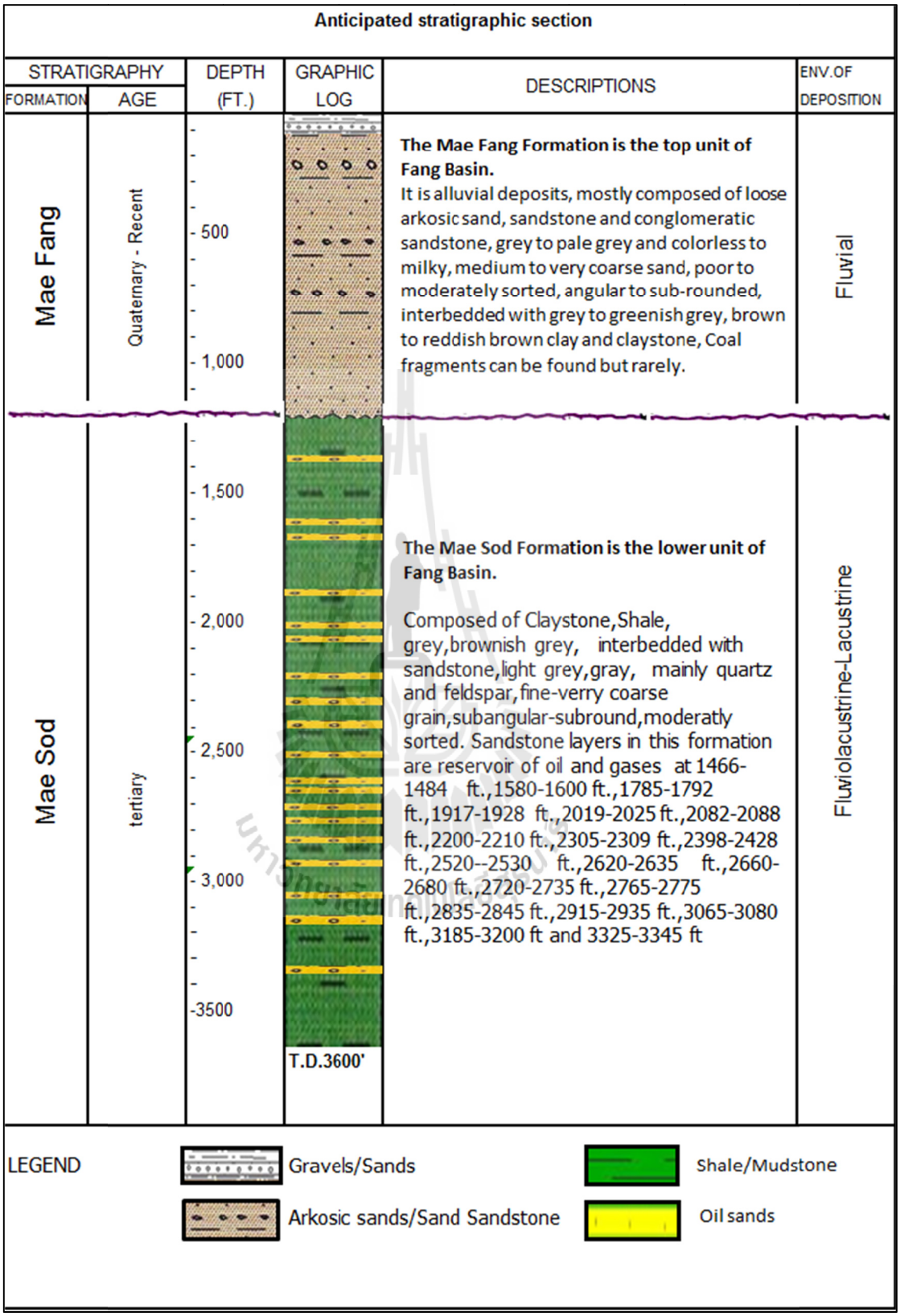

Figure 4.42 Stratigraphic section of well no. FA-MS-48-75.

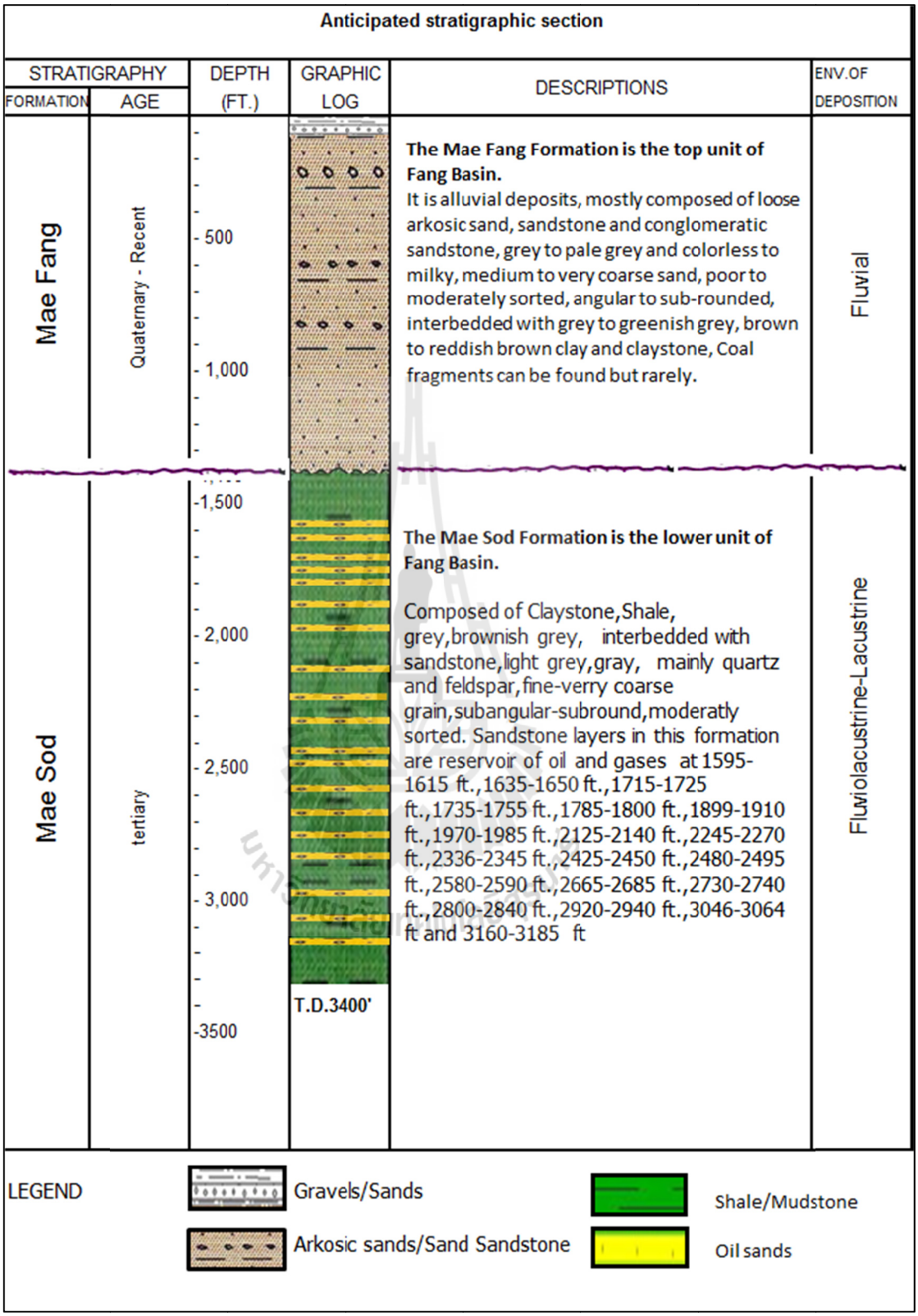

Figure 4.43 Stratigraphic section of well no. FA-MS-49-76.

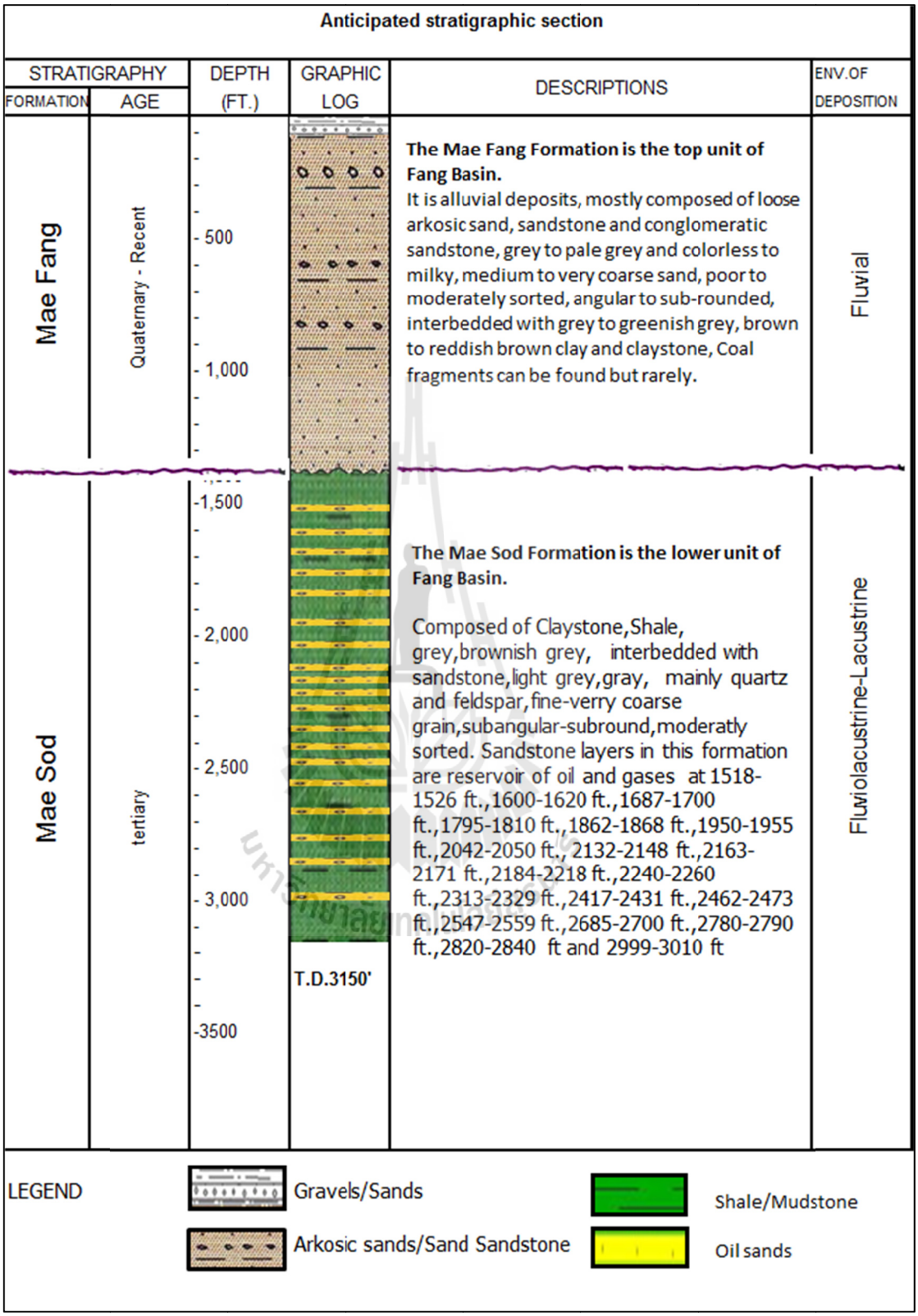

Figure 4.44 Stratigraphic section of well no. FA-MS-49-77.

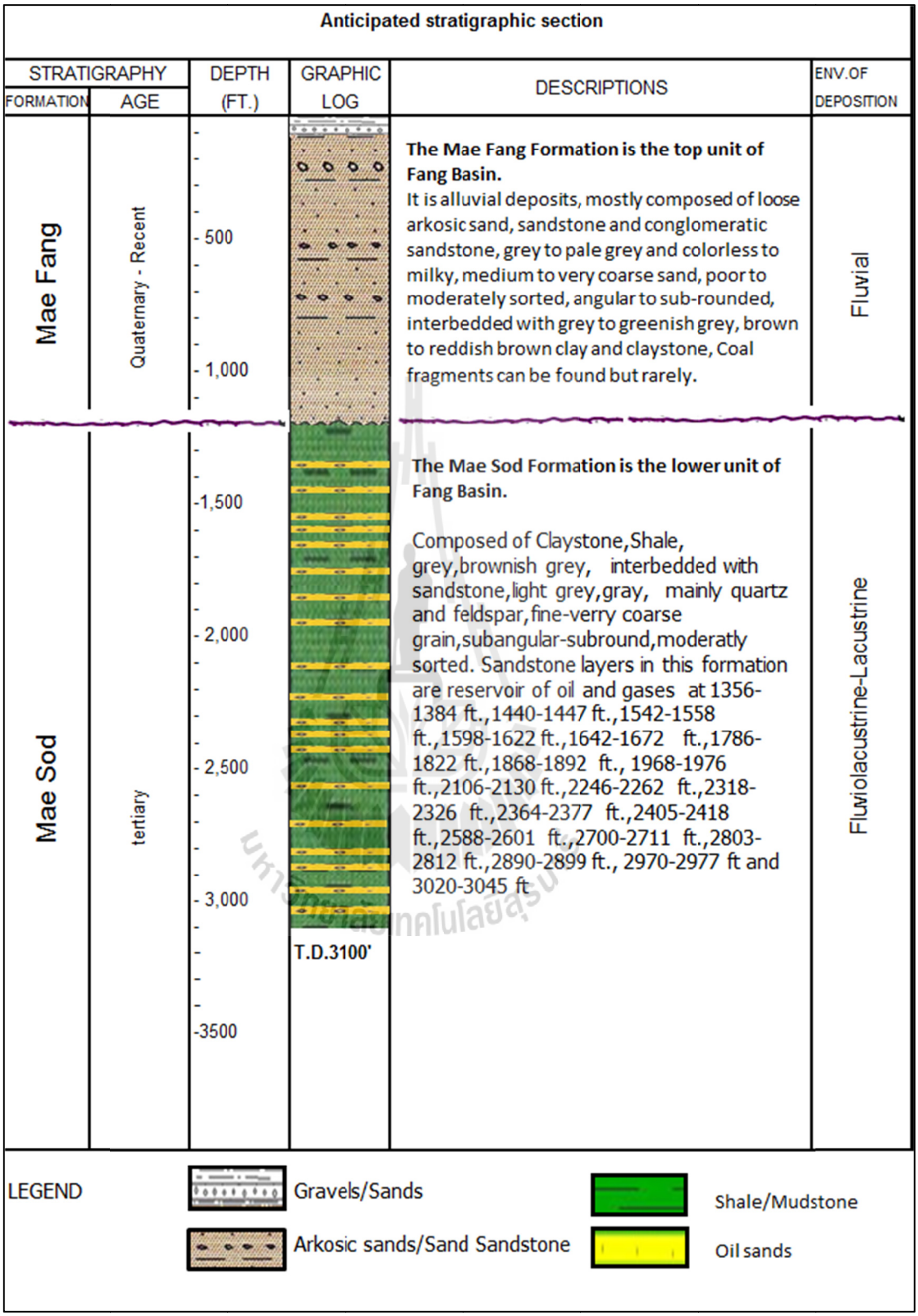

Figure 4.45 Stratigraphic section of well no. FA-MS-50-78.

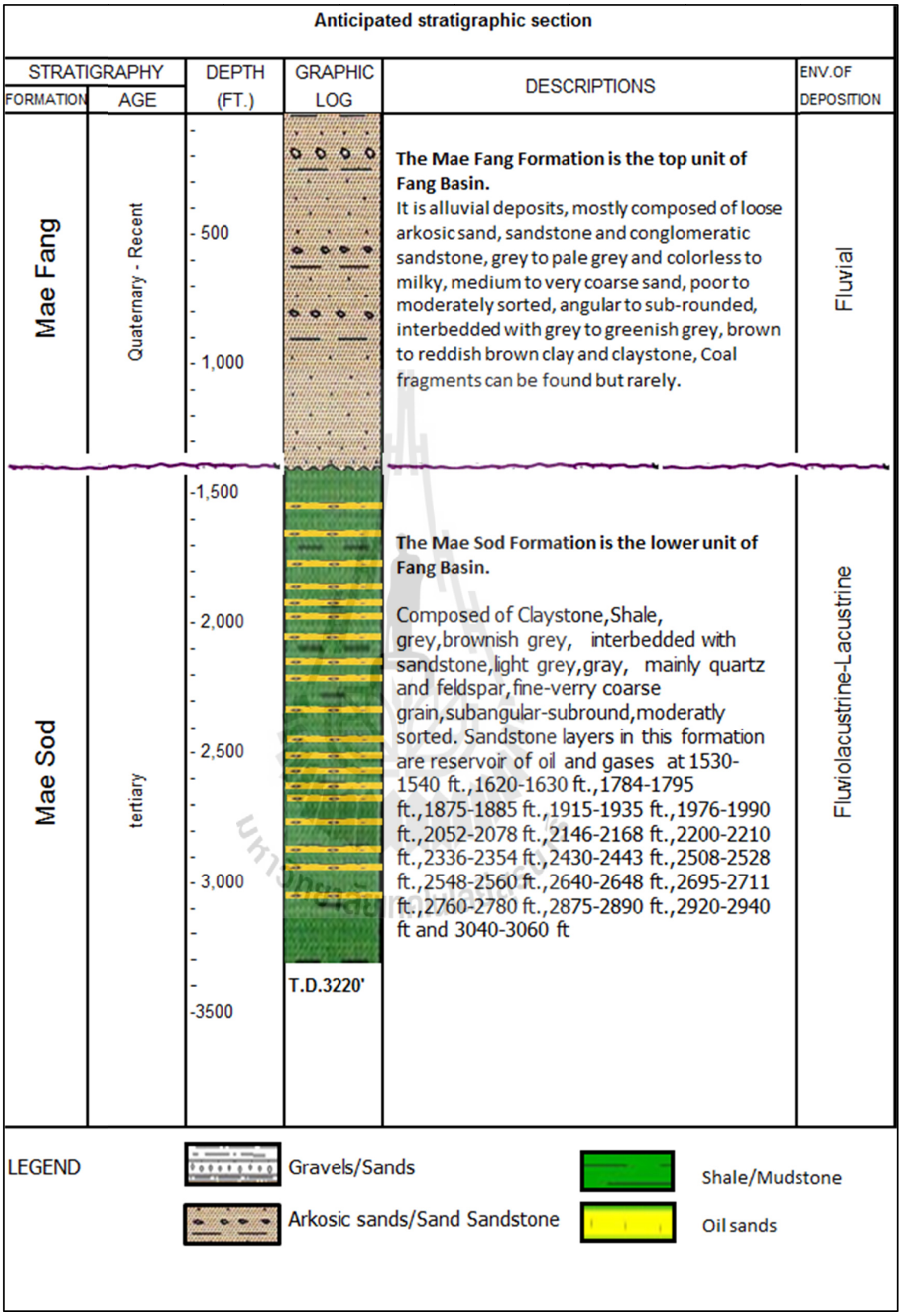

Figure 4.46 Stratigraphic section of well no. FA-MS-51-79.

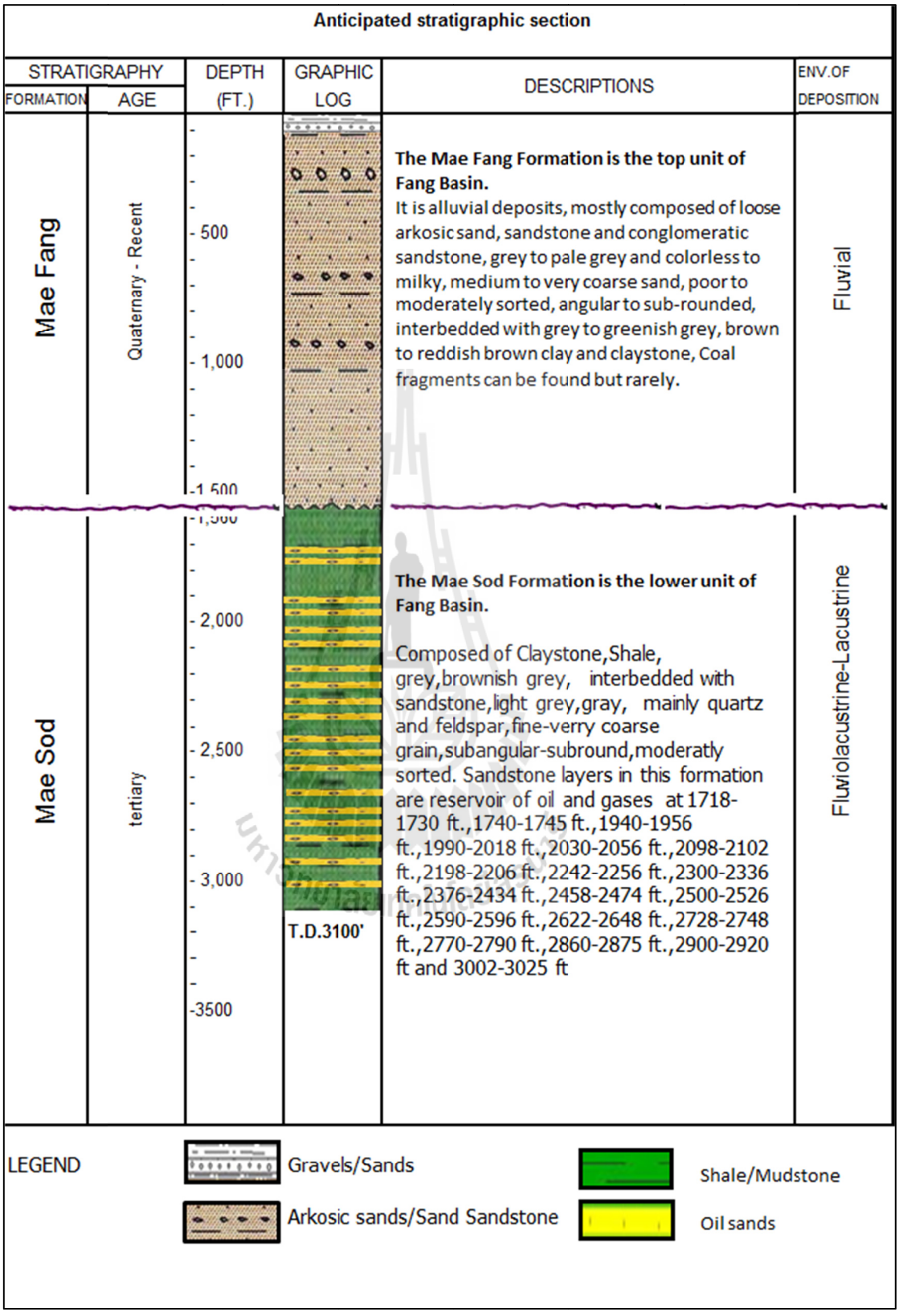

Figure 4.47 Stratigraphic section of well no. FA-MS-51-80.

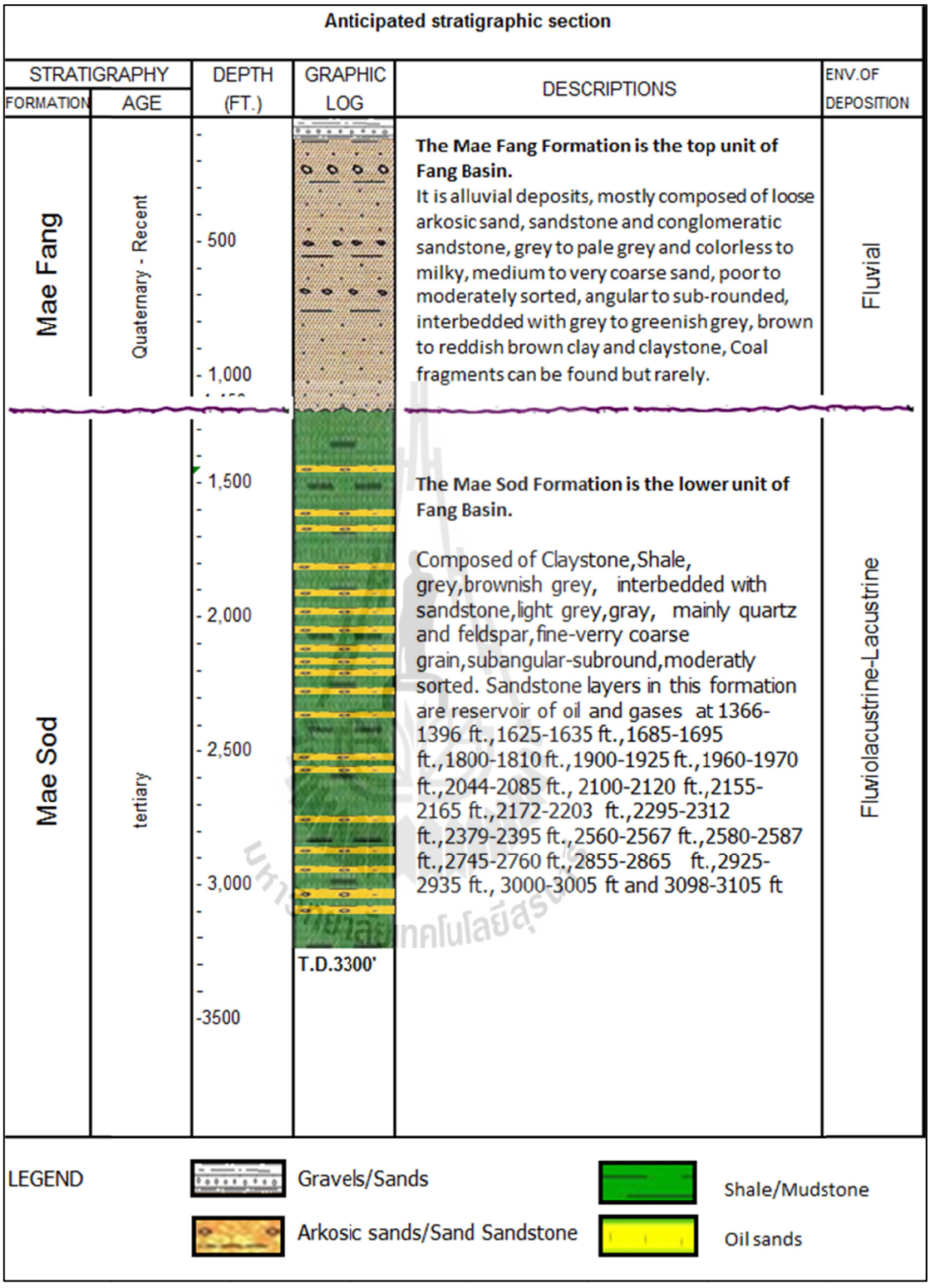

Figure 4.48 Stratigraphic section of well no. FA-MS-53-83.

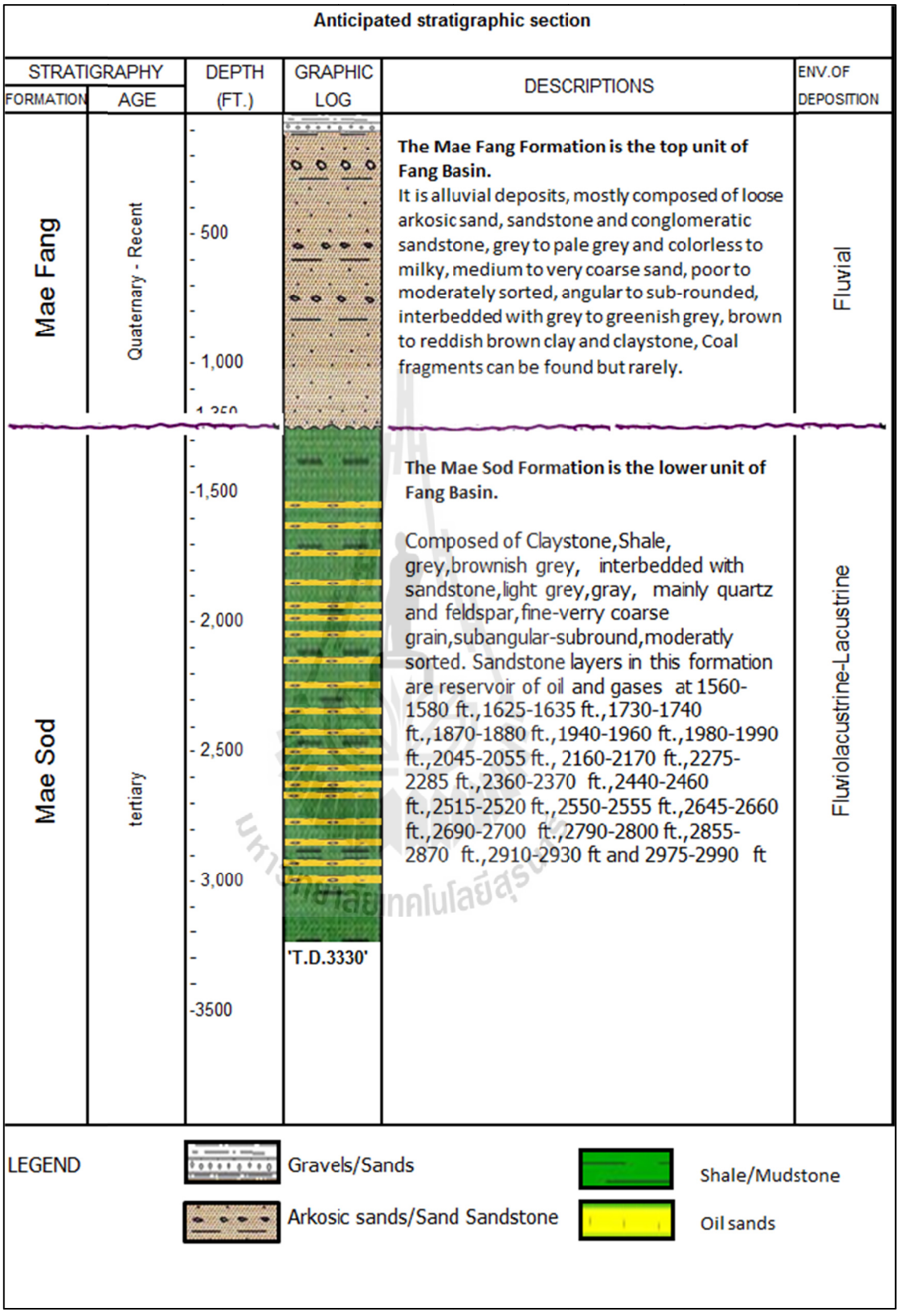

Figure 4.49 Stratigraphic section of well no. FA-MS-54-84.

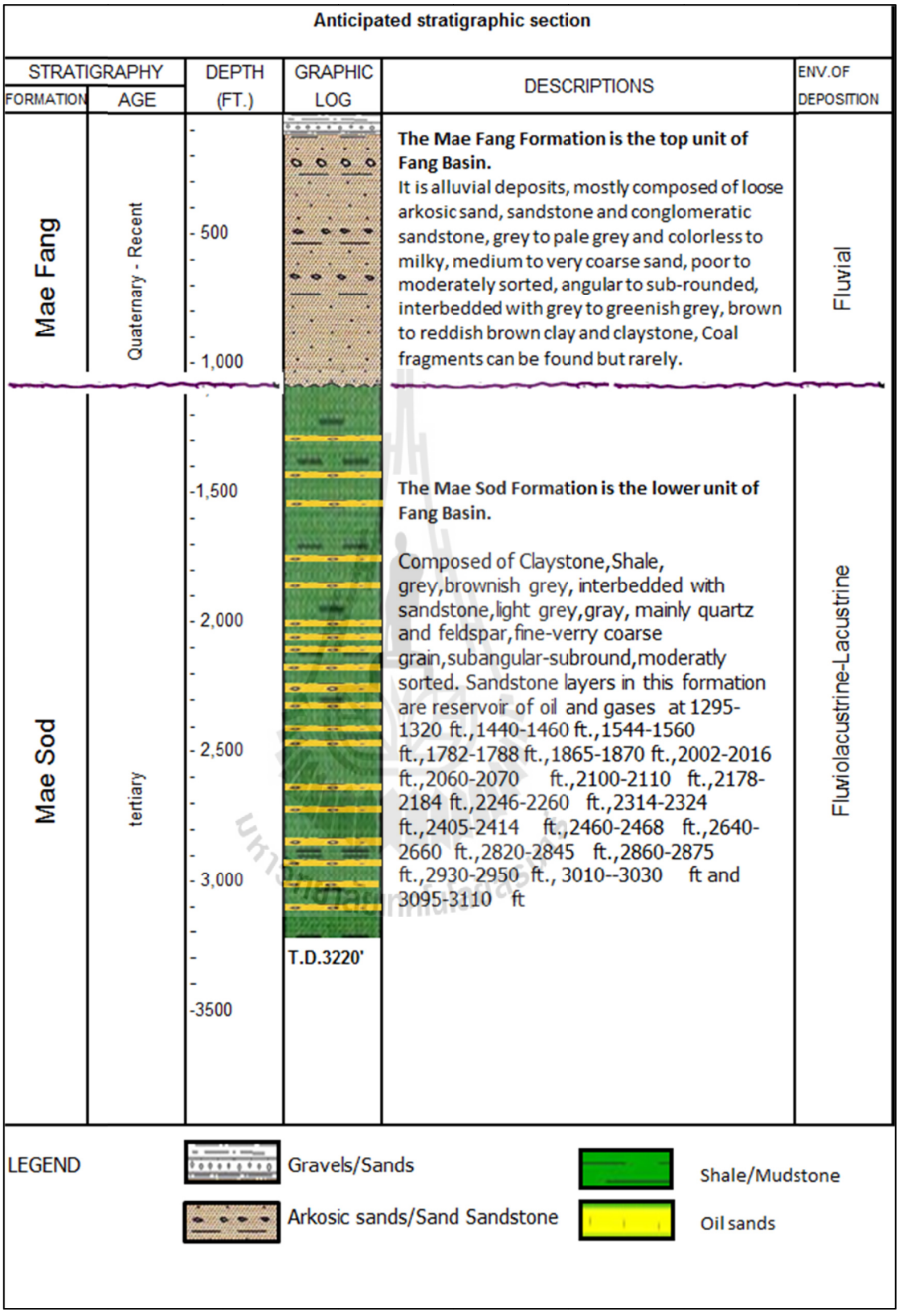

Figure 4.50 Stratigraphic section of well no. FA-MS-54-85.

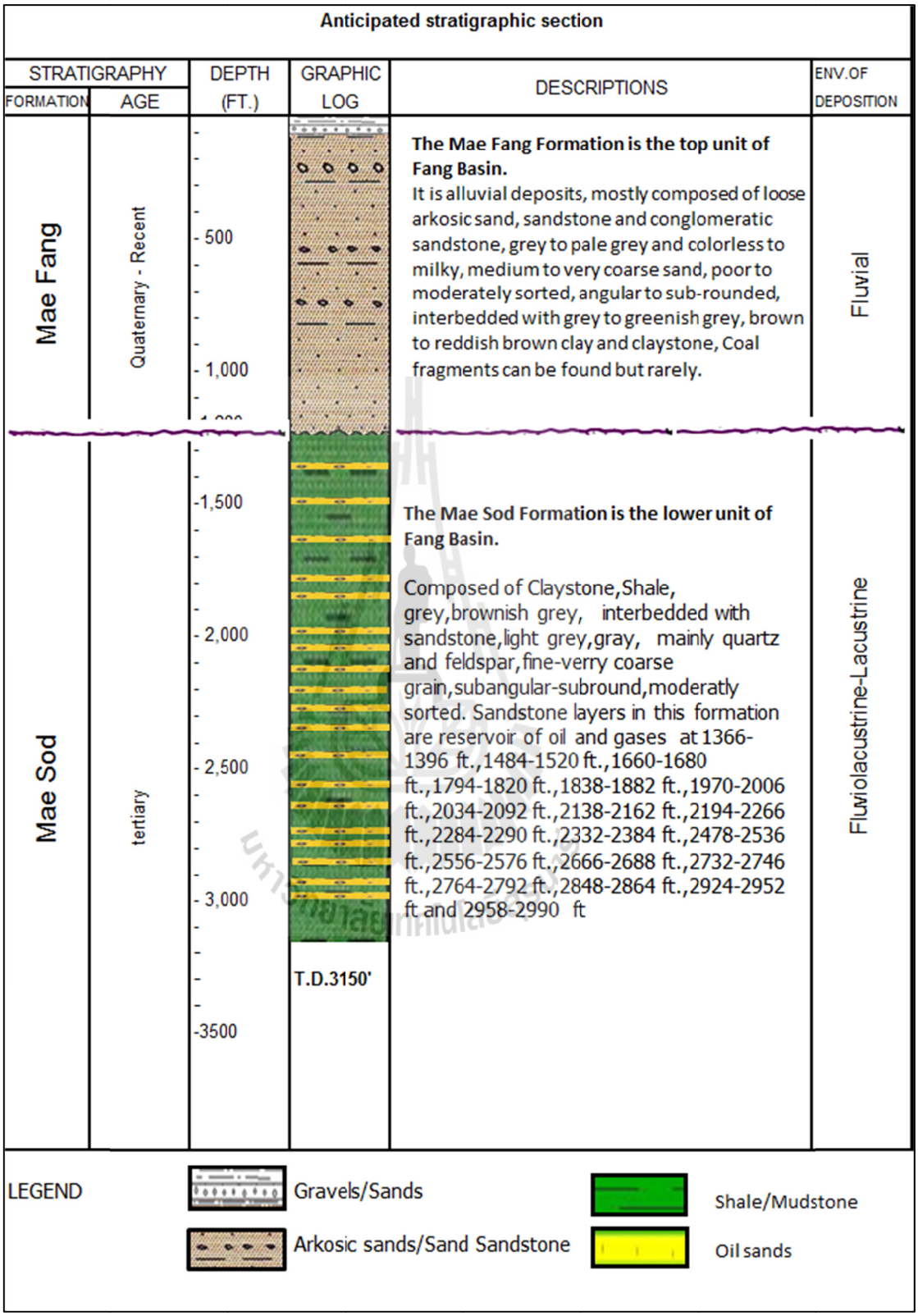

Figure 4.51 Stratigraphic section of well no. FA-MS-54-86.

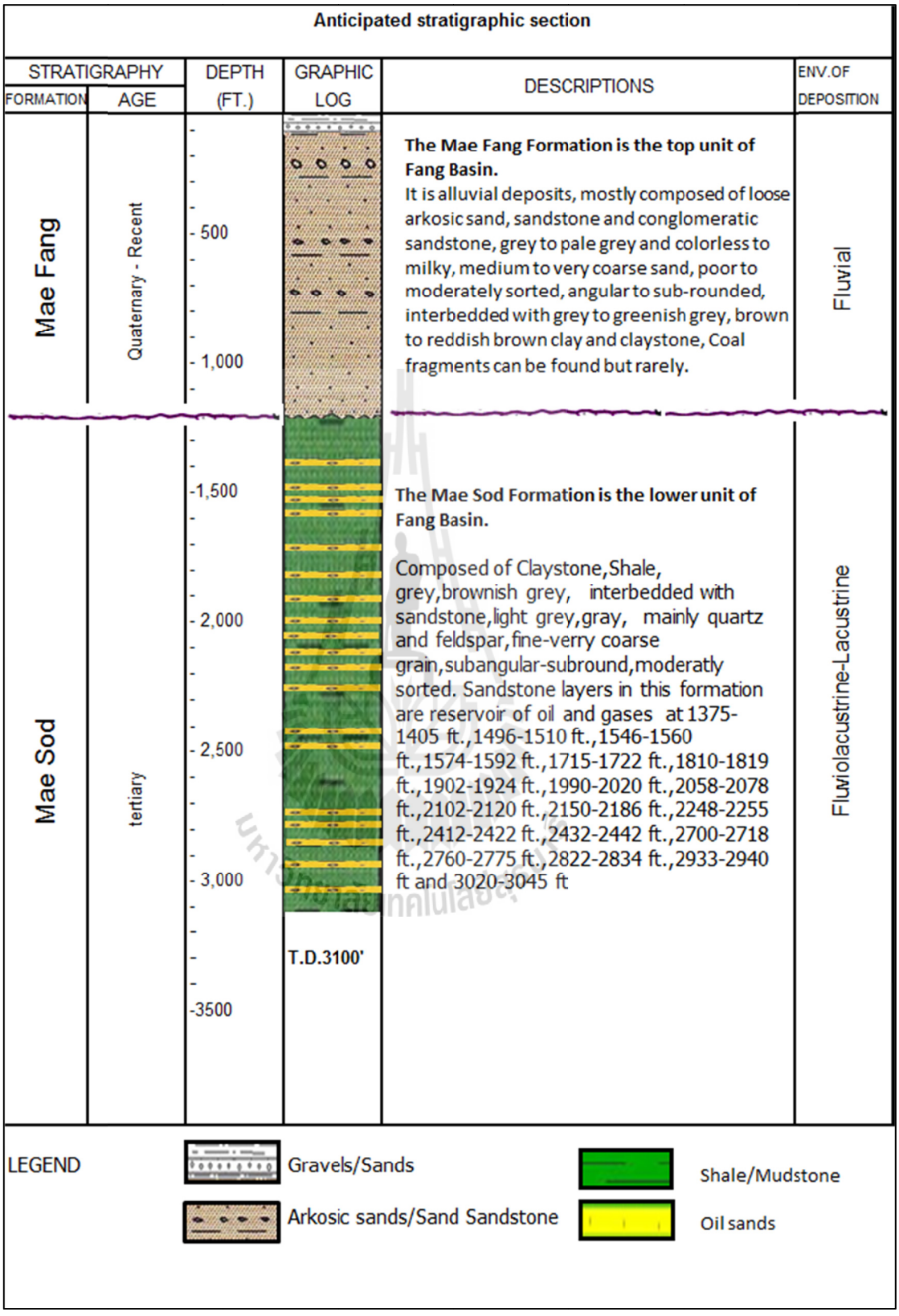

Figure 4.52 Stratigraphic section of well no. FA-MS-55-87.

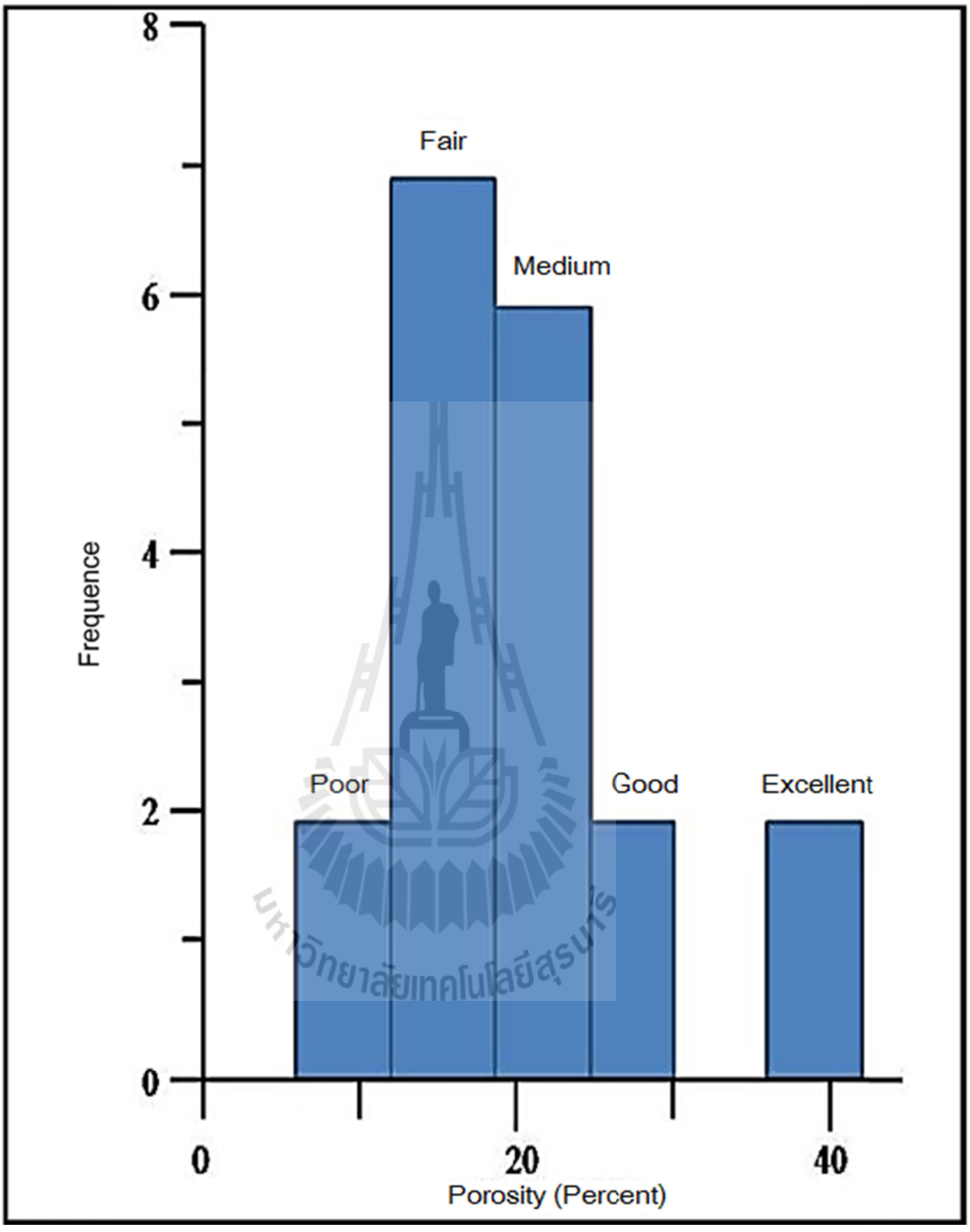

Figure 4.53 Porosity quality distribution of sandstone of Mae-Soon oil field.

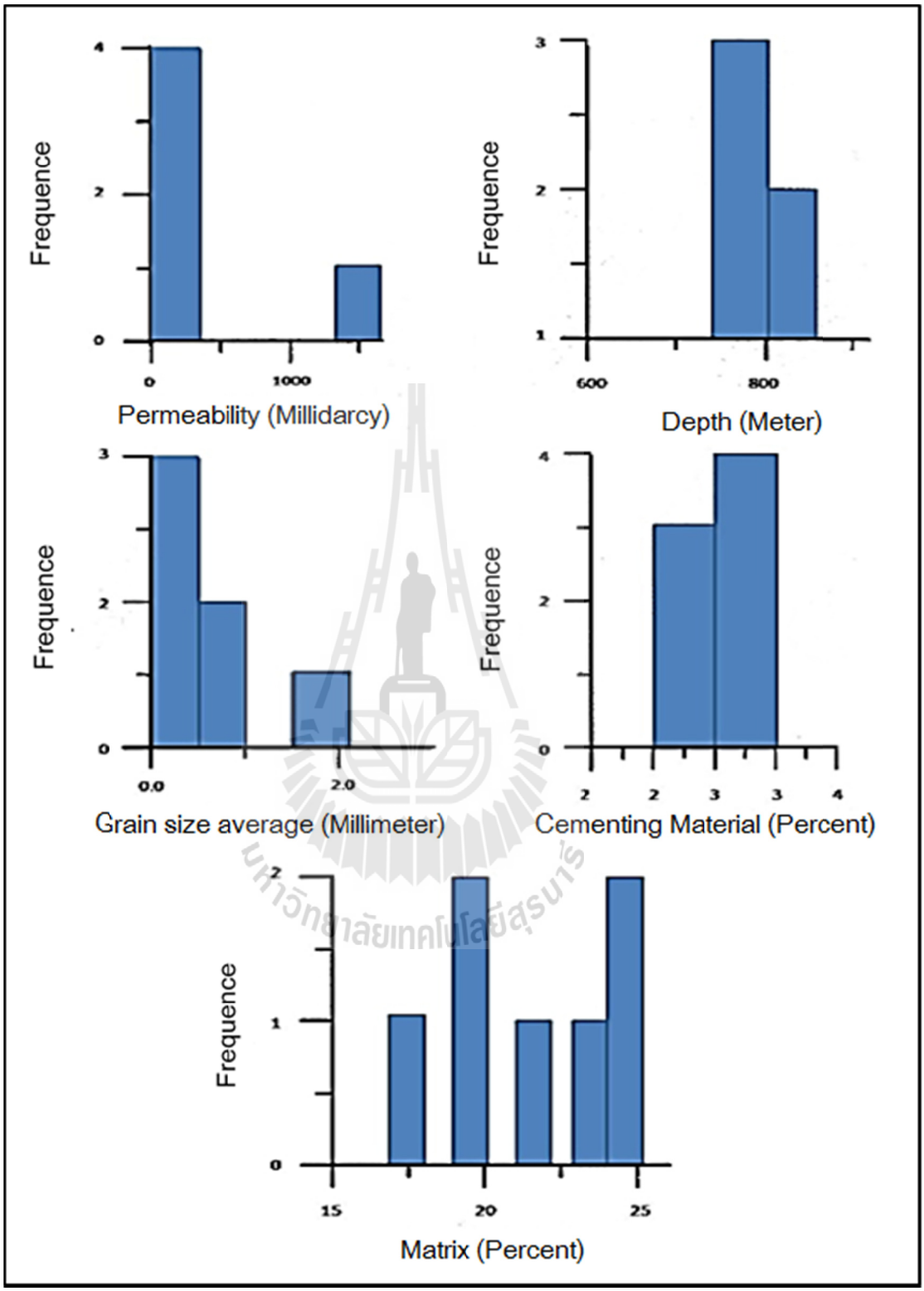

Figure 4.54 Frequency distribution of Permeability, Depth, Grain Size, Cementing Material and Matrix for fair porosity of Mae-Soon oil field.

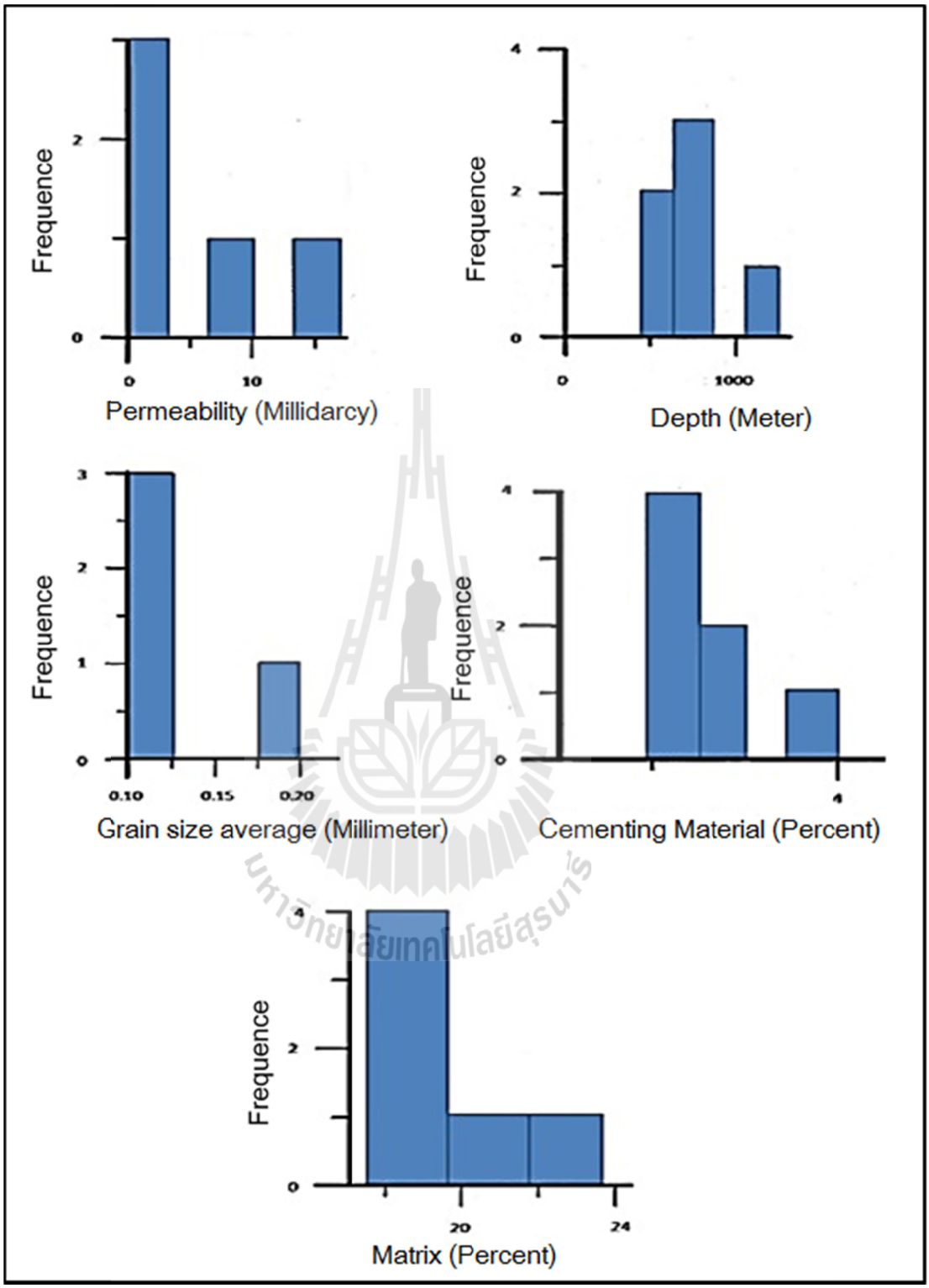

Figure 4.55 Distribution of Permeability, Depth, Grain size, Cementing material and Matrix of 19 sandstone layers of Mae-Soon oil field.

Consequently, the results of porosity and permeability analysis in order to evaluate the ability of 19 sandstone layers of Mae-Soon oil field indicate that these sandstones have capable to store hydrocarbon according to Muskat (1949) and Dickker (1985) classification.

4.3.2 The relationship between rock properties and depth

In general porosity is inversely proportional to depth. Therefore, the relationship between porosity and depth can be determined by cross-plotting these two parameters. Figure 4.56 illustrates the relationship between depth and porosity of the all 19 sandstone layers of Mae-Soon oil field. It is found that porosity is related to depth by the following equation;

$$\text{Depth (feet)} = -8.0106\ (\text{Porosity (percent)}) - 2116.4 \qquad (4.1)$$

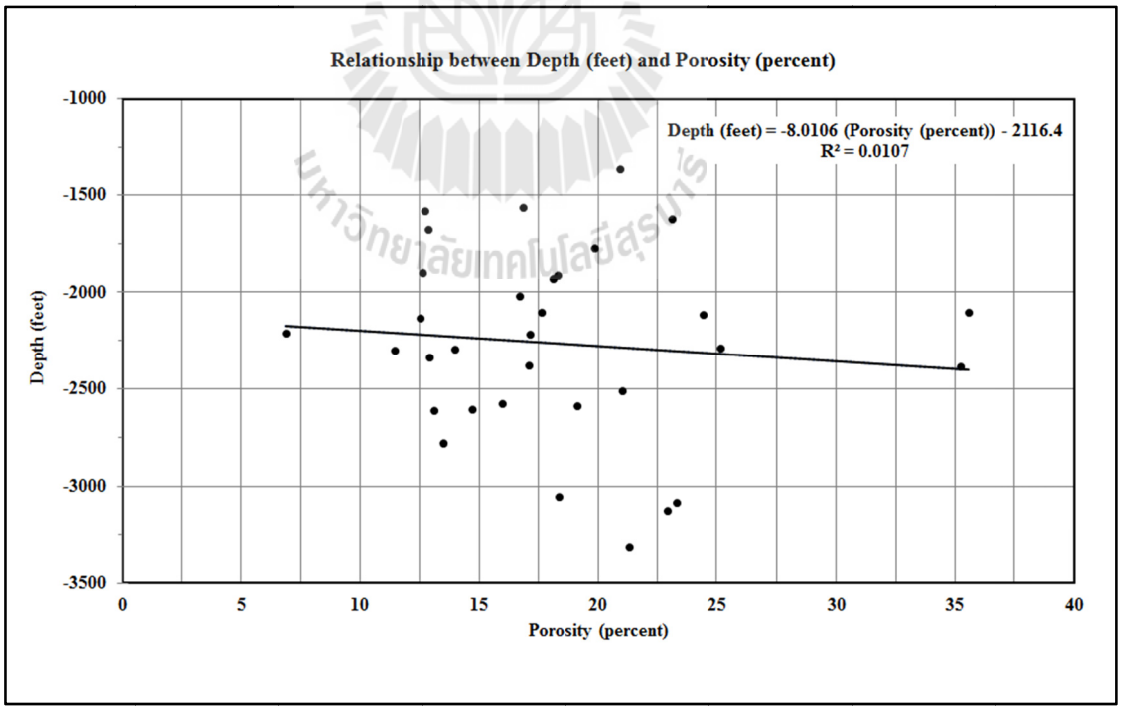

Figure 4.56 Cross-plot between porosity and depth of sandstone of Mae-Soon oil field.

Unlike the relationship between depth and porosity, permeability is directly proportional to porosity. However, the relationship between permeability and porosity can also be determined by cross-plotting these two parameters as well. Figure 4.57 shows the relationship between permeability and porosity of the all 19 sandstone layers of Mae-Soon oil field and it is found that permeability is related to porosity by the following equation;

$$\text{Porosity} = 0.0062\ (\text{Permeability, mDarcy}) + 15.95 \qquad (4.2)$$

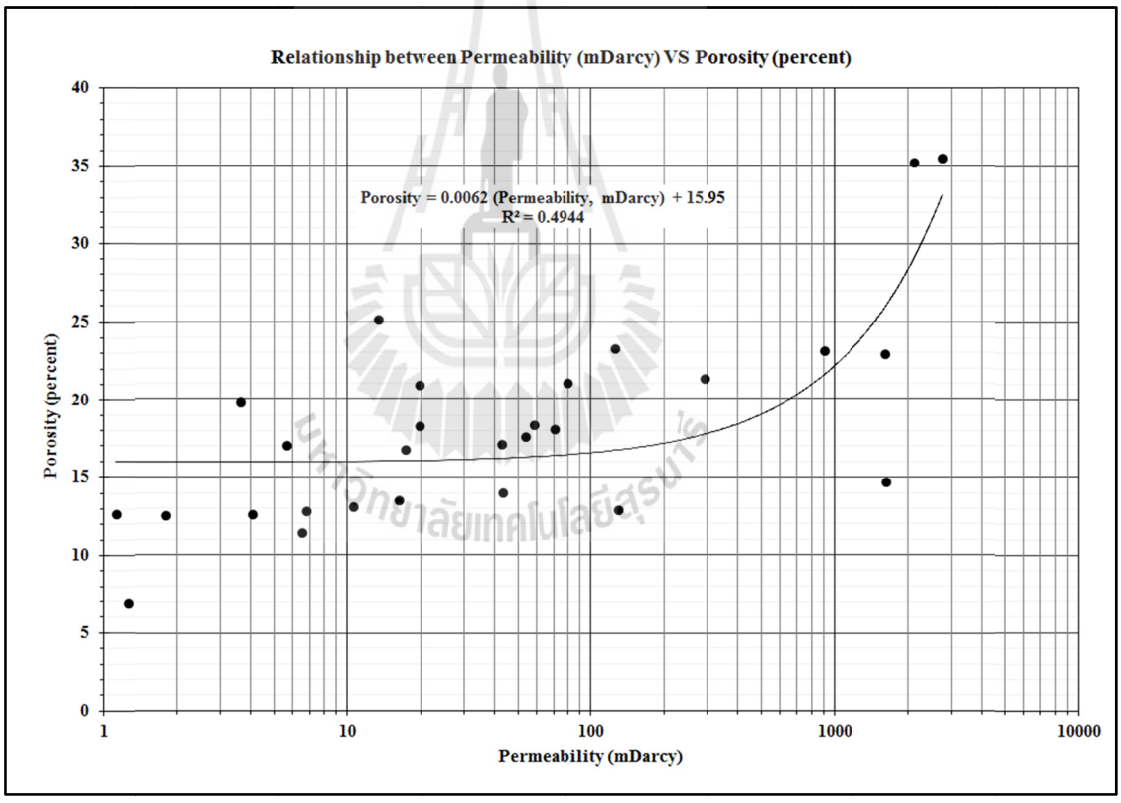

Figure 4.57 Cross-plot between porosity and permeability of sandstone of Mae-Soon oil field.

4.3.3 Grouped sandstone layers thickness, porosity, permeability and hydrocarbon saturation map

Based on lithology and petrophysical properties, including porosity and permeability, potential oil sandstone reservoirs of Mae-Soon oil field could be divided into 3 groups as follows.

Group A: sandstone layer 1 to 6

Group B: sandstone layer 7 to 13

Group C: sandstone layer 14 to 19

Consequently isopach, porosity, permeability, and hydrocarbon saturation distribution map of each sandstone group could be generated as presented in the Figure 4.58 to Figure 4.69, respectively.

Sandstone Group A of Mae-Soon oil field was found at depth 1,295-2,140 feet. It has the thickest layer of about 180 feet and the thinnest layer of about 54 feet. The thick sandstone layer appears mostly on the west side of the study area whereas the east side shows lower thickness. This sandstone is Lithic Greywacke type which is composed of very fine to medium-grained sand. The accumulation is fining upward (Figure 4.58).

Porosity of sandstone Group A of Mae-Soon oil filed is good - very good with an average porosity of 28.05%. The high porosity zone appears at the west of study area and gradually decreases to the east (Figure 4.59).

Permeability of sandstone Group A is fair – good with an average permeability of 466.62 milliDarcy. High permeability appears at the middle-west of the study area and gradually decrease to the east, the north and the south (Figure 4.60).

Hydrocarbon saturation of sandstone Group A is good - very good with an average of 0.55. High hydrocarbon saturation appears at the west side of the study area and gradually decreases to the east (Figure 4.61).

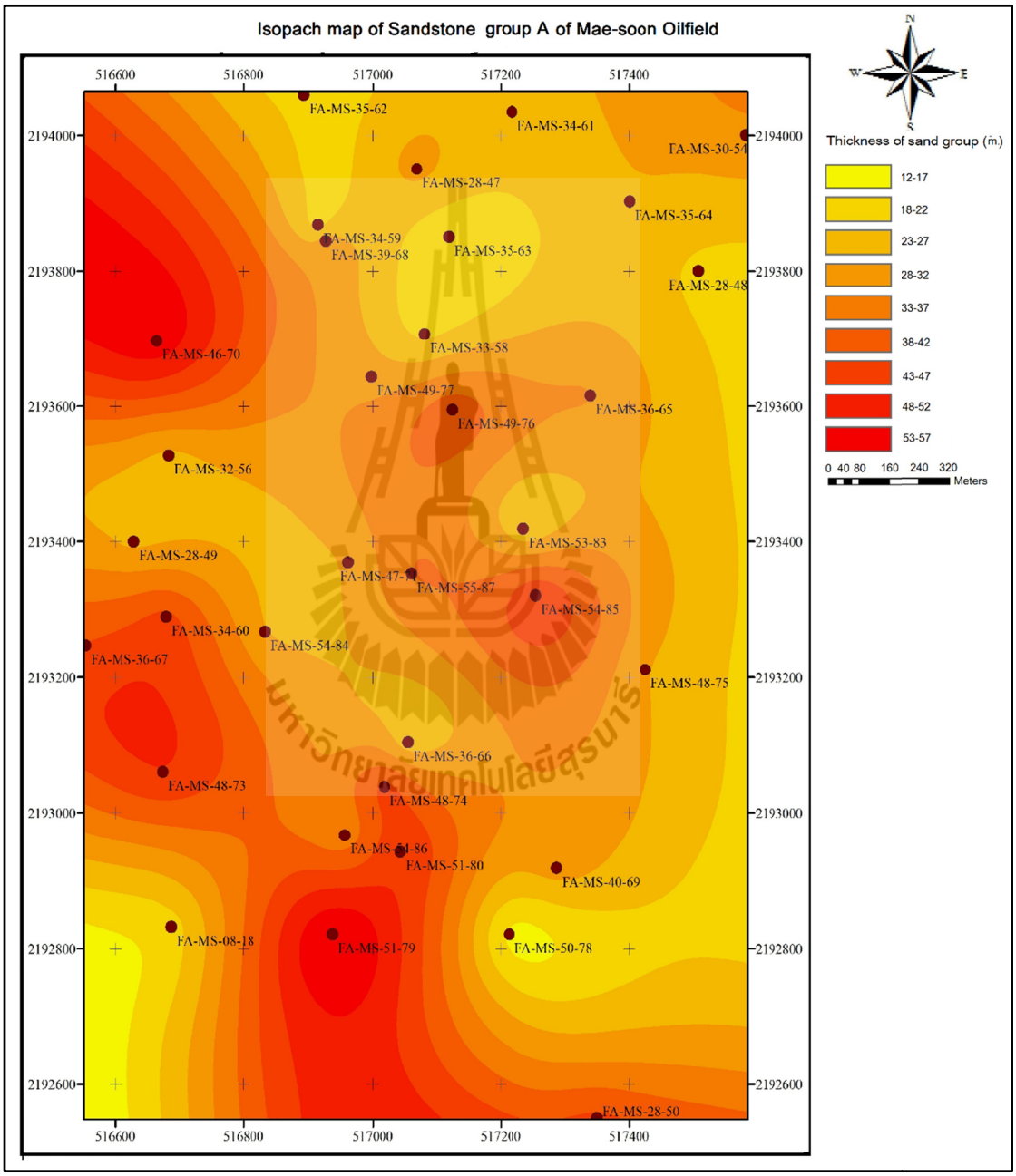

Figure 4.58 Isopach map of sandstone Group A of Mae-Soon oil field.

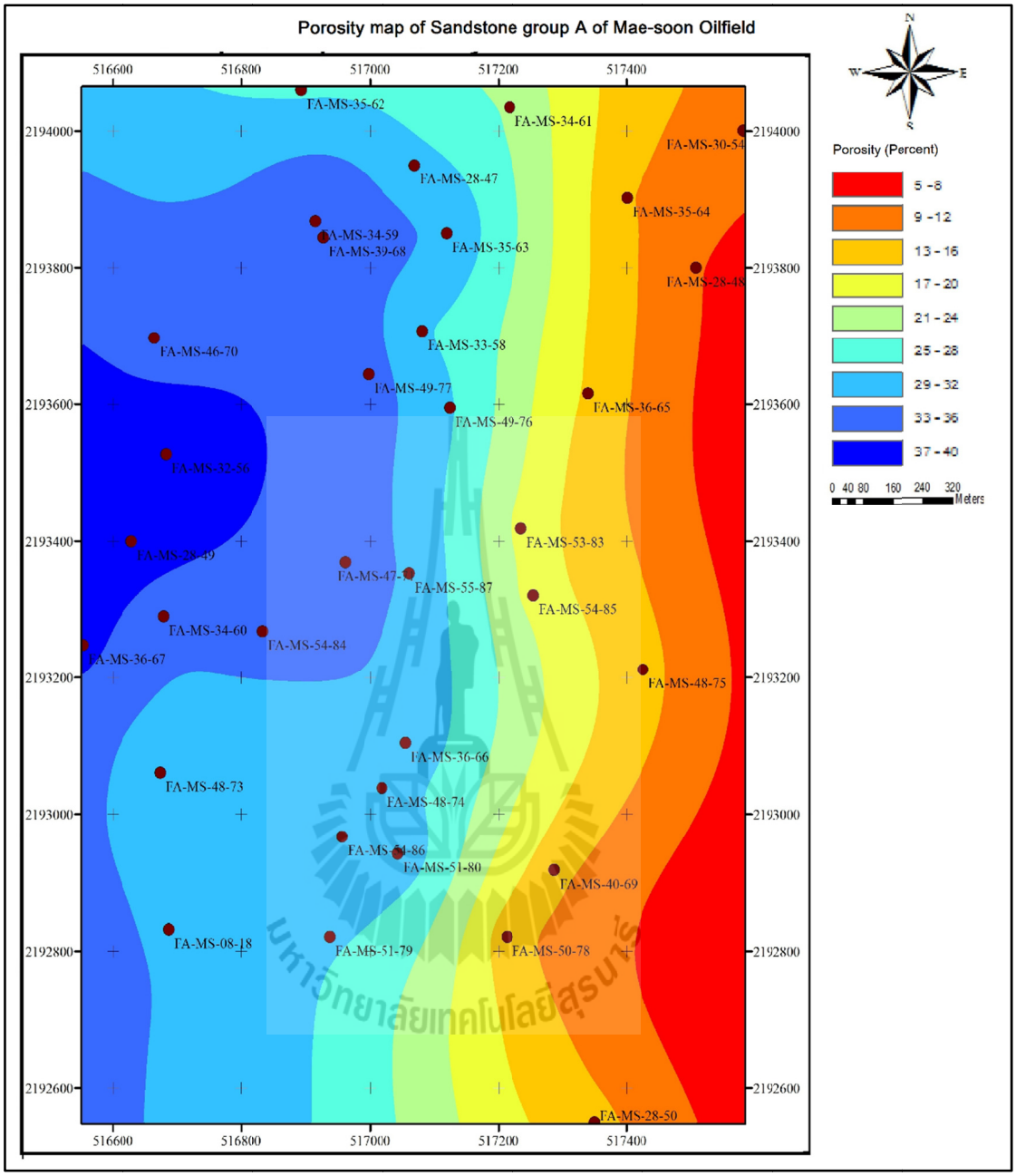

Figure 4.59 Porosity distribution map of sandstone Group A.

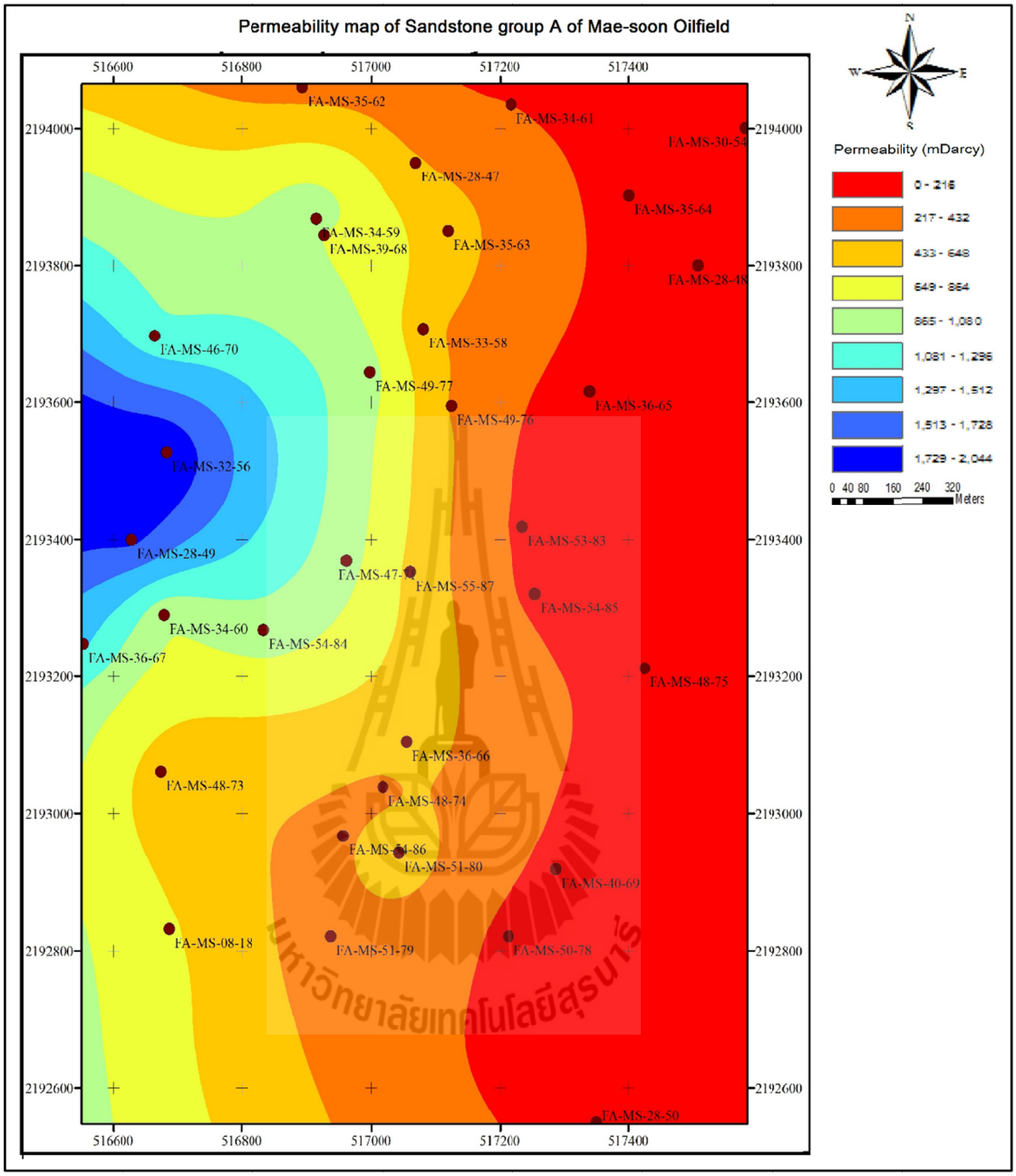

Figure 4.60 Permeability distribution map of sandstone Group A.

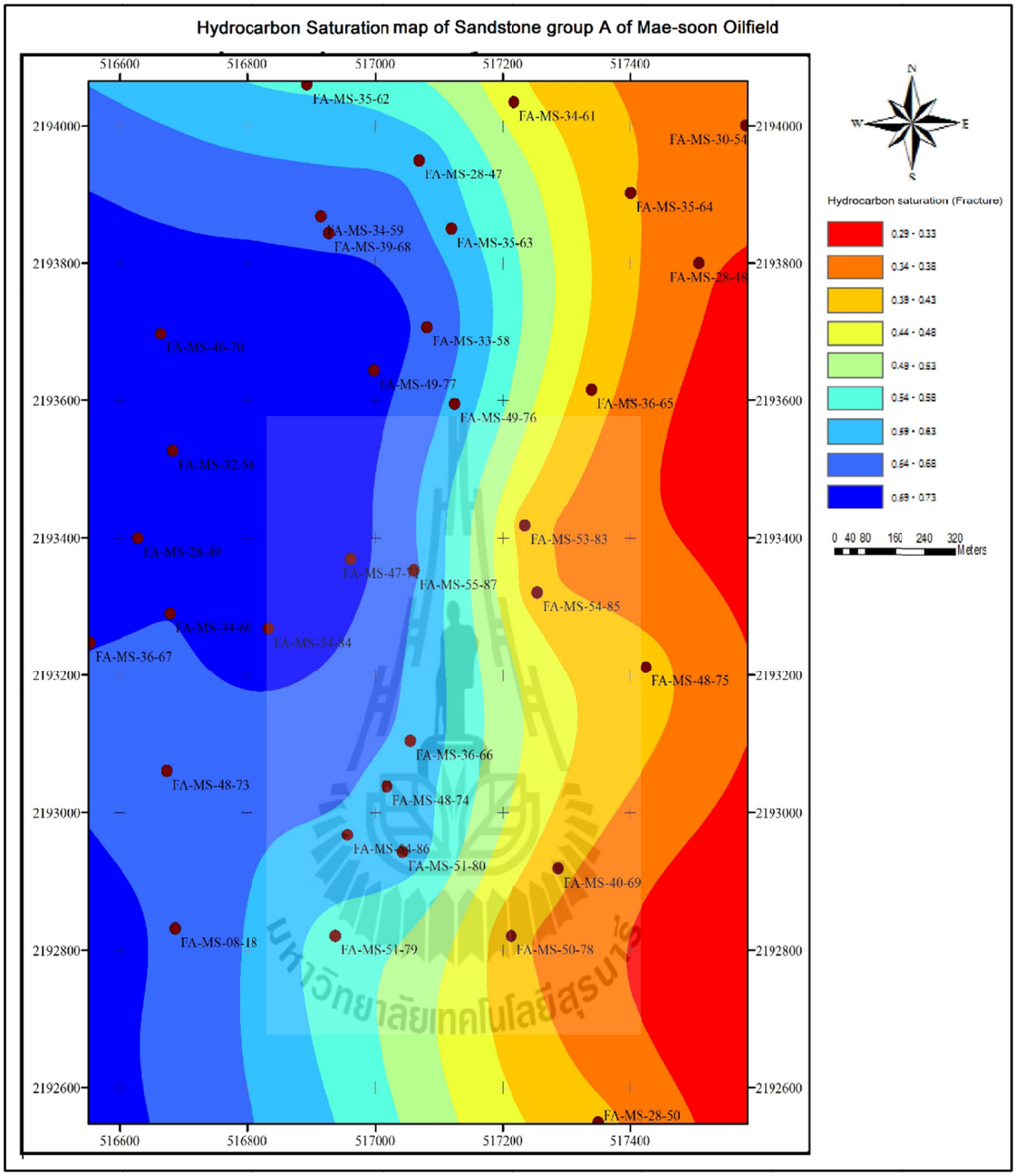

Figure 4.61 Hydrocarbon saturation distribution map of sandstone Group A.

Sandstone Group B of Mae-Soon oil field was found at depth 1,868-2,680 feet. It has the thickest layer of about 270 feet and the thinnest layer of about 57 feet. The thick sandstone layer appears mostly on the north-west side of the study area whereas the lower thickness shows mostly in the central part of the study area. This sandstone is Lithic Greywacke type which is composed of fine to coarse-grained sand. The accumulation is fining upward (Figure 4.62).

Porosity of sandstone Group B of Mae-Soon oil filed is good - very good with an average porosity of 30.77%. The high porosity zone appears at the northern part of study area and gradually decreases to the south (Figure 4.63).

Permeability of sandstone Group B is fair – good with an average permeability of 492.04 milliDarcy. Like porosity, high permeability zone appears at the northern part of the study area and gradually decrease to the south (Figure 4.64).

Hydrocarbon saturation of sandstone Group B is good - very good with an average of 0.52. Conforming to porosity and permeability, high hydrocarbon saturation zone appears at the northern part of the study area and gradually decreases to the south (Figure 4.65).

มหาวิทยาลัยเทคโนโลยีสุรนารี

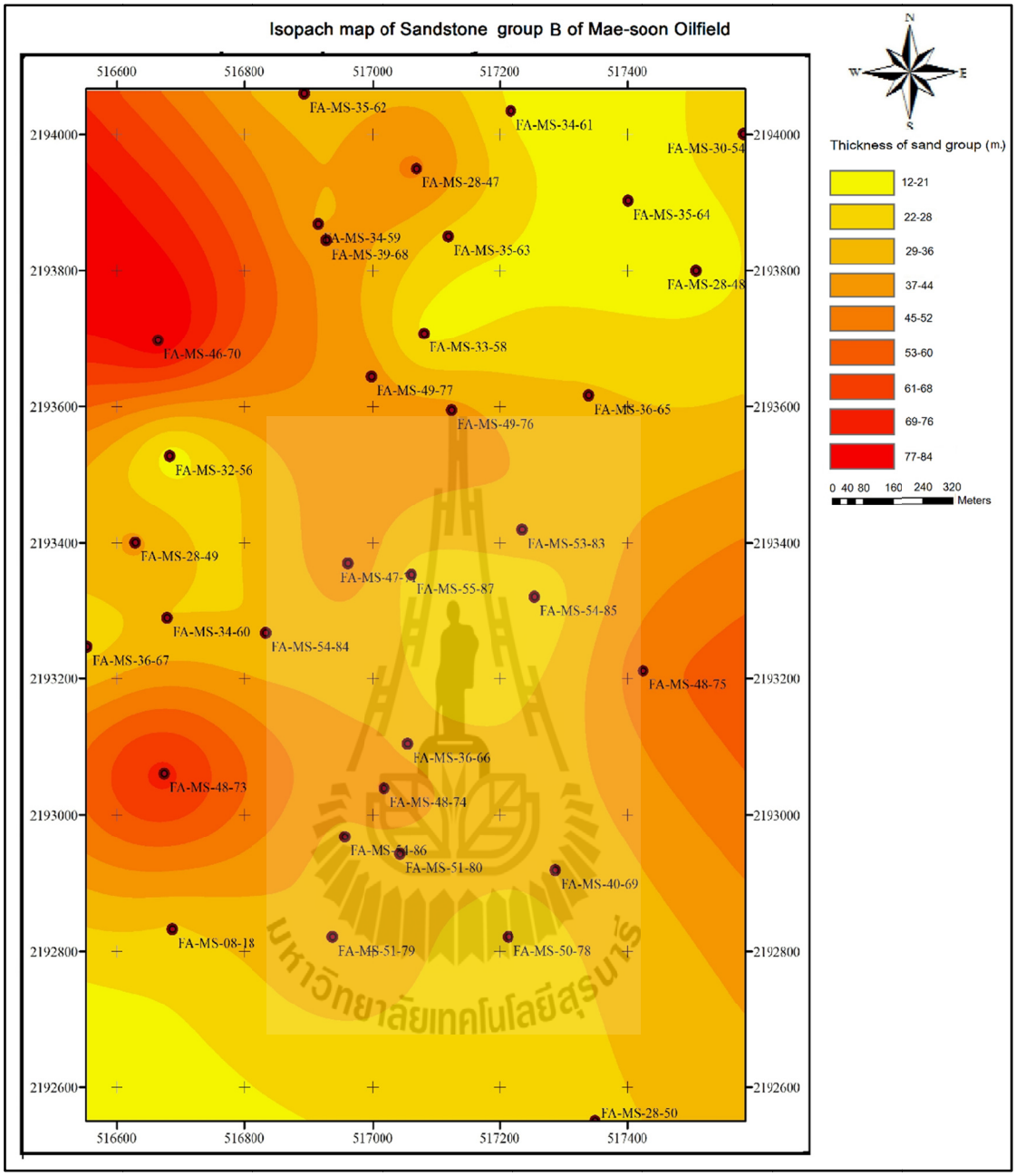

Figure 4.62 Isopach map of sandstone Group B of Mae-Soon oil field.

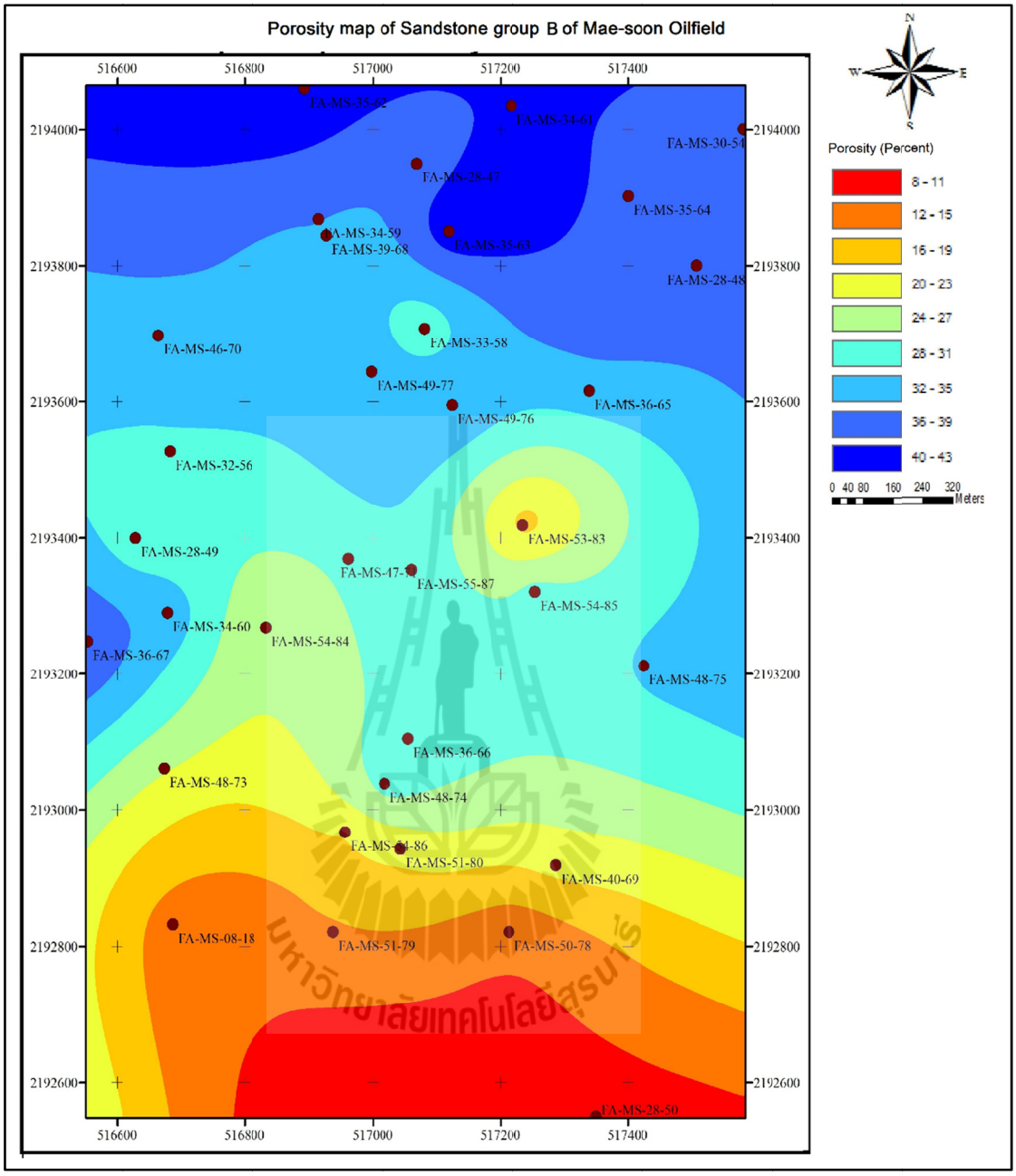

Figure 4.63 Porosity distribution map of sandstone Group B.

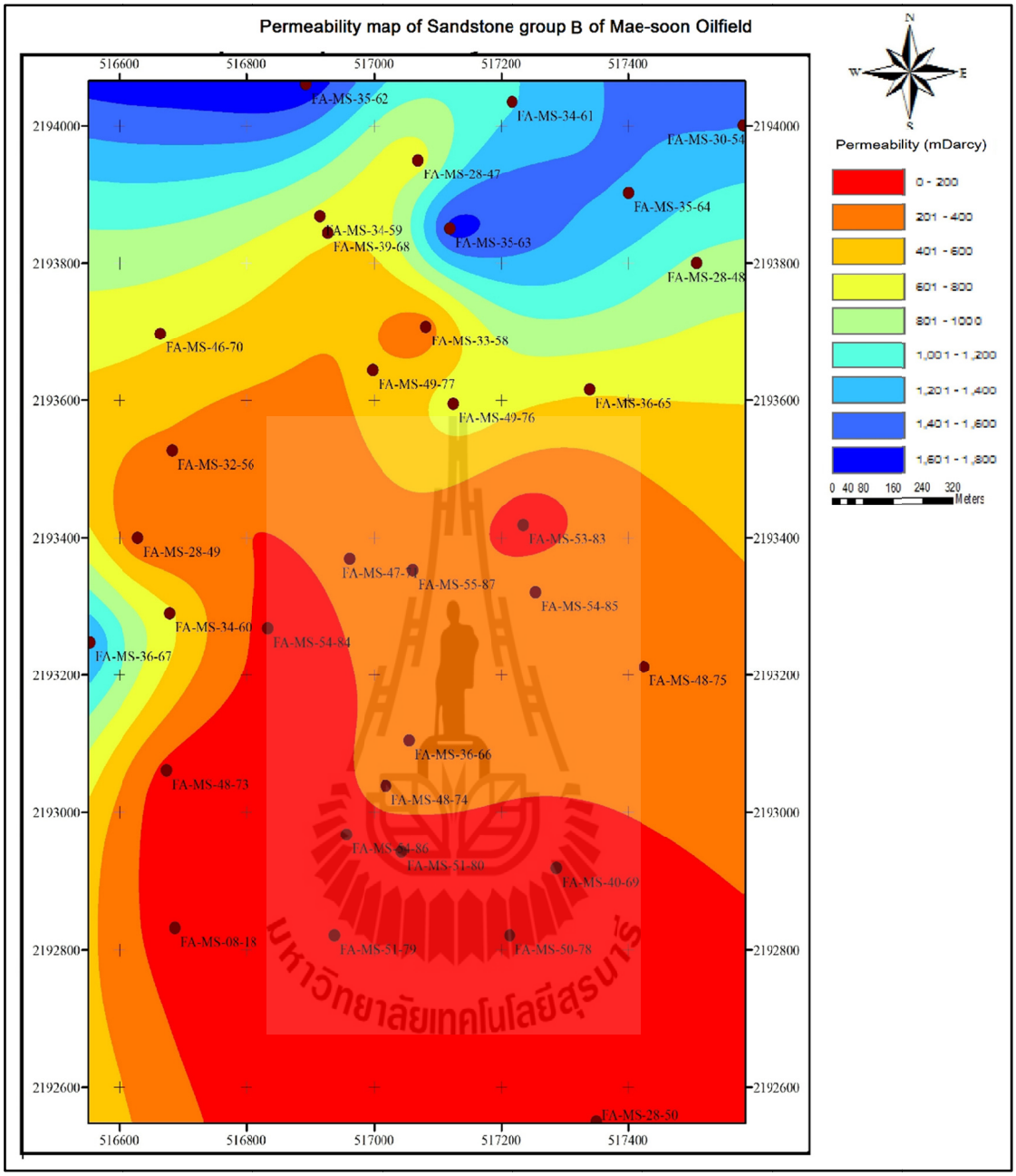

Figure 4.64 Permeability distribution map of sandstone Group B.

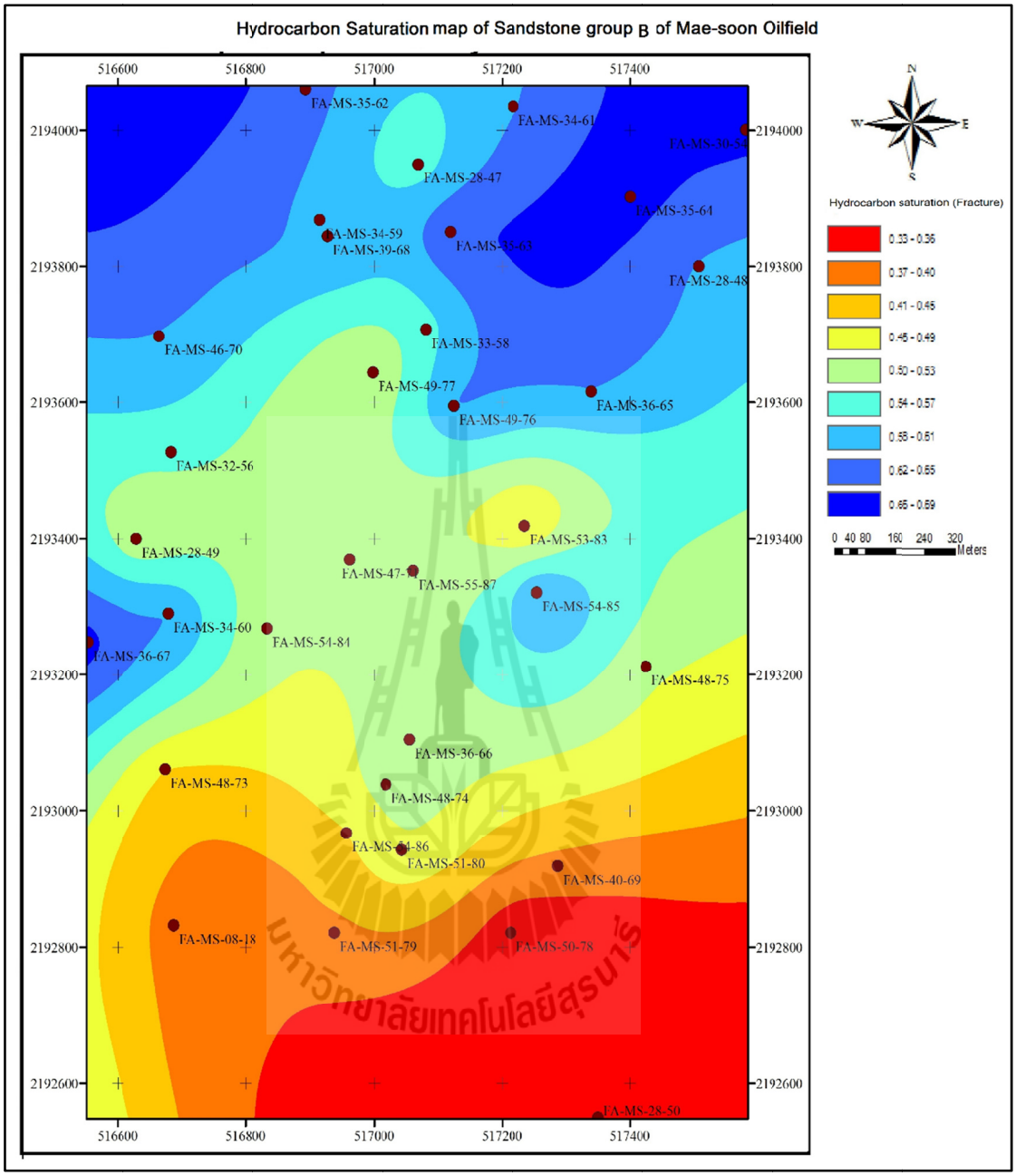

Figure 4.65 Hydrocarbon saturation distribution map of sandstone Group B.

Sandstone Group C of Mae-Soon oil field was found at depth 2,326-3,434 feet. It has the thickest layer of about 163 feet and the thinnest layer of about 60 feet. The thick sandstone layer appears mostly all parts of the study area whereas the lower thickness shows only in the central part of the study area. This sandstone is Quartz Wacke type which is composed of very fine to medium-grained sand. The accumulation is also fining upward (Figure 4.66).

Porosity of sandstone Group C of Mae-Soon oil filed is good - very good with an average porosity of 29.15%. The high porosity zones appear at the northern and the central part of study area whereas the lower porosity zones appear at the south and the west (Figure 4.67).

Permeability of sandstone Group C is good – very good with an average permeability of 599.41 milliDarcy. Like porosity, high permeability zones appear at the northern and the central part of study area whereas the lower porosity zones appear at the south and the west (Figure 4.68).

Hydrocarbon saturation of sandstone Group C is good - very good with an average of 0.52. Conforming to porosity and permeability, the high hydrocarbon saturation zones appear at the northern and the central part of study area whereas the lower porosity zones appear at the south and the west (Figure 4.69).

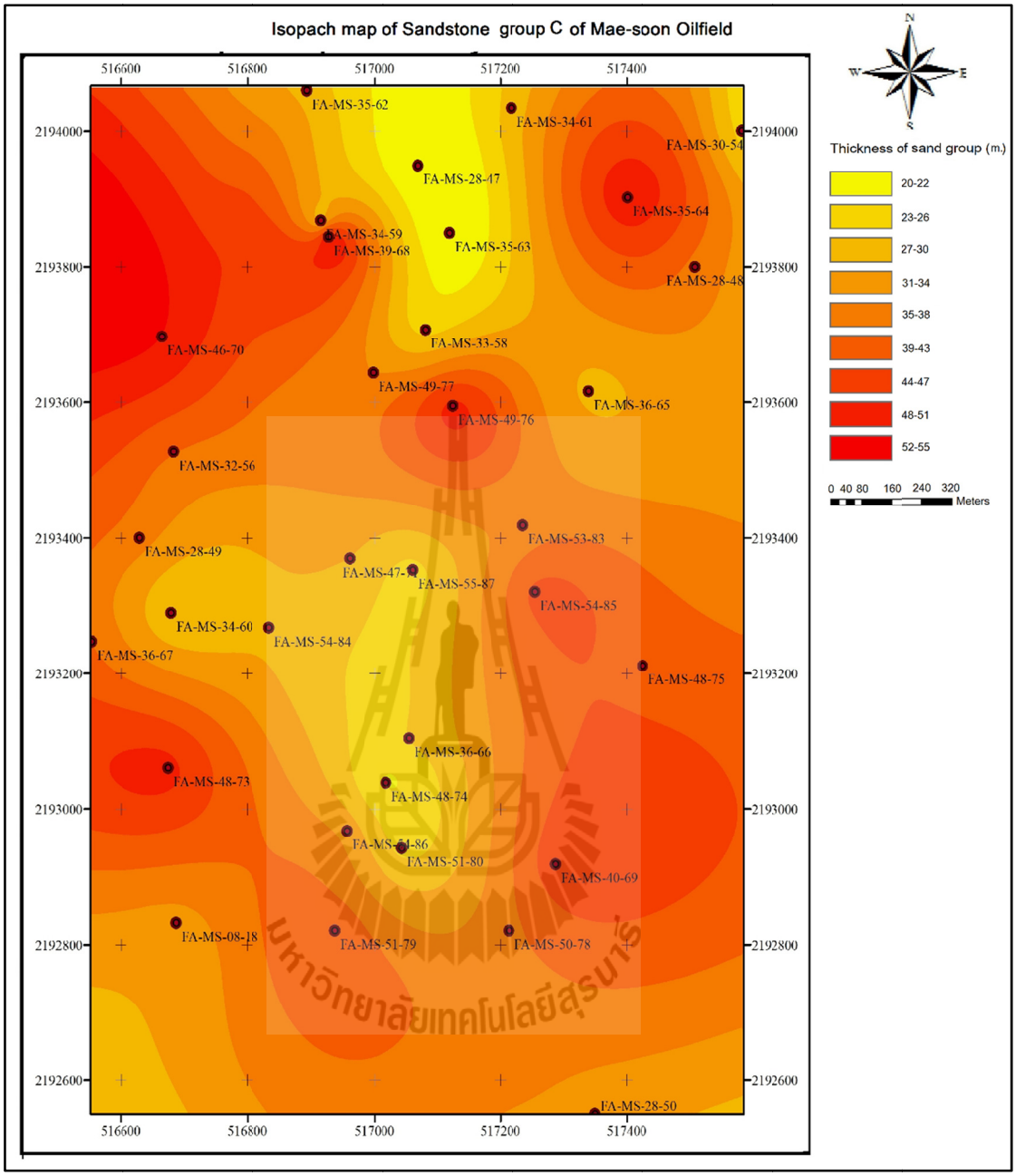

Figure 4.66 Isopach map of sandstone Group C of Mae-Soon oil field.

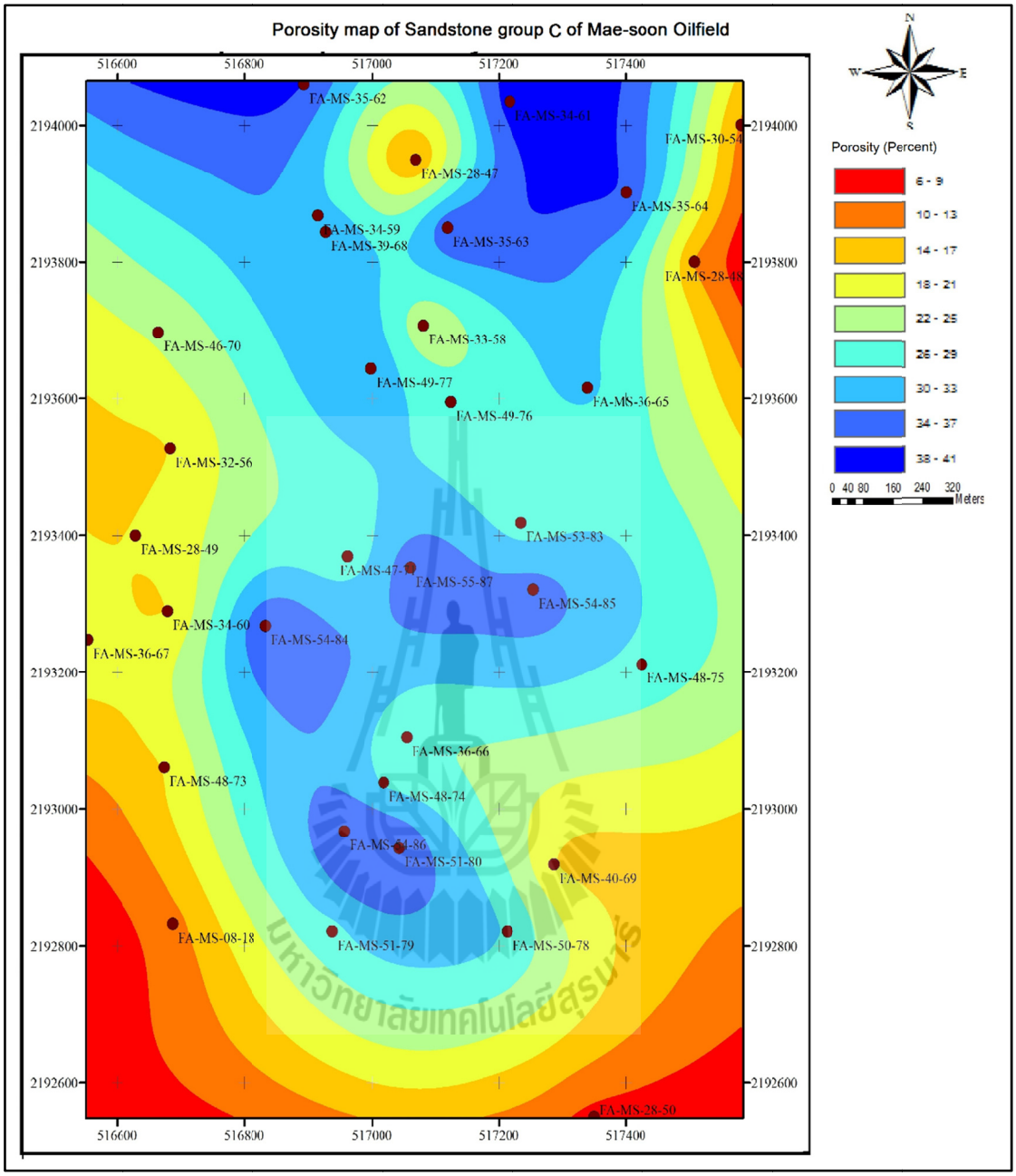

Figure 4.67 Porosity distribution map of sandstone Group C.

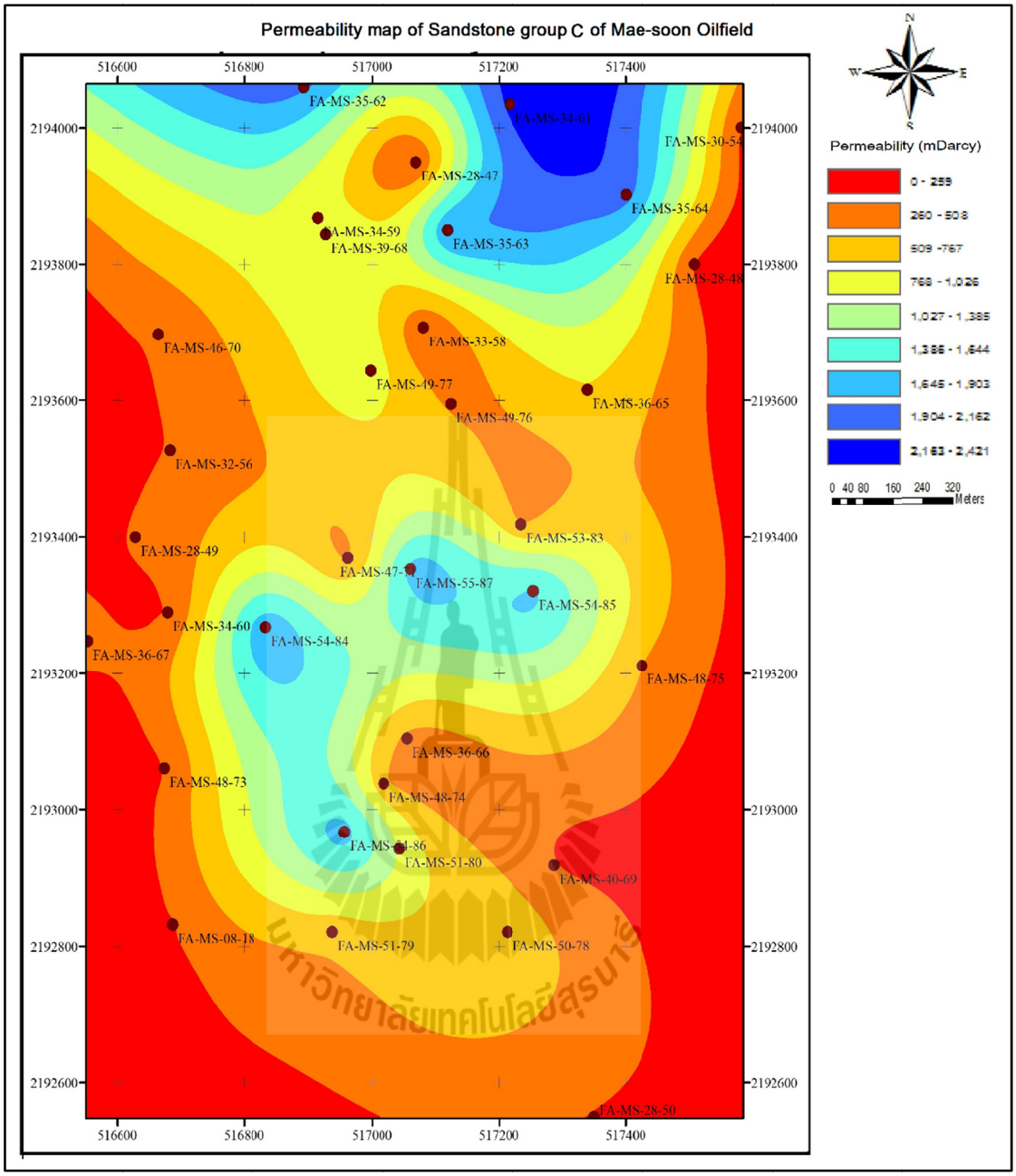

Figure 4.68 Permeability distribution map of sandstone Group C.

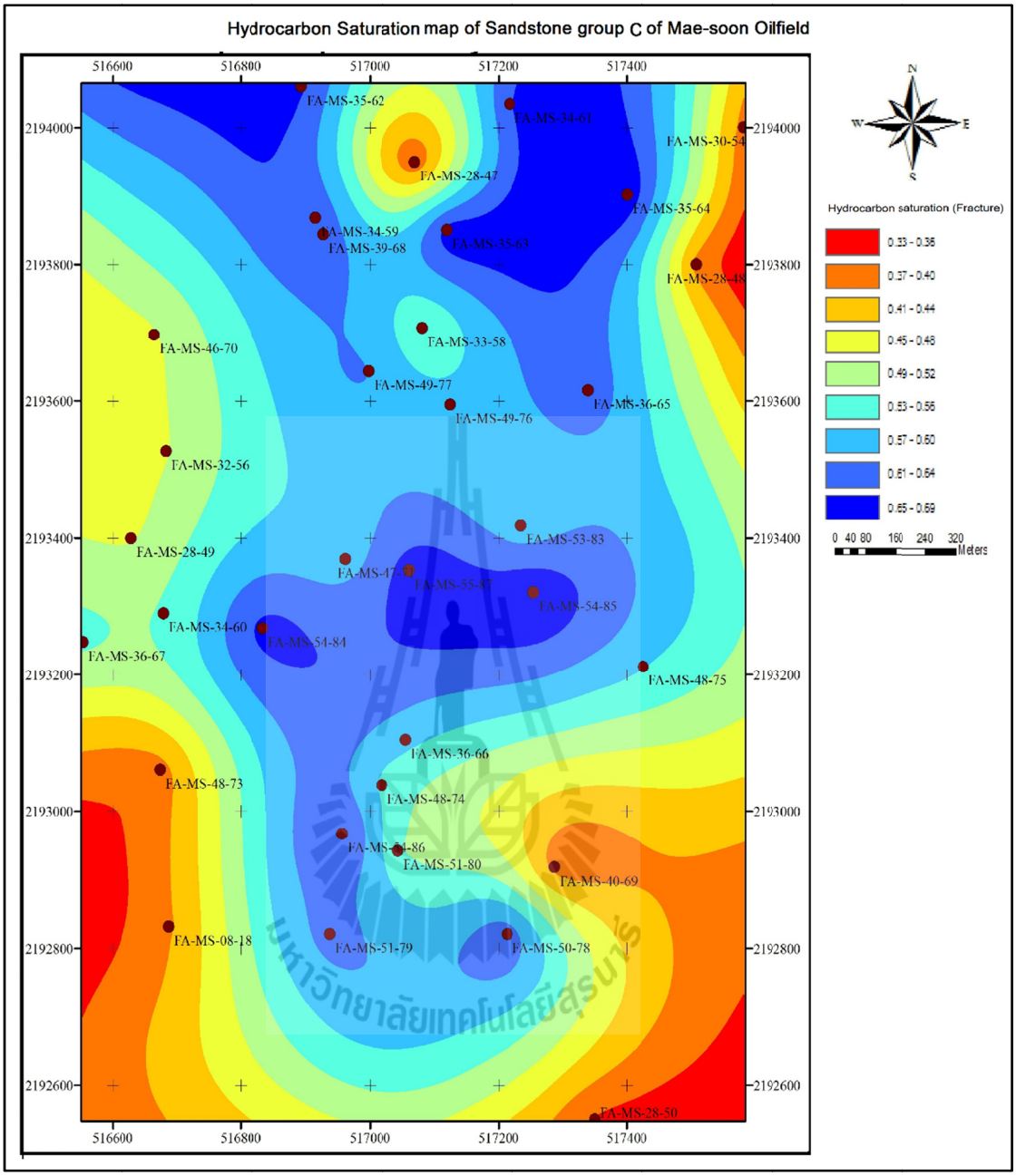

Figure 4.69 Hydrocarbon saturation distribution map of sandstone Group C.

4.4 Potential hydrocarbon-bearing zones of Mae-Soon oil field

To identify the potential hydrocarbon-bearing zone of each grouped sandstone layer of Mae-Soon oil field, isopach, porosity, permeability and hydrocarbon saturation map of each grouped sandstone layer (Figure 4.70 to Figure 4.75) were analyzed all together, and then the boundary of the potential hydrocarbon-bearing zone of each grouped sandstone layer could be drawn. The identified potential hydrocarbon-bearing zones were ranked by its potential from high to low in the order number.

Sandstone group A (Figure 4.71) has two potential hydrocarbon-bearing zones. The first zone is located in the north-western and the central part whereas the second potential zone is located in the western and the southern part of the study area. Porosity and permeability of both zones are very good to excellent.

Sandstone group B (Figure 4.73) has three potential hydrocarbon-bearing zones. The first zone is located in the north-western part of the study area. The second potential zone is located in the eastern part whereas the third zone is located in the western part of the study area. Porosity and permeability of the first zone are highest and decreased in the second zone and the third zone respectively.

Sandstone group C (Figure 4.75) has four potential hydrocarbon-bearing zones. The first zone is located in the north-western part of the study area. The second potential zone is located in the north-eastern part. The third zone is located in the eastern part of the study area where as the fourth zone is located at the south-western part of the study area.

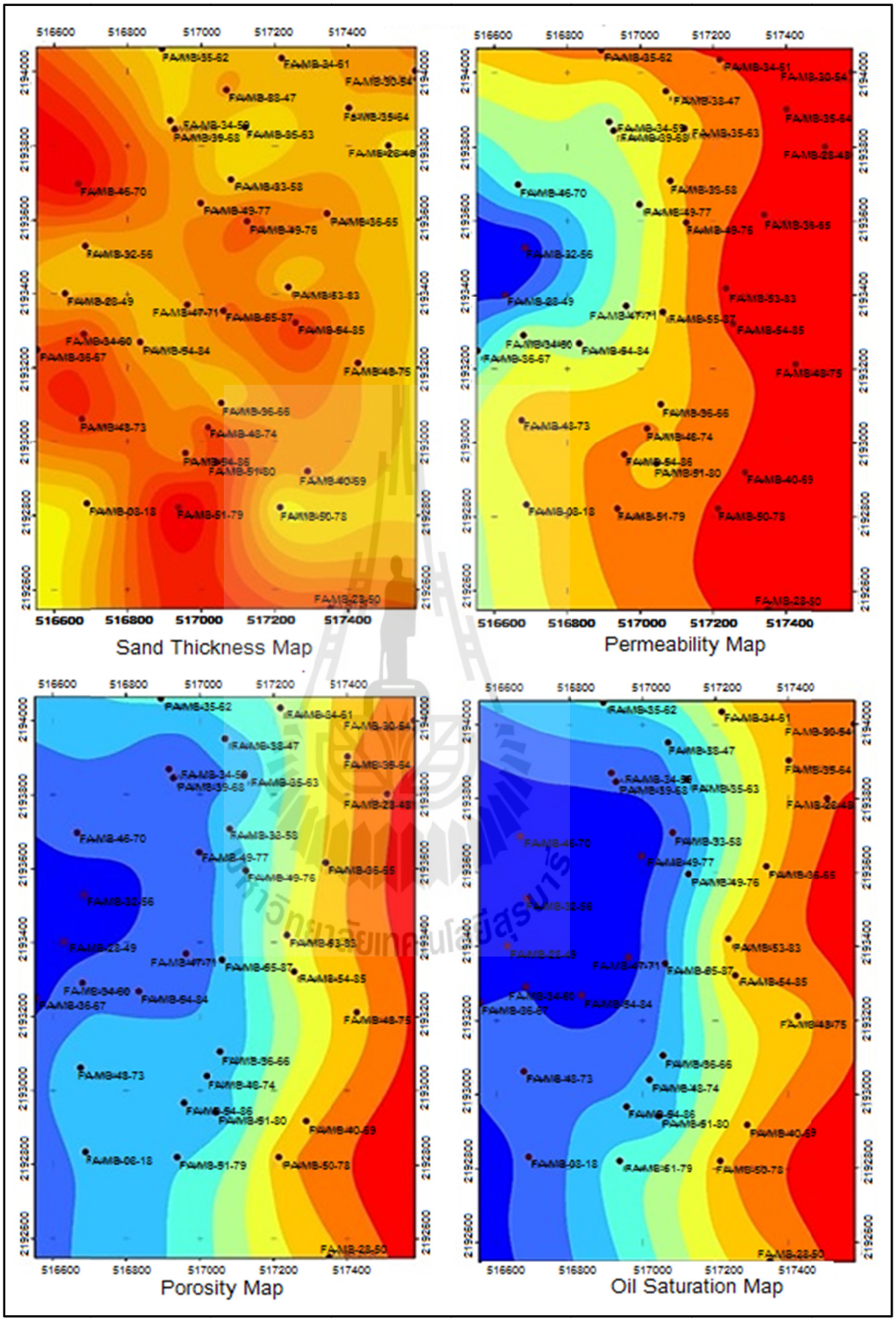

Figure 4.70 Isopach, porosity, permeability and hydrocarbon saturation map of sandstone Group A.

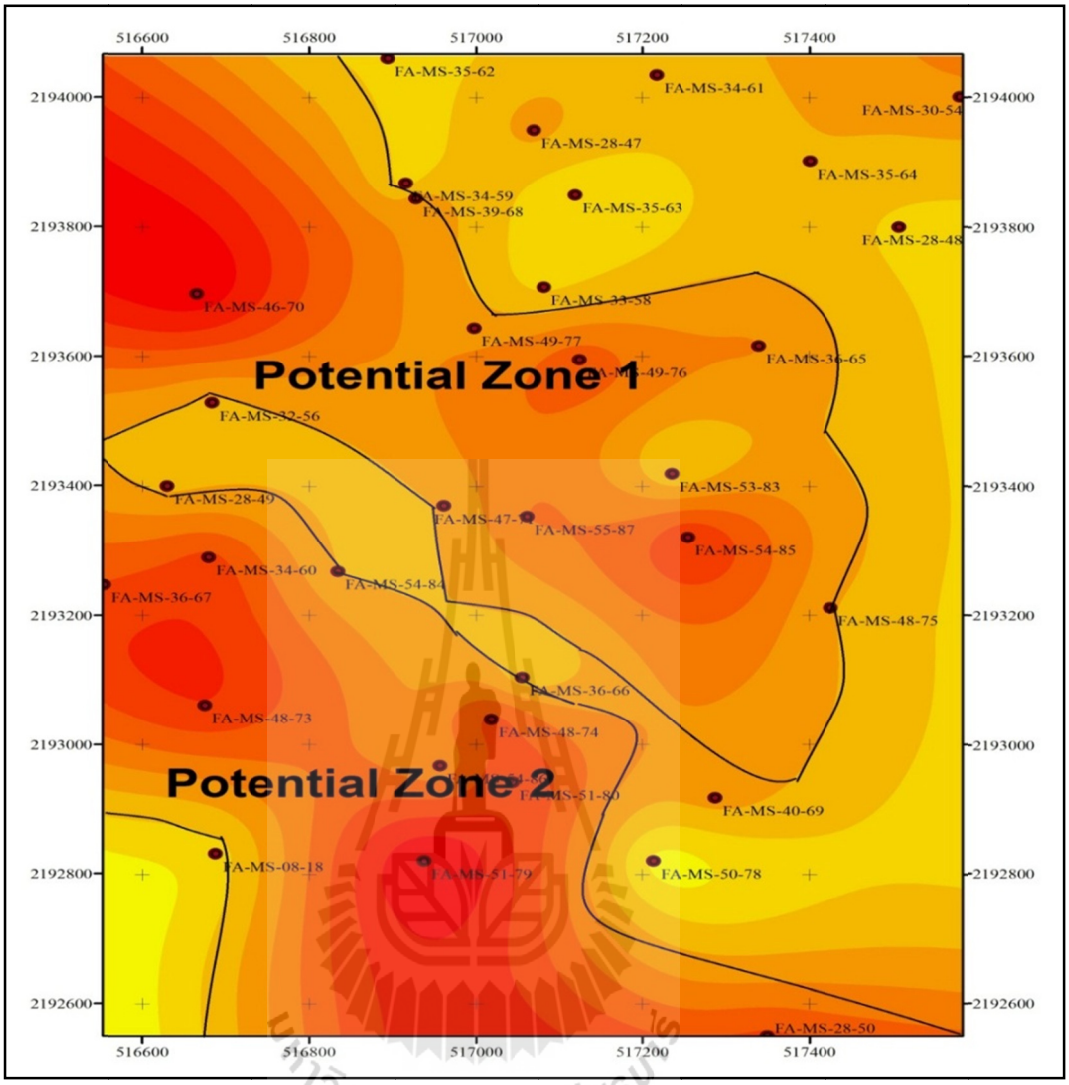

Figure 4.71 Hydrocarbon-bearing potential zone of sandstone Group A.

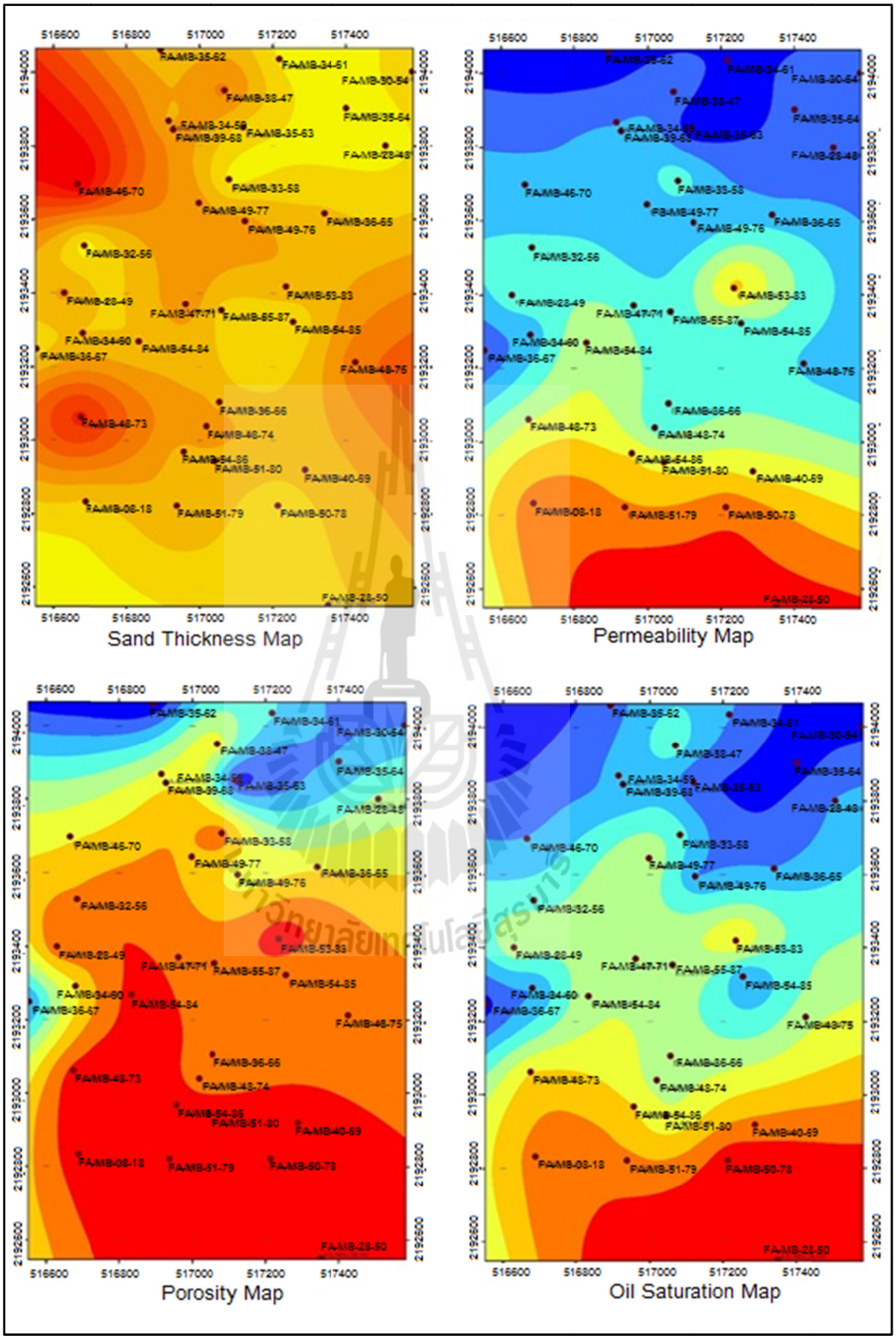

Figure 4.72 Isopach, porosity, permeability and hydrocarbon saturation map of sandstone Group B.

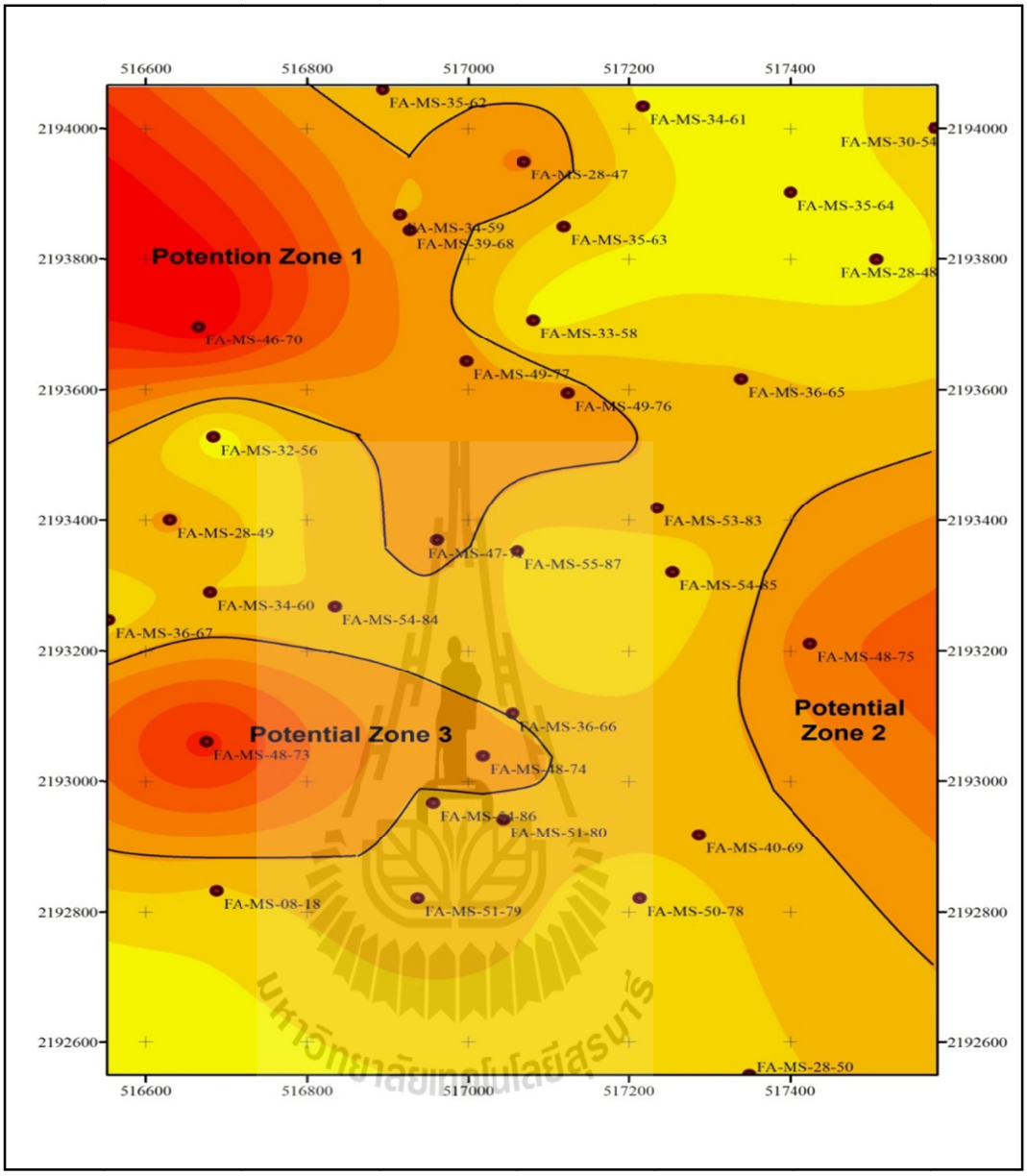

Figure 4.73 Hydrocarbon-bearing potential zone of sandstone Group B.

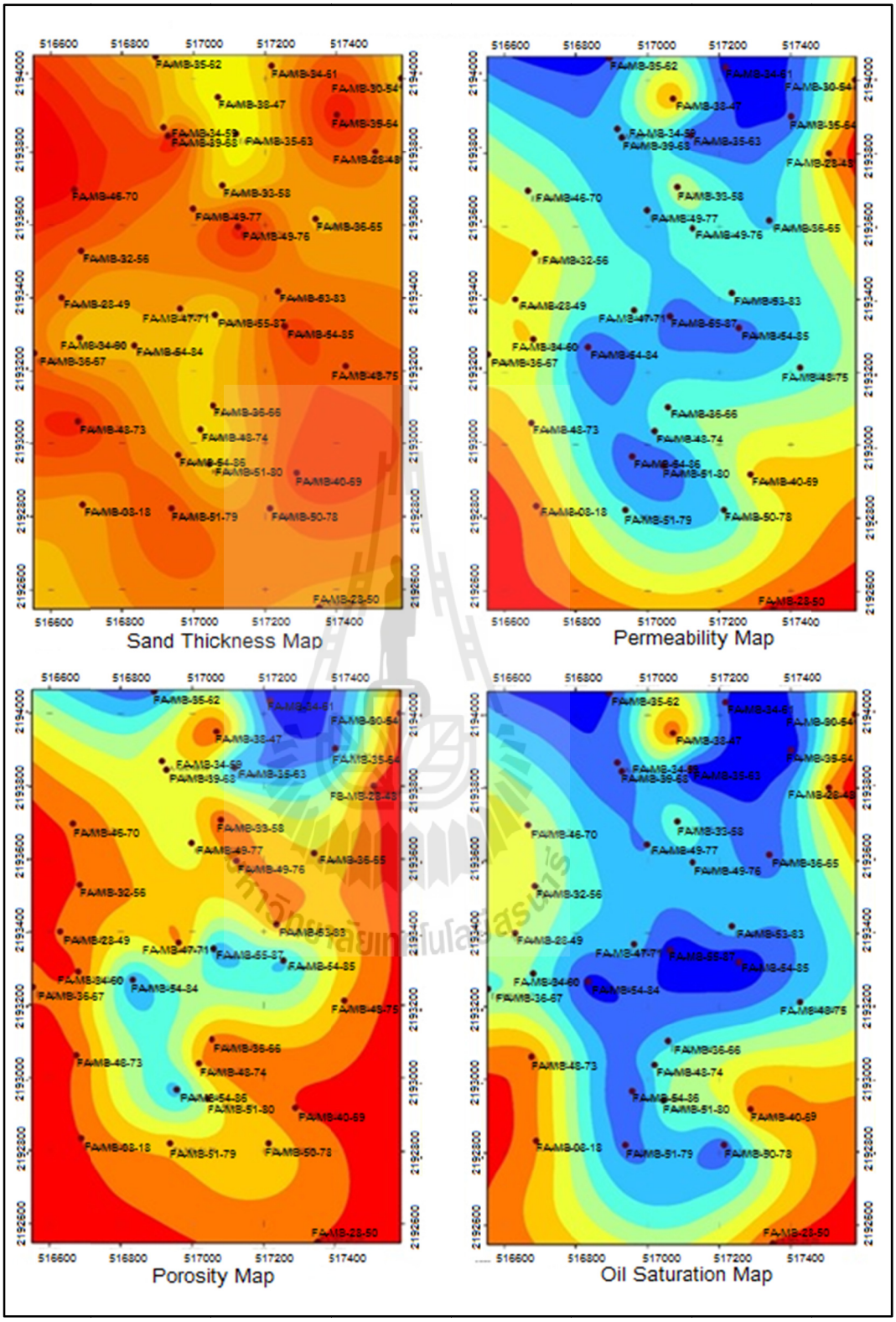

Figure 4.74 Isopach, porosity, permeability and hydrocarbon saturation map of sandstone Group C.

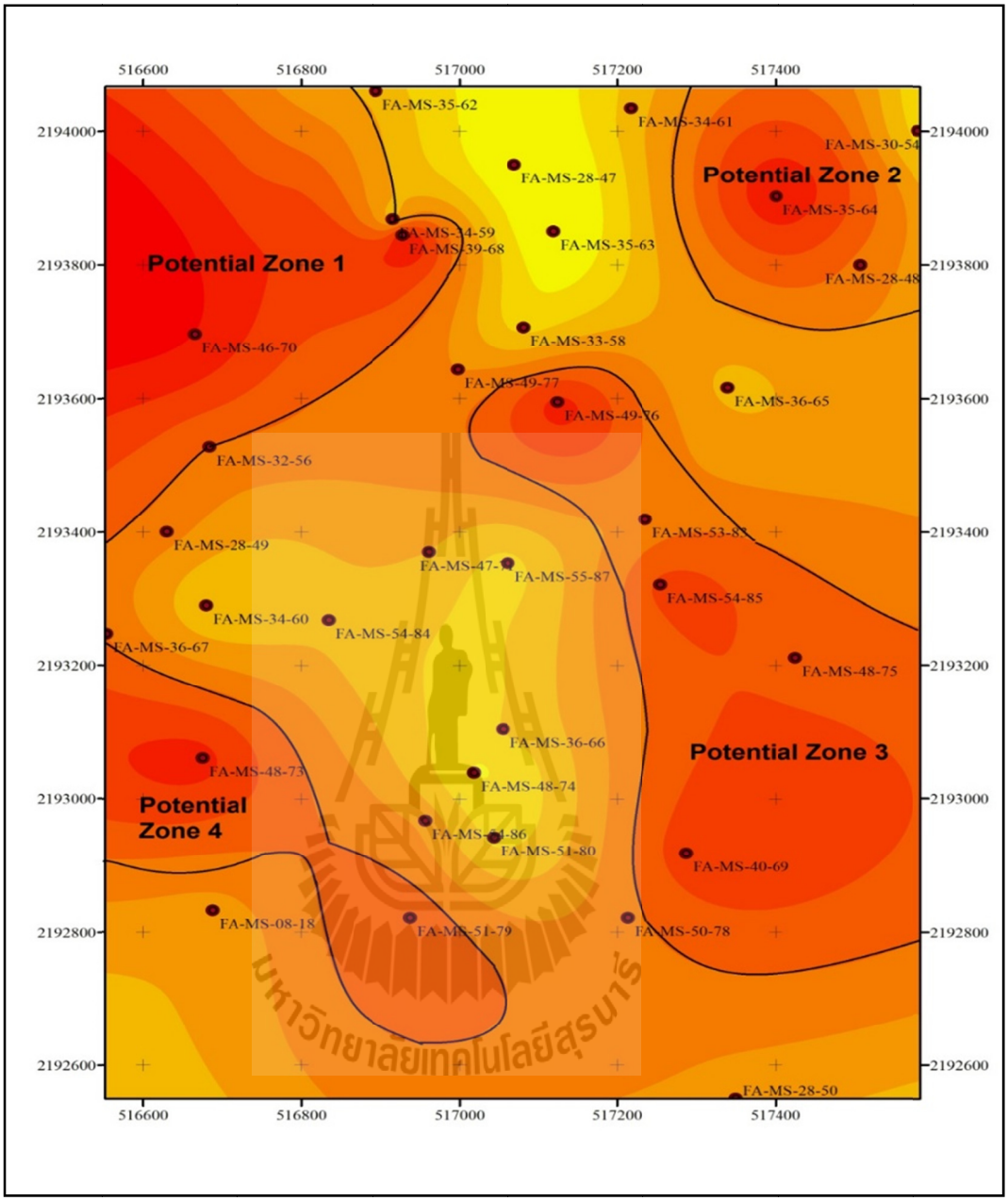

Figure 4.75 Hydrocarbon-bearing potential zone of sandstone Group C.

4.5 Three-dimensional map of the potential reservoirs

Results from literature reviews and wireline logging interpretation could be grouped 19 sandstone layers of Mae-Soon oil filed into three main groups as presented in Table 4.1.

Table 4.1 Three main grouped sandstone layer of Mae-Soon oil field.

Group	A	B	C
Kind of Sand	Litic grey wacky	Litic grey wacky	Quartz wacky
Grain Size	Very fine - intermediate	Fine - Coarse	Very fine - intermediate
Depth (feet)	1,000-2,000	2,000-3,000	3,000-4,000
Porosity (Percent)	28.05	30.77	29.15
Permeabiity (mDarcy)	466.2643	492.0391	599.4069
Oil Saturation (Fracture)	0.55	0.52	0.57

It was found that sandstone layers of Mae-Soon oil filed is fining upward in grain size. Sandstone group A and B are lithic greywacke whereas group C is quartz wake. Porosity is highest in group B while permeability is highest in group C. Hydrocarbon saturation is similar in all groups.

To illustrate the distribution of the three main groups of sandstone layers of Mae-Soon oil field, the three-dimensional model of each group were mapped as presented in Figure 4.76 to Figure 4.79, respectively.

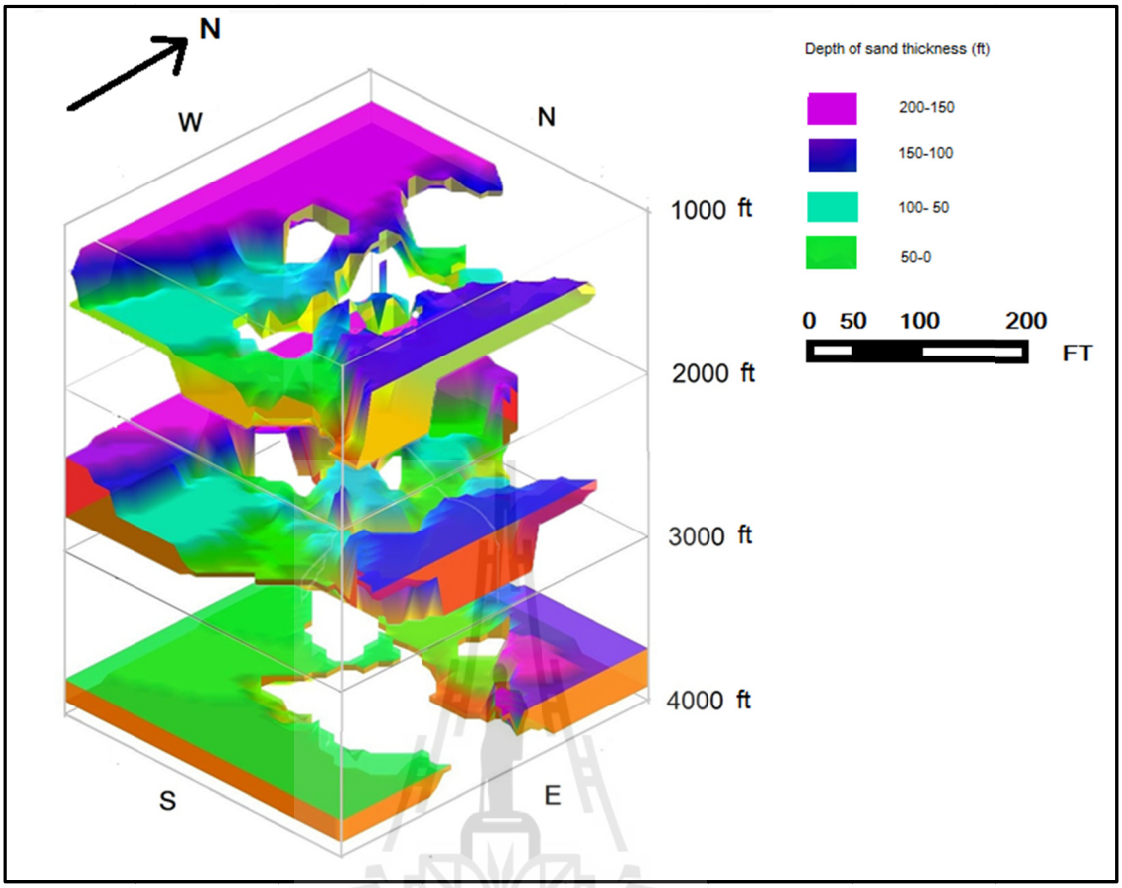

Figure 4.76 Three-dimensional model of three main sandstone groups of Mae-Soon oil field.

มหาวิทยาลัยเทคโนโลยีสุรนารี

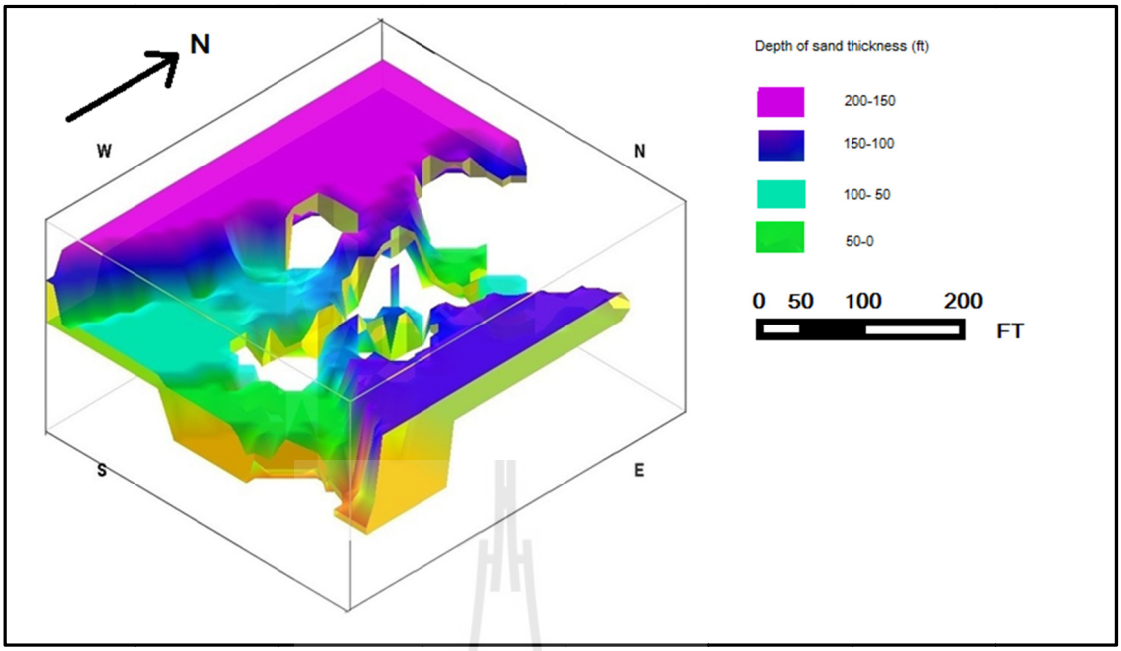

Figure 4.77 Three-dimensional model of sandstone Group A of Mae-Soon oil field.

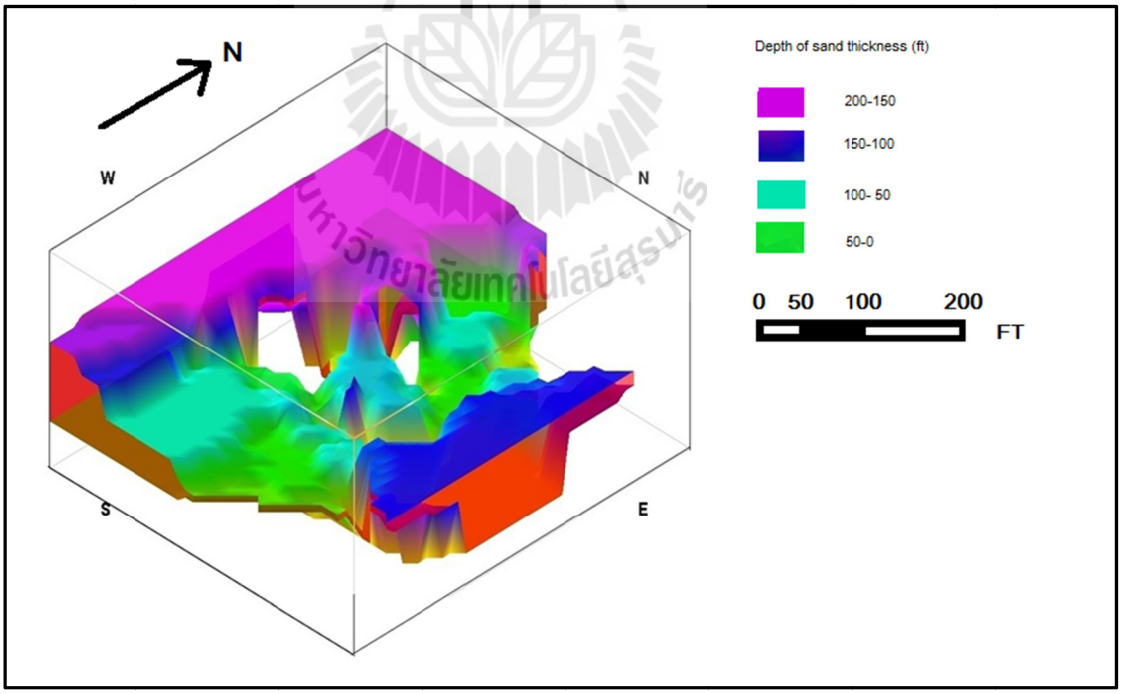

Figure 4.78 Three-dimensional model of sandstone Group B of Mae-Soon oil field.

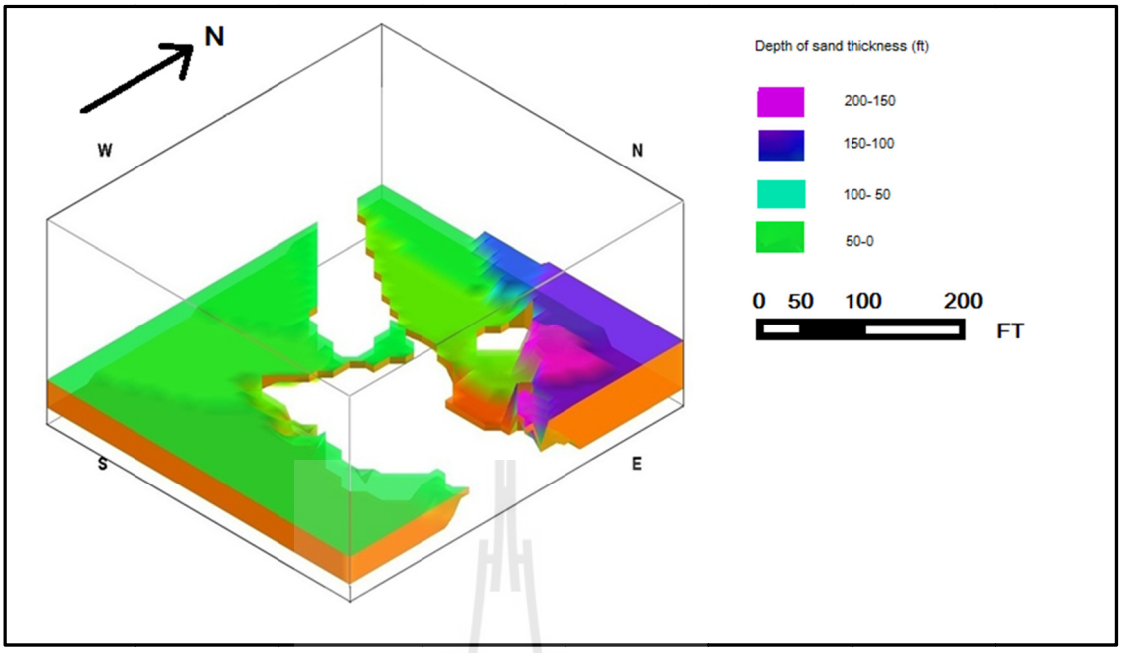

Figure 4.79 Three-dimensional model of sandstone Group C of Mae-Soon oil field.

มหาวิทยาลัยเทคโนโลยีสุรนารี

In addition to illustrate the stratigraphic correlation and subsurface structure of Mae-Soon oil field, geologic cross-section A-A' (west-east direction) and B-B' (north-south direction) had been made and are presented in Figure 4.80 to Figure 4.83, respectively.

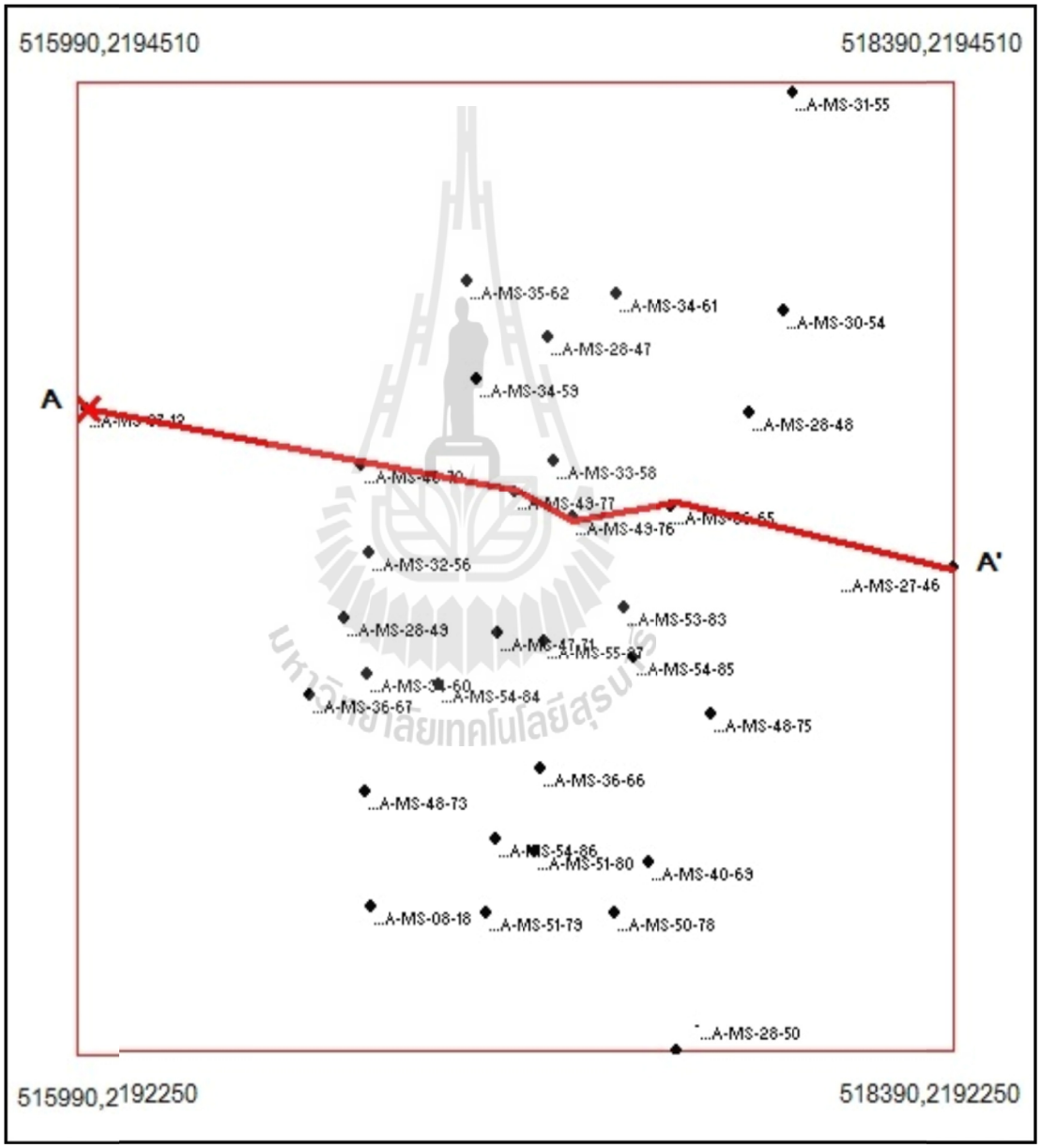

Figure 4.80 Location of geologic cross-section line A-A'.

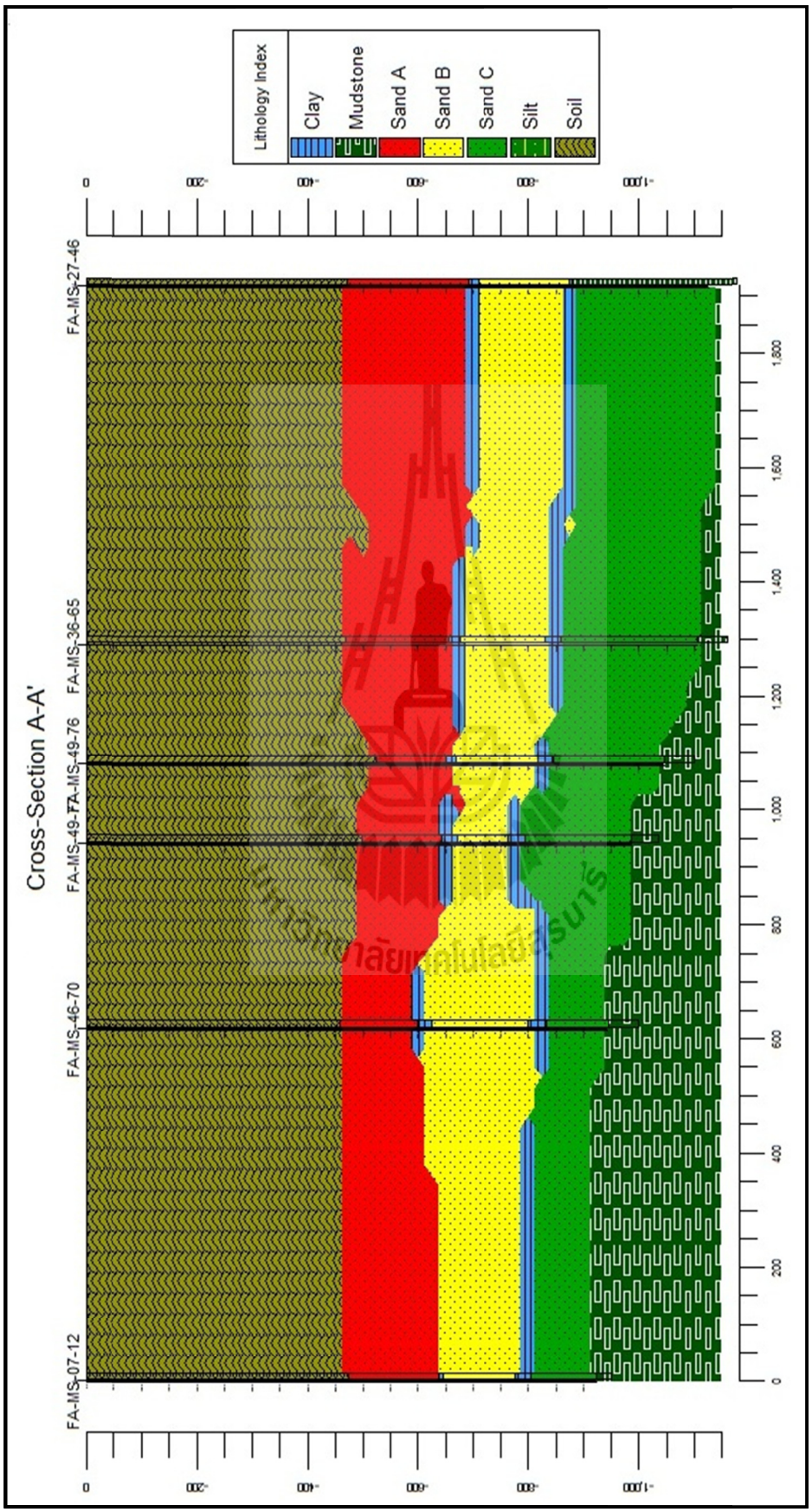

Figure 4.81 Lithologic cross-section line A-A'.

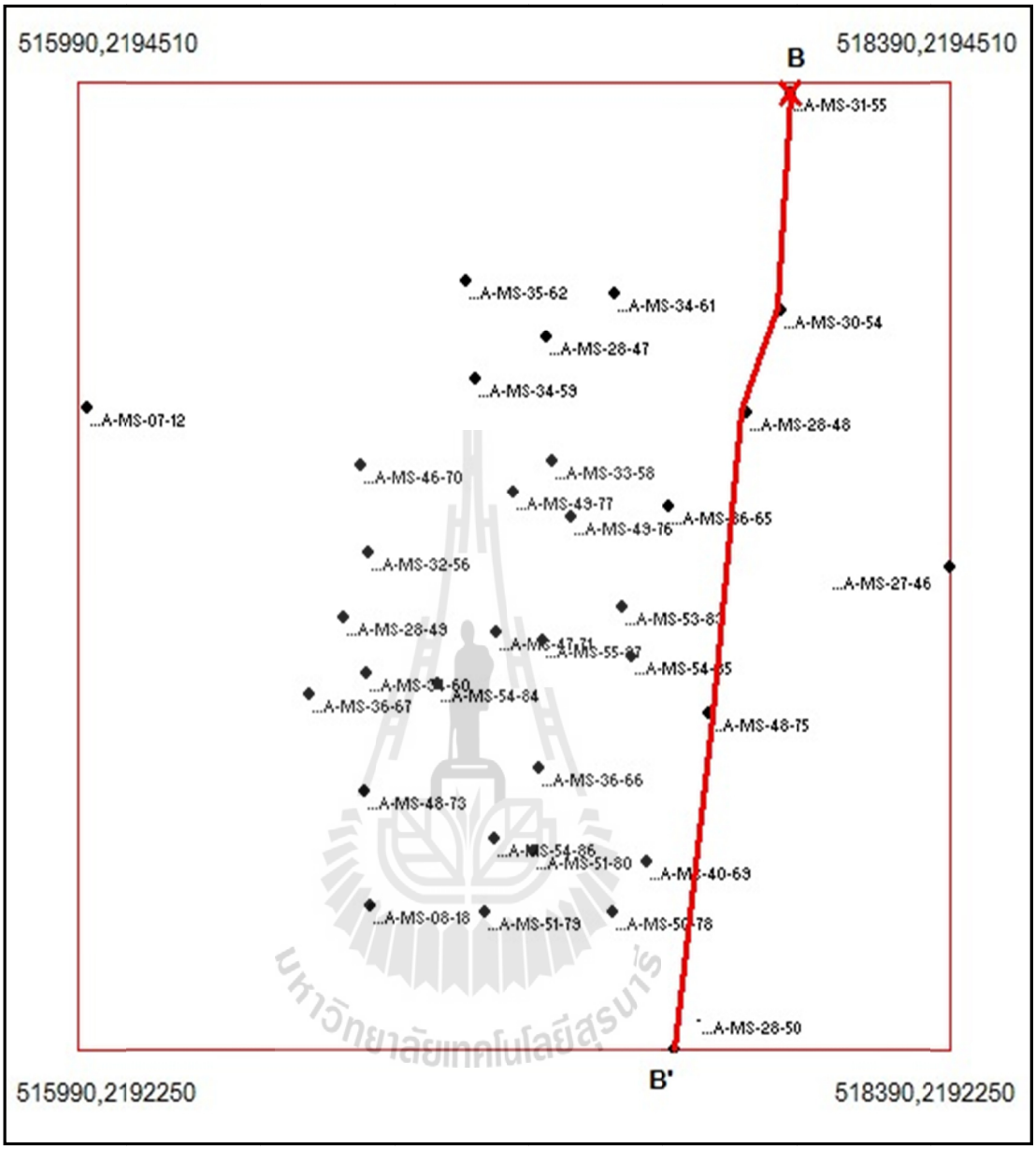

Figure 4.82 Location of geologic cross-section line B-B'.

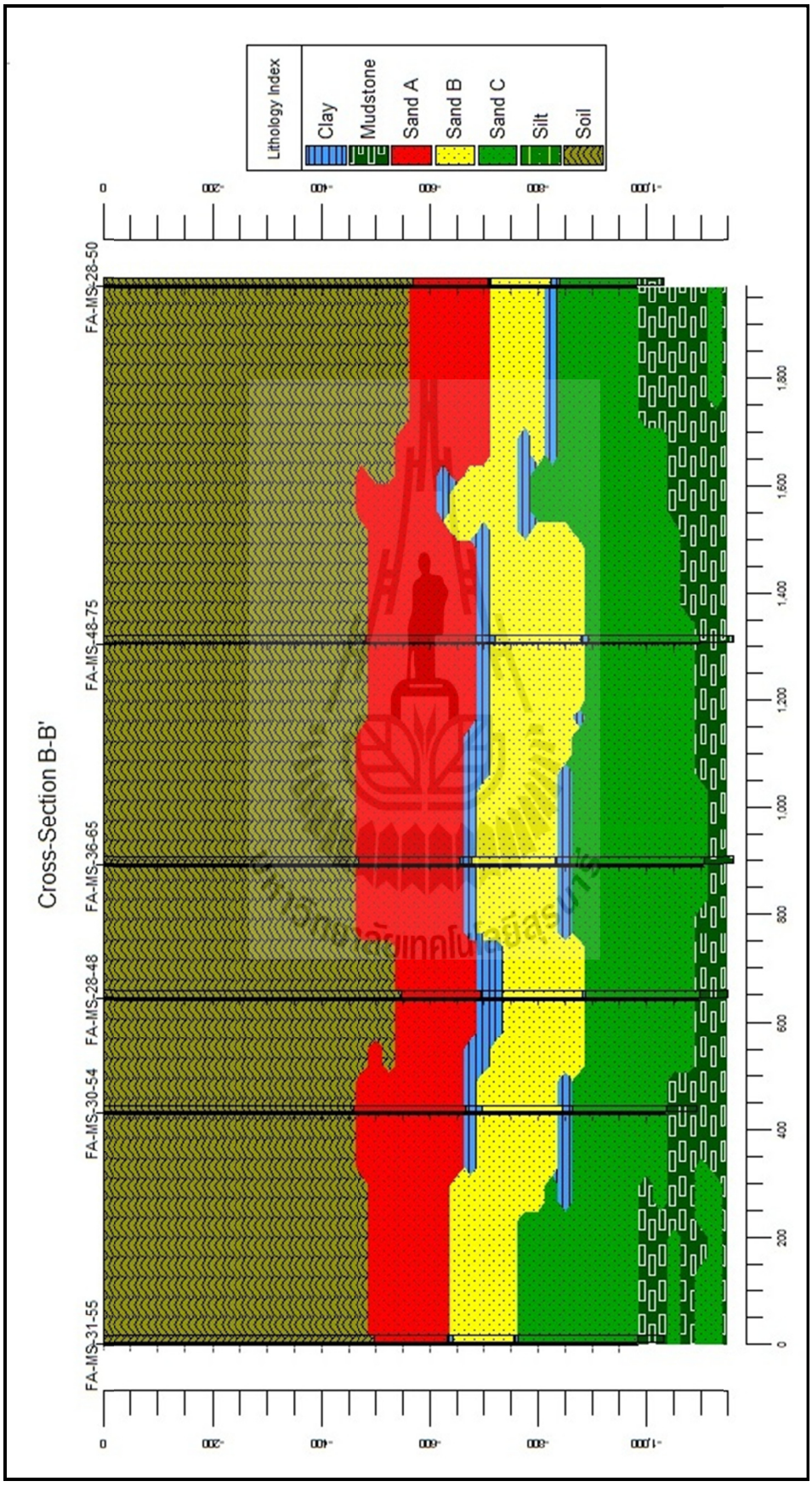

Figure 4.83 Lithologic cross-section line B-B'.

CHAPTER V

CONCLUSIONS, DISCUSSIONS AND RECOMMENDATIONS

5.1 Conclusions

Results from literature reviews, petrophysical data, and wireline logging data interpretation of 33 boreholes drilled in Mae-Soon oil field could give some information about the distribution of oil reservoirs of this filed and their properties as follows.

1. Sandstone reservoirs of this filed can be classified into 19 main layers and can be grouped into 3 main groups as group A, B, and C based on lithology, petrophysical properties, and wireline log responses. Using sandstone type classification guideline based on resistivity data and mud logging data from DED and the quality of sandstone based on porosity and permeability from Dickker.

2. Porosity of sandstones layers of this field can be determined with the respect to depth by the linear equation as

$$\text{Depth} = 0.0089\ (\text{Porosity}) + 25.415 \qquad (5.1)$$

3. Relationship between porosity and permeability of sandstone layers of Mae-soon oil field can be expressed by the linear equation as

$$\text{Permeability} = 0.0062\ (\text{Porosity}) + 16.95 \qquad (5.2)$$

4. Oil reservoir quality of Mae-Soon oil field is fair to excellent and suitable for hydrocarbon migration and storing since they have fair to excellent porosity and permeability.

5. Potential oil reservoirs orient and appear in various directions;

5.1 Sandstone group A has 2 potential hydrocarbon-bearing zones which are located in the north-western and south-western part of the field.

5.2 Sandstone group B has 3 potential hydrocarbon-bearing zones which are located in the north-western, eastern and western part of the field, respectively.

5.3 Sandstone group C has 4 potential hydrocarbon-bearing zones which are located in the north-western, north-eastern, eastern and south-western part of the field, respectively.

6. The shape and characteristic of sandstone layers as shown in the several maps revealed the deposit of sediment in the fluvial environment which occurred in different deposition time and different amount. Moreover, the uneven direction of water inlet and change of the river flow could cause the uneven and discontinuity of sediment deposition.

5.2 Discussions

This research did not study the stratigraphic correlation of Mae-soon oil filed which also has an important role in clarifying the distribution of the potential sandstone reservoirs since it much affects to the direction of migration, seal and trapping mechanism of hydrocarbon in the reservoir. Thus, this is might be effected to the reliability of the study results. Therefore, for the future study, more information on stratigraphic correlation should be taken into account to eliminate some uncertainty. However, results from this study still give some benefit and information to the Defense

Energy Department since they can help in oil production operation planning of this filed.

5.3 Recommendations

Because Fang basin is not only Mae-Soon oil field, a significant oil only. But there are other sources of oil, such as San-Sai oil field, Pong-Nok oil field etc. Therefore, it can apply the concept to create a map of the distribution of the oil layer and evaluation adapted for use with other sources of oil reservoir. It also can contribute concepts and equations of the study was capped in order to create the map. However, it must depend on the thickness of the oil reservoir and oil reservoir properties.

มหาวิทยาลัยเทคโนโลยีสุรนารี

REFERENCES

Abolins, P. (1992). **Geochemical Evaluation of Well FA-WR-35-04 Fang Basin Thailand Defence Energy, A Combined Geological Report Discussing the Biostratigraphy, Geochemistry and Sidewall Core Rock Properties**. Core Laboratories Malaysia SDN BHD.

Achalabhuti, C., and Udom-Ugsom, P. (1978). Petroleum potential in Gulf of Thailand. **Jour. Geol. Soc.** 3(1): 1-12.

Allen, P. A., and Allen J. R. (1990). **Basin Analysis: Principle and Applications.** London: Blackwell Scientific Publication.

Archie, G. E. (1950). Introduction to Petrophysics of Reservoir Rocks. **AAPG Bull.** 34(5): 943-901.

Beerbower, J. R. (1964). Cyclothems and Cyclic Depositional Mechanisms in Alluvial Plain Sedimentation, Symposium on Cyclic Sedimentation. **Bull. Kansus Geol. Sury.** 169(1): 31-42.

Belay, G. (1992). **Distribution and Characteristics of Petroleum Source Rocks in Oil Well IF 30 035 Ban Nong Yao, Fang Basin, Northern Thailand.** M.Sc. Thesis, Chiang Mai University.

Beukelaer, S. M. (2003). **Remote Sensing Analysis of Natural Oil and Gas Seeps on the Continental Slope of the Northern Gulf of Mexico.** M.S. Thesis, Texas A&M University.

Blanche, J. B., and Blanche, J. D. (1989). **Onshore Basin Evaluation and Hydrocarbon Potential.** Blanche Oil&Gas Consultants.

Braun, E. V., and Hahn, L. (1976). **Geological Map of Northern Thailand, Scale 1:250,000, Sheet Chiang Rai 2.** Federal Institute for Geo. Science and Natural Resources, Resources, Reined in Federal Republic of Germany.

Bunopas, S., and Vella, P. (1983). Opening of the Gulf of Thailand Rilfing of Continental S.E. Asia and Late Cenozoic Tectonics. **Jour. Geol. Soc.** l6(1): 1-12.

Buravas, S. (1973). **Succession of Rock in Fang and Chiang Mai Area with Reference to Thai Penisular Geology.** Unpublished report.

Burri, P. (1989). Hydrocarbon Potential of Tertiary Intermontane Basins in Thailand. In **Proceedings of the international Symposium on Intermontane Basins: Geology & Resources** (pp 3-12). Chaing Mai University, Thailand.

Chaodumrong, P., et al. (1983). A Review of the Tertiary Sedimentary Rocks of Thailand. **In Proceeding of the Workshop on Stratigraphic Correlation of Thailand and Malaysia** (pp 159-187). Haad-Yai, Thailand.

Chaturongkawanich, S., Wongwanick, T., and Chuaviroj, S. (1980). **Geology of Amphoe Fang, Changwat Chiang Mai, Scale 1:15,000.** Geothermal Studies Project, A Joint Project by EGAT, CMU and DMR. Geological Survey Division, Department of Mineral Resources, Bangkok, Thailand.

Chinbunchorn, N., Pradidtan, S., and Sattayarak, N. (1989). Petroleum Potential of Tertiary Intermontane Basin in Thailand. In **Proceedings of the International Symposium on Intermontane Basins: Geology & Resources** (pp 29-42) Chaing Mai University, Thailand.

Charoensrisomboon, S. (2007). **Lithostratigraphy of Mae Sot Formation, Fang Basin, Changwat Chiang Mai.** M.Sc. Thesis, Department of Geology, Faculty of Science, Chulalongkorn University.

Chellaiah, S. (2007). **Utility of GIS in mapping.** Map World Forum 2007.

Chinabutr, N. (1987). **Sedimentary Facies Analysis of Upper Neogene Deposits of Chaiprakarn area, Fang Basin, Chieng Mai.** Senior Project, Department of Geology, Faculty of Science, Chulalongkorn University.

Craig, F. F. Jr. (1980). **The Reservoir Engineering Aspects of Waterflooding.** Heny L. Doherty Momorial. Dallas: Society of Petroleum Engineers of AIME.

Dickinson, W. R., et al. (1983). Provinance of North America Phanerozoic Sandstones in Relation to Tectonic Setting. **GSA Bull.** 94: 222-235.

Dickker, A. J. (1985). **Geology in Petroleum Production.** Netherlands: Elsevien.

DMR (1992). **Petroleum and Coal Activities in Thailand.** Bangkok: Department of Mineral Resources.

Gawthorpe, R. L., and Hurst, J. M. (1993). Transfer Zones in Extensional Basins–Their Structural Style and Influence on Drainage Development and Stratigraphy. **Jour. Geol. Soc.** 150: 1137-1150.

Germeraad, J. H., Hopping, C. A. and Muller, J. (1968). Palynology of Tertiary Sediments from Tropical Areas. **Paleonbotany and Palynology** 6: 186-343.

Getahun, B. (1992). **Distribution Characteristics of Petroleum Rocks in Oil Well IF30 03S Ban Nong Yao, Fang Basin, Northern Thailand.** M.Sc. Thesis, Chaing Mai University.

Getahun, B., and Ratanasthien B. (1993). Botryococcus Algae in Oil Source Rocks, Fang Basin, Northern Thailand. In **Proceedings of the international Symposium on Biostratigraphy of Mainland Southeast Asia: Facies & Paleontology** (vol.2, pp 337-341). Chiang Mai, Thailand.

Hahn, L., and Siebenhuner, M. (1982). **Explanatory Notes (Paleontology) on the Geological Maps of Northern and Western Thailand 1:250,000 (Sheet Nan, Chiang Rai, Phayao, Chiang Dao, Chiang Mai, Li, Thong Pha Phum)** (pp 11-15). Bundesanstalt Fur Geowissenschaften and Rohstoffe, Hannover, Stuttgart.

Halliburton Geophysical (1991). **Final Report Interpretation of Fang Basin, Thailand 2-D Seismic Survey Volume 1 of 2 for Defense Energy Department.** William A W: Interpreter. Halliburton Geophysical Services, Inc., (Unpublished Report).

Harding, M. P. (2008). **GIS Representation and Assessment of Water Distribution System for Mae La Temporary Shelter, Thailand**. M.Eng. Thesis, Massachusetts Institute of Technology.

Hasani, H. (2013). Determination of Flood Plain Zoning in Zarigol River Using the Hydraulic Model of HEC-RAS. **Journal of Applied and Basic Sciences**. 4(12): 4300-4304.

Kaewsang, K. (1987). **Sedimentary Facies Analysis of Upper Tertiary Deposits of Fang Basin Changwat Chiang Mai.** M.Sc. Thesis, Department of Geology, Faculty of Science, Chulalongkorn University.

Khantaprab, C., and Kaewsaeng, K. (1987). **Sedimentary Facies Analysis and Petroleum Potential Assessment of the Cenozoic Intermontane Fang Basin** (pp 58-70). Department of Geology Chulalongkorn University, Bangkok.

Khantaprab, C., and Kaewsaeng, K. (1989). Sedimentary Facies and Petroleum Potential of Fang Basin (abstract). In **Proceedings of the International Symposium on Intermontane Basins: Geology & Resources** (pp 125-126). Chiang Mai University, Thailand.

Lagason, A. L. (2008). **Floodplain Visualization Using ARCVIEW GIS and HEC-RAS: A Case Study on Kota Marudu Floodplain**. Senior Project, Faculty of Civil Engineering, Universiti Teknologi Malaysia.

LeDain, A. Y., Tapponier, P., and Molnar, P. (1984). Active Faulting and Techtonics of Burma and Surrounding regions. **Jour. Geophysic Res.** 89: 453-482.

Levorsen, A. I. (1954). **Geology of Petroleum.** San Francisco: W.H. Freeman and Company.

Lian, H. M., and Bradley, K. (1986). Exploration and Development of Natural gas, Pattani Basin, Gulf of Thailand. In **Transaction of the Fourth Circum-Pacific Energy and Mineral Resources Conference** (pp 171-181).

McDonald, J., et al. (2002). Application of An Oil And Gas Fields Geographic Information System For CO2 Sequestration In Ohio. In **North-Central and Southeast Sections GSA Joint Annual Meeting 2002.**

Miall, A. D. (1985). **Principle of Sedimentary Basin Analysis** (2nd ed). New York: Springer-Verlag.

Mayer-Gurr, A. (1976). **Petroleum Engineering, Geology of Petroleum vol.3.** Germany: Pitman Publishing.

Mishra P., and Mehta, S. N. (2003). Using Remote Sensing and GIS Technologies as an Aid for Hydrocarbon Exploration in the Assam-Arakan Fold-thrust Belt Map. In **India Conference 2003**.

Müller, A. (2008). **Climate Characteristics of the Czech Republic Using ArcGIS.** Senior Project, Faculty of Civil Engineering, Department of Mapping and Cartography. Czech Technical University.

Muskat, M. (1949). **Physical Principles of Production.** New York: McGraw-Hill Book Company, Inc.

Petro-Canada Resources (PCR) (1988). **Technical appraisal of the Defense Energy Department Blocks Northern Thailand: Executive summary.** Unpublished Report.

Pettijohn, F. J. (1975). **Sedimentary Rocks** (3rd ed). New York: Harper & Row, Pubishers.

Pettijohn, F. J., Potter, P. E., and Siever, R. (1973). **Sand and Sandstone.** New York: Springer-Verlag.

Polachan, S., and Sattayarak, N. (1989). Strike-Slip Techtonics and the Development of Tertiary Basin in Thailand. In **Proceeding of international Symposium on Intermontane Basins: Geology & Resources** (pp 243-253). Chaing Mai University, Thailand.

Pradidtan, S. (1989). Characteristics and Controls of Lacustrine Depositional of some Tertiary Basin in Thailand. In **Proceeding of international Symposium on Intermontane Basins: Geology & Resources** (pp 133-145). Chaing Mai University, Thailand.

Pradidtan, S., and Tongtaow, C. (1984). Cenozoic Basins with Petroleum Potential in Thailand. In **Conference Application of Geology and the Nation Development** (pp 33-43). Chulalongkorn University, Bangkok, Thailand.

มหาวิทยาลัยเทคโนโลยีสุรนารี

Ratanasthien, B. (1997(a)). Algae Types of Oil Source Rocks in Northern Thailand. In **Proceedings of the international Conference on Stratigraphy and Techtonic Evolution of Southeast Asia and the South Pacific and the Associated, Meetings of IGCP 359 and IGCP 383 (GEOTHAI' 97)** (pp 606-612). Department of Mineral Resources, Bangkok, Thailand.

Ratanasthien, B. (1997(b)). Lithostratigraphy of Thai Neogene Sequence. In **Proceeding of Neogene Evolution of Pacific Ocean Gateways and Associated Responses to paleogeography and Paleoclimatology in Time and Space, with Spacial Emphasis on Pacific - Indian Ocean Seaways, Kyodai, Kaikan, Kyoto, IGCP-355** (pp 45-55). Japan.

Ratanasthien, B., and Haraluck, M. (1989). Palynological Evidences of Fang Oil-Bearing Formation. In **Proceeding of the Annual Technical Meeting 1988** (Spec. Publ., No.8, pp 83-98). Department of Geological Science, Chiang Mai University, Thailand.

Ratanasthien, B., and Uttamo, W. (1991). Coal Petrography of Wiang Haeng Deposits. In **Proceedings of the Annual Technical Meeting 1989 Geology and Mineral Resources of Thailand, Indochina and Myanmar and IGCP-246 Pacific Neogene Event in Southeast Asia** (Spec. Publ., No.9, pp 17-27). Department of Geological Sciences, Chiang Mai University, Thailand.

Reading, H. G. (ed.). (1986). **Sedimentary Environments and Facies** (2nd ed). Oxford: Blackwell Scientific Publications.

Richards, J. A. (1994). **Remote Sensing Digital Image Analysis.** Berlin: Springer-Verlag.

Rodjanapo, S. (1998). **Facies Analysis of Tertiary Rocks in Mae Soon and Nong Yao Oilfields, Fang Basin, Northern Thailand.** M.Sc. Thesis, Chiang Mai University.

Ruska (1985). **Instruction manual for operation and maintenance of Ruska Gas Permeameter Model 1011-801 Serial 46520.** Texas: Houston.

Ruska (1985(b)). **Operating manual for Ruska Universal Porometer Model 1053-801 Serial 46564.** Texas: Houston.

Sabins, F. F. (1997). **Remote Sensing: Principles and Interpretation.** New York: W.H. Freeman and company.

Selley, R. C. (1976). **An Introduction to Sedimentology** (2nd. ed). New York: Academic Press.

Settakul, N. (1984). Pongnok Oil field. In **Proceedings of the Symposium on Cenozoic Basins of Thailand: Geology and Resources** (pp 21-42). Chiang Mai University, Thailand.

Settakul, N. (1985). **Petroleum Geology of Fang Basin Part I.** Section of the Geology, Division of Oil Exploration and Production, Defense Energy Department. Unpublished Report.

Settakul, N., and Pimsam, V. (1991). Source Rock Screening and Oil Source Correlations in IF 30 01 and IF 30 02S. In **Proceedings of the Annual Technical Meeting 1989 Geology and Mineral Resources of Thailand, Indochina and Myanmar and IGCP-246 Pacific Neogene Event in Southeast Asia** (Spec. Publ., No.9, pp 111-140). Department of Geological Sciences, Chiang Mai University, Thailand.

Serra, O., and Sulpice, L. (1975). Sedimentary environments from wireline logs. In **SPWLA Sixteenth Annual logging symposium.**

Snansieng, S., Chaodamrong, P., Pradidtan, S., and Boripatkosol, S. (1983). The Tertiary Sedimentary Rocks of Thailand. In **Paper Presented at the conference on Geology & Mineral Resources of Thailand.** Bangkok, Thailand.

Stach, E., et al. (1982). **Stach's Textbook of Coal Petrology** (3rd ed). Berlin: Gebruder Borntraeger.

Srihiran, S. (1986). **Surface Resistivity Measurement for Oil Exploration at Mae Soon Oil Pool, Fang Basin, Changwat Chiang Mai.** M.Sc. Thesis, Chiang Mai University.

Terry, R. D., and Chilinger, G. V. (1955). Summary of "Conserning Some Additional Aids in Studying Sedimentary Formations". **Jour. Sed. Petrology** 25: 229-234.

Thurawat, C. (2003). **Application of Landsat 7 ETM+ Images and GIS Technologies for Geological Mapping in Khao Phang Ma, Amphoe Lom Kao, Changwat Petchabun.** MSc. Thesis, Chulalongkorn University. Unpublished.

Vevra, C. L., Kaldi, J. G., and Sneider, R. M. (1992). Geological Application of Capillary Pressure: A Review. **AAPG Bull.** 76(6): 840-850.

Watanasak, M. (1988). **Mid-Tertiary Palynology of Onshore and Offshore Thailand.** Ph.D. Thesis, University of Adelaide, Adelaide.

Watanasak, M. (1989). Palynological Zonation of Mid-Tertiary Intermontane Basin in Northern Thailand. In **Proceeding of international Symposium on Intermontane Basin: Geology & Resources** (pp 216-225). Chaing Mai University, Thailand.

Wentworth, C. K. (1922). A Scale of grade and class terms for clastic sediments. **Jour. Geology** 30: 377-392.

Wongpaet, K. (2005). **Geochemical Characteristics of Oil Source Rock from Mae Soon Oil Field at the Fang Basin, Chiang Mai Province.** Senior Project, Department of Geology, Faculty of Science, Chulalongkorn University.

Wood, S. H. (1996). The Chiang Saen Fault, Northern Thailand: Offset Streams and Potential Earthquakes. In **Proceeding of Submited to Techtonophysics** (15p.).

Wuyi, Y., et al. (2001). **Evaluation of Multi-sensor Remote Sensing Data Applied Oil & Gas Exploration in the Loess Highlands, Ordos Plateau, China.** Beijing: Research Institute of Petroleum Exploration and Development of Petro China Company Ltd.

มหาวิทยาลัยเทคโนโลยีสุรนารี

APPENDIX A

GAMMA RAY AND SPONTANEOUS POTENTIAL LOG INTERPRETATION

มหาวิทยาลัยเทคโนโลยีสุรนารี

Table A.1 Gamma ray and spontaneous potential log interpretation of well no. FA-MS-08-12.

Depth (feet)	**GR Log (API Unit)**	**SP Log (millivolt)**
1440-1466	15	42
1540-1570	17	48
1600-1624	24	68
1655-1670	26	68
1775-1805	19	53
1915-1940	15	42
1970-1985	22	60
2025-2035	21	58
2100-2140	17	48
2245-2263	15	41
2300-2310	22	60
2350-2366	15	43
2450-2463	18	50
2537-2555	20	55
2624-2632	22	60
2684-2688	24	60
2720-2740	16	44
2765-2778	25	70
2810-2815	18	50

มหาวิทยาลัยเทคโนโลยีสุรนารี

Table A.2 Gamma ray and spontaneous potential log interpretation of well no. FA-MS-80-18.

Depth (feet)	**GR Log (API Unit)**	**SP Log (millivolt)**
1695-1711	19	52
1720-1730	22	60
1756-1764	12	34
1860-1870	22	60
1944-1965	11	30
1980-1990	20	55
2010-2034	8	23
2065-2069	12	33
2100-2110	16	44
2165-2170	20	56
2204-2223	23	65
2285-2295	24	68
2322-2354	18	50
2410-2432	22	62
2456-2466	20	56
2534-2544	12	33
2596-2630	13	36
2704-2732	22	60
2900-2920	16	45

มหาวิทยาลัยเทคโนโลยีสุรนารี

Table A.3 Gamma ray and spontaneous potential log interpretation of well no. FA-MS-27-46.

Depth (feet)	**GR Log (API Unit)**	**SP Log (millivolt)**
1436-1460	16	45
1498-1516	13	36
1728-1746	22	61
1848-1864	24	67
1928-1956	15	43
2060-2108	13	36
2166-2234	20	56
2248-2288	15	43
2390-2406	11	30
2432-2458	9	25
2514-2544	15	41
2622-2666	20	56
2680-2706	18	50
2785-2800	16	44
2870-2880	7	20
2960-2980	11	30
3112-3144	15	43
3280-3312	20	56
3418-3434	11	31

มหาวิทยาลัยเทคโนโลยีสุรนารี

Table A.4 Gamma ray and spontaneous potential log interpretation of well no. FA-MS-28-47.

Depth (feet)	**GR Log (API Unit)**	**SP Log (millivolt)**
1400-1430	12	34
1450-1488	21	58
1606-1626	24	66
1760-1770	22	61
1855-1865	19	54
1962-1992	12	32
2062-2080	20	56
2178-2188	16	45
2244-2254	11	30
2318-2334	24	67
2412-2422	19	54
2520-2540	13	37
2620-2630	23	65
2663-2680	19	54
2760-2785	22	62
2850-2870	17	48
2900-2920	12	34
3000-3010	18	51
3070—3090	11	31

มหาวิทยาลัยเทคโนโลยีสุรนารี

Table A.5 Gamma ray and spontaneous potential log interpretation of well no. FA-MS-28-48.

Depth (feet)	**GR Log (API Unit)**	**SP Log (millivolt)**
1672-1728	22	60
1753-1770	20	56
1798-1816	15	43
1900-1920	11	30
2025-2035	9	25
2100-2120	18	50
2238-2260	22	62
2320-2340	20	56
2410-2430	12	33
2490-2500	20	56
2625-2632	16	45
2680-2688	11	30
2700-2715	20	55
2740-2755	8	23
2875-2879	12	33
2910-2920	15	42
3000-3020	17	48
3222-3230	24	68
3310-3340	24	68

มหาวิทยาลัยเทคโนโลยีสุรนารี

Table A.6 Gamma ray and spontaneous potential log interpretation of well no. FA-MS-28-49.

Depth (feet)	**GR Log (API Unit)**	**SP Log (millivolt)**
1465-1478	19	54
1540-1566	13	37
1634-1642	23	65
1700-1718	19	54
1820-1860	22	62
1984-2002	20	56
2014-2024	18	50
2220-2230	16	44
2298-2308	20	55
2344-2360	23	65
2458-2480	12	34
2544-2550	24	66
2624-2632	13	36
2674-2792	14	40
2710-2722	12	34
2785-2800	16	45
2810-2818	13	36
2910-2925	22	61
2965-2978	24	67

มหาวิทยาลัยเทคโนโลยีสุรนารี

Table A.7 Gamma ray and spontaneous potential log interpretation of well no. FA-MS-28-50.

Depth (feet)	**GR Log (API Unit)**	**SP Log (millivolt)**
1730-1742	12	34
1782-1846	16	45
1880-1890	13	36
1900-1920	22	61
1960-1990	24	67
2140-2158	16	45
2170-2180	13	36
2222-2236	20	56
2294-2304	16	45
2332-2350	11	30
2453-2461	24	67
2488-2512	19	54
2560-2580	18	50
2650-2675	22	62
2715-2735	15	42
2800-2820	22	60
2880-2890	21	58
2940-2968	17	48
2988-3000	15	41

มหาวิทยาลัยเทคโนโลยีสุรนารี

Table A.8 Gamma ray and spontaneous potential log interpretation of well no. FA-MS-30-54.

Depth (feet)	**GR Log (API Unit)**	**SP Log (millivolt)**
1400-1415	15	41
1478-1496	22	60
1635-1651	15	43
1700-1714	18	50
1916-1930	20	55
2014-2023	18	50
2124-2154	16	44
2167-2192	7	20
2323-2338	19	53
2378-2396	15	42
2468-2482	22	60
2557-2576	21	58
2630-2640	17	48
2660-2680	12	33
2785-2800	16	45
2860-2880	13	36
2940-2960	22	61
3050-3060	24	67
3140-3160	15	43

มหาวิทยาลัยเทคโนโลยีสุรนารี

Table A.9 Gamma ray and spontaneous potential log interpretation of well no. FA-MS-31-55.

Depth (feet)	**GR Log (API Unit)**	**SP Log (millivolt)**
1518-1526	16	44
1576-1598	25	70
1715-1725	18	50
1764-1778	22	61
1820-1842	23	64
1902-1924	24	67
1958-1974	25	70
2030-2045	24	66
2102-2128	16	44
2136-2180	24	67
2244-2266	12	32
2292-2302	16	45
2326-2364	21	58
2425-2450	25	71
2540-2576	23	64
2700-2710	11	30
2777-2788	20	55
2900-2910	8	23
2980-3000	12	33

มหาวิทยาลัยเทคโนโลยีสุรนารี

Table A.10 Gamma ray and spontaneous potential log interpretation of well no. FA-MS-32-56.

Depth (feet)	**GR Log (API Unit)**	**SP Log (millivolt)**
1720-1735	13	36
1832-1844	22	60
1910-1920	16	45
2014-2028	19	54
2055-2085	22	62
2120-2140	17	48
2192-2200	12	34
2260-2280	18	51
2340-2360	11	31
2458-2468	16	45
2536-2552	18	50
2570-2580	12	33
2610-2620	14	40
2640-2660	23	65
2710-2715	12	34
2798-2810	24	66
2857-2865	13	36
2915-2925	14	40
2980-2995	12	34

มหาวิทยาลัยเทคโนโลยีสุรนารี

Table A.11 Gamma ray and spontaneous potential log interpretation of well no. FA-MS-33-58.

Depth (feet)	**GR Log (API Unit)**	**SP Log (millivolt)**
1620-1640	18	50
1723-1744	22	62
1871-1877	20	56
1955-1960	12	33
2020-2040	20	56
2101-2109	16	45
2178-2184	11	30
2281-2286	20	55
2354-2358	12	34
2420-2431	21	58
2470-2475	24	66
2530-2545	22	61
2612-2632	19	54
2706-2726	11	30
2745-2760	15	43
2825-2840	24	68
2875-2890	18	50
2942-2958	22	62
3046-3064	20	56

มหาวิทยาลัยเทคโนโลยีสุรนารี

Table A.12 Gamma ray and spontaneous potential log interpretation of well no. FA-MS-34-59.

Depth (feet)	**GR Log (API Unit)**	**SP Log (millivolt)**
1510-1520	N/A	66
1697-1736	N/A	36
1812-1820	N/A	40
1865-1877	N/A	34
1920-1940	N/A	54
2024-2032	N/A	50
2108-2134	N/A	N/A
2198-2216	N/A	N/A
2248-2272	N/A	N/A
2282-2304	N/A	N/A
2322-2332	N/A	N/A
2404-2420	N/A	N/A
2486-2502	N/A	N/A
2560-2576	N/A	N/A
2648-2658	N/A	34
2800-2821	N/A	45
2870-2889	N/A	36
2990-2997	N/A	45
3045-3055	N/A	58

มหาวิทยาลัยเทคโนโลยีสุรนารี

Table A.13 Gamma ray and spontaneous potential log interpretation of well no. FA-MS-34-60.

Depth (feet)	**GR Log (API Unit)**	**SP Log (millivolt)**
1450-1461	19	54
1545-1555	22	62
1620-1635	20	56
1738-1748	18	50
1760-1775	16	44
1910-1919	20	55
2022-2034	11	30
2066-2072	9	25
2204-2223	15	41
2275-2284	20	56
2323-2334	18	50
2426-2433	16	45
2467-2481	12	34
2525-2534	24	66
2580-2590	20	56
2602-2620	16	45
2665-2670	11	30
2740-2755	20	55
2820-2830	18	50

มหาวิทยาลัยเทคโนโลยีสุรนารี

Table A.14 Gamma ray and spontaneous potential log interpretation of well no. FA-MS-34-61.

Depth (feet)	**GR Log (API Unit)**	**SP Log (millivolt)**
1375-1405	16	45
1710-1722	20	56
1770-1798	23	64
1900-1910	24	67
1980-2000	25	70
2100-2105	24	66
2175-2200	13	36
2286-2303	20	56
2360-2370	16	45
2472-2481	11	30
2510-2520	24	67
2575-2590	13	36
2640-2650	14	40
2700-2710	12	34
2740-2755	16	45
2770-2790	13	36
2845-2860	22	61
2925-2935	24	67
2975-2990	16	45

มหาวิทยาลัยเทคโนโลยีสุรนารี

Table A.15 Gamma ray and spontaneous potential log interpretation of well no. FA-MS-35-62.

Depth (feet)	**GR Log (API Unit)**	**SP Log (millivolt)**
1530-1535	19	53
1605-1610	15	42
1700-1720	22	60
1740-1750	21	58
1795-1805	17	48
1850-1860	12	33
1990-2010	16	45
2130-2150	13	36
2170-2180	24	67
2210-2220	19	54
2305-2315	18	50
2360-2375	22	62
2460-2475	15	42
2530-2540	22	60
2595-2600	21	58
2628-2635	19	53
2770-2790	15	42
2821-2831	22	60
2939-2945	21	58

มหาวิทยาลัยเทคโนโลยีสุรนารี

Table A.16 Gamma ray and spontaneous potential log interpretation of well no. FA-MS-36-65.

Depth (feet)	**GR Log (API Unit)**	**SP Log (millivolt)**
1428-1488	22	60
1530-1545	20	56
1700-1720	15	43
1758-1828	11	30
1896-1904	9	25
1988-2000	18	50
2064-2072	22	62
2180-2208	20	56
2266-2278	24	66
2322-2352	22	61
2376-2400	19	54
2520-2530	11	30
2616-2636	15	43
2717-2725	24	68
2850-2870	18	50
2950-2970	13	36
3090-3110	14	40
3222-3230	12	34
3340-3365	16	45

มหาวิทยาลัยเทคโนโลยีสุรนารี

Table A.17 Gamma ray and spontaneous potential log interpretation of well no. FA-MS-36-66.

Depth (feet)	**GR Log (API Unit)**	**SP Log (millivolt)**
1488-1512	12	34
1547-1560	24	66
1670-1682	13	36
1718-1730	14	40
1800-1820	12	34
1852-1866	16	45
1940-1956	13	36
2014-2034	12	34
2080-2100	16	45
2170-2190	13	36
2290-2306	22	61
2394-2414	24	67
2434-2470	16	45
2478-2494	13	36
2717-2725	15	41
2775-2780	20	56
2840-2850	18	50
2957-2970	16	44
3045-3067	7	20

มหาวิทยาลัยเทคโนโลยีสุรนารี

Table A.18 Gamma ray and spontaneous potential log interpretation of well no. FA-MS-36-67.

Depth (feet)	**GR Log (API Unit)**	**SP Log (millivolt)**
1455-1460	20	55
1526-1544	12	34
1624-1638	21	58
1686-1696	24	66
1728-1784	22	61
1904-1930	19	54
2040-2072	7	20
2116-2134	19	53
2165-2177	15	42
2278-2298	22	60
2366-2378	21	58
2414-2444	17	48
2492-2504	12	34
2528-2572	21	58
2642-2666	24	66
2686-2724	22	61
2735-2745	19	54
2770-2785	12	32
2815-2822	20	56

มหาวิทยาลัยเทคโนโลยีสุรนารี

Table A.19 Gamma ray and spontaneous potential log interpretation of well no. FA-MS-40-69.

Depth (feet)	**GR Log (API Unit)**	**SP Log (millivolt)**
1434-1445	24	66
1495-1500	16	44
1550-1560	24	67
1720-1744	12	32
1796-1822	16	45
1834-1848	21	58
1914-1930	25	71
1972-1990	20	55
2006-2012	8	23
2184-2210	12	33
2256-2274	15	42
2310-2322	17	48
2404-2420	24	68
2544-2550	24	68
2663-2674	15	43
2755-2761	18	50
2844-2860	20	55
2987-3002	22	60
3165-3188	22	60

มหาวิทยาลัยเทคโนโลยีสุรนารี

Table A.20 Gamma ray and spontaneous potential log interpretation of well no. FA-MS-46-70.

Depth (feet)	**GR Log (API Unit)**	**SP Log (millivolt)**
1392-1406	13	36
1476-1508	20	56
1550-1565	16	45
1636-1648	11	30
1706-1762	24	67
1810-1822	19	54
1902-1924	18	50
1936-1960	22	62
2054-2082	15	42
2234-2264	22	60
2318-2330	21	58
2414-2440	24	67
2542-2554	16	45
2570-2582	13	36
2615-2620	15	41
2642-2655	20	56
2745-2750	18	50
2820-2833	11	31
2868-2880	20	56

มหาวิทยาลัยเทคโนโลยีสุรนารี

Table A.21 Gamma ray and spontaneous potential log interpretation of well no. FA-MS-47-71.

Depth (feet)	**GR Log (API Unit)**	**SP Log (millivolt)**
1634-1648	14	40
1701-1711	12	32
1740-1745	16	45
1784-1795	19	53
1804-1812	21	59
1940-1952	12	32
1976-1990	15	42
2023-2037	20	56
2046-2062	13	35
2300-2314	24	67
2352-2364	12	32
2404-2420	13	35
2440-2450	17	48
2512-2532	22	61
2686-2714	15	43
2724-2744	19	54
2780-2800	9	24
2895-2900	24	68
2999-3015	21	57

มหาวิทยาลัยเทคโนโลยีสุรนารี

Table A.22 Gamma ray and spontaneous potential log interpretation of well no. FA-MS-48-73.

Depth (feet)	**GR Log (API Unit)**	**SP Log (millivolt)**
1460-1475	22	60
1545-1555	21	58
1662-1675	24	67
1764-1772	16	45
1826-1838	13	36
1930-1940	15	41
2023-2030	16	44
2170-2178	20	55
2222-2272	11	30
2338-2368	9	25
2422-2432	15	41
2487-2499	11	31
2587-2600	24	67
2677-2700	18	51
2745-2755	22	62
2798-2810	15	43
2835-2850	13	37
2900-2920	23	65
2970-2980	25	70

มหาวิทยาลัยเทคโนโลยีสุรนารี

Table A.23 Gamma ray and spontaneous potential log interpretation of well no. FA-MS-48-75.

Depth (feet)	**GR Log (API Unit)**	**SP Log (millivolt)**
1466-1484	22	62
1580-1600	17	48
1785-1792	12	34
1917-1928	18	51
2019-2025	11	31
2082-2088	16	45
2200-2210	18	50
2305-2309	12	33
2398-2428	12	34
2520--2530	21	58
2620-2635	24	66
2660-2680	22	61
2720-2735	19	54
2765-2775	12	32
2835-2845	20	56
2915-2935	16	45
3065-3080	16	45
3185-3200	11	30
3325-3345	20	55

มหาวิทยาลัยเทคโนโลยีสุรนารี

Table A.24 Gamma ray and spontaneous potential log interpretation of well no. FA-MS-49-76.

Depth (feet)	**GR Log (API Unit)**	**SP Log (millivolt)**
1595-1615	11	30
1635-1650	15	43
1735-1755	24	68
1785-1800	18	50
1899-1910	22	62
1970-1985	20	56
2040-2050	17	48
2125-2140	12	34
2245-2270	18	51
2336-2345	11	31
2425-2450	16	45
2480-2495	18	50
2580-2590	12	33
2665-2685	13	36
2730-2740	20	56
2800-2840	16	45
2920-2940	11	30
3046-3064	24	67
3160-3185	16	45

มหาวิทยาลัยเทคโนโลยีสุรนารี

Table A.25 Gamma ray and spontaneous potential log interpretation of well no. FA-MS-49-77.

Depth (feet)	**GR Log (API Unit)**	**SP Log (millivolt)**
1518-1526	16	45
1600-1620	12	34
1687-1700	24	66
1795-1810	20	56
1862-1868	16	45
1950-1955	11	30
2042-2050	15	42
2132-2148	22	60
2163-2171	21	58
2184-2218	17	48
2240-2260	12	34
2313-2329	19	54
2417-2431	11	30
2462-2473	15	43
2547-2559	24	68
2685-2700	18	50
2780-2790	13	36
2820-2840	14	40
2999-3010	12	34

มหาวิทยาลัยเทคโนโลยีสุรนารี

Table A.26 Gamma ray and spontaneous potential log interpretation of well no. FA-MS-50-78.

Depth (feet)	**GR Log (API Unit)**	**SP Log (millivolt)**
1356-1384	24	68
1440-1447	15	43
1542-1558	18	50
1598-1622	20	55
1642-1672	22	60
1786-1822	22	60
1868-1892	15	43
1968-1976	20	56
2106-2130	16	45
2246-2262	24	67
2318-2326	12	32
2364-2377	12	34
2405-2418	18	50
2588-2601	22	62
2700-2711	20	56
2803-2812	12	33
2890-2899	20	56
2970-2977	16	45
3020-3045	18	51

มหาวิทยาลัยเทคโนโลยีสุรนารี

Table A.27 Gamma ray and spontaneous potential log interpretation of well no. FA-MS-51-79.

Depth (feet)	**GR Log (API Unit)**	**SP Log (millivolt)**
1530-1540	9	25
1620-1630	18	50
1784-1795	22	62
1875-1885	20	56
1915-1935	24	66
1976-1990	22	61
2052-2078	19	54
2146-2168	20	56
2200-2210	18	50
2336-2354	11	31
2430-2443	20	56
2508-2528	12	34
2548-2560	24	66
2640-2648	13	36
2695-2711	14	40
2760-2780	12	34
2875-2890	16	45
2920-2940	12	32
3040-3060	21	59

มหาวิทยาลัยเทคโนโลยีสุรนารี

Table A.28 Gamma ray and spontaneous potential log interpretation of well no. FA-MS-51-80.

Depth (feet)	**GR Log (API Unit)**	**SP Log (millivolt)**
1718-1730	20	56
1740-1745	16	45
1940-1956	11	30
1990-2018	24	67
2030-2056	13	36
2098-2102	14	40
2198-2206	12	34
2242-2256	11	30
2300-2336	15	43
2376-2434	24	68
2458-2474	18	50
2500-2526	13	36
2590-2596	14	40
2622-2648	12	34
2728-2748	16	45
2770-2790	12	34
2860-2875	24	66
2900-2920	20	56
3002-3025	16	45

มหาวิทยาลัยเทคโนโลยีสุรนารี

Table A.29 Gamma ray and spontaneous potential log interpretation of well no. FA-MS-53-83.

Depth (feet)	**GR Log (API Unit)**	**SP Log (millivolt)**
1366-1396	22	62
1625-1635	15	42
1685-1992	22	60
1800-1810	21	58
1900-1925	17	48
1960-1970	24	66
2044-2085	13	36
2100-2120	14	40
2155-2165	9	25
2172-2203	15	41
2295-2312	11	31
2379-2395	24	67
2560-2567	18	51
2580-2587	22	62
2745-2760	15	43
2855-2865	20	56
2925-2935	17	48
3000-3005	12	34
3098-3105	18	51

มหาวิทยาลัยเทคโนโลยีสุรนารี

Table A.30 Gamma ray and spontaneous potential log interpretation of well no. FA-MS-54-84.

Depth (feet)	**GR Log (API Unit)**	**SP Log (millivolt)**
1560-1580	20	55
1625-1635	11	30
1730-1740	9	25
1870-1880	15	41
1940-1960	20	56
1980-1990	18	50
2045-2055	16	45
2160-2170	12	34
2275-2285	22	61
2360-2370	19	54
2440-2460	11	30
2515-2520	15	43
2550-2555	24	68
2645-2660	18	50
2690-2700	20	56
2790-2800	18	50
2855-2870	16	44
2910-2930	20	55
2975-2990	16	44

มหาวิทยาลัยเทคโนโลยีสุรนารี

Table A.31 Gamma ray and spontaneous potential log interpretation of well no. FA-MS-54-85.

Depth (feet)	**GR Log (API Unit)**	**SP Log (millivolt)**
1295-1320	20	56
1440-1460	12	32
1544-1560	15	43
1782-1788	20	55
1865-1870	24	67
2002-2016	17	47
2060-2070	16	45
2100-2110	31	87
2178-2184	25	69
2246-2260	18	49
2314-2324	23	64
2405-2414	14	38
2460-2468	22	61
2640-2660	21	57
2820-2845	19	54
2860-2875	23	65
2930-2950	13	35
3010--3030	13	37
3095-3110	11	30

มหาวิทยาลัยเทคโนโลยีสุรนารี

Table A.32 Gamma ray and spontaneous potential log interpretation of well no. FA-MS-54-86.

Depth (feet)	**GR Log (API Unit)**	**SP Log (millivolt)**
1366-1396	15	41
1484-1520	16	45
1660-1680	23	63
1794-1820	13	36
1838-1882	14	38
1970-2006	27	74
2034-2092	20	56
2138-2162	15	42
2194-2266	31	85
2284-2290	17	47
2332-2384	20	56
2478-2536	13	36
2556-2576	14	38
2666-2688	27	76
2732-2746	12	34
2764-2792	18	51
2848-2864	22	61
2924-2952	24	67
2958-2990	21	59

มหาวิทยาลัยเทคโนโลยีสุรนารี

Table A.33 Gamma ray and spontaneous potential log interpretation of well no. FA-MS-55-87.

Depth (feet)	**GR Log (API Unit)**	**SP Log (millivolt)**
1375-1405	14	38
1496-1510	22	61
1546-1560	21	57
1574-1592	19	54
1715-1722	23	65
1810-1819	13	35
1902-1924	13	37
1990-2020	11	30
2058-2078	12	34
2102-2120	18	50
2150-2186	22	62
2248-2255	20	56
2412-2422	12	33
2432-2442	20	56
2700-2718	16	45
2760-2775	18	51
2822-2834	16	45
2933-2940	21	57
3020-3045	25	70

มหาวิทยาลัยเทคโนโลยีสุรนารี

APPENDIX B

RESISTIVITY LOG INTERPRETATION

มหาวิทยาลัยเทคโนโลยีสุรนารี

Table B.1 Resistivity log interpretation of well no. FA-MS-80-12.

Depth (feet)	Thickness (feet)	Long resistivity (ohm-m)	Short resistivity (ohm-m)	Lithology
1440-1466	26	40	15.5	very fine Lithic Greywacke
1540-1570	30	84	25	very fine Lithic Greywacke
1600-1624	24	94	31	fine Lithic Greywacke
1655-1670	15	105	33	fine Lithic Greywacke
1775-1805	30	121	27.5	Medium Lithic Greywacke
1915-1940	25	134	39	Medium Lithic Greywacke
1970-1985	10	60	28	fine Lithic Greywacke
2025-2035	10	106	31	fine Lithic Greywacke
2100-2140	40	110	45	Medium Lithic Greywacke
2245-2263	18	121	47	Medium Lithic Greywacke
2300-2310	10	140	54	Coarse Lithic Greywacke
2350-2366	16	152	56	Coarse Lithic Greywacke
2450-2463	13	20	8.5	very fine Quartz Wacke
2537-2555	18	40	12	very fine Quartz Wacke
2624-2632	8	50	21	very fine Quartz Wacke
2684-2688	4	71	30	fine Quartz Wacke
2720-2740	20	94	43	fine Quartz Wacke
2765-2778	13	124	56	Medium Quartz Wacke
2810-2815	5	131	43.5	Medium Quartz Wacke

มหาวิทยาลัยเทคโนโลยีสุรนารี

Table B.2 Resistivity log interpretation of well no. FA-MS-08-18.

Depth (feet)	Thickness (feet)	Long resistivity (ohm-m)	Short resistivity (ohm-m)	Lithology
1695-1711	16	110	43.5	very fine Lithic Greywacke
1720-1730	10	64	19	very fine Lithic Greywacke
1756-1764	8	70	23	fine Lithic Greywacke
1860-1870	10	87	27.5	fine Lithic Greywacke
1944-1965	21	103	25.5	Medium Lithic Greywacke
1980-1990	21	130	40	Medium Lithic Greywacke
2010-2034	24	35	15.5	fine Lithic Greywacke
2065-2069	4	56	15.5	fine Lithic Greywacke
2100-2110	10	73	30	Medium Lithic Greywacke
2165-2170	5	87	31	Medium Lithic Greywacke
2204-2223	5	99	36.5	Coarse Lithic Greywacke
2285-2295	10	131	61	Coarse Lithic Greywacke
2322-2354	32	50	21.5	very fine Quartz Wacke
2410-2432	22	71	31.5	very fine Quartz Wacke
2456-2466	10	84	35	very fine Quartz Wacke
2534-2544	10	94	38	fine Quartz Wacke
2596-2630	34	105	47.5	fine Quartz Wacke
2704-2732	28	121	54.5	Medium Quartz Wacke
2900-2920	20	134	49	Medium Quartz Wacke

มหาวิทยาลัยเทคโนโลยีสุรนารี

Table B.3 Resistivity log interpretation of well no. FA-MS-27-46.

Depth (feet)	Thickness (feet)	Long resistivity (ohm-m)	Short resistivity (ohm-m)	Lithology
1436-1460	24	46	17.5	very fine Lithic Greywacke
1498-1516	18	51	15.5	very fine Lithic Greywacke
1728-1746	18	65	22	fine Lithic Greywacke
1848-1864	16	77	24	fine Lithic Greywacke
1928-1956	28	89	22	Medium Lithic Greywacke
2060-2108	48	101	30	Medium Lithic Greywacke
2166-2234	68	41	20	fine Lithic Greywacke
2248-2288	40	53	16	fine Lithic Greywacke
2390-2406	16	66.5	27.5	Medium Lithic Greywacke
2432-2458	26	78	30	Medium Lithic Greywacke
2514-2544	30	96	36.5	Coarse Lithic Greywacke
2622-2666	44	108	56	Coarse Lithic Greywacke
2680-2706	26	59	25.5	very fine Quartz Wacke
2785-2800	15	67	30	very fine Quartz Wacke
2870-2880	10	84	35	very fine Quartz Wacke
2960-2980	20	98.5	40	fine Quartz Wacke
3112-3144	32	114	50	fine Quartz Wacke
3280-3312	32	127	60	Medium Quartz Wacke
3418-3434	16	143	52	Medium Quartz Wacke

มหาวิทยาลัยเทคโนโลยีสุรนารี

Table B.4 Resistivity log interpretation of well no. FA-MS-28-47.

Depth (feet)	Thickness (feet)	Long resistivity (ohm-m)	Short resistivity (ohm-m)	Lithology
1400-1430	30	44	17.5	very fine Lithic Greywacke
1450-1488	38	50	15	very fine Lithic Greywacke
1606-1626	20	65	22	fine Lithic Greywacke
1760-1770	10	73	23	fine Lithic Greywacke
1855-1865	10	82	21	Medium Lithic Greywacke
1962-1992	30	96	30	Medium Lithic Greywacke
2062-2080	18	35	15.5	fine Lithic Greywacke
2178-2188	10	43	12.5	fine Lithic Greywacke
2244-2254	10	65	25	Medium Lithic Greywacke
2318-2334	16	71	25.5	Medium Lithic Greywacke
2412-2422	10	88	35	Coarse Lithic Greywacke
2520-2540	20	104	47.5	Coarse Lithic Greywacke
2620-2630	10	80	34	very fine Quartz Wacke
2663-2680	17	91	40	very fine Quartz Wacke
2760-2785	25	106	45	very fine Quartz Wacke
2850-2870	20	112.5	41	fine Quartz Wacke
2900-2920	20	121	54.5	fine Quartz Wacke
3000-3010	10	136	60	Medium Quartz Wacke
3070-3090	20	152	56	Medium Quartz Wacke

มหาวิทยาลัยเทคโนโลยีสุรนารี

Table B.5 Resistivity log interpretation of well no. FA-MS-28-48.

Depth (feet)	Thickness (feet)	Long resistivity (ohm-m)	Short resistivity (ohm-m)	Lithology
1672-1728	56	90	35	very fine Lithic Greywacke
1753-1770	17	95	28	very fine Lithic Greywacke
1798-1816	18	100	32.5	fine Lithic Greywacke
1900-1920	20	105	32	fine Lithic Greywacke
2025-2035	10	110	27	Medium Lithic Greywacke
2100-2120	20	130	38.5	Medium Lithic Greywacke
2238-2260	22	200	90	fine Lithic Greywacke
2320-2340	20	30	8.5	fine Lithic Greywacke
2410-2430	20	65	25	Medium Lithic Greywacke
2490-2500	10	90	32.5	Medium Lithic Greywacke
2625-2632	7	120	46	Coarse Lithic Greywacke
2680-2688	8	130	62	Coarse Lithic Greywacke
2700-2715	15	210	88	very fine Quartz Wacke
2740-2755	15	50	22	very fine Quartz Wacke
2875-2879	4	75	32	very fine Quartz Wacke
2910-2920	10	85	33	fine Quartz Wacke
3000-3020	20	105	47	fine Quartz Wacke
3222-3230	8	120	54	Medium Quartz Wacke
3310-3340	30	125	45	Medium Quartz Wacke

มหาวิทยาลัยเทคโนโลยีสุรนารี

Table B.6 Resistivity log interpretation of well no. FA-MS-28-49.

Depth (feet)	Thickness (feet)	Long resistivity (ohm-m)	Short resistivity (ohm-m)	Lithology
1465-1478	13	45	16.5	very fine Lithic Greywacke
1540-1566	26	40	12	very fine Lithic Greywacke
1634-1642	8	47.5	16	fine Lithic Greywacke
1700-1718	18	63	20	fine Lithic Greywacke
1820-1860	40	84	21	Medium Lithic Greywacke
1984-2002	18	103	29	Medium Lithic Greywacke
2014-2024	10	34	14.5	fine Lithic Greywacke
2220-2230	10	106	31	fine Lithic Greywacke
2298-2308	10	112.5	46	Medium Lithic Greywacke
2344-2360	16	121	44.5	Medium Lithic Greywacke
2458-2480	22	136	50	Coarse Lithic Greywacke
2544-2550	6	152	70	Coarse Lithic Greywacke
2624-2632	8	50	21.5	very fine Quartz Wacke
2674-2792	18	46	19	very fine Quartz Wacke
2710-2722	12	55	22	very fine Quartz Wacke
2785-2800	15	87.5	33	fine Quartz Wacke
2810-2818	8	94	40	fine Quartz Wacke
2910-2925	15	116	55	Medium Quartz Wacke
2965-2978	13	134	45	Medium Quartz Wacke

มหาวิทยาลัยเทคโนโลยีสุรนารี

Table B.7 Resistivity log interpretation of well no. FA-MS-28-50.

Depth (feet)	Thickness (feet)	Long resistivity (ohm-m)	Short resistivity (ohm-m)	Lithology
1730-1742	12	64	25	very fine Lithic Greywacke
1782-1846	64	66.5	21	very fine Lithic Greywacke
1880-1890	10	73	26	fine Lithic Greywacke
1900-1920	20	86	25	fine Lithic Greywacke
1960-1990	30	109	27	Medium Lithic Greywacke
2140-2158	18	138	60	Medium Lithic Greywacke
2170-2180	10	50	23	fine Lithic Greywacke
2222-2236	14	51	15.5	fine Lithic Greywacke
2294-2304	10	62	20	Medium Lithic Greywacke
2332-2350	18	74	25.5	Medium Lithic Greywacke
2453-2461	8	88	33.5	Coarse Lithic Greywacke
2488-2512	24	95	29	Coarse Lithic Greywacke
2560-2580	20	50	21	very fine Quartz Wacke
2650-2675	15	60	24	very fine Quartz Wacke
2715-2735	20	72	30	very fine Quartz Wacke
2800-2820	20	80	30	fine Quartz Wacke
2880-2890	10	91	40	fine Quartz Wacke
2940-2968	28	103	46	Medium Quartz Wacke
2988-3000	12	120	43	Medium Quartz Wacke

มหาวิทยาลัยเทคโนโลยีสุรนารี

Table B.8 Resistivity log interpretation of well no. FA-MS-30-54.

Depth (feet)	Thickness (feet)	Long resistivity (ohm-m)	Short resistivity (ohm-m)	Lithology
1400-1415	15	40	16	very fine Lithic Greywacke
1478-1496	18	45	13.5	very fine Lithic Greywacke
1635-1651	16	60	20	fine Lithic Greywacke
1700-1714	14	80	25	fine Lithic Greywacke
1916-1930	14	100	25	Medium Lithic Greywacke
2014-2023	9	140	42	Medium Lithic Greywacke
2124-2154	30	30	13.5	fine Lithic Greywacke
2167-2192	25	40	11.5	fine Lithic Greywacke
2323-2338	15	60	23	Medium Lithic Greywacke
2378-2396	18	80	29	Medium Lithic Greywacke
2468-2482	14	100	38	Coarse Lithic Greywacke
2557-2576	19	125	59	Coarse Lithic Greywacke
2630-2640	10	70	30	very fine Quartz Wacke
2660-2680	20	90	40	very fine Quartz Wacke
2785-2800	15	105	45	very fine Quartz Wacke
2860-2880	20	110	44	fine Quartz Wacke
2940-2960	20	120	53.5	fine Quartz Wacke
3050-3060	10	135	61	Medium Quartz Wacke
3140-3160	20	140	50	Medium Quartz Wacke

Table B.9 Resistivity log interpretation of well no. FA-MS-31-55.

Depth (feet)	Thickness (feet)	Long resistivity (ohm-m)	Short resistivity (ohm-m)	Lithology
1518-1526	8	70	27.5	very fine Lithic Greywacke
1576-1598	22	87	26	very fine Lithic Greywacke
1715-1725	10	95	32	fine Lithic Greywacke
1764-1778	14	106	33	fine Lithic Greywacke
1820-1842	22	113	28	Medium Lithic Greywacke
1902-1924	22	129	40	Medium Lithic Greywacke
1958-1974	16	35	15.7	fine Lithic Greywacke
2030-2045	15	51	14.5	fine Lithic Greywacke
2102-2128	26	64	24.5	Medium Lithic Greywacke
2136-2180	44	77	28	Medium Lithic Greywacke
2244-2266	22	95	36	Coarse Lithic Greywacke
2292-2302	10	110	51.5	Coarse Lithic Greywacke
2326-2364	38	47	20	very fine Quartz Wacke
2425-2450	38	60	26.5	very fine Quartz Wacke
2540-2576	36	78	32	very fine Quartz Wacke
2700-2710	10	91	37	fine Quartz Wacke
2777-2788	11	106	46.5	fine Quartz Wacke
2900-2910	10	115	52	Medium Quartz Wacke
2980-3000	20	132	47.5	Medium Quartz Wacke

มหาวิทยาลัยเทคโนโลยีสุรนารี

Table B.10 Resistivity log interpretation of well no. FA-MS-32-56.

Depth (feet)	Thickness (feet)	Long resistivity (ohm-m)	Short resistivity (ohm-m)	Lithology
1720-1735	15	140	56	very fine Lithic Greywacke
1832-1844	12	40	12	very fine Lithic Greywacke
1910-1920	10	50	17	fine Lithic Greywacke
2014-2028	14	70	22	fine Lithic Greywacke
2055-2085	30	90	22	Medium Lithic Greywacke
2120-2140	20	120	36	Medium Lithic Greywacke
2192-2200	8	30	13.5	fine Lithic Greywacke
2260-2280	20	45	13	fine Lithic Greywacke
2340-2360	20	70	27	Medium Lithic Greywacke
2458-2468	10	80	29	Medium Lithic Greywacke
2536-2552	16	105	40	Coarse Lithic Greywacke
2570-2580	10	130	64	Coarse Lithic Greywacke
2610-2620	10	90	38	very fine Quartz Wacke
2640-2660	20	105	47	very fine Quartz Wacke
2710-2715	5	60	25	very fine Quartz Wacke
2798-2810	12	90	35	fine Quartz Wacke
2857-2865	8	110	49	fine Quartz Wacke
2915-2925	10	130	58	Medium Quartz Wacke
2980-2995	15	150	50	Medium Quartz Wacke

มหาวิทยาลัยเทคโนโลยีสุรนารี

Table B.11 Resistivity log interpretation of well no. FA-MS-33-58.

Depth (feet)	Thickness (feet)	Long resistivity (ohm-m)	Short resistivity (ohm-m)	Lithology
1620-1640	20	200	80	very fine Lithic Greywacke
1723-1744	11	80	24	very fine Lithic Greywacke
1871-1877	6	95	31	fine Lithic Greywacke
1955-1960	5	105	33	fine Lithic Greywacke
2020-2040	20	125	31	Medium Lithic Greywacke
2101-2109	8	140	42	Medium Lithic Greywacke
2178-2184	20	30	13	fine Lithic Greywacke
2281-2286	5	45	13	fine Lithic Greywacke
2354-2358	4	60	24	Medium Lithic Greywacke
2420-2431	11	85	31	Medium Lithic Greywacke
2470-2475	5	100	40	Coarse Lithic Greywacke
2530-2545	15	125	55	Coarse Lithic Greywacke
2612-2632	20	90	38	very fine Quartz Wacke
2706-2726	20	100	44.5	very fine Quartz Wacke
2745-2760	15	110	45.5	very fine Quartz Wacke
2825-2840	15	115	46	fine Quartz Wacke
2875-2890	15	130	58	fine Quartz Wacke
2942-2958	16	140	63	Medium Quartz Wacke
3046-3064	18	160	60	Medium Quartz Wacke

มหาวิทยาลัยเทคโนโลยีสุรนารี

Table B.12 Resistivity log interpretation of well no. FA-MS-34-59.

Depth (feet)	Thickness (feet)	Long resistivity (ohm-m)	Short resistivity (ohm-m)	Lithology
1510-1520	10	53	21	very fine Lithic Greywacke
1697-1736	39	38	11.5	very fine Lithic Greywacke
1812-1820	8	45	15	fine Lithic Greywacke
1865-1877	12	58.5	18.5	fine Lithic Greywacke
1920-1940	20	78	16.5	Medium Lithic Greywacke
2024-2032	8	85.5	24.5	Medium Lithic Greywacke
2108-2134	26	60	27	fine Lithic Greywacke
2198-2216	18	76.5	23.5	fine Lithic Greywacke
2248-2272	24	67	25	Medium Lithic Greywacke
2282-2304	22	76	30	Medium Lithic Greywacke
2322-2332	10	82	35.5	Coarse Lithic Greywacke
2404-2420	16	118	53.5	Coarse Lithic Greywacke
2486-2502	16	40	17	very fine Quartz Wacke
2560-2576	16	47	21	very fine Quartz Wacke
2648-2658	10	66	27.5	very fine Quartz Wacke
2800-2821	21	80	31	fine Quartz Wacke
2870-2889	19	100	42	fine Quartz Wacke
2990-2997	7	125	59	Medium Quartz Wacke
3045-3055	10	152	54	Medium Quartz Wacke

มหาวิทยาลัยเทคโนโลยีสุรนารี

Table B.13 Resistivity log interpretation of well no. FA-MS-34-60.

Depth (feet)	Thickness (feet)	Long resistivity (ohm-m)	Short resistivity (ohm-m)	Lithology
1450-1461	11	60	24	very fine Lithic Greywacke
1545-1555	10	70	21	very fine Lithic Greywacke
1620-1635	15	80	27	fine Lithic Greywacke
1738-1748	10	90	28	fine Lithic Greywacke
1760-1775	15	100	25	Medium Lithic Greywacke
1910-1919	9	120	35	Medium Lithic Greywacke
2022-2034	6	30	13	fine Lithic Greywacke
2066-2072	12	50	14	fine Lithic Greywacke
2204-2223	19	60	24.5	Medium Lithic Greywacke
2275-2284	9	70	26	Medium Lithic Greywacke
2323-2334	11	90	32	Coarse Lithic Greywacke
2426-2433	7	100	49	Coarse Lithic Greywacke
2467-2481	14	50	22	very fine Quartz Wacke
2525-2534	9	60	26	very fine Quartz Wacke
2580-2590	10	70	30	very fine Quartz Wacke
2602-2620	18	80	31	fine Quartz Wacke
2665-2670	5	90	39	fine Quartz Wacke
2740-2755	15	105	44	Medium Quartz Wacke
2820-2830	10	115	40	Medium Quartz Wacke

มหาวิทยาลัยเทคโนโลยีสุรนารี

Table B.14 Resistivity log interpretation of well no. FA-MS-34-61.

Depth (feet)	Thickness (feet)	Long resistivity (ohm-m)	Short resistivity (ohm-m)	Lithology
1375-1405	30	78	30	very fine Lithic Greywacke
1710-1722	12	85	26	very fine Lithic Greywacke
1770-1798	28	97	32	fine Lithic Greywacke
1900-1910	10	105	32	fine Lithic Greywacke
1980-2000	20	119	30	Medium Lithic Greywacke
2100-2105	5	132	40	Medium Lithic Greywacke
2175-2200	25	35	16	fine Lithic Greywacke
2286-2303	17	42	12	fine Lithic Greywacke
2360-2370	10	54	21	Medium Lithic Greywacke
2472-2481	9	68	25	Medium Lithic Greywacke
2510-2520	20	94	36	Coarse Lithic Greywacke
2575-2590	15	106	53	Coarse Lithic Greywacke
2640-2650	10	50	21	very fine Quartz Wacke
2700-2710	10	66	30	very fine Quartz Wacke
2740-2755	15	78	32	very fine Quartz Wacke
2770-2790	20	91	36	fine Quartz Wacke
2845-2860	15	106	48	fine Quartz Wacke
2925-2935	10	121	55.5	Medium Quartz Wacke
2975-2990	15	140	50	Medium Quartz Wacke

มหาวิทยาลัยเทคโนโลยีสุรนารี

Table B.15 Resistivity log interpretation of well no. FA-MS-35-62.

Depth (feet)	Thickness (feet)	Long resistivity (ohm-m)	Short resistivity (ohm-m)	Lithology
1530-1535	5	49	20	very fine Lithic Greywacke
1605-1610	5	67	20	very fine Lithic Greywacke
1700-1720	20	79	25.5	fine Lithic Greywacke
1740-1750	10	98	30	fine Lithic Greywacke
1795-1805	10	112	28.5	Medium Lithic Greywacke
1850-1860	10	144	44	Medium Lithic Greywacke
1990-2010	20	20	9	fine Lithic Greywacke
2130-2150	20	37	10.5	fine Lithic Greywacke
2170-2180	10	46	17.5	Medium Lithic Greywacke
2210-2220	10	78	28.5	Medium Lithic Greywacke
2305-2315	10	104	40	Coarse Lithic Greywacke
2360-2375	15	121	60	Coarse Lithic Greywacke
2460-2475	15	45	19.5	very fine Quartz Wacke
2530-2540	10	51	22.5	very fine Quartz Wacke
2595-2600	5	66	28	very fine Quartz Wacke
2628-2635	7	74.5	30	fine Quartz Wacke
2770-2790	7	93	41	fine Quartz Wacke
2821-2831	10	108.5	49	Medium Quartz Wacke
2939-2945	6	132	50	Medium Quartz Wacke

มหาวิทยาลัยเทคโนโลยีสุรนารี

Table B.16 Resistivity log interpretation of well no. FA-MS-36-65.

Depth (feet)	Thickness (feet)	Long resistivity (ohm-m)	Short resistivity (ohm-m)	Lithology
1428-1488	60	40	18	very fine Lithic Greywacke
1530-1545	15	51	15	very fine Lithic Greywacke
1700-1720	20	76	21	fine Lithic Greywacke
1758-1828	70	88	29	fine Lithic Greywacke
1896-1904	8	110	25	Medium Lithic Greywacke
1988-2000	12	125	30	Medium Lithic Greywacke
2064-2072	8	85	35	fine Lithic Greywacke
2180-2208	28	47	11.5	fine Lithic Greywacke
2266-2278	12	62	23	Medium Lithic Greywacke
2322-2352	30	81	30	Medium Lithic Greywacke
2376-2400	24	100	38	Coarse Lithic Greywacke
2520-2530	10	125	59	Coarse Lithic Greywacke
2616-2636	20	60	27	very fine Quartz Wacke
2717-2725	20	45	19.5	very fine Quartz Wacke
2850-2870	20	51	22.5	very fine Quartz Wacke
2950-2970	20	64	28	fine Quartz Wacke
3090-3110	20	68	30	fine Quartz Wacke
3222-3230	8	96	41	Medium Quartz Wacke
3340-3365	25	118.5	42	Medium Quartz Wacke

มหาวิทยาลัยเทคโนโลยีสุรนารี

Table B.17 Resistivity log interpretation of well no. FA-MS-36-66.

Depth (feet)	Thickness (feet)	Long resistivity (ohm-m)	Short resistivity (ohm-m)	Lithology
1488-1512	24	108	48	very fine Lithic Greywacke
1547-1560	13	67	20	very fine Lithic Greywacke
1670-1682	12	79	25.5	fine Lithic Greywacke
1718-1730	14	99	30	fine Lithic Greywacke
1800-1820	20	122	28.5	Medium Lithic Greywacke
1852-1866	14	144	44	Medium Lithic Greywacke
1940-1956	32	20	8.5	fine Lithic Greywacke
2014-2034	20	43	12.5	fine Lithic Greywacke
2080-2100	20	65	25	Medium Lithic Greywacke
2170-2190	20	71	25.5	Medium Lithic Greywacke
2290-2306	16	88	33	Coarse Lithic Greywacke
2394-2414	20	104	47.5	Coarse Lithic Greywacke
2434-2470	36	40	17.5	very fine Quartz Wacke
2478-2494	16	103	44.5	very fine Quartz Wacke
2717-2725	8	111	45.5	very fine Quartz Wacke
2775-2780	5	124	46	fine Quartz Wacke
2840-2850	10	131	58	fine Quartz Wacke
2957-2970	13	146	63	Medium Quartz Wacke
3045-3067	22	160	57	Medium Quartz Wacke

มหาวิทยาลัยเทคโนโลยีสุรนารี

Table B.18 Resistivity log interpretation of well no. FA-MS-36-67.

Depth (feet)	Thickness (feet)	Long resistivity (ohm-m)	Short resistivity (ohm-m)	Lithology
1455-1460	5	50	18	very fine Lithic Greywacke
1526-1544	18	73	21.5	very fine Lithic Greywacke
1624-1638	14	87	29	fine Lithic Greywacke
1686-1696	10	91	28	fine Lithic Greywacke
1728-1784	56	106	26.5	Medium Lithic Greywacke
1904-1930	26	118	35.5	Medium Lithic Greywacke
2040-2072	32	35	16	fine Lithic Greywacke
2116-2134	18	52	14.5	fine Lithic Greywacke
2165-2177	12	63	24	Medium Lithic Greywacke
2278-2298	20	88	32	Medium Lithic Greywacke
2366-2378	12	113	47	Coarse Lithic Greywacke
2414-2444	30	132	60	Coarse Lithic Greywacke
2492-2504	12	50	21	very fine Quartz Wacke
2528-2572	44	62	28	very fine Quartz Wacke
2642-2666	24	75	32	very fine Quartz Wacke
2686-2724	38	91	36.5	fine Quartz Wacke
2735-2745	10	114	51	fine Quartz Wacke
2770-2785	15	126	57	Medium Quartz Wacke
2815-2822	7	135	46	Medium Quartz Wacke

มหาวิทยาลัยเทคโนโลยีสุรนารี

Table B.19 Resistivity log interpretation of well no. FA-MS-40-69.

Depth (feet)	Thickness (feet)	Long resistivity (ohm-m)	Short resistivity (ohm-m)	Lithology
1434-1445	11	55	22	very fine Lithic Greywacke
1495-1500	5	51	15.5	very fine Lithic Greywacke
1550-1560	10	68	23	fine Lithic Greywacke
1720-1744	24	70	21	fine Lithic Greywacke
1796-1822	26	94	24	Medium Lithic Greywacke
1834-1848	14	103.5	29	Medium Lithic Greywacke
1914-1930	16	39	18.5	fine Lithic Greywacke
1972-1990	18	75	23	fine Lithic Greywacke
2006-2012	6	91	35.5	Medium Lithic Greywacke
2184-2210	26	114	41	Medium Lithic Greywacke
2256-2274	18	126	50	Coarse Lithic Greywacke
2310-2322	12	135	62	Coarse Lithic Greywacke
2404-2420	12	44	16.5	very fine Quartz Wacke
2544-2550	12	61	27.5	very fine Quartz Wacke
2663-2674	11	75	30.5	very fine Quartz Wacke
2755-2761	6	86.5	34	fine Quartz Wacke
2844-2860	16	102	45.5	fine Quartz Wacke
2987-3002	15	118	53.5	Medium Quartz Wacke
3165-3188	23	128	47	Medium Quartz Wacke

มหาวิทยาลัยเทคโนโลยีสุรนารี

Table B.20 Resistivity log interpretation of well no. FA-MS-46-70.

Depth (feet)	Thickness (feet)	Long resistivity (ohm-m)	Short resistivity (ohm-m)	Lithology
1392-1406	14	55	22	very fine Lithic Greywacke
1476-1508	32	61	18	very fine Lithic Greywacke
1550-1565	15	76	24	fine Lithic Greywacke
1636-1648	12	83	25	fine Lithic Greywacke
1706-1762	56	92	22	Medium Lithic Greywacke
1810-1822	12	113.5	33	Medium Lithic Greywacke
1902-1924	24	40	18.5	Fine Lithic Greywacke
1936-1960	24	44	12.5	Fine Lithic Greywacke
2054-2082	28	67	26	Medium Lithic Greywacke
2234-2264	30	95.5	33	Medium Lithic Greywacke
2318-2330	12	107.5	40	Coarse Lithic Greywacke
2414-2440	26	118	54	Coarse Lithic Greywacke
2542-2554	12	50	21	Very fine Quartz Wacke
2570-2582	12	61	27	Very fine Quartz Wacke
2615-2620	5	76	31	Very fine Quartz Wacke
2642-2655	13	85	34	fine Quartz Wacke
2745-2750	5	96	42	fine Quartz Wacke
2820-2833	13	148	66	Medium Quartz Wacke
2868-2880	12	148	55	Medium Quartz Wacke

มหาวิทยาลัยเทคโนโลยีสุรนารี

Table B.21 Resistivity log interpretation of well no. FA-MS-47-71.

Depth (feet)	Thickness (feet)	Long resistivity (ohm-m)	Short resistivity (ohm-m)	Lithology
1634-1648	14	100	35	very fine Lithic Greywacke
1701-1711	10	49	15	very fine Lithic Greywacke
1740-1745	5	61	20	fine Lithic Greywacke
1784-1795	5	83	25	fine Lithic Greywacke
1804-1812	8	125	31.5	Medium Lithic Greywacke
1940-1952	12	155	45	Medium Lithic Greywacke
1976-1990	14	95	40	fine Lithic Greywacke
2023-2037	14	47	11.5	fine Lithic Greywacke
2046-2062	16	62	23	Medium Lithic Greywacke
2300-2314	14	81	30	Medium Lithic Greywacke
2352-2364	12	100	38	Coarse Lithic Greywacke
2404-2420	16	125	59	Coarse Lithic Greywacke
2440-2450	10	70	30	very fine Quartz Wacke
2512-2532	20	45	19.5	very fine Quartz Wacke
2686-2714	28	51	22.5	very fine Quartz Wacke
2724-2744	20	66	28	fine Quartz Wacke
2780-2800	20	74.5	30	fine Quartz Wacke
2895-2900	5	93	41	Medium Quartz Wacke
2999-3015	16	108.5	36	Medium Quartz Wacke

มหาวิทยาลัยเทคโนโลยีสุรนารี

Table B.22 Resistivity log interpretation of well no. FA-MS-48-73.

Depth (feet)	Thickness (feet)	Long resistivity (ohm-m)	Short resistivity (ohm-m)	Lithology
1460-1475	15	25	10	very fine Lithic Greywacke
1545-1555	10	30	9	very fine Lithic Greywacke
1662-1675	13	45	15	fine Lithic Greywacke
1764-1772	8	60	19	fine Lithic Greywacke
1826-1838	12	85	21	Medium Lithic Greywacke
1930-1940	10	90	27	Medium Lithic Greywacke
2023-2030	7	40	18	fine Lithic Greywacke
2170-2178	8	50	14	fine Lithic Greywacke
2222-2272	50	90	33	Medium Lithic Greywacke
2338-2368	30	110	38	Medium Lithic Greywacke
2422-2432	10	130	50	Coarse Lithic Greywacke
2487-2499	12	150	70	Coarse Lithic Greywacke
2587-2600	13	50	21.5	very fine Quartz Wacke
2677-2700	13	70	33	very fine Quartz Wacke
2745-2755	10	75	30	very fine Quartz Wacke
2798-2810	12	80	35	fine Quartz Wacke
2835-2850	15	100	43.5	fine Quartz Wacke
2900-2920	20	120	59.5	Medium Quartz Wacke
2970-2980	10	135	50	Medium Quartz Wacke

มหาวิทยาลัยเทคโนโลยีสุรนารี

Table B.23 Resistivity log interpretation of well no. FA-MS-48-75.

Depth (feet)	Thickness (feet)	Long resistivity (ohm-m)	Short resistivity (ohm-m)	Lithology
1466-1484	16	31	12	very fine Lithic Greywacke
1580-1600	20	49	15	very fine Lithic Greywacke
1785-1792	7	61	20	fine Lithic Greywacke
1917-1928	11	83	25	fine Lithic Greywacke
2019-2025	6	125	30	Medium Lithic Greywacke
2082-2088	6	153.5	45	Medium Lithic Greywacke
2200-2210	10	55	25	fine Lithic Greywacke
2305-2309	4	72	20	fine Lithic Greywacke
2398-2428	30	92.5	35	Medium Lithic Greywacke
2520-2530	10	110	40	Medium Lithic Greywacke
2620-2635	15	130	50	Coarse Lithic Greywacke
2660-2680	20	150	70	Coarse Lithic Greywacke
2720-2735	15	35	15	very fine Quartz Wacke
2765-2775	10	45	20	very fine Quartz Wacke
2835-2845	10	60	25	very fine Quartz Wacke
2915-2935	20	75	30	fine Quartz Wacke
3065-3080	15	90	40	fine Quartz Wacke
3185-3200	15	100	45	Medium Quartz Wacke
3325-3345	20	135	50	Medium Quartz Wacke

มหาวิทยาลัยเทคโนโลยีสุรนารี

Table B.24 Resistivity log interpretation of well no. FA-MS-49-76.

Depth (feet)	Thickness (feet)	Long resistivity (ohm-m)	Short resistivity (ohm-m)	Lithology
1595-1615	20	100	35	very fine Lithic Greywacke
1635-1650	15	63	18.5	very fine Lithic Greywacke
1735-1755	20	78	26.5	fine Lithic Greywacke
1785-1800	15	85	25.5	fine Lithic Greywacke
1899-1910	11	99.5	24	Medium Lithic Greywacke
1970-1985	15	107	33	Medium Lithic Greywacke
2040-2050	10	40	17.5	fine Lithic Greywacke
2125-2140	15	62	18.5	fine Lithic Greywacke
2245-2270	25	74	27.5	Medium Lithic Greywacke
2336-2345	9	87	30	Medium Lithic Greywacke
2425-2450	25	104	40	Coarse Lithic Greywacke
2480-2495	15	140	70	Coarse Lithic Greywacke
2580-2590	10	50	22	very fine Quartz Wacke
2665-2685	20	64	28	very fine Quartz Wacke
2730-2740	10	75	31	very fine Quartz Wacke
2800-2840	40	89	35	fine Quartz Wacke
2920-2940	20	94	42	fine Quartz Wacke
3046-3064	18	117	52	Medium Quartz Wacke
3160-3185	25	128	47	Medium Quartz Wacke

มหาวิทยาลัยเทคโนโลยีสุรนารี

Table B.25 Resistivity log interpretation of well no. FA-MS-49-77.

Depth (feet)	Thickness (feet)	Long resistivity (ohm-m)	Short resistivity (ohm-m)	Lithology
1518-1526	8	42	16.5	very fine Lithic Greywacke
1600-1620	20	55	16.5	very fine Lithic Greywacke
1687-1700	13	64	22	fine Lithic Greywacke
1795-1810	15	83	25	fine Lithic Greywacke
1862-1868	6	97	24.5	Medium Lithic Greywacke
1950-1955	5	103	30	Medium Lithic Greywacke
2042-2050	8	20	9.5	fine Lithic Greywacke
2132-2148	16	33	9	fine Lithic Greywacke
2163-2171	8	47	18.5	Medium Lithic Greywacke
2184-2218	34	61	21.5	Medium Lithic Greywacke
2240-2260	20	74	28.5	Coarse Lithic Greywacke
2313-2329	16	81	37.5	Coarse Lithic Greywacke
2417-2431	14	40	16.5	very fine Quartz Wacke
2462-2473	11	53	23.5	very fine Quartz Wacke
2547-2559	12	61	25	very fine Quartz Wacke
2685-2700	15	76	30	fine Quartz Wacke
2780-2790	10	82	35.5	fine Quartz Wacke
2820-2840	20	118	53.5	Medium Quartz Wacke
2999-3010	11	134	50	Medium Quartz Wacke

มหาวิทยาลัยเทคโนโลยีสุรนารี

Table B.26 Resistivity log interpretation of well no. FA-MS-50-78.

Depth (feet)	Thickness (feet)	Long resistivity (ohm-m)	Short resistivity (ohm-m)	Lithology
1356-1384	28	50	21	very fine Lithic Greywacke
1440-1447	7	65	20	very fine Lithic Greywacke
1542-1558	16	80	27	fine Lithic Greywacke
1598-1622	24	100	32	fine Lithic Greywacke
1642-1672	30	115	30	Medium Lithic Greywacke
1786-1822	36	130	40	Medium Lithic Greywacke
1868-1892	24	30	15	fine Lithic Greywacke
1968-1976	8	45	12	fine Lithic Greywacke
2106-2130	24	55	21.5	Medium Lithic Greywacke
2246-2262	16	70	26.5	Medium Lithic Greywacke
2318-2326	8	85	29.5	Coarse Lithic Greywacke
2364-2377	13	110	52	Coarse Lithic Greywacke
2405-2418	13	90	38.5	very fine Quartz Wacke
2588-2601	13	95	42	very fine Quartz Wacke
2700-2711	11	105	42.5	very fine Quartz Wacke
2803-2812	9	115	46	fine Quartz Wacke
2890-2899	9	120	53	fine Quartz Wacke
2970-2977	7	140	63	Medium Quartz Wacke
3020-3045	25	170	64	Medium Quartz Wacke

มหาวิทยาลัยเทคโนโลยีสุรนารี

Table B.27 Resistivity log interpretation of well no. FA-MS-51-79.

Depth (feet)	Thickness (feet)	Long resistivity (ohm-m)	Short resistivity (ohm-m)	Lithology
1530-1540	10	50	20	very fine Lithic Greywacke
1620-1630	10	75	22	very fine Lithic Greywacke
1784-1795	11	85	27.5	fine Lithic Greywacke
1875-1885	10	105	33	fine Lithic Greywacke
1915-1935	20	120	30	Medium Lithic Greywacke
1976-1990	14	125	39.5	Medium Lithic Greywacke
2052-2078	26	60	17	fine Lithic Greywacke
2146-2168	22	63	18.5	fine Lithic Greywacke
2200-2210	10	78	29	Medium Lithic Greywacke
2336-2354	18	87.5	30	Medium Lithic Greywacke
2430-2443	13	99.5	37	Coarse Lithic Greywacke
2508-2528	20	107	49	Coarse Lithic Greywacke
2548-2560	12	53	18	very fine Quartz Wacke
2640-2648	12	78	33.5	very fine Quartz Wacke
2695-2711	16	85	39	very fine Quartz Wacke
2760-2780	20	97	37	fine Quartz Wacke
2875-2890	15	105	45	fine Quartz Wacke
2920-2940	20	119	55	Medium Quartz Wacke
3040-3060	20	132	40	Medium Quartz Wacke

มหาวิทยาลัยเทคโนโลยีสุรนารี

Table B.28 Resistivity log interpretation of well no. FA-MS-51-80.

Depth (feet)	Thickness (feet)	Long resistivity (ohm-m)	Short resistivity (ohm-m)	Lithology
1718-1730	12	100	36	very fine Lithic Greywacke
1740-1745	5	43	12.5	very fine Lithic Greywacke
1940-1956	16	51	17.5	fine Lithic Greywacke
1990-2018	28	75	23	fine Lithic Greywacke
2030-2056	26	101.5	25	Medium Lithic Greywacke
2098-2102	4	115	34.5	Medium Lithic Greywacke
2198-2206	8	30	13.5	fine Lithic Greywacke
2242-2256	14	42	12	fine Lithic Greywacke
2300-2336	36	57	21.5	Medium Lithic Greywacke
2376-2434	58	86	31	Medium Lithic Greywacke
2458-2474	16	95	37	Coarse Lithic Greywacke
2500-2526	26	134	65	Coarse Lithic Greywacke
2590-2596	6	45	19.5	very fine Quartz Wacke
2622-2648	26	51	22.5	very fine Quartz Wacke
2728-2748	20	82	34	very fine Quartz Wacke
2770-2790	20	95.5	37.5	fine Quartz Wacke
2860-2875	15	107	48.5	fine Quartz Wacke
2900-2920	20	114	52.5	Medium Quartz Wacke
3002-3025	23	129	47	Medium Quartz Wacke

มหาวิทยาลัยเทคโนโลยีสุรนารี

Table B.29 Resistivity log interpretation of well no. FA-MS-53-83.

Depth (feet)	Thickness (feet)	Long resistivity (ohm-m)	Short resistivity (ohm-m)	Lithology
1366-1396	30	40	16	very fine Lithic Greywacke
1625-1635	10	55	16.5	very fine Lithic Greywacke
1685-1992	7	65	21	fine Lithic Greywacke
1800-1810	10	90	28	fine Lithic Greywacke
1900-1925	25	110	27	Medium Lithic Greywacke
1960-1970	10	125	37	Medium Lithic Greywacke
2044-2085	31	20	9	fine Lithic Greywacke
2100-2120	41	40	11.5	fine Lithic Greywacke
2155-2165	10	70	28	Medium Lithic Greywacke
2172-2203	31	120	44	Medium Lithic Greywacke
2295-2312	17	140	56	Coarse Lithic Greywacke
2379-2395	16	150	67	Coarse Lithic Greywacke
2560-2567	7	80	34	very fine Quartz Wacke
2580-2587	7	88	38.5	very fine Quartz Wacke
2745-2760	15	90	37	very fine Quartz Wacke
2855-2865	10	95	38.5	fine Quartz Wacke
2925-2935	10	103	45	fine Quartz Wacke
3000-3005	5	127	58	Medium Quartz Wacke
3098-3105	7	145	54	Medium Quartz Wacke

มหาวิทยาลัยเทคโนโลยีสุรนารี

Table B.30 Resistivity log interpretation of well no. FA-MS-54-84.

Depth (feet)	Thickness (feet)	Long resistivity (ohm-m)	Short resistivity (ohm-m)	Lithology
1560-1580	20	34	13.5	very fine Lithic Greywacke
1625-1635	10	46	14	very fine Lithic Greywacke
1730-1740	10	55	18.5	fine Lithic Greywacke
1870-1880	10	77.5	23.5	fine Lithic Greywacke
1940-1960	20	91	22.5	Medium Lithic Greywacke
1980-1990	10	116	35.5	Medium Lithic Greywacke
2045-2055	10	25	11	fine Lithic Greywacke
2160-2170	10	40	11.5	fine Lithic Greywacke
2275-2285	10	55	21	Medium Lithic Greywacke
2360-2370	10	78	27	Medium Lithic Greywacke
2440-2460	20	80	31	Coarse Lithic Greywacke
2515-2520	5	103.5	51	Coarse Lithic Greywacke
2550-2555	5	30	13	very fine Quartz Wacke
2645-2660	15	57	25	very fine Quartz Wacke
2690-2700	10	79	32.5	very fine Quartz Wacke
2790-2800	10	91	35.5	fine Quartz Wacke
2855-2870	15	112	50	fine Quartz Wacke
2910-2930	20	131	58.5	Medium Quartz Wacke
2975-2990	15	144	54	Medium Quartz Wacke

มหาวิทยาลัยเทคโนโลยีสุรนารี

Table B.31 Resistivity log interpretation of well no. FA-MS-54-85.

Depth (feet)	Thickness (feet)	Long resistivity (ohm-m)	Short resistivity (ohm-m)	Lithology
1295-1320	25	35	14.5	very fine Lithic Greywacke
1440-1460	20	50	15	very fine Lithic Greywacke
1544-1560	16	70	21	fine Lithic Greywacke
1782-1788	6	85	29	fine Lithic Greywacke
1865-1870	5	110	35	Medium Lithic Greywacke
2002-2016	14	125	30	Medium Lithic Greywacke
2060-2070	10	30	9	fine Lithic Greywacke
2100-2110	10	45	20	fine Lithic Greywacke
2178-2184	6	50	15	Medium Lithic Greywacke
2246-2260	14	75	29	Medium Lithic Greywacke
2314-2324	10	95	32	Coarse Lithic Greywacke
2405-2414	7	130	50	Coarse Lithic Greywacke
2460-2468	8	70	35	very fine Quartz Wacke
2640-2660	20	80	37	very fine Quartz Wacke
2820-2845	25	90	38	very fine Quartz Wacke
2860-2875	15	110	49	fine Quartz Wacke
2930-2950	20	115	55	fine Quartz Wacke
3010-3030	20	125	59	Medium Quartz Wacke
3095-3110	15	130	51	Medium Quartz Wacke

มหาวิทยาลัยเทคโนโลยีสุรนารี

Table B.32 Resistivity log interpretation of well no. FA-MS-54-86.

Depth (feet)	Thickness (feet)	Long resistivity (ohm-m)	Short resistivity (ohm-m)	Lithology
1366-1396	30	70	25	very fine Lithic Greywacke
1484-1520	24	77	23	very fine Lithic Greywacke
1660-1680	20	90	30	fine Lithic Greywacke
1794-1820	26	96	30	fine Lithic Greywacke
1838-1882	44	114.5	28	Medium Lithic Greywacke
1970-2006	36	130.5	38.5	Medium Lithic Greywacke
2034-2092	58	35	15.5	fine Lithic Greywacke
2138-2162	24	52	14.5	fine Lithic Greywacke
2194-2266	72	66	25.5	Medium Lithic Greywacke
2284-2290	6	74	26.5	Medium Lithic Greywacke
2332-2384	52	91	36	Coarse Lithic Greywacke
2478-2536	58	120	60	Coarse Lithic Greywacke
2556-2576	20	50	21.5	very fine Quartz Wacke
2666-2688	22	62	28	very fine Quartz Wacke
2732-2746	14	77	32	very fine Quartz Wacke
2764-2792	28	82	33	fine Quartz Wacke
2848-2864	16	94.5	42	fine Quartz Wacke
2924-2952	28	121	55	Medium Quartz Wacke
2958-2990	32	129	45	Medium Quartz Wacke

มหาวิทยาลัยเทคโนโลยีสุรนารี

Table B.33 Resistivity log interpretation of well no. FA-MS-55-87.

Depth (feet)	Thickness (feet)	Long resistivity (ohm-m)	Short resistivity (ohm-m)	Lithology
1375-1405	30	52.5	19.5	very fine Lithic Greywacke
1496-1510	14	63	19	very fine Lithic Greywacke
1546-1560	14	71	24	fine Lithic Greywacke
1574-1592	18	83	25.5	fine Lithic Greywacke
1715-1722	7	95	23	Medium Lithic Greywacke
1810-1819	9	107	33	Medium Lithic Greywacke
1902-1924	20	30	13.5	fine Lithic Greywacke
1990-2020	30	43	11.5	fine Lithic Greywacke
2058-2078	20	68	25.5	Medium Lithic Greywacke
2102-2120	18	74	27	Medium Lithic Greywacke
2150-2186	36	98.5	38	Coarse Lithic Greywacke
2248-2255	7	106	50	Coarse Lithic Greywacke
2412-2422	10	50	21	very fine Quartz Wacke
2432-2442	10	61	27	very fine Quartz Wacke
2700-2718	18	74	30	very fine Quartz Wacke
2760-2775	15	83	33	fine Quartz Wacke
2822-2834	12	96	42	fine Quartz Wacke
2933-2940	7	109	50	Medium Quartz Wacke
3020-3045	25	119	39.5	Medium Quartz Wacke

มหาวิทยาลัยเทคโนโลยีสุรนารี

APPENDIX C

PERMEABILITY AND POROSITY OF SANDSTONE LAYER OF MAE-SOON OIL FIELD

มหาวิทยาลัยเทคโนโลยีสุรนารี

Table C.1 Permeability and porosity of sandstone layer of Mae-Soon oil field (after DED).

Well Name	Depth of the sample measured from KBE (feet)	Sandstone name	Permeability (millidarcy)	Porosity (Percent)	Average grain size of the sediments contained in the rock (millimeter)	Cementing material (Percent)	Matrix (Percent)
FA-MS-30-54	2020.05	Very coarse sandstone Lithic Grey Wacke	-*	16.68	2	2	22
FA-MS-30-54	2570.54	Coarse sandstone Lithic Grey Wacke	-*	15.98	0.7	2	19.5
FA-MS-32-56	1359.21	Very fine sandstone Lithic Grey Wacke	19.62	20.90	0.125	3	16
FA-MS-32-56	1776.04	Fine sandstone Lithic Grey Wacke	3.63	19.87	0.25	3	19
FA-MS-32-56	2101.10	Fine sandstone Lithic Grey Wacke	53.45	17.60	0.25	3	18
FA-MS-32-58	2383.36	Fine sandstone Lithic Grey Wacke	2118.2	35.23	0.25	2	20
FA-MS-32-58	3120.85	Fine sandstone Lithic Grey Wacke	1603.4	22.90	0.25	2	22

มหาวิทยาลัยเทคโนโลยีสุรนารี

Table C.1 Permeability and porosity of sandstone layer of Mae-Soon oil field (after DED) (cont).

Well Name	Depth of the sample measured from KBE (feet)	Sandstone name	Permeability (millidarcy)	Porosity (Percent)	Average grain size of the sediments contained in the rock (millimeter)	Cementing material (Percent)	Matrix (Percent)
FA-MS-32-59	1625.56	Fine sandstone Lithic Grey Wacke	904.44	23.13	0.25	2	19
FA-MS-32-59	2101.57	Fine sandstone Lithic Grey Wacke	2765.3	35.55	0.25	2	20
FA-MS-33-60	1909.84	Fine sandstone Lithic Grey Wacke	19.70	18.31	0.25	4	18
FA-MS-33-60	2300.98	Fine sandstone Lithic Grey Wacke	6.54	11.43	0.15	4	20
FA-MS-35-62	2287.40	Fine sandstone Lithic Grey Wacke	13.35	25.16	0.25	2	23
FA-MS-35-62	2294.88	Medium sandstone Lithic Grey Wacke	43.22	13.99	0.3	3	25
FA-MS-35-63	2582.67	Coarse sandstone Lithic Grey Wacke	-*	19.12	0.6	2	20

มหาวิทยาลัยเทคโนโลยีสุรนารี

Table C.1 Permeability and porosity of sandstone layer of Mae-Soon oil field (after DED) (cont).

Well Name	Depth of the sample measured from KBE (feet)	Sandstone name	Permeability (millidarcy)	Porosity (Percent)	Average grain size of the sediments contained in the rock (millimeter)	Cementing material (Percent)	Matrix (Percent)
FA-MS-35-64	2603.60	Coarse sandstone Lithic Grey Wacke	1623.8	14.70	0.6	3	19
FA-MS-35-66	2206.29	Fine sandstone Lithic Grey Wacke	1.25	6.91	0.15	3	22
FA-MS-35-66	2607.28	Very Fine sandstone Lithic Grey Wacke	10.55	13.09	0.125	3	23
FA-MS-39-68	2117.12	Fine sandstone Lithic Grey Wacke	-*	24.47	0.19	3	25
FA-MS-48-74	2508.92	Medium sandstone Lithic Grey Wacke	80.12	21.00	0.27	2	21
FA-MS-49-76	1930.28	Fine sandstone Lithic Grey Wacke	70.46	18.10	0.125	2	16
FA-MS-49-77	2333.13	Fine sandstone Lithic Grey Wacke	129.21	12.90	0.125	2.5	15

มหาวิทยาลัยเทคโนโลยีสุรนารี

Table C.1 Permeability and porosity of sandstone layer of Mae-Soon oil field (after DED) (cont).

Well Name	Depth of the sample measured from KBE (feet)	Sandstone name	Permeability (millidarcy)	Porosity (Percent)	Average grain size of the sediments contained in the rock (millimeter)	Cementing material (Percent)	Matrix (Percent)
FA-MS-51-78	1582.28	Fine sandstone Lithic Grey Wacke	1.12	12.69	0.125	2.5	18
FA-MS-51-79	1899.72	Fine sandstone Lithic Grey Wacke	4.08	12.59	0.125	2	17
FA-MS-51-79	1680.38	Medium sandstone Lithic Grey Wacke	6.82	12.83	0.5	2	16
FA-MS-52-80	1563.58	Fine sandstone Lithic Grey Wacke	17.22	16.82	0.15	2.5	20
FA-MS-52-80	2216.53	Fine sandstone Lithic Grey Wacke	42.75	17.15	0.2	2.5	21
FA-MS-53-83	2376.96	Very Fine sandstone Lithic Grey Wacke	5.62	17.09	0.1	3	18
FA-MS-53-83	3081.88	Fine sandstone Lithic Grey Wacke	125.60	23.29	0.25	2	20

มหาวิทยาลัยเทคโนโลยีสุรนารี

Table C.1 Permeability and porosity of sandstone layer of Mae-Soon oil field (after DED) (cont).

Well Name	Depth of the sample measured from KBE (feet)	Sandstone name	Permeability (millidarcy)	Porosity (Percent)	Average grain size of the sediments contained in the rock (millimeter)	Cementing material (Percent)	Matrix (Percent)
FA-MS-54-85	2773.81	Fine sandstone Lithic Grey Wacke	16.20	13.50	0.12	2	20
FA-MS-54-85	3048.65	Fine sandstone Quartz Arenite	58.25	18.36	0.2	3	4
FA-MS-54-86	3314.88	Fine sandstone Quartz Arenite	292.54	21.33	0.2	3	5
FA-MS-55-87	2131.88	Fine sandstone Lithic Grey Wacke	1.80	12.51	0.2	2	22

มหาวิทยาลัยเทคโนโลยีสุรนารี

Table C.1 Permeability and porosity of sandstone layer of Mae-Soon oil field (after DED) (cont).

Well Name	Depth of the sample measured from KBE (feet)	Sandstone name	Permeability (millidarcy)	Porosity (Percent)	Average grain size of the sediments contained in the rock (millimeter)	Cementing material (Percent)	Matrix (Percent)
Max.	3314.88	-	2765.4	35.55	2	4	25
Min	1359.21	-	1.12	6.91	0.1	2	4
Average	1989.55	-	1383.26	21.23	1.05	3	14.5
Mean	1754.70	-	49.23	17.38	0.21	2.62	19
Median	-	-	-	-	0.19	2	20
Deviation	540.81		539.35	5.55	0.27	0.55	3.99

มหาวิทยาลัยเทคโนโลยีสุรนารี

BIOGRAPHY

Mr. Makara Laikanok was born on September 7, 1988, in Surat Thani Province, Thailand. He received his Bachelor's Degree in Engineering (Geotechnology) from Suranaree University of Technology in 2009. He continued with his graduate study in the Petroleum Engineering Program, Institute of Engineering, Suranaree University of Technology.